Profiling Medulloblastoma and Juvenile Pilocytic Astrocytoma Brain Tumours in a South African Paediatric Cohort

Thesis Presented for the Degree of

DOCTOR OF PHILOSOPHY

In the Division of Neurosurgery

UNIVERSITY OF CAPE TOWN

March 2017

Omesan Nair

Supervisor: Professor Anthony Figaji

Co-supervisor: Professor Jonathan Blackburn

 The financial assistance of the National Research Foundation of South Africa and the German Academic Exchange Programme (NRF-DAAD) towards this research is hereby acknowledged. Opinions expressed and conclusions arrived at, are those of the author and are not necessarily to be attributed to the NRF-DAAD.

For my parents, JG and K Nair

…who have worked tirelessly and supported both my sister and myself throughout our academic endeavours and doctoral journey's. You, together, are our first and greatest teachers; this project is dedicated to you for all your love and encouragement in everything we do.

Acknowledgements

Firstly, I wish to acknowledge and thank the participants and their parents and families who were involved in the studies of this thesis. Both the retrospective and prospective cohort participants have contributed immensely to the molecular oncology knowledgebase from a unique South African context. Furthermore, I wish to acknowledge the financial support from the NRF/DAAD for investing in my personal development and local capacity development through this degree as well as the Cancer Association of South Africa (CANSA/CARISA) and the University of Cape Town Cancer Research Trust for supporting the broader study.

To my supervisor, Prof Anthony Figaji and the neurosurgical team at the Red Cross War Memorial children's Hospital, I owe much gratitude for your astute leadership, supervision and going above the call of duty in your support of this project. I am grateful for the opportunity to have worked in the translational research space that you have so graciously made accessible to the broader research community through this project.

To my co-supervisor Prof Jonathan Blackburn and the functional proteomics team at the Department of Integrative Biomedical Sciences at the University of Cape Town, I would like to acknowledge and thank you for providing the resources and renowned expertise in the proteomics field, as well as for the support, motivation and insightful discussions around clinical and translational proteomics. The team at the Blackburn lab has been immensely supportive during my doctoral journey.

I would also like to acknowledge the contributions from the Oncology/Heamatology and Radiology Departments at the Groote Schuur Hospital, Prof Alan Davids, Prof Jeanette Parkes and Dr Johann Reiderman for the keen interest, insights, clinical outcome data insights and discussions throughout this project. Additionally, I wish to acknowledge the support from Prof Graham Fieggen the Head of Department of Paediatric Neurosurgery and now the Head of Department of Surgery at Groote Schuur Hospital. I also wish to acknowledge the neurosurgery team, Dr Llewellyn Padayachy, Dr Nico Enslin and the staff at the Red Cross Children's Hospital who have managed the patients and facilitated the collection of biological samples for this work and others to follow. Many thanks also go to the Medical Records team at Red Cross for all the assistance and guidance with accessing patient folders from the archives.

The contributions from the Histopathology unit at the Red Cross Hospital are acknowledged, A/Prof Komala Pillay and team, many thanks for your incredible support during these research activities. I would like to acknowledge the collaboration from your department together with Dr Patricia Akiro and Dr Naeem Osman for their inputs on the MB and JPA study respectively.

I wish to acknowledge and thank Prof Michael Taylor and team at the Hospital for SickKids in Toronto for providing the resources, expertise and hosting us in your labs for Nanostring subtyping of the MB cases. In particular, I wish to thank Dr Vijay Ramaswamy, Betty Luu and Xiaochong Wu for all the guidance and assistance during the Nanostring subtyping of the MB samples.

A specific mention to my colleagues, Dr Ursula Rohlwink and Dr Andrew Nel for all your support, guidance, motivation and for providing a sympathetic ear during the particularly difficult times during my PhD journey.

To my family, parents, sister and dear friends, many thanks for the encouragement throughout my academic career. You all provided an invaluable support system through this highly challenging endeavour.

Lastly, I would like to note the progress of this work during a time of broad economic liberation movements', particularly the student-led movements for more accessible and inclusionary higher education in South Africa. I am supportive of this ideal and am grateful that the essential work and academic freedom for the studies in this thesis was valued throughout.

I am grateful for the opportunity to have worked at the Red Cross War Memorial Children's Hospital and for the opportunity to present some of this work at local and international conferences during my PhD studies.

Profiling Medulloblastoma and Juvenile Pilocytic Astrocytoma Brain Tumours in a South African Paediatric cohort

Candidate: Omesan Nair, Supervisor: Professor Anthony Figaji, Co-supervisor: Prof Jonathan Blackburn

ABSTRACT

Brain tumours in children are one of the most challenging diseases to treat, and so outcomes are variable and often lacking. There are currently no reliable data of presentation of disease, the spectrum of tumours treated, how these are treated, and what the outcomes are for children in South Africa, and certainly no molecular biology data. In this respect, this thesis investigated the two commonest types of childhood brain tumour, the highly malignant Medulloblastoma (MB) and the generally less aggressive Juvenile Pilocytic Astrocytoma (JPA) with relation to their molecular biology and their clinical correlates to begin to address this gap and build capacity for further molecular-based studies in an African context. The study design in this thesis takes a systematic approach and is structured into MB and JPA biochemical characterisation followed by 4 studies of their respective proteomic profiles. The study design involved creating appropriate patient cohorts and determining sample characteristics for interpretation of results.

The statistical power achieved in this thesis showed a minimum of 2-fold difference for a power greater than 0.8 in each case. Proteomic clustering was used to validate or delineate any discrepancies in subtype assignments for MB. Molecular profiles together with proteomic data of MB and JPA cases in this thesis provide evidence for some novel molecular pathways, proteins and peptides associated with pathogenesis. This work therefore provides extensive data that is hypothesis generating for further studies that could build upon molecular understanding in a South African and larger African context.

Summary of findings

The cohorts were determined by the availability of banked specimens and clinical data. In the first instance, a summary of the molecular characteristics of a retrospective cohort of MB patients in a South African context was determined using Nanostring-based molecular subtyping and IHC, any discrepancies were resolved by proteomic clustering analysis to assign subtype. There are 19% WNT, 27% SHH, 29% Group 3 and 25% Group 4 consolidated subtypes presented in this cohort of 48 cases between 1988 - 2014 with follow up until 2016. Demographic and phenotypic data are reasonably consistent with data from other international cohorts, with the exception of a greater proportion of female patients with MB and greater proportion of NMYC amplified cases in the current cohort. The 5-year overall survival rate was 74% and 10-year overall survival rate was 62%.

The JPA cohort consisted of 14 cases spanned 1993 - 2014, with follow-up until 2016. There are 9 cerebellar cases and 5 non-cerebellar cases. There was a favourable 5-year overall survival rate of 93%, and a progression free survival rate of 86%. The molecular characteristics investigated in the current cohorts show that BRAF amplifications (as determined by FISH) suggest a strong association with cerebellar JPA cases and showed a trend towards poorer outcomes in this cohort. pERK positivity by IHC as a marker of MAPK pathway activation is consistent in the majority of the patients in this study and further confirms the role of this pathway in JPA pathogenesis. P16 (CDKN2A) inactivation as determined by the IHC producing a weakly staining pattern, trended towards poorer prognosis. This is also consistent with other international cohorts.

Proteomic work in this thesis involved investigating the onco-proteomic profile of the retrospective cohorts of MB and JPA using a discovery proteomic approach with label-free quantitation. Thereafter, a subsequent proteomic validation approach validated the findings in a prospective cohort.

Medulloblastoma WNT-specific associations revealed enrichment of endoplasmic reticulum, immunoglobulin and ribonuclear complex associations. The highly abundant protein groups

related to WNT were VIM, DKK factors, COLA and RNA elongation factors. Validated peptides included HSPA5, DAD1, FBN1 and INA protein groups specific to the WNT subtype.

SHH-specific associations showed enrichment of proteins associated with the excitatory synapse, SWI/SNF complex and membrane vesicles. PDLIMs, GAB, heat shock proteins and NEFM neurofilament proteins and peptides for DPSY2-5, PRR36 and GAB1 were specific for SHH. In all, the chromatin remodelling factors as well as the SWI/SNF, DPYSL protein, cell motility proteins and RNA transcript degradation pathways are suggested in this thesis to be implicated in SHH-specific tumours in the cohort.

Group 3-specific associations revealed ATPase degradation complexes, ribonuclear and DNA replication associations with NFκB binding. COX, PYCR1 and sumoylation proteins and peptides for TGFBI, ARAP1 and LUC were significantly implicated for this subtype.

The protein groups associated with favourable prognosis in Group 3 include RAB5A, ANP32A, DDX5, RPS13, CCT2 and DYNC1H1. Those associated with poor outcomes include VIM, LAMC1, IGKCs, NCAM and GSN protein groups.

Group 4-specific associations include protein folding, splicing and motor protein associations with serine proteases RELN and serine protease inhibitors PEBP1, neurodevelopment proteins, TNIK and VAT1. Specific peptides including markers for RHOA, FRY and HAGH are specifically linked to Group 4 subgroups. Proteins associated with Group 4 MB favourable outcomes include RPL13, SERPINA3, RPS12 and C1QBP, while those associated with a poorer outcome in Group 4 tumours include HIST1, PDXP, IDH2, AKR1B1 and C14orf166 protein groups. Taken together the protein groups related to favourable prognosis in Group 4 MB are ribosomal and protein translation-linked with pro-coagulation proteins and inflammatory related proteins, while the proteins linked to poorer outcomes are histone and ploidy related, mitosis, IDH onco-metabolite-related and chemotherapy resistance related proteins. A region on chromosome 6p, VARS, RPS12 and HIST1H3A are associated with good outcomes in MB overall and more specifically for the Group 4 and SHH subtypes respectively.

Juvenile Pilocytic Astrocytoma Data from this thesis suggest that specific proteins linked with poor outcomes in cerebellar JPA were MYH10, RPS8, RPS4X and PRDX. The non-

cerebellar specific proteins were seen enriched for dopamine, GABA, serotonin-associated proteins and Rho cell motility processes. Chemo-osmotic and vasopressin associated water reabsorption protein groups are shown overrepresented in these cases. Protein groups associated specifically with poorer outcomes were MYH9, PSMC1, RPL7A.

Abbreviations list

Abbreviation	Expansion
CGH	Comparative genomic hybridisation
Conc.	Concentration
DNA	Deoxyribose nucleic acid
FISH	Fluorescence *in situ* hybridisation
ICP	Intra-cranial pressure
IHC	Immunohistochemistry
IV	Intravenous administration
JPA	Juvenile pilocytic astrocytoma
LC/MS	Liquid chromatography mass spectrometry
MB	Medulloblastoma
MS	Mass spectrometry
NCJPA	Non-cerebellar JPA
NS	NanoString
PNET	Primitive Neuroectodermal tumour
PO	Per os (oral administration)
RCCH	Red Cross Children's Hospital
RNA	Ribose nucleic acid
SA	South Africa
SHH	Sonic hedgehog
SNP	Single nucleotide polymorphisms
US	United States of America
WHO	World Health Organisation
WNT	Wingless

Table of Contents

Section A - Introduction

Chapter 1 – Introduction and Background

1.1 Context

Brain tumours in children are one of the most challenging diseases to treat, and so outcomes are often poor. Mortality is high and survivors are often neurologically disabled. Treatment of such disease optimally requires an experienced team of multidisciplinary health professionals and availability of resources to monitor progress and recurrence. The accessibility of such resources is limited in developing nations such as South Africa. Moreover, the disease is more common than most people realise: it is the second commonest malignancy in children in the US and worldwide (Figure 1.1). Unlike international efforts that are more comprehensive and include vast molecular data on the genomic, transcriptomic and epigenomic profiles of this disease, data is limited in the South African context (Northcott et al., 2014). In particular, a coherent dataset, which includes information on the presentation of disease, the spectrum of tumours treated, how these are treated, the patient outcomes and their biochemical presentation in our local context, is urgently needed. In fact, there are no reliable comprehensive data for brain tumours in children in the whole of Africa. This data is becoming increasingly important for a more precise diagnosis, more accurate prognosis, and an advanced molecular understanding of brain cancers.

Absence of this data restricts our understanding of the burden of childhood brain tumours in South African children, our knowledge of how our outcomes compare with international standards and so what needs to be addressed, and our involvement in international trials of novel therapies and protocols of treatment. To this effect, this thesis aims to examine two types of childhood brain tumours from two ends of the spectrum of disease, the malignant tumour medulloblastoma (MB) and the generally less aggressive and slower growing juvenile pilocytic astrocytoma (JPA), with relation to their molecular biology and their clinical correlates. The overall aim is to develop novel data on molecular profiles of these tumours in a local Southern African cohort of children. Given that such work currently does not exist in our context, our aim was also to develop capacity in this area for future work.

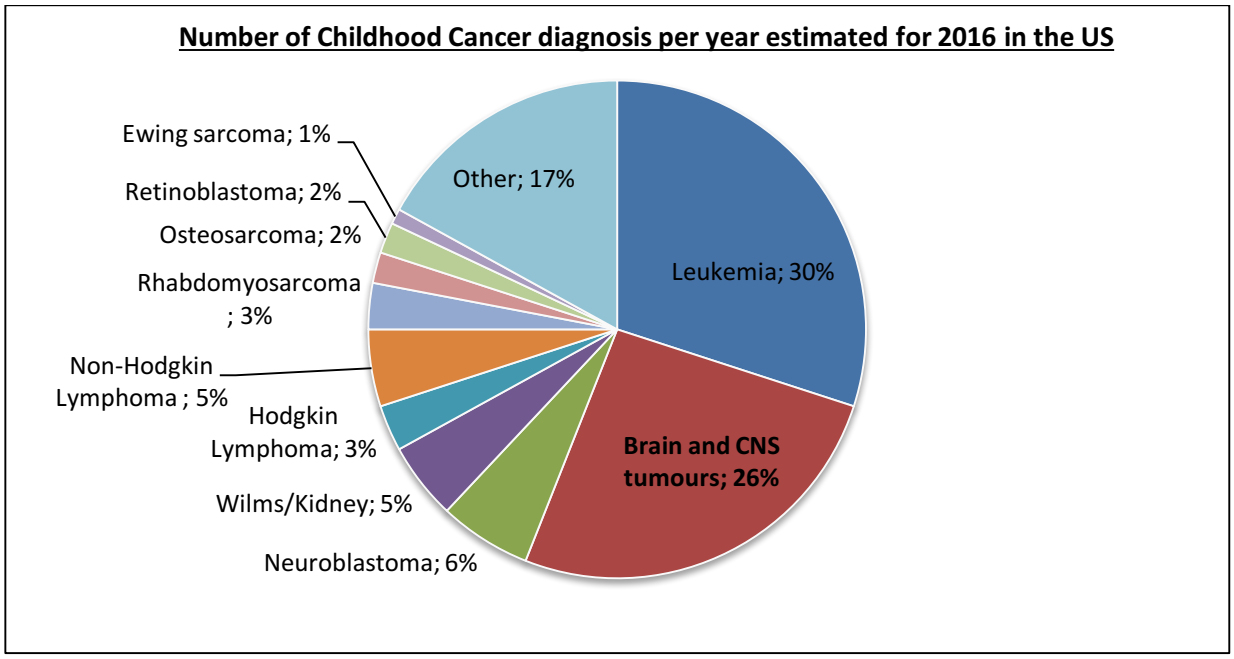

Figure1.1: Incidence of Childhood tumours from American Cancer society, 2016 (*Cancer Facts and Figures 2016*, 2016)

1.2 Brain tumour overview

Brain tumours are abnormal growths (neoplasms) in the brain and CNS regions that can disrupt normal brain function. These tumours may be benign or malignant, but there is a spectrum. Benign tumours are slower growing and responsive to surgery if they are in an accessible location. However, in difficult locations even benign tumours may be difficult to cure. Tumours arising or identified as originating in the brain region are known as primary brain tumours and those that spread to the brain from other cancerous sites in the body are known as secondary malignancies. Primary tumours in the CNS are classified and described based on region and histological resemblance (Louis et al., 2016; Read, Hegedus, Wechsler-reya, & Gutmann, 2006). There are two broad categories, gliomas and non-gliomas. Gliomas include tumours such as astrocytoma, ependymoma – ependymal cell tumour appearance, oligodendroglioma – oligodendrocyte or mixed glial cell appearances. Non-gliomas include CNS tumours such as meningiomas – arising from cells in meninges, CNS lymphomas – arising from lymphoid tissues and germ cell tumours appearing from germ cell origins.

Furthermore, they are described and classified into the specific regions in which they occur such as optic gliomas and pineoblastoma, which occur in the optic nerve or pineal gland respectively (Figure1.2). While some tumour types can occur in any brain region, often they tend to occur in specific brain regions with in a particular frequency. Gliomas occur in the suprasellar region, hemispheres and cerebellum, craniopharyngiomas occur almost always in the suprasellar region, medulloblastomas and ependymomas tend to occur in the posterior fossa (Figure1.3).

1.3 Occurrences

Tumours of the CNS can occur anywhere in the brain and spinal cord. They can be primary tumours arising in the CNS or secondary tumours arising elsewhere in the CNS or from other cancer sites from other organs in the body. Tumours are particularly common in the posterior fossa in young children (Gajjar et al., 2015).

The posterior cranial fossa is located at the base of the skull and contains the cerebellum and brainstem, limited inferiorly by the skull base and superiorly by the tentorium. This region is suggested to contain multipotent and progenitor cells which may be linked to tumourigenesis (Turner, Mckean-cowdin, Fisher, & Philip, 2014). Lesions here often cause hydrocephalus, as the fourth ventricle becomes obstructed by the tumour mass (Turner et al., 2014). It is suggested that these tumours occur by aberrant cerebellar development processes. As the majority (±70%) of paediatric brain tumours occur in this brain region compared to only about 15% in adult brain tumour types and cells in this region have growth, migration and differentiation responsive signals in some paediatric cerebellar tumours (Turner et al., 2014).

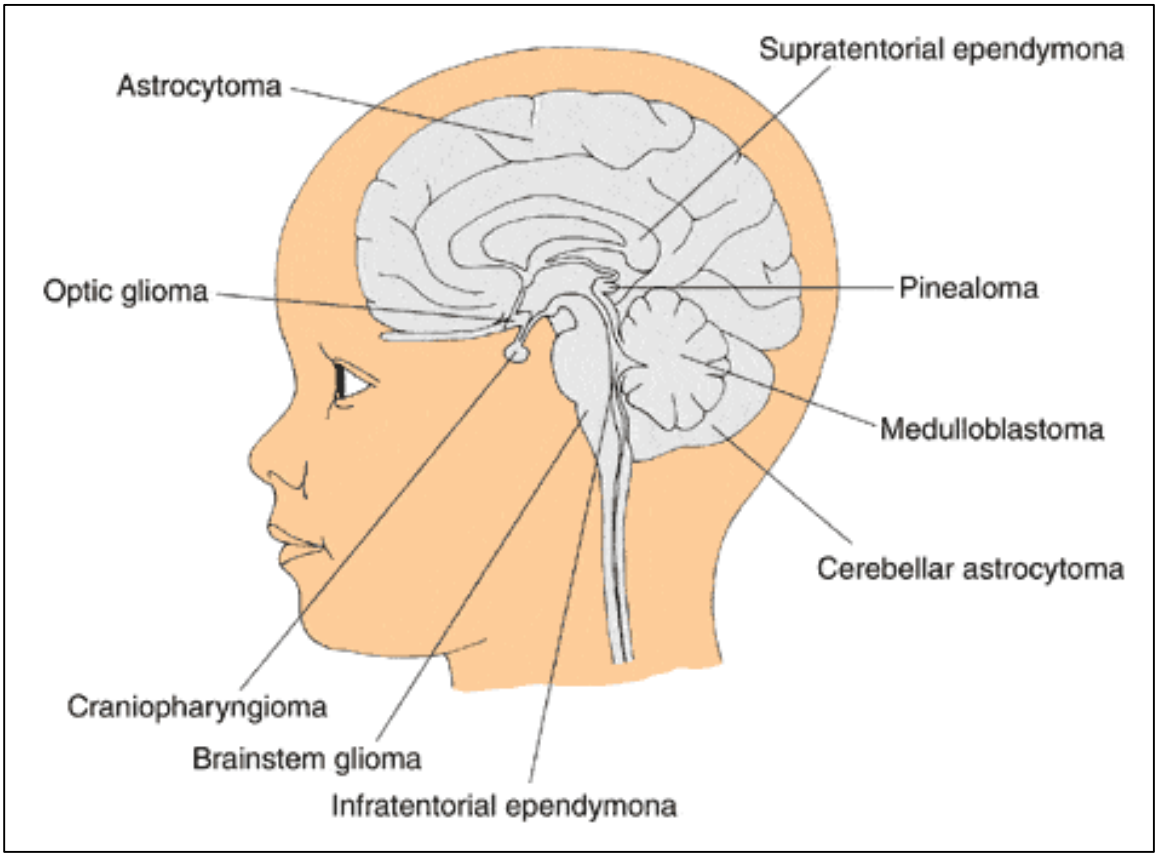

Figure1.2: Different type of brain tumour occurrences ("Brain tumors," 2016).

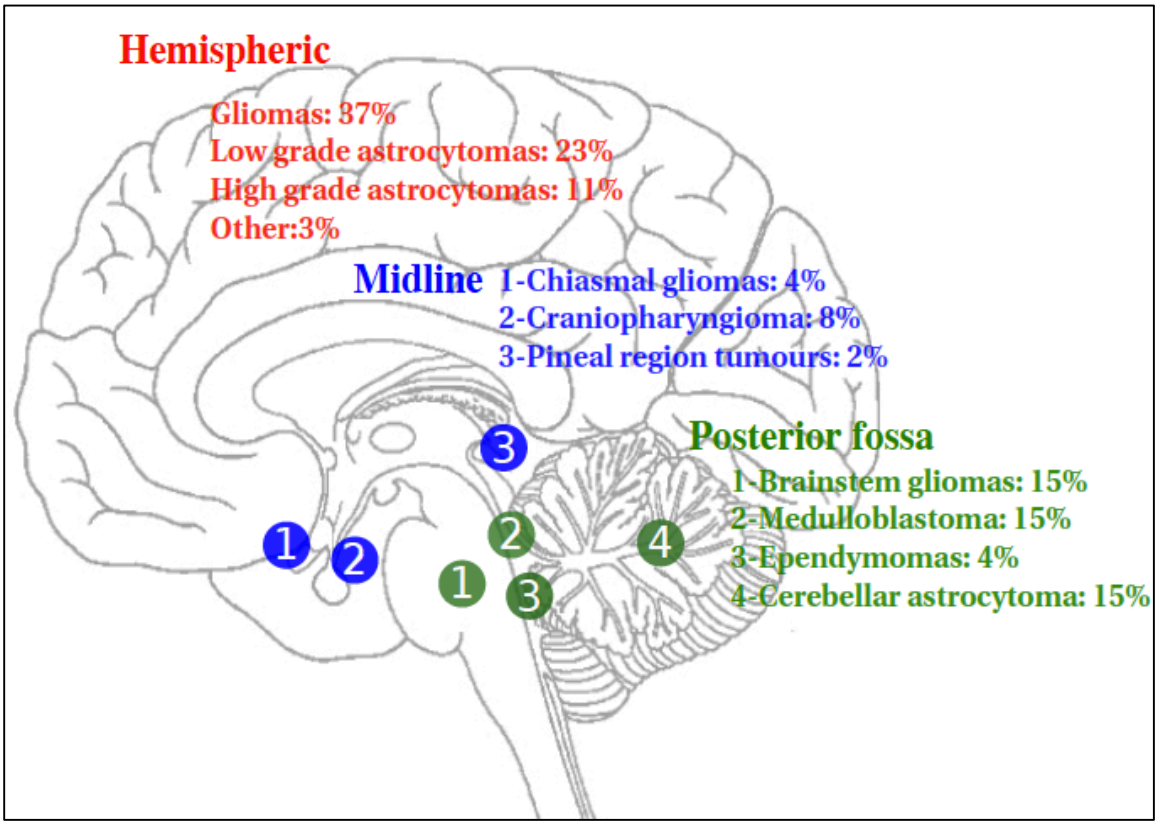

Figure1.3: Location and frequency of childhood brain tumours adapted (Albright, 1993).

1.4 Clinical presentation

The clinical presentation of brain tumours varies depending on the brain location of the tumour. Generally, patients with brain tumours may present with generalised symptoms such as headaches, seizures, nausea, vomiting, syncope (a loss of consciousness due to a sudden rise in intracranial pressure resulting in a loss of blood pressure) and cognitive dysfunction. More focal symptoms include muscle weakness, sensory deficits, aphasia (communication deficits) and visual dysfunctions. Symptoms of cerebellar tumours usually include vomiting, headache, uncoordinated movements, and ataxia (walking deficits) (Table 1.1). The diagnostic interval (from time of symptoms to time of diagnosis) is one of the longest in all of childhood cancers, usually up to 14 weeks in developed nations (Dhurgsharma, Walker, Liu, & Wilne, 2015). Some suggested reasons for long diagnostic interval times are that the nonspecific symptoms of brain tumours and the likely misdiagnosis with other more common conditions and behavioural disorders, the relative rarity of brain tumours and the lack of awareness amongst clinicians and families (Dhurgsharma et al., 2015). Despite this enormous challenge, there are awareness campaigns being implemented in many countries throughout the world and international advocacy groups such as the international brain tumour alliance that assist and support the community of involved patients, families, researchers and clinicians.

Table 1.1: Clinical presentation of posterior fossa tumours adapted (Packer, Macdonald, & Verzina, 2010)

Tumour type	Relative incidences	Clinical presentation	Diagnosis	Prognosis
Medulloblastoma	35-40%	2-3 months of headaches, vomiting, truncal ataxia	Hetero or homogenously enhancing fourth ventricular mass, may disseminate	65-80% survival, dependent on stage/type, poorer in infants (20-70%)
Cerebellar astrocytoma	35-40%	3-6 months of limb ataxia, headaches, vomiting	Cerebellar hemisphere mass, usually cystic and solid (mural nodule) components	90-100% in gross total resected pilocytic type
Brain stem glioma	10-15%	1-4 months double vision, unsteadiness, weakness, other cranial nerve deficits, facial weakness, swallowing deficits	Diffusely expanded, minimally or partially enhancing mass in 80%, 20% more focal tectal or cervicomedullary lesion	>90%, 18-month mortality in diffuse tumours, better in localised
Ependymoma	10-15%	2-5 months of unsteadiness, headaches, double vision, facial asymmetry	Usually enhancing, fourth ventricular mass with cerebellopontine predilection	>75% in gross total resected cases
Atypical Teratoid/Rhabdoid	>5%	Same as medulloblastoma, mostly in infants, facial weakness, strabismus	As in medulloblastoma, often more laterally extended	<10-20% in infants

1.5 Causes

While little is known of the causes of childhood brain cancers, there is a small proportion of brain cancers that are linked to germline mutations or alterations such as Neurofibromitosis 1 which is associated with an increased risk of gliomas and central nervous system lesions (Pollack & Jakacki, 2011) (Table1.2). There are some suspected environmental and dietary exposures during pregnancy, such as alcohol exposure and tobacco use etc.; however, there are no proven causal relationships. It has also been suggested that there is a link between SV 40 virus and medulloblastoma (Farwell, Dohrmann, & Flannery, 1984). However, this is contentious in the field and other groups have shown that a closely related virus, the JC virus, cannot been seen in the tissues of any of their medulloblastoma cases using southern hybridisation or direct sequencing (Okamoto et al., 2005). Polyomaviruses such as BK, JC and SV40 have not been detected in the majority of primary MBs unlike ependymomas and choroid plexus tumours (Kim et al., 2002). The frequently contradictory literature on causation does not fare well for the development of preventative measures for brain cancers and therefore limit any form of prophylaxis for this disease type. Currently, there only exists genetic counselling for couples who may display a significant risk from known inherited or genetic predisposition syndromes. It has also been shown in multinational cohorts that the inheritance pattern of family members with brain cancers or other cancers without any predisposition syndromes is not related to an increased risk for brain tumours in childhood and so pedigree inheritance analysis is often of limited utility (Searles et al., 2008). This results in the lack of stringent predictors of brain cancer risks in childhood.

Table1.2: Germline syndromes linked to brain cancers adapted (Pollack & Jakacki, 2011)

Syndrome	Gene affected	Gene Function
Neurofibromatosis1, 2	NF1, NF2	GTPase
Tuberous sclerosis	TSC1, TSC2	GTPase
Von Hipple-Lindau	VHL	Component of VCB-CUL2, HIF-2alpha transcription factor regulator
Li-Fraumeni	TP53	Transcription factor
Turcot	APC, other mismatch repair genes	WNT signalling
Gorlin	PTCH1	Hedgehog signalling receptor
Nijmegan breakage (Frappart & Mckinnon, 2006)	NBN	DNA damage repair
Rubinstein-Taybi (R. W. Miller & Rubinstein, 1995)	CBP, EP300, 16p deletion	Histone acetyltransferase, DNA damage repair, cell differentiation
Fanconi anemia (Offit et al., 2003)	BRCA2, FA pathway mutations	DNA interstrand break repair

1.6 Diagnosis

When a patient presents with the symptoms of brain tumour, neuro-radiologic imaging is usually employed both to inform the diagnosis and as a surgical planning tool. The most common tool is magnetic resonance imaging (MRI), which is based on nuclear magnetic resonance that uses high-powered magnetic fields to determine the location of water and fats (measurement of abundance of hydrogen atoms) in the body. MRI can generate T1-weighted images, which are short electromagnetic excitation time and short magnetic relaxation times that is integrated into images showing lipid rich tissues such as white matter brighter and

water appearing darker and CSF very dark (Walter et al., 2010). This allows for a wide contrast especially between grey and white matter of the brain, however the quality of the T1 images are enhanced by contrast agents such as gadolinium (Chun-yan Cao, Shen, Wang, Li, & Liang, 2013). This enhancement is useful to distinguish the tumour from the surrounding oedema artefacts common in brain tumours. The utility of enhancement in paediatric brain tumours has some limitations - some malignant gliomas enhance poorly, while many low grade gliomas such as juvenile pilocytic astrocytomas enhance brightly (Scott, Brasher, Sevick, Rewcastle, & Forsyth, 2002). T2-weighted images make use of long excitation and relaxation times producing images where CSF appears bright and lipids less bright. To minimise the CSF effects the fluid-attenuated inversion recovery (FLAIR) sequence is commonly used to image non-enhancing tumours (Rees, 2003). Newer imaging techniques are increasingly being developed for applications such as intraoperative MRI, functional MRI spectroscopy for identification of metabolites and biomolecules in diagnosis, treatment planning and treatment response monitoring (Fink, Muzi, Peck, & Krohn, 2015). MRI also enables assessment of leptomeningial spread and metastasis in the brain and spinal cord.

Computed tomography (CT) imaging has largely been replaced by MRI but is still useful in selected cases to diagnose tumour calcifications. Although CT may be more readily available and less costly, it is limited by poor soft tissue characterisation, posterior fossa beam hardening artefacts and the long term risk of radiation (Brenner, Elliston, Hall, & Berdon, 2001).

Radioimaging such as positron emission tomography (PET) imaging makes use of a radiotracer such as radiolabelled fluorodeoxyglucose (^{18}F-FDG) and is a label for energy metabolism (Fink et al., 2015). However, the complex nature of the brain makes the utility of current PET imaging in brain tumours problematic as the brain has typically a high metabolic rate. Normal grey matter often takes up the radiolabel and appears enhancing in images, there is variable uptake in heterogeneous tumours, and necrosis artefacts all confound the utility of PET in aiding a clinical diagnosis (Fink et al., 2015). Future prospects of PET imaging are increasingly promising as newer radiotracers are being developed with labelled small molecules, amino acid derivatives, and protein functional based probes to target a wide

variety of neurotransmitters, receptors and other targets for brain tumour imaging (Zimmer & Luxen, 2011).

1.7 Cellular and histological diagnosis

Although imaging is useful in diagnosis, accurate diagnosis requires tissue histology (or increasingly, tissue molecular biology). Specific tumour histology characteristics are discussed in later sections in this chapter. Usually, mitotic activity is assessed as well as evaluation of metastatic cells in the CSF. CSF is sometimes sampled intraoperatively from cisternal or ventricular fluid; however, it is more commonly sampled from lumbar puncture taken two weeks post operatively to avoid false positives associated with cytology related to surgery (Souweidane et al., 2009).

1.8 Molecular diagnosis

Molecular characterisation of brain tumours is rapidly expanding with modern next generation technologies in genomics and epigenetics. The latest updated World Health Organisation (WHO) classification of brain and CNS tumours in 2016 included, for the first time, molecular diagnostic characteristics for brain tumours. These include several molecular characteristics that relate to prognosis or susceptibility to treatment with certain drugs (Table1.3) (Louis et al., 2016). While this latest update allows for molecular phenotypes there are as yet no guidelines on standardisation of the methods for molecular characterisation, and this is required given the rapid advancement of the technology in the field. Ideally, an integrative approach to make a comprehensive diagnosis is warranted, using clinical, imaging, histological and molecular data.

Table 1.3: Molecular markers for brain tumours in latest WHO classification for CNS tumours

Molecular marker	Brain tumour type	Clinical utility
Chromosome 1p and 19q co-deletion with IDH mutant	Oligodendroglioma	Generally better prognosis (Boots-Sprenger et al., 2013) Treatment specificity for Temozolamide (Kaloshi et al., 2007)
IDH mutation	Astrocytoma, Glioblastoma	Good prognosis Treatment specificity for Temozolamide (Songtao et al., 2012)
ATRX loss, TP53 mutation	Diffuse astrocyomta	Good prognosis (Wiestler et al., 2013)
H3K27M mutant	Glioma	Poor prognosis (Khuong-quang et al., 2012)
RelA fusions	Ependymoma	Supratentorial with very poor prognosis (Pajtler et al., 2015)
C19MC gains	Embryonal tumours multilayer rosettes	Poor prognosis (M. Li et al., n.d.)
ALK positive	Lymphoma	Secondary, Possible metastatic risk (Chiarle, Voena, Ambrogio, Piva, & Inghirami, 2008)
MGMT promoter methylation	Glioblastoma	Treatment specificity for Temozolamide (Hamou et al., 2005)
WNT, SHH, Group 3, Group 4 activated	Medulloblastoma	Prognosis, WNT subtype best outlook, others varyingly poor (Ellison et al., 2011)

1.9 Treatment protocols

Brain tumours are generally treated with surgical resection, followed by chemo and radiotherapy (Karajannis & Allen, 2008). The location and characteristics of the tumour, such as defined borders (circumscribed) or diffuse tumours, determine the extent of which resection is possible. Gross total resection is usually targeted however near-total or subtotal resections may be preferable for the low grade or less aggressive tumour subtypes (E. M. Thompson et al., 2016). While gross total resection remains ideal if possible, more aggressive surgery may result in adverse outcomes and possible poor quality of life in survivors (Sajjad, Kaliaperumal, Yousaf, Bhatti, & Sullivan, 2016).

Chemotherapy is usually administered within 4 weeks after surgery. It is given as a systemic drug combination of approved drugs such as Carboplatin, Vincristine and Etoposide that can last up to 8 courses or more, which can run concurrent with radiotherapy (Karajannis & Allen, 2008).
Chemotherapy regimens are constantly being investigated to apply the most appropriate regime for the specific tumour, patient age, as well as now to the molecular phenotype that is most likely to respond a particular drug or treatment regime (Gottardo & Gajjar, 2009). There are however potential side effects including neurodevelopmental, neurocognitive, endocrine, reproductive, neurologic and neurosensory sequelae. There is great interest in developing new drugs for better, more specific, and less toxic effects with targeted therapeutic care strategies (Srivastava et al., 2016).

Radiotherapy is a dose of ionising radiation given to the site of the primary tumour bed, sometimes more widely to the cranial and spinal axis commonly in the form of photon radiation or particle radiation. Although necessary, radiotherapy also has potential short and long term risks (Bunin, 2000). There are however, several radiology techniques employed to minimise the exposure of normal tissue to the ionisation or to specifically target disease. These include techniques such as hyper-fraction therapy or modern gamma knife neuroradiology which has been suggested to improve the quality of life in survivors (Skeie et al., 2016). Nevertheless, because there are still high levels of neurotoxicity related to radiotherapy, this treatment is usually delayed in very young patients below the age of 3 years

old and deferred to even older patients where possible, such as with hypothalamic gliomas (Duffner et al., 1993). Delaying radiotherapy has been successful in brain cancers and is effective in avoidance of the neurocognitive decline associated with radiotherapy exposure in young children (S. Rutkowski et al., 2008). The use of prolonged chemotherapy in delayed radiotherapy cases in young children has been suggested to be of benefit but only in selected tumours (Strother et al., 2014). Methods of improving radiotherapy in brain cancers have been investigated particularly with the use of radiosensitizers. These are chemical agents that can improve the radiation effect on tumour cells and limit their effects on surrounding normal cells thereby preventing the adverse effects of the treatment. However, the utility of these agents are being investigated as many of these agents are either poor at crossing the blood-brain-barrier or are taken up by the metabolically active normal brain cells. Nonetheless, approved drugs such as Temozolamide have been suggested to confer radiosensitivity and might be particularly useful in induction therapy regimes (Milker-zabel, 2006).

1.10 Follow up monitoring

Survivors are monitored for many years to detect relapse and the development of long-term sequalae of therapy with support from endocrine and neuropsychology. Surveillance imaging is usually performed at routine intervals, more frequent in the initial years and less frequent in later years.

1.11 Follow up treatment and relapse

Relapse can occur locally to the primary tumour site or at distant sites (Packer, Zhou, Holmes, Vezina, & Gajjar, 2013). The treatment of relapse depends on the type of brain tumour being managed and whether the recurrence is local or distant. They may require second surgery, chemotherapy, and even radiotherapy occasionally. Relapsed patients that are resistant to treatment may have the option to enrol into clinical trials if they are eligible and there are many ongoing trials investigating new drug targets that have shown early phase and preclinical promise.

Neuroendocrine deficits in brain tumour some survivors are related to the tumour, treatment effects as well as individual childhood development, and often require endocrine interventions (Laughton et al., 2008).

1.12 Brain tumour molecular biology

The molecular phenotypes of brain tumours increasingly have a more direct impact in the clinic because there is growing consensus that molecular characteristics impact on clinical decisions. The molecular data are in many cases a complex interplay of cellular and tissue markers. Biomarkers are specific molecular cues that can assist with diagnosis, tumour staging and prognosis; there are also biomarkers that may predict individual response to treatment.

However, for consensus to be reached on any set of markers generated from large molecular datasets, the statistical, methodological and clinical significance has to be rigorously validated. In future, more advanced molecular markers will be identified and validated for utility in accurate diagnosis, prognostication and treatment stratification but the field is still far from the ideal of optimally utilising molecular biomarkers. Furthermore, application of genetic and protein markers that are identified in relatively genetically homogenous populations may not be entirely generalizable to poorly represented and diverse geographic populations. Notwithstanding, the applications of biomarkers in a population with a vast genetic diversity such as the genetic background in Southern African populations, have not been established. One area in which South Africa specifically, and Africa more generally, have not kept pace with international trends has been the recognition of molecular characterisation of childhood brain cancers and its potential implications for treatment. This is important for several reasons, including the confirmation of generalizability of data developed in the global North, enabling the benefit of these techniques (and targeted therapies) to local populations, and the expectation that identification of these subtypes will be required for entry into future clinical trials.

Chapter 2 Medulloblastoma (MB)

2.1 Background

MBs are malignant primary brain tumours that mostly occur in children and are a leading cause of paediatric brain tumour deaths (Turner et al., 2014). Rare in adults, they have a childhood incidence of 0.2 - 0.6 per 100, 000 and account for 15 - 25% of all CNS tumours in international cohorts (Turner et al., 2014). The incidence of medulloblastoma in the North America is 1.6 per million; the incidence rate in children is 6.0 and adults 0.6, and this rate has not significantly changed since the 1970s (Smoll & Drummond, 2012).

2.2 Clinical presentation

Overall, MB affects males 1.5 times more frequently than females (Kool et al., 2012). There has been no conclusive evidence suggesting that MB occurs in seasonal fluctuations, as reports from international cohorts from Denmark and the UK suggest (Basta, James, Craft, & McNally, 2010; L. S. Schmidt et al., 2009).

Most MBs are located in the midline of the cerebellum, occasionally with brain stem involvement. MB patients can present clinically with the general characteristics of brain tumours as specified in Chapter 1, with specific indications of cerebellar involvement such as symptoms of difficulty swallowing, nausea, vomiting, balance deficiencies or ataxic gait (Packer, Friedman, Kun, & Fuller, 2002).

2.3 Histological presentation of MB

The international classification of diseases for oncology (ICD-O) has developed guidelines for the classification of neoplasms in cancer registries for coding topography (tumour site in the brain) and morphology (shape and structure) of the tumour. MBs are histologically classified as follows: classic, large cell/anaplastic, desmoplastic/nodular, MB with extensive nodularity (Louis et al., 2016).

2.3.1 Classic variants

Classic MB displays as small round blue nuclei, may be cigar-shaped, with hyperchromatic nuclei in routine cyto-architecture H & E stains. Cells appear undifferentiated and have little cytoplasm (Pfister, Hartmann, & Korshunov, 2009).

2.3.2 Large cell variants/anaplastic MB

Spherical cells with round nuclei and prominent nucleoli, high mitotic and apoptosis rate are seen with this variant. There is a lot of overlap in characteristics between anaplastic and large cell variants of medulloblastoma. This variant of medulloblastoma is characterised by high mitotic activity and highly variable size/shaped nucleus (pleomorphic). Large cell variant usually present with spherical cells with round nuclei, open chromatin and prominent nucleoli (Louis et al., 2007).

2.3.3 Desmoplastic/nodular variants

These variants are characterised histologically by the presence of nodules, with reticulin rich intermodal regions (Louis et al., 2007). These have been associated with a favourable outcome (Gerber et al., 2014).

2.3.4 Medulloblastoma with extensive nodularity

There is commonality between this type and the desmoplastic/nodular MB type. This type usually displays an expanded lobular architecture with reticulin-free zones becoming filled with a neuropil-like tissue. These zones contain small cells in a streaming pattern. Desmoplastic/nodular MB usually present with nodules and reticulin-rich internodular zones (Louis et al., 2007). Both these types are associated with a better prognosis.

2.4 Possible causal links in MB inheritance and predisposition

It has been reported in the Connecticut tumour registry that in some cases children presenting with MB had a higher chance of having immediate family members with brain tumours, leukaemia or childhood cancers when compared to controls (Farwell et al., 1984). Two inherited syndromes have been shown to be associated with a higher risk of MB occurrence,

namely, Gorlin and Turcot syndromes. Gorlin syndrome is associated with basal cell carcinoma of the skin, while, a specific subtype of Turcot syndrome, in particular those with mutations in FAP and APC, results in a higher risk for MB in these cases (Huang et al., 2000). Although the role of viral mediators is inconclusive, some studies such as the ones carried out at the Karolinska Institute between 1994 and 2005 (Baryawno et al., 2011) have identified the human cytomegalovirus (HCMV) in primary MB tumours. However, other studies have shown that while some patients may be serologically positive for HCMV there was no evidence for HCMV presence in the neoplasm tissue (Sardi et al., 2015).

2.5 MB molecular biology

MB patients are usually stratified in clinical trials based on age, extent of surgical resection, presence of metastatic spread, and histological appearance. However, it has been suggested that these are suboptimal methods since MBs are an ideal group to consider the recent advances in the understanding of tumour biology.

Current molecular evidence demonstrates that the entity of MB comprises at least 4 distinct subgroups that have clinical correlates and predict the risk for recurrent disease (WNT, SHH, Group 3, and Group 4) (Northcott, Korshunov, et al., 2011). Each group demonstrates a pattern of demographics, genomics, and outcomes (Figure 2.1). Furthermore, while much is known about the genomics of MB, translating those that are known and validated as well as identifying additional biomarkers of disease that correlate with clinical presentation and disease outcome are urgently needed. Additionally, insights of molecular presentation of MB in local South African cohorts are also urgently needed in the form of translational research for optimal treatment as well as for representation of diverse genetic backgrounds into clinical research into new treatments. To this end there is more and more genomic data being generated globally and contributing to global understanding of MB, but there are limited details of the proteomic correlation of the genomic findings and the nature of this disease. Generating proteomic datasets of these tumours can yield further insights into MB and can lead to the discovery and validation of much needed additional biomarkers of the disease and probable treatment outcome. A combination of gene expression profiling along with proteome analysis would further the understanding of MB pathogenesis.

2.6 MB Treatment

Recently there have been improvements in the treatments of this tumour largely in radiotherapy; however, the overall survival rate has not been significantly enhanced, with evidence from a small study of 19 MB cases in South Africa during 1983-1995 suggesting an overall survival of 60% in childhood MB (Hesseling, Wessels, & Riet, 1995). This further emphasises the complexity of this disease and the limitations of our traditional understanding of the disease phenotype. Despite the improvements in treatment of patients with MB, survivors often have impaired long-term outcomes, such as problems with learning and delays in physical growth and development (Johnson et al., 1994).

The integrative treatment of MB involves surgical resection followed by chemo- and radiotherapy. However, radiotherapy can be delayed in children younger than 3 years of age to limit the adverse developmental and neurocognitive effects (Müller et al., 2014). There are ongoing studies investigating the specific treatment protocols for relapsed or treatment resistant MB. Additionally, there are also molecularly guided treatment protocols being investigated for subgroup specific treatment such as treatment de-escalation in the less aggressive WNT subtype.

Gross total resection of tumours appeared better that subtotal tumour resection historically (Park, Hoffman, Hendrick, Humphreys, & Becker, 1983). However, recent molecularly-informed treatment stratification suggests that more aggressive surgical strategies do not confer a greater progression-free or overall survival benefit, if subgrouping is taken into account. This was reported for the WNT, SHH, and Group 3 subgroups (E. M. Thompson et al., 2016). Aggressive surgical strategies in Group 4 subtype appears to have some benefit and more so in patients experiencing metastasis. Of course, this is limited by the fact that at initial surgery such subgrouping is not available.

2.7 Evolution of risk stratification

MB patients were traditionally stratified in clinical trials based on age, extent of surgical resection, presence of metastatic spread, and histological appearance. There is now consensus that the entity of MB comprises 4 distinct subgroups that have clinical correlates and predict

the risk for recurrent disease (WNT, SHH, Group 3, and Group 4) (Northcott, Korshunov, et al., 2011). To further characterise each group pattern of demographics, genomics, and outcomes; Figure 2.1 and Table 2.1 summarises the current consensus.

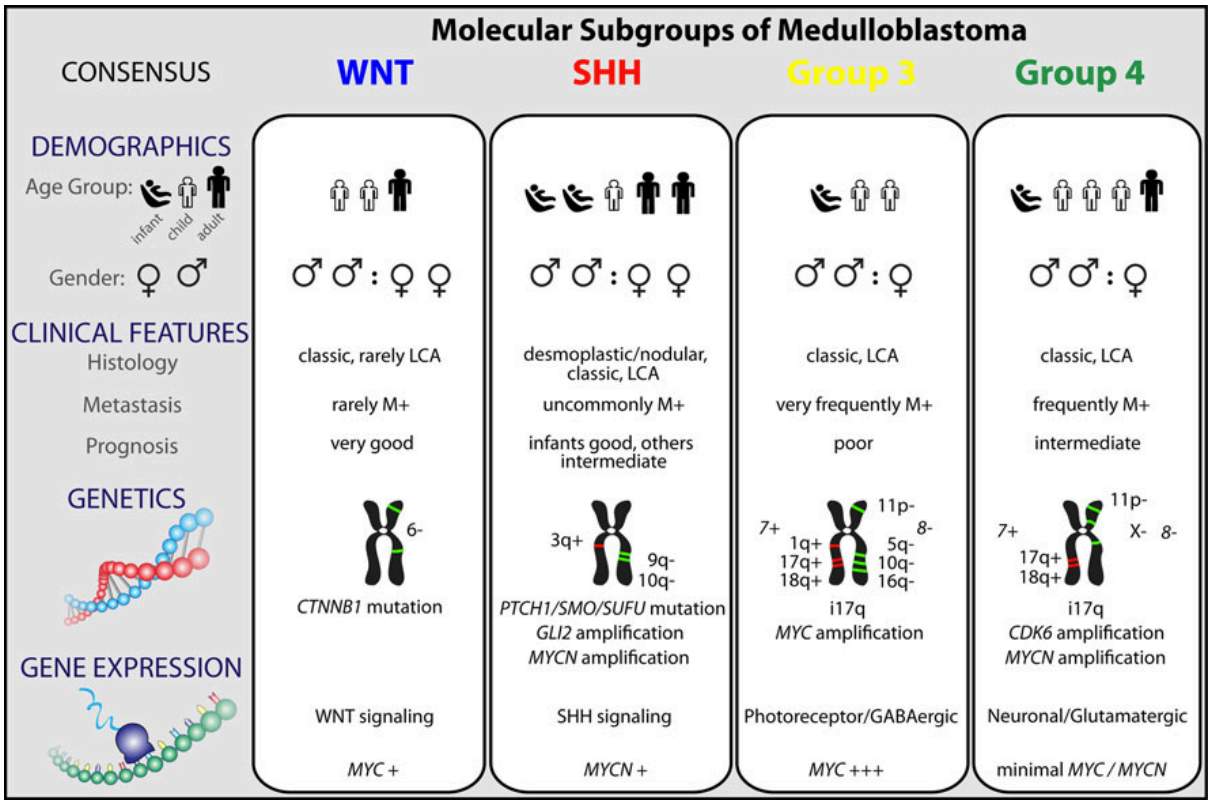

Figure 2.1: An overview of the clincopathological associations of MB molecular subtypes adapted (Taylor et al., 2012)

Table 2.1: Medulloblastoma can be divided into 4 categories namely the WNT, SHH, Group 3 and Group 4. The table summarises their reported association with prognosis, mutation and suggested molecular markers.

Category	**Prognosis** (Ellison et al., 2011)	**Mutations** (Kagawa et al., 2006)	**Histology** (Louis et al., 2016)	**Molecular Markers** (Northcott, Korshunov, et al., 2011)
WNT	Very good	APC (Turcot syndrome), CTNNB1, Monosomy 6	Classic, Rarely LCA	Beta-catenin, DKK1 positive High MYC
SHH	Good/Poor	PTCH (Gorlin syndrome), SUFU, Del 9q, TP53 (high risk group)	All	SFRP positive High MYCN
Group 3	Very Poor	Maybe gain 1q, del 5q, 10q	Classic Rarely LCA	NPR3 positive High MYC
Group 4	Good/Poor	Iso 17q, loss of X in females	Classic LCA	KCNA1 positive Low MYC and MYCN Few high MYCN

2.8 Methods of subtyping

Although to date there is an acceptable consensus on the clinical utility of MB molecular subtypes, as incorporated in the WHO definition of MB, there is no standardised methodology of determining MB subtype. Several techniques have been reported with varying accuracies and accessibilities (Table 2.2). Furthermore, the utility of some of these techniques depend on several factors, such as poor RNA stability associated with routine histopathological tissue processing.

2.9 Recurrence

MB histotypes frequently change at recurrence (Pöschl, Koch, & Schüller, 2015). Interestingly, the molecular subtype have been suggested to be stable upon recurrence (X. Wang et al., 2015). Recurrences are treated based on the initial treatment. If radiotherapy was delayed, it may be considered as a treatment option for the recurrence, localised radiotherapy if the recurrence is non-disseminated. In children who have been treated with both chemo- and radiotherapy initially; re-surgical resection, chemotherapy with different drugs and/or radiotherapy boosts may be considered as treatment options. In some centres of excellence there is also the option for recurrent patients to enrol in ongoing clinical trials if eligible (Gottardo et al., 2014).

Table 2.2: Methods of MB subtyping employed in other cohorts

Analyte	Method	Description	Reference
Gene expression	RT-PCR, ddPCR, GeXP, Nanostring RNA profiling, gene expression microarray, RNA-sequencing	RNA based expression is subgroup specific, however this is susceptible to RNA degradation processes	(Northcott, Korshunov, et al., 2011)
Genomics	Whole genome sequencing, single nucleotide polymorphism arrays, PCR, sequencing, FISH	Copy number aberrations, single nucleotide polymorphisms display subgroup specific associations	(Northcott et al., 2012)
miRNA expression profiling	RT-PCR, RNA-sequencing	A combined miRNA and protein coding gene based panel to accurately determine MB subtype, susceptible to RNA degradation processes	(T. Gupta et al., 2013)
Protein expression	Immunohistochemistry	Panel of antibody based technology easily accessible in histopathology labs	(Northcott, Korshunov, et al., 2011)
Epigenetic profiling	Epigenetic microarray (Illumina 450k), Sequenom (Mass spectrometry based)	Methylation profiling of bisulphite converted DNA, MB displays distinct subgroup specific epigenetic patterns	(Edward C Schwalbe et al., 2015)
Metabolite profiling	MRI based spectroscopy	5 metabolite based classifier used to determine Group3/4 and SHH types fairly accurately	(Blüml et al., 2015)
Imaging characteristics	MRI based imaging	MRI location and enhancement patterns has been reported to act as surrogate markers for MB subtypes, less sensitive	(Perreault et al., 2014)

2.10 Genomic landscape of medulloblastoma

There are many somatic copy number aberrations that have been reported which are subtype specific; these are speculated to be either disease drivers or as a result of the pathogenesis. Some of the most common include NMYC gene duplication, MSH2, EGFR, AKT3 gene duplications, chromosomes 7q/17q gain, 1p, 8, 10, 11p, 13q, 16q, 17p and X minor losses (Kagawa et al., 2006). There are also reports of activation of kinase associated pathways such as pERK and pAKT signalling pathways in MB that are linked to cell cycle progression and apoptosis protection (Włodarski, Grajkowska, Łojek, Rainko, & Jóźwiak, 2006). The most common biomarkers and mutations linked to subtypes are reviewed elsewhere (Figure 2.2) (Gajjar et al., 2015).

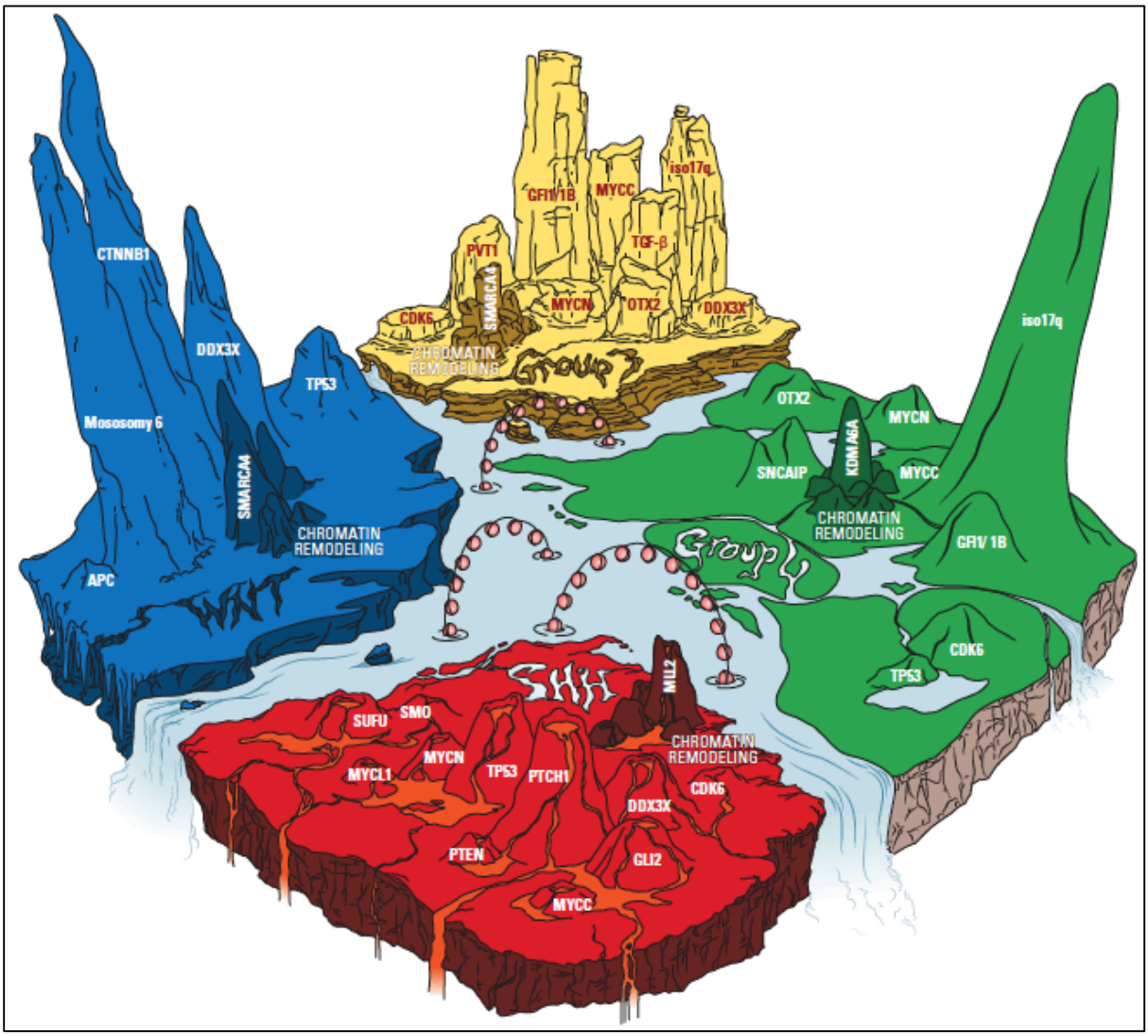

Figure 2.2: A cartoon schematic representation of the overview of the genetic landscape of MB with genomic and epigenetic components (Gajjar et al., 2015)

2.11 β-catenin, NMYC and CMYC associations with MB

β-catenin has been reported to be associated to the less aggressive WNT subtype with extensive nuclear staining, but there is a subset of focal nuclear staining that is associated with a poor outcome (Fattet et al., 2010) (Table 2.3).

Amplifications of NMYC and CMYC have been reported to be linked with large cell/ anaplastic histotypes and a poorer survival (Pfister, Remke, et al., 2009) (Table 2.3). NMYC has been reported in many subtypes including SHH and Group 4, while CMYC only almost

exclusively in Group 3 subtypes (Northcott, Korshunov, et al., 2011). The association with poor prognosis has resulted in its use in stratification for entry into certain clinical trials (Korshunov et al., 2012).

Table 2.3: β-catenin, NMYC and CMYC clinical and molecular associations

Biomarker	Technique	Finding	Detail	Linked with	Reference
β-catenin	Immunostaining with β-catenin antibody	Extensive nuclear staining	>50%	Chr 6 loss	(Fattet et al., 2010)
		Focal nuclear staining	<10%	Disease severity Deaths of all within 36months	
β-catenin	Mutation screening	G34R, S33F, I35K, D32Y		Classic histology, average risk,	
		WT		Metastasis seen	
C-MYC	FISH	Amplification in 5-10% of cases		Aggressive neoplasms within 7 months cases	(Aldosari et al., 2002; Pfister, Remke, et al., 2009)
N-MYC	FISH, array based CGH	Amplification in 5-10% of cases		Poor outcome	
C-MYC and N-MYC	Array based CGH	Both		Shortened survival	

2.12 Review of MB molecular subtypes

2.12.1 WNT subtype

This subtype occurs at the lowest frequency of all subtypes at about 10%, it has a predisposition in older children and it is also associated with the best outcomes (Kool et al., 2012). These tumours are most often associated with the classic histotype and are rarely LCA (Table 2.1) (Kool et al., 2008; M. C. Thompson et al., 2006). WNT cells of origin is suggested to originate from the dorsal brain stem and rhombomeres (Gibson et al., 2010).

Activating mutations in CTNNB1 have been reported to be associated with WNT subtypes (Kool et al., 2008; M. C. Thompson et al., 2006). Nuclear positivity for beta catenin tends to yield better survival (Ellison et al., 2005).

2.12.2 SHH subtype

These tend to arise in young children <3years old, have large cell anaplastic or desmoplastic histology, and usually have a poor prognosis (Kool et al., 2008; M. C. Thompson et al., 2006). They occur in approximately 30% in international cohorts. There exists within the SHH group a rare subset of tumours carrying TP53 mutations that confers a poor outcome. The WHO recommends classification of the latter subgroup as TP53 mutant with high risk and TP53 wild-type with standard risk (Louis et al., 2016). SHH has been shown to trigger epigenetic alterations such as cooperation with the Gli factors to induce changes in SHH target genes (Shi et al., 2014). Links to the GPCRs to MB have been suggested with recent research highlighting the GαS subunit when ablated can give rise to SHH-driven MB as shown in mice models (X. He et al., 2014). The origin of SHH tumour cells is believed to be derived from the cerebellum (Gibson et al., 2010). SHH MB is often characterised by mutations in PTCH1 (M. C. Thompson et al., 2006).

Furthermore, it has also been shown that cerebellar granule neuron precursors cells of origin can form MB SHH type tumours (Schu et al., 2008). It has also been reported that after stem cells have committed to neural development, subsequent activation of SHH pathway can lead to tumour formation (Z. Yang et al., 2008).

2.12.3 Group 3 subtype

These occur at approximately 25% of MBs and are predominant in younger patients, more often in males, and are more likely to present with metastases at diagnosis (Gerber et al., 2014). There is a reported incidence of 35-40% of metastatic disease in this subtype. A mechanism of gene upregulation has been observed in a subset of Group 3 and Group 4 MBs. This involves the target genes hinging onto other enhancer elements proximal or distant loci and appropriating physiologically active gene signatures (enhancer hijacking mechanism) (Erkek et al., 2014).

2.12.4 Group 4 subtype

These are one of the most prevalent occurring at approximately 35% of all MB. These have an intermediate prognosis, with a predominance in males appearing three times as often as females (Gajjar & Robinson, 2014). There is a reported incidence of 35-40% of metastatic disease in this subtype (Gajjar & Robinson, 2014). This group of tumours are associated with the worst outcomes and therefore are the target of many preclinical research aims and clinical trials. BET bromodomain inhibitors which interrupt MYC transcriptional activity are promising candidates for clinical research into MYC amplified MB (Bandopadhayay et al., 2015).

2.13 MB Laboratory models

It has been shown that there are some marked differences in primary cells compared to some MB cell lines and can be seen at the genomic level (C. Y. Lin et al., 2016). MB tumours have been reported to contain neural stem-like cells that are hypothesised to be the cause of tumour hyper-proliferation and origin (Hemmati et al., 2003). Primary MB has been reported to be stem-like, self-renewing, can propagate in culture forming neurospheres and can propagate and migrate in mouse xenograft models for several weeks (Hemmati et al., 2003). The lack of consistent and accurate models of MB subtypes lead to the importance of clinical and translational research to further understand MB pathogenesis.

2.14 Investigational treatments

Some subtypes present with poor outcomes and recurrence, and many patients experience adverse effects due to aggressive treatment strategies. There is recent interest in more targeted therapy strategies, possibly with the subtype guiding treatment in the future (Cloughesy, Cavenee, & Mischel, 2014). An example of this is the possible treatment de-escalation in WNT subtypes; these subtypes have the best prognosis and therefore are candidates to be spared the adverse effects of aggressive treatment. Furthermore, there is also interest in alternate drug delivery routes of administration, as CNS tumours are in a protected anatomic compartment shielded by the blood-brain-barrier, providing a significant pharmacokinetic challenge (Guerit & Liebner, 2016). Treatments by direct administration of chemotherapeutic drugs by the intrathecal route of administration, in the lumbar fluid, or the intraventricular route, in ventricular fluid, and by implanted ventricular Ommaya reservoirs, are also being investigated (Gerber et al., 2014).

2.15 MB molecular biology and issues facing developing nations such as South Africa

There are few resources available to subtype tumours in the developing world. There does exist some easily implemented diagnostic assays for the attempted histopathological assessment of subtype, therefore, a simplified lower cost approach has been suggested, classifying MB into just 3 groups, WNT, SHH and the Non-WNT/SHH group which would include both Group 3 and Group 4 (Kaur, Kakkar, Kumar, Mallick, & Julka, 2016). This is due to the lower cost of assigning WNT and SHH and the non-WNT/SHH group using a fewer costly antibodies, reagents and other costs associated with standard IHC some of which are already accessible in lower resource settings. Other diagnostic methods can be more time consuming, costly or require specialised equipment/personnel that are not accessible in resource-limited settings.

3. Chapter 3 – Juvenile Pilocytic astrocytoma (JPA)

3.1 Introduction

JPAs are the most common glial cell tumour type found in children and can occur at any age. They can occur anywhere in the CNS however; they are more likely to occur in the cerebellum, the optic pathways, hypothalamus or brainstem. They occur with regional variances in incidences and histotypes (Rodriguez, Lim, Bowers, & Eberhart, 2013) (Table 3.1). Pilocytic is used to describe the histopathological phenomenon of "hair-like with bipolar processes" (Collins, Jones, & Giannini, 2015). JPAs are low grade gliomas that are benign, slow growing, typically WHO grade I tumours (Louis et al., 2007). JPAs are a predominantly single pathway disease, with genetic abnormalities found presenting largely with the MAPK pathway (Jones et al., 2013).

3.2 JPA molecular biology

Mutations or gene fusions in this growth promoting ERK-MAPK pathway have been associated with JPAs. These include the KIAA1549-BRAF, the FAM131B fusions and the ARAF fusions (Y.-H. Chen & Gutmann, 2014; Chiang & Ellison, 2017). All these result in the loss of the auto inhibitory signal in RAF which leads to constitutive kinase activity (Forshew et al., 2009). There are sporadic JPA types associated with KIAA1549-BRAF fusion and these are likely to arise in cerebellar regions. The BRAF V600E point mutation has been reported in about 10% of cases of JPA (Schindler et al., 2011). There is also an association to the extra-cerebellar region of occurrence. BRAF V600E has been reported to occur in mostly Grade II-IV astrocytomas and not so common in Grade I JPAs (Schiffman et al., 2010). Additionally, there are also the NF1 associated types that are more likely to arise in the optic pathway and brainstem (Louis et al., 2007). Given the molecular associations to specific brain regions, studies on JPA should take note of the brain region in their JPA molecular analyses.

3.3 Histological profile of JPAs

Pilocytic astrocytoma is characterised by compacted bipolar cells and microcysts with loose texture, eosinophilic staining bodies of Rosenthal fibres and mitotic features only present in a small proportion of these tumours (Rodriguez et al., 2013). Macroscopically astrocytomas are often cystic. Microscopically, appear as bipolar cells with hair-like processes. May contain Rosenthal fibres that are corkscrew shaped eosinophilic fibre bundles. Piloid areas are GFAP positive while spongy areas are GFAP weakly positive that are associated with microcysts (Becker, Scapulatempo-neto, Neder, Chimelli, & Reis, 2013).

3.4 JPA treatment

Since JPA is a low grade tumour, treatment is first decided by observation in order to monitor progression due to reports of spontaneous regressions in this grade of glioma (Schmandt, Packer, Gilbert, & Jane, 2000). Treatment often starts with surgical resection dependent on location with gross total resection aimed for as the primary treatment. However, in the case of diffuse JPA or optic nerve and hypothalamus tumour involvement, extensive surgical resection carries a high risk of neurological sequelae. In these cases only biopsy is considered (Mamelak, Prados, Obana, Cogen, & Edwards, 1994). Symptomatic relief of hydrocephalus is often surgically achieved using ventricular shunt for CSF diversion. In addition, follow up imaging is undertaken to monitor recurrences.

Chemo- and radio-therapy is often only administered in select cases of JPAs, these are in the case of residual tumour or evidence of recurrence. In the case of non-surgically resectable tumours, chemotherapy is often employed involving carboplatin and vincristine or a combination thereof (“Childhood Astrocytomas Treatment,” 2015). In the case of recurrence, a second surgery is likely performed followed by chemotherapy.

3.5 Future treatments

There is a need for new treatment for surgically inaccessible JPA, since current chemotherapies are largely cytotoxic leading to neurological and neurodevelopmental deficits (Qaddoumi, Sultan, & Broniscer, 2016). There are several promising drugs e.g. immunomodulatory lenalidomide, BRAF and AKT inhibitors of the MAPK pathway in

clinical trials for recurrent JPAs as well as other gliomas (Qaddoumi et al., 2016; Warren et al., 2011).

3.6 JPA mouse models

There are several types of laboratory models for astrocytomas, these include established cell lines from human and mice however there are limitations to these models and these are becoming more evident from genomics data which suggest there are some genetic drift effects resulting in the culture model not fully resembling the primary tumour (Mcneill, Vitucci, Wu, & Miller, 2015). An advance to the technology is the development of patient derived xenograft models, which are derived from patient tumours and implanted into immune, compromised mice and can be propagated in laboratory culture for orthotopic transplantation in mice. Engineered human cell models are another variant of laboratory model, where defined genomic alterations are created in normal brain or glial cells resulting in controlled genetic abnormalities in cells that can then be implanted into mice for propagation.

While these laboratory models exist, they have limitations of being expensive, and not timeous due to multiple successive breeding. Of note, all these models are almost exclusively relevant for high grade gliomas, the low grade gliomas such as the JPAs are difficult to model in *in vitro* culture or *in vivo* mouse models (Klose et al., 2002). There is a lack of reliable lab models for JPAs and even characteristic features such as IDH status in models are not robust as yet. Therefore, in trying to understand the biology of JPA, tumours directly from patients are a crucial resource. While these tumours are variable they do represent the JPA in the context of extracellular microenvironment and are a largely valuable resource. However, these samples are rare and restricted to neurosurgical centres often in dedicated paediatric facilities. If accessible and consented, these will allow accurate and reflective insights into JPA pathogenesis and understandings into the elements that drive its non-malignancy.

3.7 Clinical presentation

The majority of JPA are cerebellar with a smaller proportion being non-cerebellar. Clinical symptoms depend on the location of the tumour and often include headache, neck pain and common symptoms of cerebellar involvement as mentioned previously. In non-cerebellar JPA, those that are tentorial and associated with cortical regions often lead to symptoms of seizures. If there is hypothalamic involvement, symptoms include growth abnormalities, obesity and diabetes insipidus and optic nerve impairments (Becker et al., 2013). JPAs patients are more likely to have a relative who presented with childhood seizures (Kuijten et al., 1993). However, it has been reported that there is no significant relationship of childhood cancers (PNETs and astrogliomas) in family members even when controlling for known links of heredity cancers such as NF1 (Searles et al., 2008). JPA imaging often shows these tumours appearing well circumscribed, non infiltrative and cystic in nature, they are rarely associated with leptomeningial spread (Collins et al., 2015).

3.8 Conclusions

JPAs are low-grade tumours that are usually responsive to treatment. Treatment usually only involves surgical resection and a “watch and wait” approach. In many instances treatment is patient specific and is determined by operability, age of patient and site of tumour. Due to toxicities associated with chemo- and radiotherapy its utility in treating low-grade tumours, some of which may reside spontaneously, is limited. In developing countries such as South Africa these treatment related decisions are taken with additional factors such as regular assess to treatment centres for rounds of chemotherapy. Low-grade malignancies in these settings often go misdiagnosed as patients usually present at a late stage and have symptoms for a prolonged time interval. This late patient presentation might result in low-grade tumours acquiring additional cancer progressing factors and possible transformation into high-grade tumours. Often most confounding factors are patients co-presenting with infectious disease and incidental findings of JPA. Additionally, JPA patients in this context have limited representation in international clinical trials. Inclusion in these trials provides clinical testing of novel therapies in a diverse genetic background that if effective has wide applicability.

Building up the molecular knowledgebase of JPAs in South African context aids in this effort, as it builds on our current understanding of molecular information from international cohorts and adds or validate findings across a wide genetic background. The studies presented in this work aims to deduce this information in a South African context.

Section B – Study outline

4. Chapter 4 Hypothesis and aims

4.1 Background

The molecular biology knowledgebase of brain tumours in children has been rapidly increasing in the past decades. The accessibility of such resources is limited in developing nations such as in South Africa. Moreover, the disease is more common than most people realise, it is the second commonest malignancy in children worldwide. There are currently no reliable datasets of brain tumours in children in South Africa. We have no data on the presentation of disease, the spectrum of tumours treated, how these are treated, what the outcomes are and biochemical presentation. This data is urgently needed. Absence of this data restricts our understanding of the burden of brain tumours in South African children. It further restricts our knowledge of how our outcomes compare with international standards and what needs to be addressed. Eventually this knowledge will allow our involvement in international trials of novel therapies and protocols of treatment. In general, the recognition of molecular characterisation of childhood brain cancers has been lacking in South Africa as well as in Africa.

Increasingly, molecular studies are revealing important aspects of childhood brain tumours that may revolutionise treatment in the future. MB is the leading cause of death in children with brain tumours that can now be classified into 4 main subgroups. These MB classifications have a specific prognosis that opens the way for an exciting era of development of subgroup specific targeted treatments. It is expected that identification of these subtypes will be required for entry into clinical trials and will eventually guide targeted therapeutic decisions in the future.

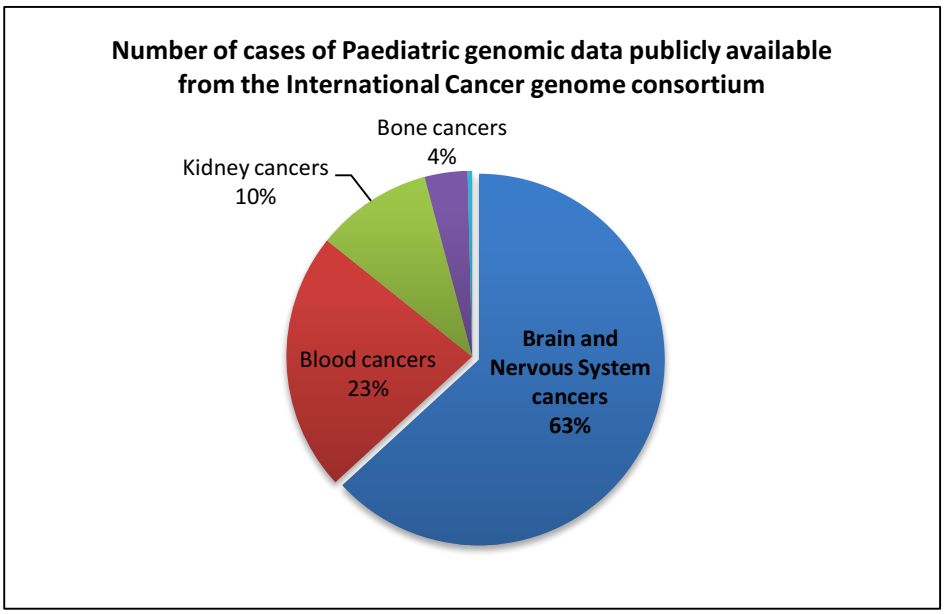

Figure 4.1: Genomic data for paediatric cancer by number of cases represented in international repository genomic data ("NCI, GDC Data portal," 2016).

There is a vast collection of genomic data for paediatric cancers available in repositories worldwide. The representation of brain and nervous system cancers forms the majority of this data (Figure 4.1). Much of this data stems from large multinational projects utilising array based and next generation sequencing technologies ("NCI, GDC Data portal," 2016). In stark contrast to this, validation of this data is primarily limited to low to medium throughout orthogonal techniques such as cell and animal based gene mutagenesis, knock-in, knock-downs and antibody based methods of validation assays. Analysis of the brain proteome has been limited in the context of brain tumour studies, and represent the minority of cases in publically available proteomics repositories (Martens et al., 2006). The utility of mass spectrometry based proteomics technology in clinical and translational research is recognised as a robust technology in biomarker discovery, validation and taking unbiased global snapshot of the proteomic state in disease presentation. The current technology has become increasingly reproducible when applied to clinical samples that are commonly preserved as formalin-fixed paraffin embedded (FFPE) tissue blocks. Furthermore, the usefulness of FFPE blocks for certain gene profiling and

next generation “omics” technologies is becoming increasingly promising due to newer nucleic acid and protein restoration protocols.

4.2 Formalin-fixed and paraffin embedded (FFPE) preserved tissue specimens

These are tissue specimens obtained from clinical samples from surgical biopsy or sampled from surgical resections. Such specimens are subject to chemical cross-linking or fixation commonly using formaldehyde, the more stable paraformaldehyde, or other crosslinking agents (Srinivasan & Sedmak, 2002). FFPE tissue blocks are routinely used worldwide to analyse cellular and tissue architecture involving chemical or antibody based staining, FFPE allows for good structural preservation and storage at room temperature for prolonged periods. While FFPE preservation is suited to structural observations the utility of FFPE preservation for biomolecular preservation is less fitting. FFPE blocks are suited for thin sectioning and mounting on glass slides for observation under light or fluorescence microscopy. This process of FFPE block embedding involves several rounds of fixation, dehydration by solvent exchange and casting in paraffin wax. To allow for chemical or antibody based staining and for biomolecule isolation from FFPE blocks, further processing involving removing of the paraffin wax and rehydrating back to aqueous solvents are required. All this processing, as well as the time held in storage, causes chemical changes on biomolecules. Some of these include hydrolysis, methylol and crosslinked methylene bridges in nucleic acids, and in proteins a much more complex array of chemical modifications result, mostly involving basic amino acids (Magdeldin & Yamamoto, 2012; Srinivasan & Sedmak, 2002). There has been much progress in adequately isolating the biomolecules from FFPE blocks and they are sufficient for modern molecular biology uses (April et al., 2009; Magdeldin & Yamamoto, 2012). Furthermore, the ability to isolate and analyse both nucleic acids and proteins from FFPE blocks provides a more comprehensive snapshot of the molecular state of the samples. Taking this multi biomolecular approach illuminates more of the complex processes occurring within cells and tissues, providing information on cellular dysregulation and anomalies associated with cancer processes. Findings of such

irregularities provide useful targets for therapeutic strategies or for more accurate prognosis. Furthermore, the age of the tissue blocks have been suggested to be considerably much less detrimental compared to fixation time and blocks surviving 30 years usually leads to a similar number of protein identifications compared to younger FFPE blocks (Tanca, Pagnozzi, & Addis, 2012). This suggests that in the study design, older FFPE blocks are suitable for inclusion into the study design without any significant storage age related bias as all FFPE blocks were processed according to the same fixation time.

In aiming to determine molecular profiles of brain tumours in a previously under-investigated disease in developing world countries such as South Africa, the use of retrospective FFPE blocks is a rich source of clinical samples. Furthermore, the utility of retrospective cohorts provides the much-needed patient outcome information that can be used to identify outcome-related molecular markers and use this as a predictor in other cohorts for validation.

4.3 Overall Aims

This study has the overall aim to analyse paediatric MB and JPA samples by taking a combined nucleic acid and proteomic approach. This study takes a systematic approach to generate molecular profiles of MB and JPA. Firstly, MB and JPA are characterised in terms of demographics, histology and investigated using specific molecular markers previously identified in other international cohorts. The markers are investigated for their association with demographics, clinical presentation and prognosis.

The aims of this research would focus on the characterisation of a South African MB cohort. This South African MB cohort is compared to international cohort standards by their representation of the 4 subgroups by using both Nanostring RNA technology and a panel of immunohistochemistry markers. Furthermore, those same samples would be analysed by using a quantitative MS based proteomic approach. The approach of this research would be as follows: initial determination of subgroup

specific proteomic markers using supervised grouping by Nanostring and IHC as a classifier; and secondly, to identify proteomic markers of poor outcome within the MB cohort. The specimens used in this research are paediatric brain tumours from a retrospective cohort curated over the past 20 years at the Red Cross Memorial Children's Hospital (RCCH). The results of the proteomic work were further validated using a targeted proteomic approach on an additional smaller cohort of samples collected prospectively.

JPA samples are divided into a retrospective cohort and a prospective validation cohort. JPA samples are clinically classified into tumours in the cerebellar region, and tumours in non-cerebellar regions. These samples are characterised by histology, phosphorylated-ERK (pERK) and p16 activation by IHC. Furthermore, proteomic profiles are determined to investigate, firstly, proteins that are specifically associated with cerebellar JPA versus non-cerebellar JPA tumours. Secondly, to identify malignancy associated proteins in comparing the malignant MB to the generally less aggressive JPA. Similarly, these findings were validated using a targeted proteomic approach in the prospective cohort.

5. Chapter 5 – Cohort study design

5.1 Study design overview

As an overview of the study design used in this research; the aims of the current investigation are structured into 4 studies. Study 1 and 2 characterise the demographics and molecular profiles of the MB and JPA clinical cohorts. Study 3 and 4 undertake to determine and validate proteomic profiles of MB and JPA with specific sub-aims (Figure 5a). The study designs were conceptualised by creating appropriate cohorts and estimating the sample characteristics and sample size required to achieve adequate statistical power and to aid in interpretation of the results.

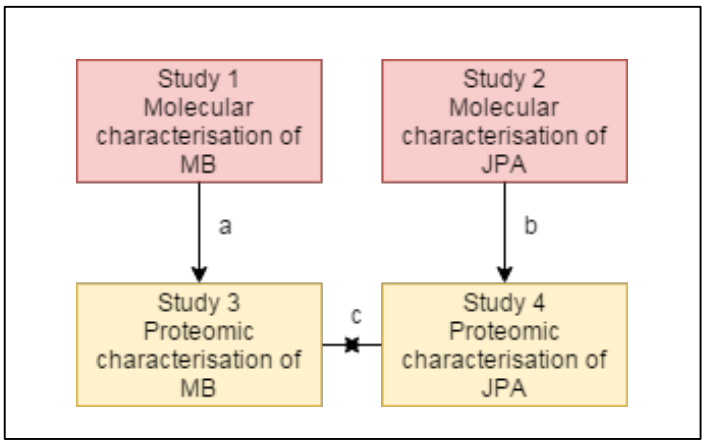

Figure 5a: Schematic overview of the study design used in this investigation

a,b – molecular, subtype and clinical characterisation data used to aid in interpretation of proteomic results, c – Proteomic comparison between two brain tumour types for malignancy associations

5.1.1 Study design

As outlined in the aims section in the previous chapter, this study focuses on MB and JPA molecular characterisation and their association with clinical variables. For both cohorts, clinical data were collected from patient records. Demographic data such as age, sex, together with outcome data was collected. Additionally, histotype data was collected with the physical tissue blocks and the age of the tissue blocks. Furthermore,

all evaluated samples were from treatment naïve patients, as prior treatment with either chemotherapy or radiotherapy might alter the gene expression or proteomic profile of the samples.

Study 1 investigates the molecular profile of MB and uses two techniques for prediction of MB subtype. The appropriateness and description of the techniques are highlighted in the previous chapter. The cohort used in this study is a retrospective cohort of 48 children between 1988 and 2014 with a histological diagnosis of MB. These are patients who have had a tumour resection and available biopsy sample preserved as FFPE. Our aim was to subtype these tumours according to recent descriptions of 4 molecular subgroups of medulloblastoma (Figure 5.1A). While this is not designed as a population study, it is a first description of MB molecular subtypes in the diverse South African genetic background. We investigate several molecular variables such as a panel of 6 IHC markers, a panel of 24 RNA markers, and 1 FISH marker. This study then correlates the molecular markers to clinical variables such as age, gender, disease progression and mortality.

Study 2 investigates the molecular characteristics in a retrospective cohort in children with a histological diagnosis of JPA. This study characterises these JPAs based on the molecular expression of p-ERK and p16 IHC markers (Figure 5.1B). The molecular markers are then correlated to clinical variables as for the MB in study 1.

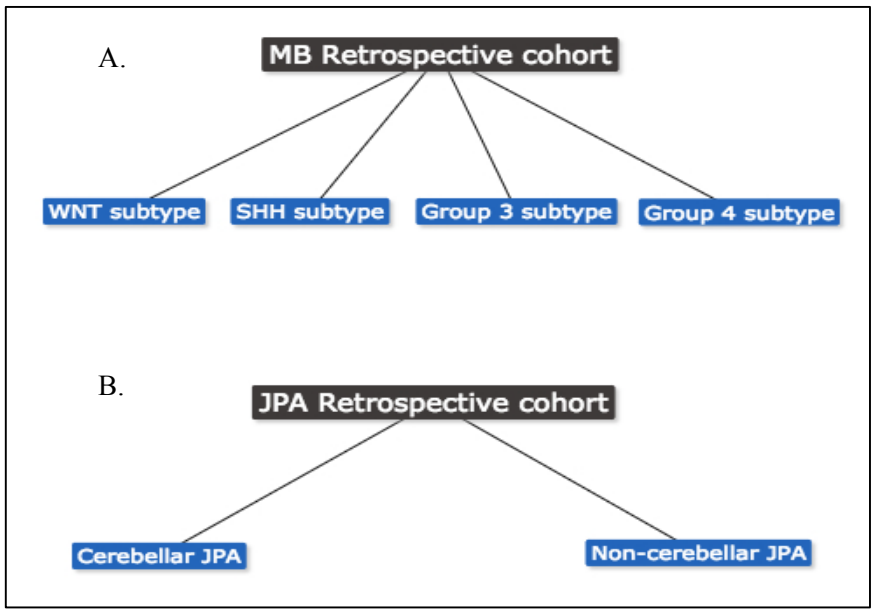

Figure 5.1: Retrospective cohorts used in Study 1 and Study 2 used in MB and JPA molecular characterisation

A – MB cohort description and the subcategories that it contains. B – JPA cohort description and the categories that make up this cohort.

Additionally, the proteomic investigations are designed to address the aims of the proteomic profiles as outlined in the previous chapter. Study 3 and Study 4 are discovery-based proteomic experiments that generate proteomic profiles in MB and JPA retrospective cohorts respectively. The protein markers are then correlated to both molecular variables and to clinical variables such as prognosis or relapse. Furthermore, study 3 and study 4 make use of an orthogonal prospective cohort for validation of those findings (Figure 5.2). The prospective cohort includes both MB and JPA tumours and all their subgroupings, where JPA tumours serve as the negative controls for the MB proteins of interest and vice versa. This type of study is more complex than a simple case-control design utilised in many routine proteomics experiments. The validation approach necessitated here is as a result of insufficient access to healthy brain controls. There are ethical limitations to accessing healthy brain tissue during a biopsy for brain tumour resection. Methodologies such as laser capture micro-dissection are used to isolate histologically healthy looking cells from

the same biopsy but are limited in their utility as many tumours contain histologically appearing cells that are being might be in an altered molecular state due to stressors induced by the tumour or bear genetic or epigenetic accumulations (Martirosian, Chen, Lin, & Neman, 2016).

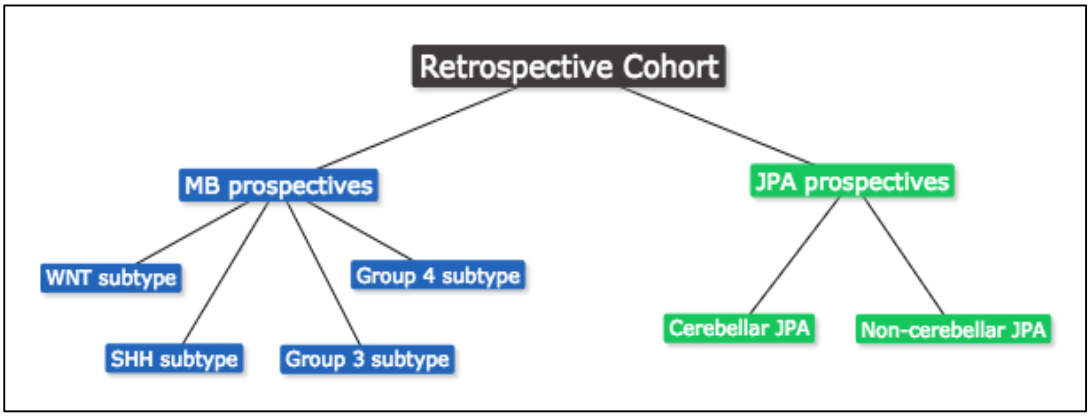

Figure 5.2: Graphical description of the retrospective cohort used in this study

Study 3 investigated proteomic profiles of tumours, the utility of single sample runs, and the methodology was tested against a more complex and extensive fractionation run. The power of the proteomic study has to be interpreted taking the level of coverage into account, similar to genomic studies where genome coverage is considered. Study 3A involves proteomic profiles investigated using subgroup classifications gained from Study 1 for MB. The MB retrospective cohort is analysed and those samples that met the proteomic inclusion criteria were used for subgroup specific protein enrichment. These findings were thereafter tested in the prospective cohort. The prospective cohort was characterised using a panel of IHC markers as in Study 1 to assign MB subgroups. The proteomic findings were then structured in targeted assays across the entire prospective cohort, using the JPA samples as negative controls. Study 3B investigated MB tumours and the proteomic links to clinical variables such as prognosis and disease progression. These were validated against the prospective cohort with the latest follow up data.

Study 4A was similar to Study 3A, but using the JPA retrospective cohort. The proteomic changes were investigated between cerebellar and non-cerebellar JPA samples. Study 4B investigated both cerebellar and non-cerebellar JPA proteomic links to outcome. Study 4C looked at JPA and MB specific proteome associations to identify malignancy and non-malignancy or lower grade malignancy protein groups.

5.2.1 Statistical power of characterisation studies 1 and 2

The characterisation studies namely Study 1 and 2 are targeted studies monitoring a small number of known biomarkers and clinical variables. The statistical tests used to determine significance in these studies were ANOVA with correction for multiple testing. While not designed as a population based epidemiological study the power estimated to be achieved by the experimental design can be determined using the measures of the characteristics of the data. Such characteristics include the number of comparison groups, number of measures, the variance or correlation of repeated measures and the error probabilities. By modelling these measures from low to mid throughout Nanostring transcription panels, IHC panels and FISH measures we can determine the appropriate sample size needed to achieve a statistically significant power in these studies. These measures were modelled *a priori* here and are revisited in later sections to validate the actual power achieved. The power achieved improves with increasing sample size and is proportional to the effect size (Figure 5.a). The effect size might be an important factor in taking biological meaning from low to mid-throughput data as it suggests any statistically significant comparisons where the means differ by less than 0.2 standard deviations then such differences are minor (Faul, Erdfelder, Lang, & Buchner, 2007).

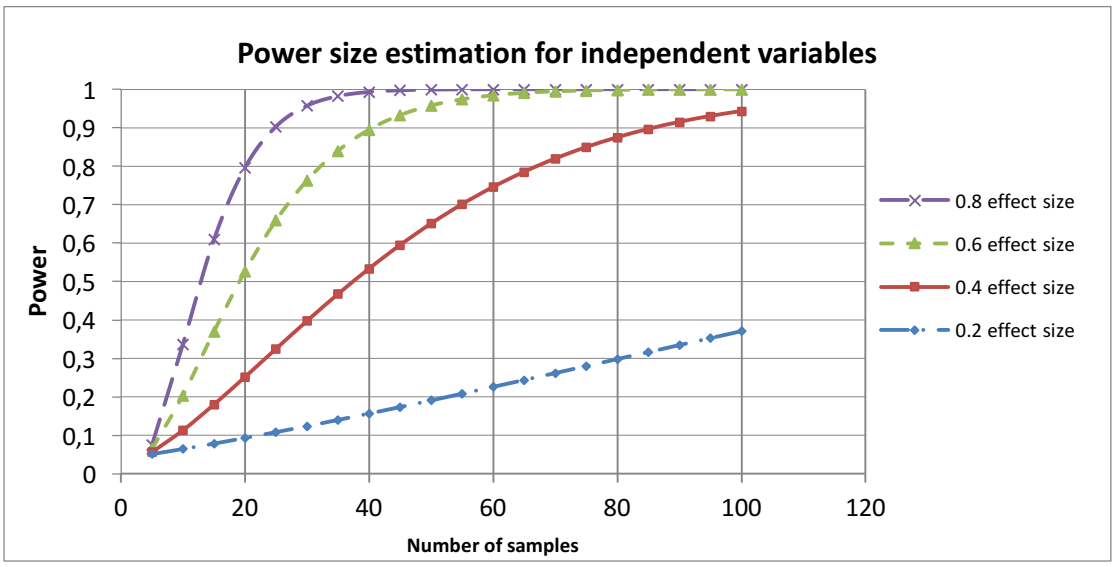

Figure 5.a: Modelling statistical power expected to be achieved by varying sample sizes using G*Power 3 software version 3.1.9.2 (2017) with the following parameters:

ANOVA test for multiple comparisons between factors, 4 groups, 5-25 measures each, 0.9 correlations with repeated measures and an α-error probability of 0.05.

The study design of Study 1 therefore has the expected power of 0.8-1 from a medium to high effect size difference between 48 patients spread over 4 MB subgroups with panels of 6 IHC, 1 FISH and 24 transcript panels of Nanostring characterisation and subsequent comparisons to clinical characteristics. The design of Study 2 had a smaller sample size and therefore has an expected power of 0.4-0.6 from comparisons between 2 groups of 14 patients, using a 2 panel IHC, 1-panel FISH measures and correlations to clinical characteristics.

5.2.1 Clinical proteomics study design and statistical power of studies 3 and 4

Clinical proteomic studies often start off with addressing a biological question, and then use an appropriate study design to sufficiently investigate that aim. Biological sampling, measurement, data process and analysis then follow to identify potential biomarkers. These possible markers have to be stringently and statistically validated prior to experimental validation in an orthogonal or independent clinical cohort (Smit, Hoefsloot, & Smilde, 2008)(Figure 5.3).

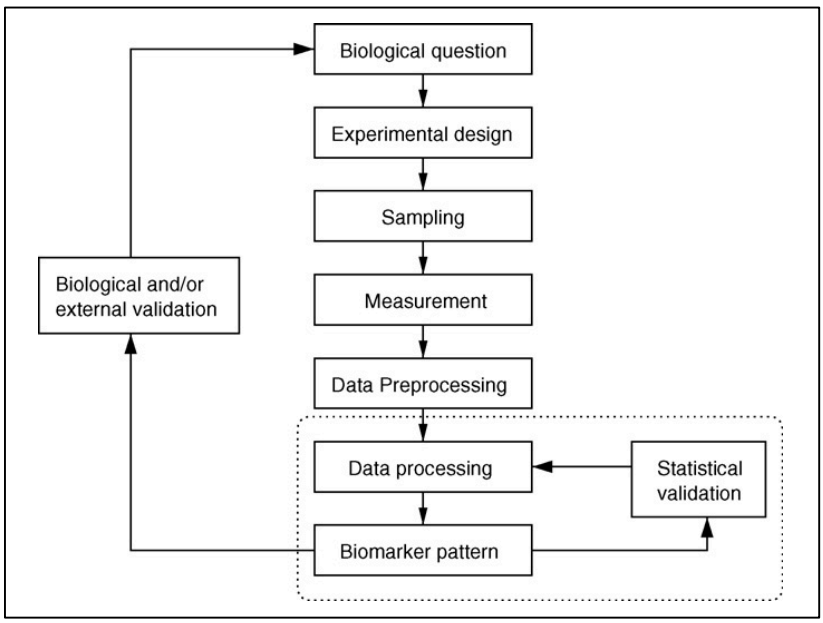

Figure 5.3: Proteomic biomarker discovery workflow from the biological question to the candidate biomarkers adapted (Smit et al., 2008)

Since proteomic studies are complex and the objectives are diverse, there is as yet no standardisation in estimating sample size in order to provide adequate statistical power. Furthermore, as high-resolution proteomics studies usually produce thousands of proteins and use limited numbers of samples, this leads to a large number of variables and a relatively small sample size causing high-dimensionality small-sample size issues. Two strategies are usually implemented to address this issue, firstly reducing the dimensionality and secondly to cross-validate the results in an orthogonal cohort (Smit et al., 2008). Therefore Study 3 and 4 presented here employs both strategies, the reduced dimensionality measure by single MS runs without extensive fractionations and cross-validation in the prospective cohort to identify subtype and clinically relevant MB and JPA biomarkers.

5.3 Power calculations and sample size determination

There are two main issues related to statistical power when applied to clinical proteomic experiments, these are the known effect size and the high multivariate nature of proteomic data (Smit et al., 2008). Sample size calculations are non-standardised in clinical proteomics experiments however they have been applied in orthogonal clinical study designs for microarray-based experiments. There are specific sources of variations for MS based proteomics such as protein extraction, digestion, fractionation, instrument variations and stability (Piehowski et al., 2013). Statistical power and sample size estimations can be achieved using microarray based equations, as power is determined in a global context and not specific to any particular 'omics' platform. Power in this context refers to the probability that the result if a false negative (Levin, 2011). Calculations suggest that given an expected fold change between the proteins, as well as the variations within the samples, simulated power curves can be generated to gauge the number of samples likely needed to gain statistical power.

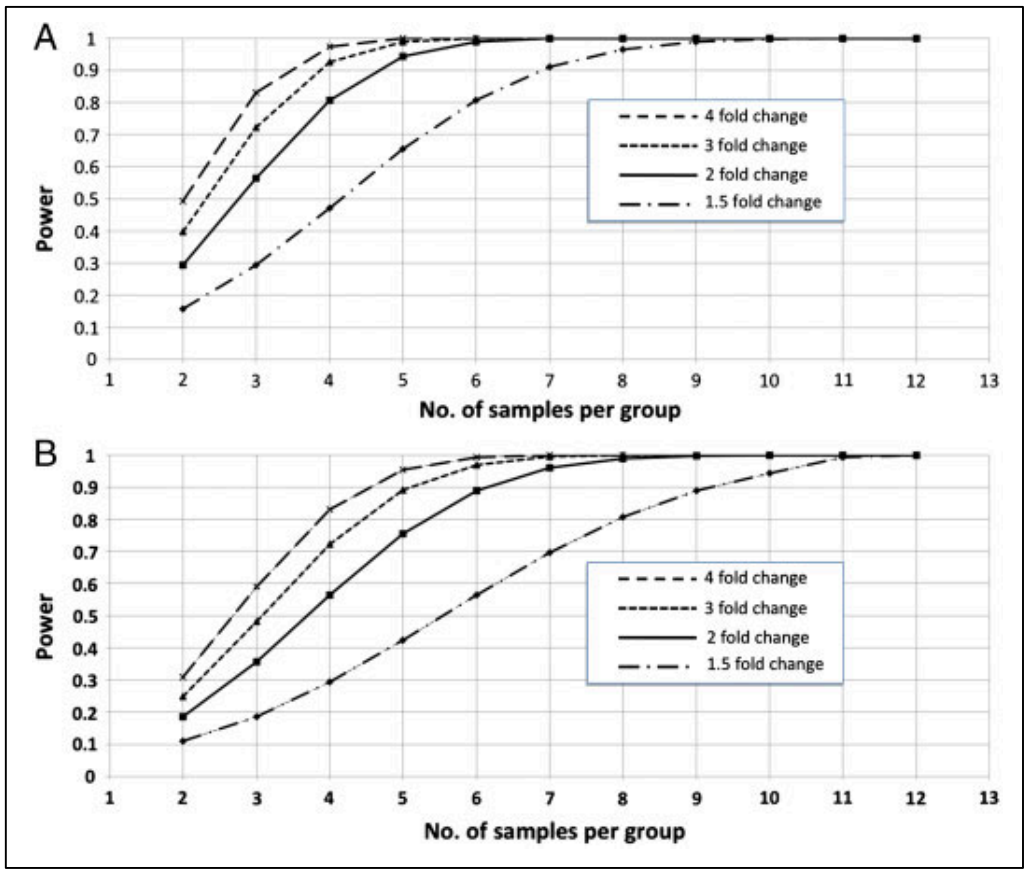

Figure 5.4: Power estimations against number of samples per group as adapted (Levin, 2011)

A – With a 20% variation, B – With a 40% variation

Previously published biological and technical total variations in similar proteomics study designs where in the range of 18-40% or greater (Levin, 2011). Therefore, estimating the variation from previously reported simulations is in that range, the number of samples in each group should be greater that 5 with a minimum of 2-fold difference for a power greater than 0.8 (Figure 5.4).

This formed the basis of sampling in this research, the statistical power is revisited later in interpreting the findings of this study and to determine the power achieved.

5.4 Study design conclusions

The study design in the current study aimed to appropriately use the methodology and clinical cohort to generate data to answer the biological questions as stated in each of the aims of the current research. The design is structured into 4 studies, namely, Studies 1 and 2 that characterised the demographics and molecular profiles of the MB and JPA clinical cohorts and Studies 3 and 4, which determined and validated proteomic profiles of MB and JPA. The statistical power achieved was conceptualised by modelling variances and effect sizes and thereby creating appropriate cohorts and estimating the sample characteristics and sample size required to achieve adequate statistical power and to aid in interpretation of the results and identify biomarkers of these diseases.

Section C – Molecular Characterisation of MB and JPA

6. Chapter 6 - Medulloblastoma molecular subtyping in cohort – Study 1

6.1 Introduction

Brain tumours have been classified for the past years based on their histological appearance, observing tissue morphology, structure, likely resemblance of cells of origin and levels of differentiation. The utility of tumour classification in modern times is useful in several aspects in oncology. Firstly, classifying tumours based on aggressiveness or metastatic status might be useful for treatment decisions, which might be useful in suggesting a conservative treatment regime for lower aggressive tumours and the converse for highly aggressive tumours. Secondly, classifying based on molecular phenotype is useful in guiding and developing targeted therapy that might be specific and highly effective only in certain subtypes based on rational therapeutic designs. Furthermore, it might play a role in understanding the variation in drug responses in similar kinds of tumours that are histologically alike. The later aids in the advancement of targeted treatments that advocates the "right drug for the right patient". Current clinical trials make use of histologically defined disease states, which can have negative effects such as skewing responses in cancers that have essentially molecularly distinct subtypes. A prime example of this is in the brain tumour field, particularly with the case of MB subtypes. MB is now widely recognised as containing at least 4 distinct molecular subtypes as mentioned previously. MB subtypes can indicate likelihood of favourable outcomes as is the case of WNT subgroup in MB (Ellison et al., 2011).

MB have been suggested to be the most common CNS neoplasm in childhood in some African countries such as Morocco and Nigeria (Idowu, Akang, & Malomo, 2007; Karkouri, Zafad, Khattab, & Benjaafar, 2010). One area in which South Africa specifically, and Africa more generally, have not kept pace with international trends has been the recognition of molecular characterisation of childhood brain cancers and its potential implications for treatment.

Increasingly, molecular studies are revealing important aspects of childhood brain tumours that may revolutionise treatment in the future. MB, can be histologically classified into histotypes displaying classic, desmoplastic/nodular, large cell/anaplastic and MB with extensive nodularity morphological characteristics (Louis et al., 2016). Moreover, there is now consensus that MB can be classified molecularly into 4 main subgroups each of which correlates with prognosis which opens the way for an exciting era of targeted treatment according to subtype (WNT, SHH, Group 3, and Group 4) (Northcott, Korshunov, et al., 2011)(Table 6.1). It is expected that identification of these subtypes will be required for entry into clinical trials and will eventually guide targeted therapeutic decisions in the future. The most recent WHO guidelines for CNS tumours recommend a marriage of the histological and molecular classification schemes for MB (Louis et al., 2016). There is also now wide accord on risk stratification involving molecular subtypes (Ramaswamy et al., 2016). Both histotype and molecular subtype information are becoming more clinically important and this emphasises the relevance of subtyping MBs in the modern molecular era.

Although, one of the challenges we face is that there is currently no reliable data on molecular characterisation of brain tumours in children in SA. We have no data on the genomic aberrations, the protein expression and what their association to outcomes are in this local context. Absence of this data restricts our understanding of the molecular profile of childhood brain tumours in South African children, our knowledge of how our outcomes compare with international standards. With this data and analysis thereof we will better be able to identify our local requirements and being to participate in international trials of novel therapies and protocols of treatment.

MBs are an ideal group to consider the recent advances in the understanding of tumour biology. Several molecular markers have been associated with outcome, including nuclear β-catenin, ERBB2, TP53, and TRKC positivity, as well as cytogenetic markers such as aberrations of chromosome 17, CTNNB mutation, and MYC family amplification (Northcott, Korshunov, et al., 2011).

The MYC family proteins have been described in genomic studies of MB, they appear to demonstrate different roles in the different MB subgroups (Northcott et al., 2012; Ramaswamy et al., 2016). The expression and amplification of MYC and MYCN in medulloblastoma have been evaluated extensively, as they have previously been associated with poor outcomes and highly aggressive tumours (Cho et al., 2011; Pfister, Remke, et al., 2009).

MYCN amplifications are seen to most commonly occur in the SHH subgroup, with a few occurring in Group 4 tumours, and rarely in Group 3 (Cho et al., 2011). Patients with MYCN amplification have a substantially worse prognosis than those without amplification (Korshunov et al., 2012). Bearing in mind the fairly specific finding of nodular desmoplastic histology in SHH tumours, the finding of these two features is fairly specific for this subgroup, and would allow the evaluation of outcomes in this subgroup that are generally regarded as having favourable outcomes. It is now being suggested that NMYC amplified within the SHH subtypes be a candidate in the high rick category of risk stratification (Ramaswamy et al., 2016).

Evidence of the involvement of the WNT cell signalling pathway in medulloblastoma first came to light from genetic studies of patients with Turcot syndrome, characterized by germ-line mutations in the *Adenomatous Polyposis Coli (APC)* gene, who exhibit a higher risk of developing medulloblastoma (Attard, Giglio, Koppula, Snyder, & Lynch, 2007; Huang et al., 2000; Okota et al., 2002).

Sporadic medulloblastoma shows mutations in *CTNNB1* (β-catenin), *Axin-1*, and *APC*, whose phenotypic demonstration can be elucidated by IHC nuclear localization of β-catenin (Huang et al., 2000). This finding is fairly specific for WNT group of MBs, making this a fairly specific marker of this subgroup, and is associated with a favourable outcome (Ellison et al., 2005, 2011).

Table 6.1: Implicated subtype specific biomarkers and their association with prognosis (Ramaswamy, Northcott, & Taylor, 2011)

Subtype	Prognosis	Biomarkers implicated
WNT	Very good	Beta-catenin, DKK1 positive High MYC
SHH	Good/Poor	High MYCN
Group 3	Very Poor	NPR3 positive High MYC
Group 4	Good/Poor	KCNA1 positive Low MYC and MYCN Few high MYCN

6.2 Aims

1) To determine the histological presentation, demographic profile and outcomes from a retrospective cohort of MB patients in a South African cohort.
2) To create molecular profiles of MB in a local context using a validated nanoString assay.
3) To investigate the utility of using accessible techniques involving IHC and FISH to elucidate molecular subtypes from a retrospective cohort.
4) To examine the relations between group type and outcome and how this compares to international standards.

6.3 Methods

6.3.1 Cohort and patient samples

MB patients were identified from several sources including Neurosurgery and Radiation Oncology databases, and searched for against pathology records at the Red Cross Memorial Children's Hospital (RCCH), Western Cape, South Africa. The cohort used for this study does not reflect the full cohort of children treated for MB at

the centre, but rather the patients who had sufficient sample available for analysis by Nanostring, IHC and/or proteomics. This resulted in 48 patients who comprised the MB retrospective cohort. Ethical approval for this study has been obtained from the University of Cape Town Faculty of Health Sciences Human Research Ethics Committee (HREC 149/2014). Demographic and outcome data was collected together with age of the tissue blocks. Archived slides and tissue blocks were retrieved and anonymised from the Anatomical Pathology Department at RCCH. Outcome data is presented with follow up medians and ranges in each case. Poor outcomes are defined here as patients who are confirmed as deceased. Favourable outcomes are defined as patients who are confirmed as alive and not confined to palliative care.

6.3.2 MB Treatment

Following imaging, surgical resection of the tumour was undertaken resulting in samples preserved in FFPE blocks. Chemotherapy followed within 4 weeks after surgery. The treatment regime was as follows: Week 0: Day 1: Carboplatin 500mg/m^2 IV, Vincristine 1.5mg/m^2, Etoposide 100mg/m^2 IV. Day 2-5 Etoposide 200mg/m^2 PO daily. Week 1-6 Vincristine 1.5mg/m^2 IV Weekly. (Dosage for infants: Carboplatin 16.5mg/kg, Etoposide 3.3mg/kg, Vincristine 1.5mg/kg). Patients under 3 years of age: repeated Carboplatin 16.5mg/kg + Etoposide 3.3mg/kg every 3 weeks for a total of 8 courses.

Radiotherapy is given after course 2 of chemotherapy. On completion, chemotherapy is recommenced immediately (if blood counts permits) to a total of 8 courses.

6.3.4 NanoString subtyping

Total RNA was extracted from 8-10 10µm sections of FFPE blocks using RNeasy FFPE RNA extraction kit as per the manufacturers recommendations (Qiagen). Sections were first deparaffinised in xylene and xylene removed with absolute ethanol. All chemicals were of molecular biology grade (Sigma-Aldrich). RNA quality and concentration was determined using a Nanodrop instrument. 100ng of total RNA was used for subtyping on the nanoString nCounter system (University Health Network Microarray centre, Toronto, Canada) and a nanoString codeset as

published elsewhere (Northcott, Shih, et al., 2011). Briefly the codeset consisted of 5-6 gene transcripts per subtype and 3 housekeeping genes used for biological normalisation. RNA hybridisation, detection and scanning were carried out as per nanoString technologies recommendations.

6.3.5 Data processing and class prediction

Raw nanoString counts were normalised to positive control gene counts as a technical normalisation and to the housekeeping gene controls as a biological normalisation. A training dataset was used to predict the subtypes of this cohort. The training set consisted of 101 clinical samples and is published elsewhere (Northcott, Shih, et al., 2011). All prediction models were performed in R statistical programming environment using the NanoStringNorm and PAMR packages.

6.3.6 Immunohistochemistry staining

FFPE blocks were sectioned into 5µm sections and mounted on glass slides following routine histology staining with haematoxylin and eosin. All slides were re-examined by a neuropathologist to confirm the MB diagnosis. Sections were deparaffinised in xylene and rehydrated in a graded ethanol series (70%, 80% and 100% ethanol in distilled water) and subsequently rinsed in distilled water. The following antibodies and FISH probes were used to identify groups as per the manufacturers recommendations (Table 6.2).

Table 6.2: List of antibodies and probes used in characterising MB subtypes

MB subtype	**WNT**	**SHH**	**Group 3**	**Group 4**	**ATRT (Exclusion)**	**β-catenin**	**N-MYC FISH**
Marker	DKK1	SFRP1	NPR3	KCNA	INI1 (1/200)	NCL-B-CAT	07J72 001
Dilution	(1/100)	(1/800)	(1/500)	(1/1000)	(3ug/ml)	(1/100)	(2ul Probe)
Conc.	(10ug/ml)	(4ug/ml)		(0,7mg/ml)	(ab58209)	(nclcat)	(Vysis)
Prod no.	(ab61034)	(ab4193)	(ab97389)	(ab32433)	(Abcam)	(roche)	
Manuf.	(Abcam)	(Abcam)	(Abcam)	(Abcam)			

Positive control tissues for the antibody panel used were heart muscle tissue for DKK1, liver tissue for SFRP1, kidney tissue for both NPR3 and KCNA. INI1 immunoreactivity was used as exclusion criteria for ATRT tumours, ATRT tumours are known to contain a distinct loss of INI1 protein expression (Pfister, Hartmann, et al., 2009). Heat-mediated antigen retrieval was performed with the β-catenin antibody. Briefly, slides were blocked in 0,5% hydrogen peroxide/methanol for 10 minutes and rinsed in distilled water. Slides were held heated at a pressure of 15psi in 0.1M citrate buffer pH6.0 for 1 minute, and thereafter rinsed 3 times for 5 minutes each in TBS-Tween (20mM Tris, 0.65mM EDTA, 0.65% Tween 20, pH 9.0). All slides were incubated with blocking reagent (10% bovine serum albumin, in TBS-Tween) and thereafter incubated with primary antibody for 1 hour at room temperature or overnight at 4 °C. Slides were rinsed in TBS and incubated with biotinylated secondary antibody and visualised using the Real Envision peroxidase/DAB kit (DAKO) according to the manufacturers recommendations. Slides were counterstained with haematoxylin, dehydrated in an ethanol series and mounted for imaging.

6.3.7 FISH staining

Deparaffinised slides were treated with enzymatic digestion and heat denaturation (Leica, Tissue digestion II), heated to 73°C for 5 minutes in denaturation buffer (0.1M citrate buffer pH6.0) as per manufacturers recommendations. Slides were then dehydrated in a graded series of ethanol for 1 minute each and dried at 45°C until ethanol evaporated completely. FISH probes were denatured at 73°C for 5 minutes and snap cooled on ice for 2 mins. 10 µl of probe mixture (2µl probe, 8µl denaturation buffer) was added to each slide, cover slipped and incubated for 16 hours at 37°C. Slides were rinsed, counterstained with DAPI nuclear fluorescent stain and mounted for imaging.

6.3.8 Imaging of slides for IHC and FISH

Stained slides were imaged using Olympus multi header microscope (Olympus)/Zeiss Axiovert 200M (Zeiss) fluorescence microscopes (for FISH) or light microscope (for IHC) (Nikon). Counting stained cells of at least 50 non-overlapping nuclei from representative 10 high-powered fields of views.

6.3.9 Data analysis

Clinical data are presented as mean, median, range and percentages of total patients in the cohort. Incidences are plotted by spline function using GraphPad prism (version 7.0). Chord diagrams are plotted using the Circos tool (version 0.69) (Krzywinski et al., 2009). Principle component analysis was performed using clustering of quantitative data from both methods of subtyping, and distribution plots shown as mosaic diagrams both done in SAS university edition (version 2.3.9.4M3, 2016). Statistical power analysis was determined using G*Power (version 3.1.9.2, 2014) (Faul et al., 2007).

6.4 Results

We present data (Table 6.3) for a retrospective cohort taken from the archives spanning 26 years (1988 – 2014) with a median follow up time of 1.6 years and a maximum follow up of 23 years.

The cohort consisted of children (aged 4 months to 13 years old at diagnosis) with a median age of 6 years old and overall gender ratio of 0,7 males to females. The histological profile of patients consisted of mostly large cell anaplastic variant (LCA) 38.5%, followed closely by classic variant 34.6%, and a small incidence of MB with extensive nodularity, nodular/desmoplastic and a proportion of mixed desmoplastic and large cell anaplasia 9,61% (Table 6.3). Most tumours occurred in the midline cerebellum (93,5%), and were large (>4cm) (72,1%). Given the predominance of LCA histotype, high-risk disease predominated (64,2%) as compared to standard risk (35,8%). All patients were treated surgically with the majority undergoing gross total resection (46,3%), closely followed by near total resection (40,7%), and a small minority of patients undergoing subtotal resection (7,4%) or biopsy only (5,6%). In line with treatment protocols most patients underwent radiotherapy (81,5%) and chemotherapy (74,1%), with delayed onset of chemotherapy for patients younger than 3 years of age. In terms of outcomes, overall metastasis was seen in 40,5% of patients (7,5% at time of initial diagnosis and 33,0% at recurrence) and 13,8% showed leptomeningial spread; there was 14,8% (8 cases) of tumour recurrence (Table 6.3). However, it should be noted that not all patients had access to a full brain and spine MRI at evaluation due to developing world circumstances and resource availability (only 30 of 54 patients had MRI scans). Thus, there were 14 of 30 (46,7%) cases that had full brain and spine MRI scans available that showed overall metastatic disease, 13,3% at initial diagnosis and 33,4% at recurrence. This might be a bias in metastatic incidence but can be a representation of the actual overall metastatic incidence.

The 5-year overall survival was 74,1% and 10-year overall survival was 62,4% of cases with a 27,7% loss to follow up in this cohort. When stratifying by risk status, there was an 86,4% overall survival in standard risk cases and a 56,1% survival in high-risk cases, with a hazard ratio of 2,7 suggestive of a faster and poorer outcome in

high-risk cases (Figure 6.1A). In terms of extent of resection, 5-year survival was 80,0% in patients with gross total resection, 63,6% in near-total resection, and 44,2% in patients with subtotal resection (Figure 6.1B, *, p = 0.0482).

Table 6.3: MB cohort characteristics showing demographics, clinical and molecular summaries

Age	Mean	5,45	
	Median	6	
	Range	0,25 - 13	
Sex	Male	21 (43,8%)	
	Female	27 (56,2%)	
Histology	LCA	11 (22,9%)	
	Classic	27 (56,3%)	
	MBEN	3 (6,2%)	
	Nodular/Desmo	7 (14,6%)	
Year of diagnosis	Range	1988 -2014	
Follow up until		2016	
Tumour location	Midline	43 (93,5%)	
	Left	1 (2,2%)	
	Right	2 (4,3%)	
Tumour Size	>4cm	31 (72,1%)	
	<4cm	12 (27,9%)	
Risk	Standard	19 (35,8%)	
	High	34 (64,2%)	
Treatment	Surgery	GTR	25 (46,3%)
		NTR	22 (40,7%)
		STR	4 (7,4%)
		Biopsy	3 (5,6%)
	Chemotherapy		40 (74,1%)
	Radiotherapy		44 (81,5%)
Recurrence			8 (14,8%)
5-year overall survival			40 (74,1%)
Metastasis			15 (40,5%)
Leptomeningial spread			4 (13,8%)

Age, age at presentation (in years), follow up duration in years (median: 13,5 years; Range: 3 years – 29 years), Metastasis – if presented with metastasis at time of diagnosis or at time of relapse, Leptomeningial spread – at time of diagnosis.

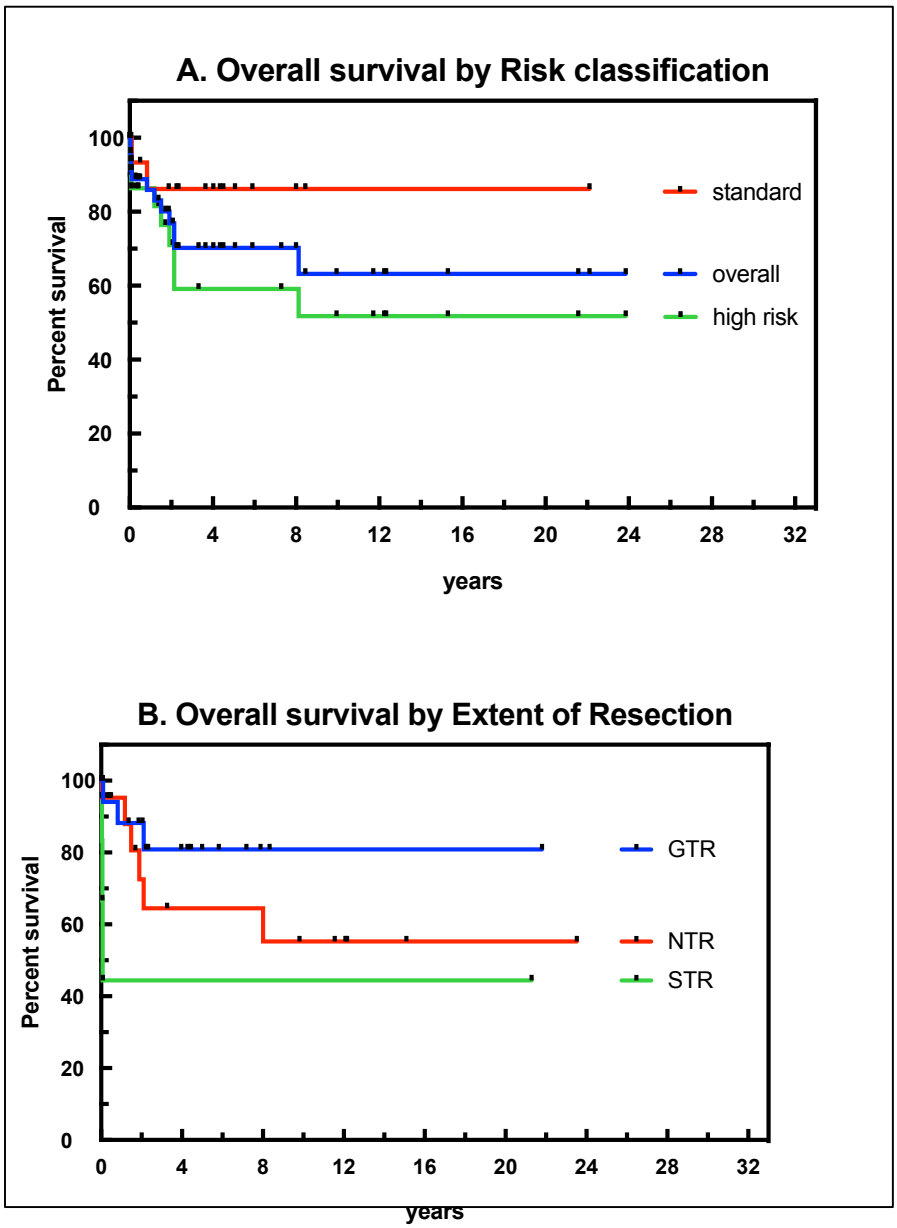

Figure 6.1: Overall survival by risk group based on standard and high-risk groups and combined overall survival (A). Overall survival curves by extent of surgical resection, Gross total resection (GTR), Near-total resection (NTR), Sub-total resection (STR) (B). Dots represent last time point patients were seen or lost to follow up.

The molecular subtype profile results by nanoString show 22,9% WNT, 27,1% SHH, 29,2% Group 3 and 20,8% Group 4 subtype distribution. The IHC method used tended to deplete the WNT (13,0%) and Group 3 (23,9%) classifications and reclassify into SHH (32,6%) and Group 4 (30,4%) respectively. There are 19% WNT, 27% SHH, 29% Group 3 and 25% Group 4 overall consolidated subtypes presented in this cohort. The β-catenin status largely correlated with WNT subtype by NS displaying 6 cases (12,5%) positivity. N-MYC status were largely presented as balanced overall (76,7%) and a proportion of amplification (7 cases, 30,4%) (Table 6.4).

The age-balanced incidence displayed in this cohort peaked earlier (age <5 years old) in SHH and Group 3 types and later (age >7 years old) in WNT and Group 4 (Figure 6.2.1A).

The age-balanced incidence was similar to other cohorts reported with slightly younger patients in the WNT subtype. The younger WNT subtype patients are less common. The WNT subtype displayed the most favourable outcome, with the other groups showing a similar 10-year overall survival (WNT - 100 %, SHH - 67,5 %, Group 3 - 56,0 % and Group 4 - 77,0 %) (Figure 6.2.1B). The follow up times for survivals are indicated in the figure legends, median and range follow up times are as follows; WNT - 23 months (2 months – 20 years), SHH – 10 months (2 months – 8 years), Group 3 – 5 months (2 months – 12 years), Group 4 – 21 months (1 month – 23 years).

The distribution of subtypes shown per method shows a similar SHH and Group 3 and NS showed slight WNT enrichment with Group 4 depletion, the consolidated subtypes show a slight enrichment for the WNT subtype and slight Group 4 depletion (Figure 6.2.1C). Any conflicting subtype assignments between NS and the IHC panel were further resolved by MS based proteomic clustering, this data is presented in the supplementary section (Figure s1).

The gender distribution shows a balanced 1:1 male female ratio between the SHH and Group 3, while the WNT shows a predominantly female representation (0.2 male:

female), and the Group 4 a predominant male representation (1,6 male: female) (Figure 6.2.1D).

Further distributions of the subtype were stratified based on age of the tissue blocks, as shown in Figure 6.2.2. There is a slightly higher incidence of WNT types in the post-2007 (7 WNT cases) as compared to the pre-2007 (4 WNT cases) groups identified by NS (Figure 6.2.2A). While there appears to be a slight depletion of the WNT types using the IHC method for subtyping, namely 4 WNT cases pre-2007 and 2 WNT cases post-2007 (Figure 6.2.2B). Additionally, comparing across methodologies, there appears to be consistency in the pre-2007 cases across both methods used, with a deviation in subtype assignment in the post-2007 group, namely, a depletion of WNT types (7 assigned WNT types using NS to 3 assignments using IHC) and an increase in Group 4 assigned cases (2 Group 4 cases assigned using NS to 6 assigned cases using IHC) (Figure 6.2.2). To consolidate this the NS results were presented to clinical correlates, with any disparities resolved by later mass spectrometry based proteomic clustering (data in supplementary Figure s1).

Table 6.4: Subtype profile as determined by nanoString and IHC and consolidated.

	WNT	**SHH**	**Group 3**	**Group 4**
NS	11 (22,9 %)	13 (27,1 %)	14 (29,2 %)	10 (20,8 %)
IHC	6 (13,0 %)	15 (32,6%)	11 (23,9 %)	14 (30,4 %)
Consolidated	9 (19,0 %)	13 (27,0 %)	14 (29,0 %)	12 (25,0%)
β-catenin				
Positive	6 (54,5 %)	0 (0,0 %)	2 (14,3 %)	0 (0,0 %)
Negative	5 (45,5 %)	13 (100 %)	12 (85,7 %)	10 (100 %)
N-MYC				
Amplified	2 (20,0 %)	3 (33,4 %)	4 (44,4 %)	1 (12,5 %)
Balanced	8 (80,0 %)	9 (66,6 %)	9 (55,6 %)	8 (87,5 %)

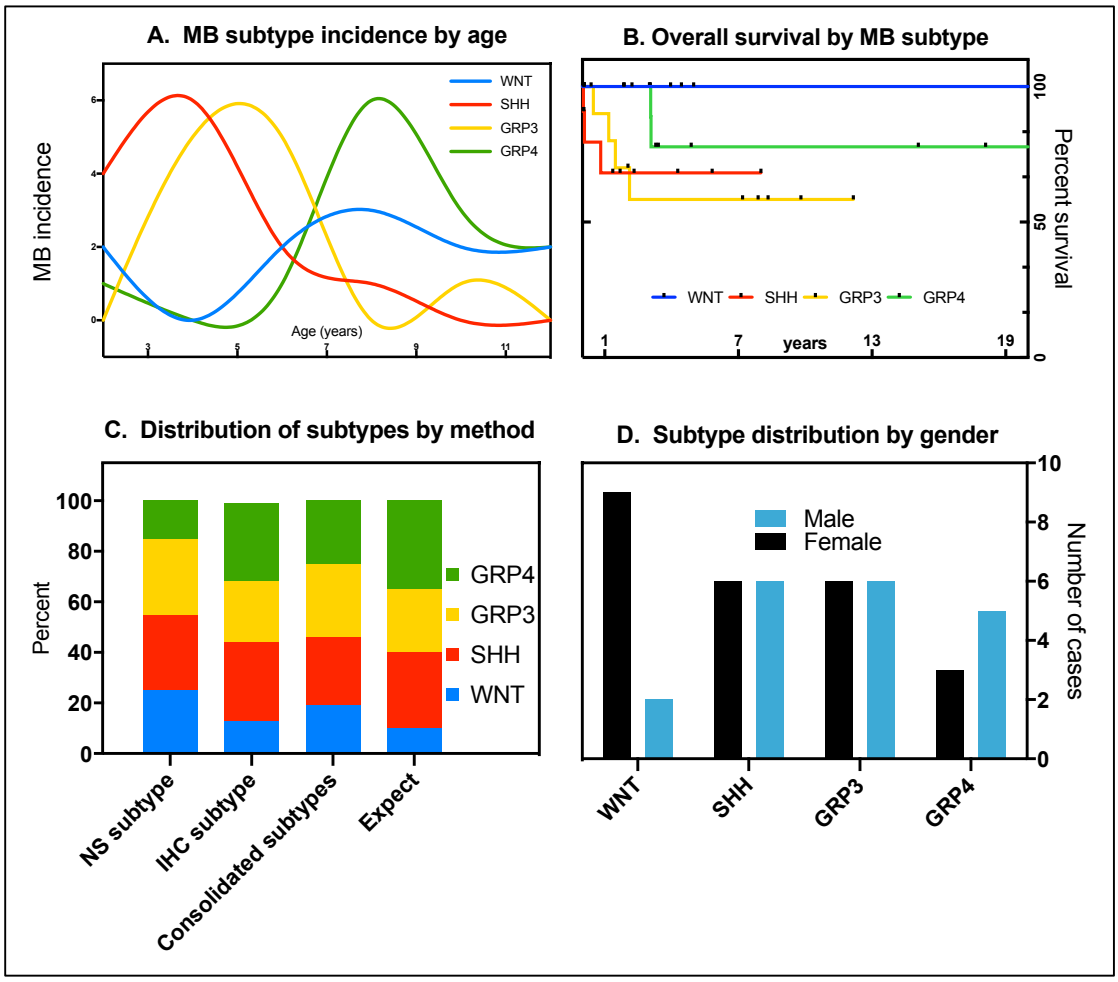

Figure 6.2.1: Incidence, survival and distributions classified by molecular subtype. A) MB consolidated subtype incidence by age from this cohort; B) Overall survival curves by consolidated subtype, dots represent last time point patients were seen or lost to follow up, median and range follow up times are as follows; WNT - 23 months (2 months – 20 years), SHH – 10 months (2 months – 8 years), Group 3 – 5 months (2 months – 12 years), Group 4 – 21 months (1 month – 23 years); C) representation of subtypes in this cohort showing the NS, IHC method of subtype determination with the consolidated subtype and the expect cohort based on international norms; D) Consolidated MB molecular subtype showing sex distributions.

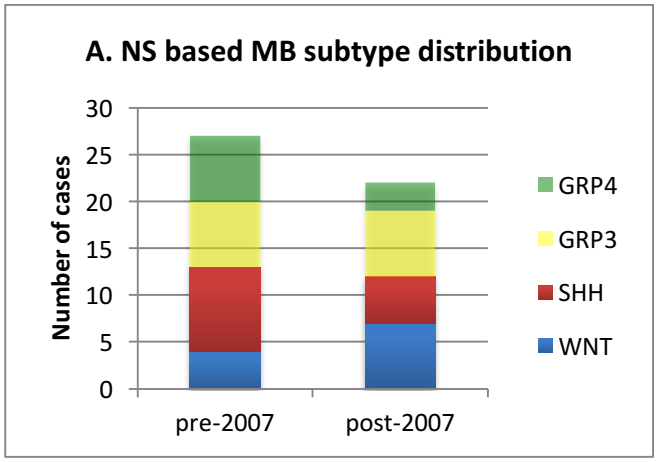

NS	WNT	SHH	GRP3	GRP4
pre-2007	4	9	7	7
post-2007	7	5	7	3

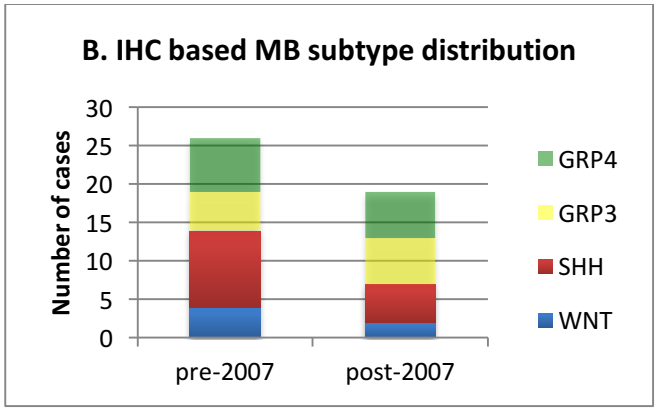

IHC	WNT	SHH	GRP3	GRP4
pre-2007	4	10	5	7
post-2007	2	5	6	6

Figure 6.2.2: MB subtype by techniques and year of retrospective tissue blocks.

A-Distribution of the molecular subtypes assigned using Nanostring (NS) methodology based on age of the tissue blocks retrieved from the retrospective cohort pre-2007 (blocks older than 8 years) and post-2007 (more recent blocks not older than

8 years old). B-The distribution of the subtypes using IHC methodology with a panel of protein specific stains on those same tissue block over the age of the tissue blocks.

The MB histologic profile shown in this cohort was mostly classic and LCA and showed slight variability amongst the subtypes. One of the most notable findings is that the SHH subgroup is depleted in LCA histotypes, while the MB with extensive nodularity (MBEN) and nodular/desmoplastic histotypes are absent from the WNT subgroup in this cohort (Figure 6.3).

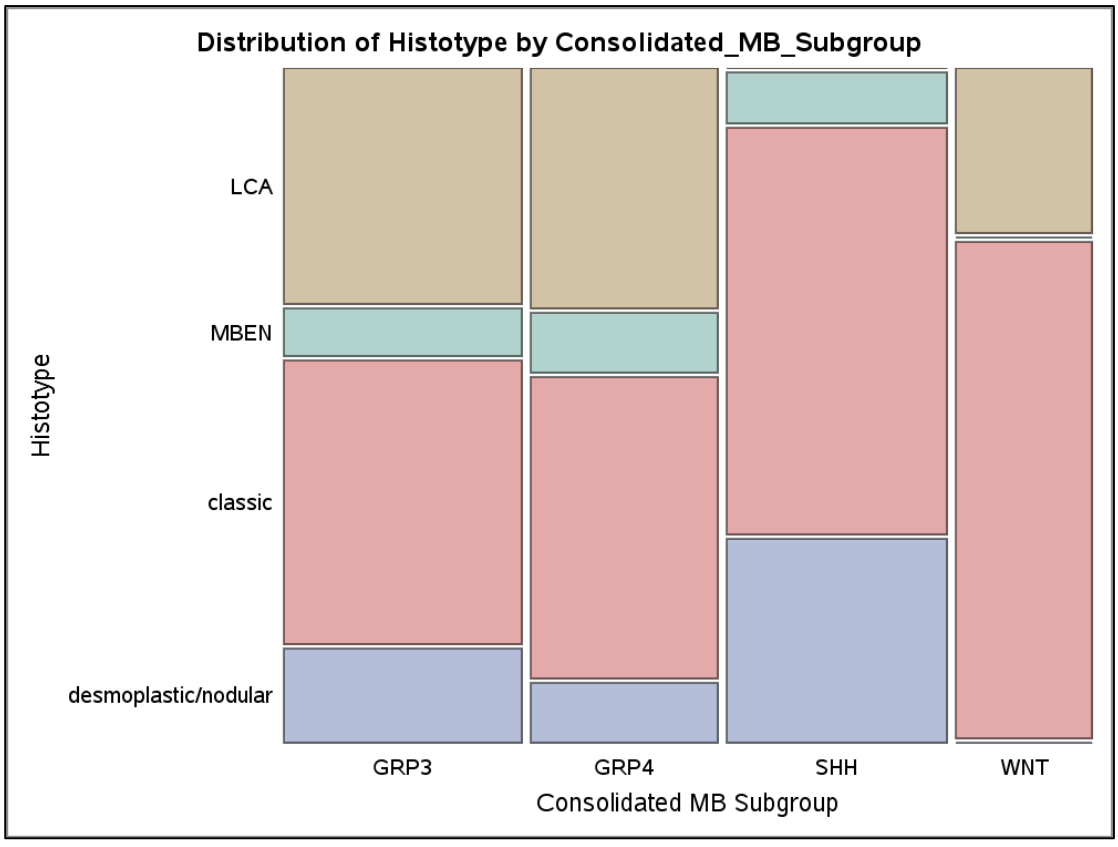

Figure 6.3: Distribution of histological classification between the molecular subtypes. LCA - large cell anaplastic; MBEN - MB with extensive nodularity; classic and desmoplastic/nodular histotypes is shown.

There were slightly more metastases in Group 3 patients compared to the other subgroups (Figure 6.4). In terms of leptomeningial spread, these occurred exclusively in Group 3 and Group 4 molecular subtypes (Figure 6.5).

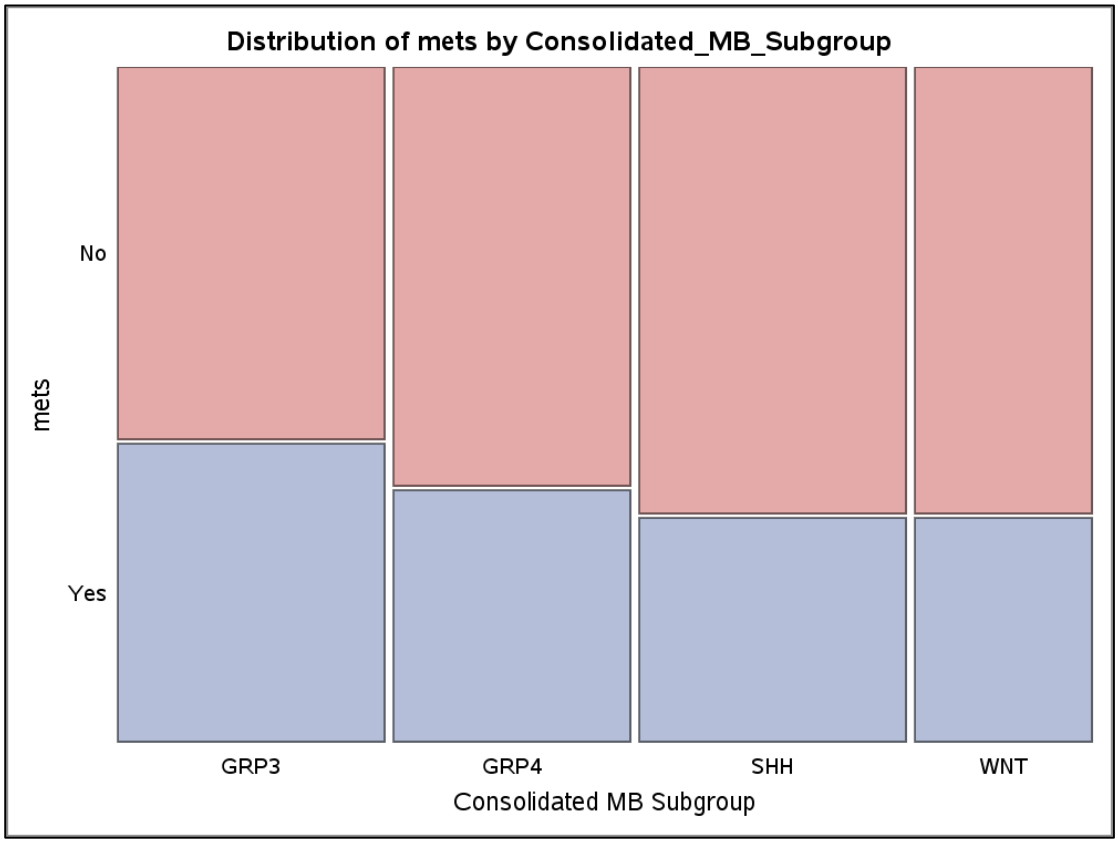

Figure 6.4: Metastasis and its incidence between the molecular subtypes. Metastasis was identified either by the patient MRI imaging report or by CSF malignant cells at 2 weeks or follow up post operatively.

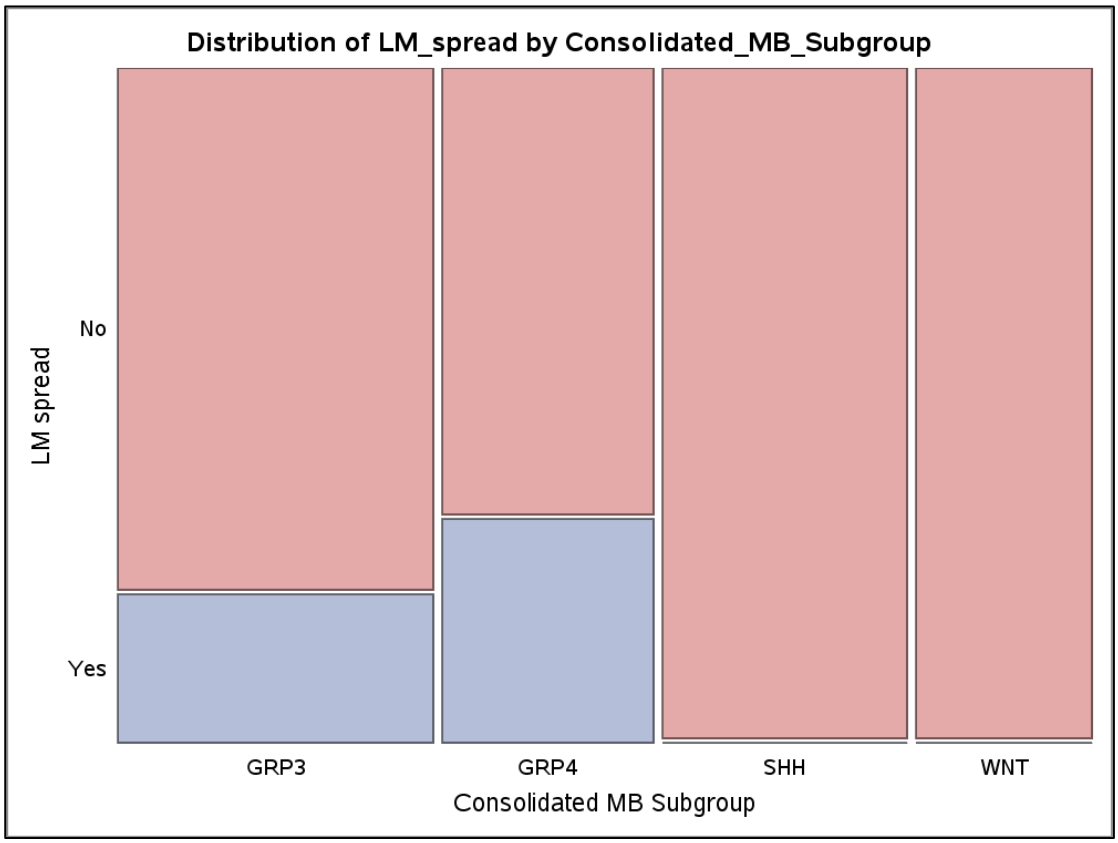

Figure 6.5: Leptomeningial spread between the molecular subtypes.

The cohort N-MYC status by survival shows a more favourable outcome with N-MYC balanced status (77,9% 5-year overall survival rate) (follow up time median 19 months (2months – 21 years)) and the N-MYC amplified patients showing a poorer survival outcome (50,8% survival rate) (follow up time median 14 months (2 months – 8 years), hazard ratio of 2.2. (Figure 6.6A).

A notable association seen in this cohort is the Group 3 and Group 4 N-MYC status with outcome. The N-MYC amplified cases showed enrichment for poorer outcome and the opposite with N-MYC balanced having a favourable outcome however not exclusively (Figure 6.6B and 6.6C). As a more general indicator, N-MYC status seems to have a subgroup independent association with outcome but there may also exist associations, particularly in the absence of N-MYC amplifications in the Group 4 subtype (Figure 6.6B and 6.6C).

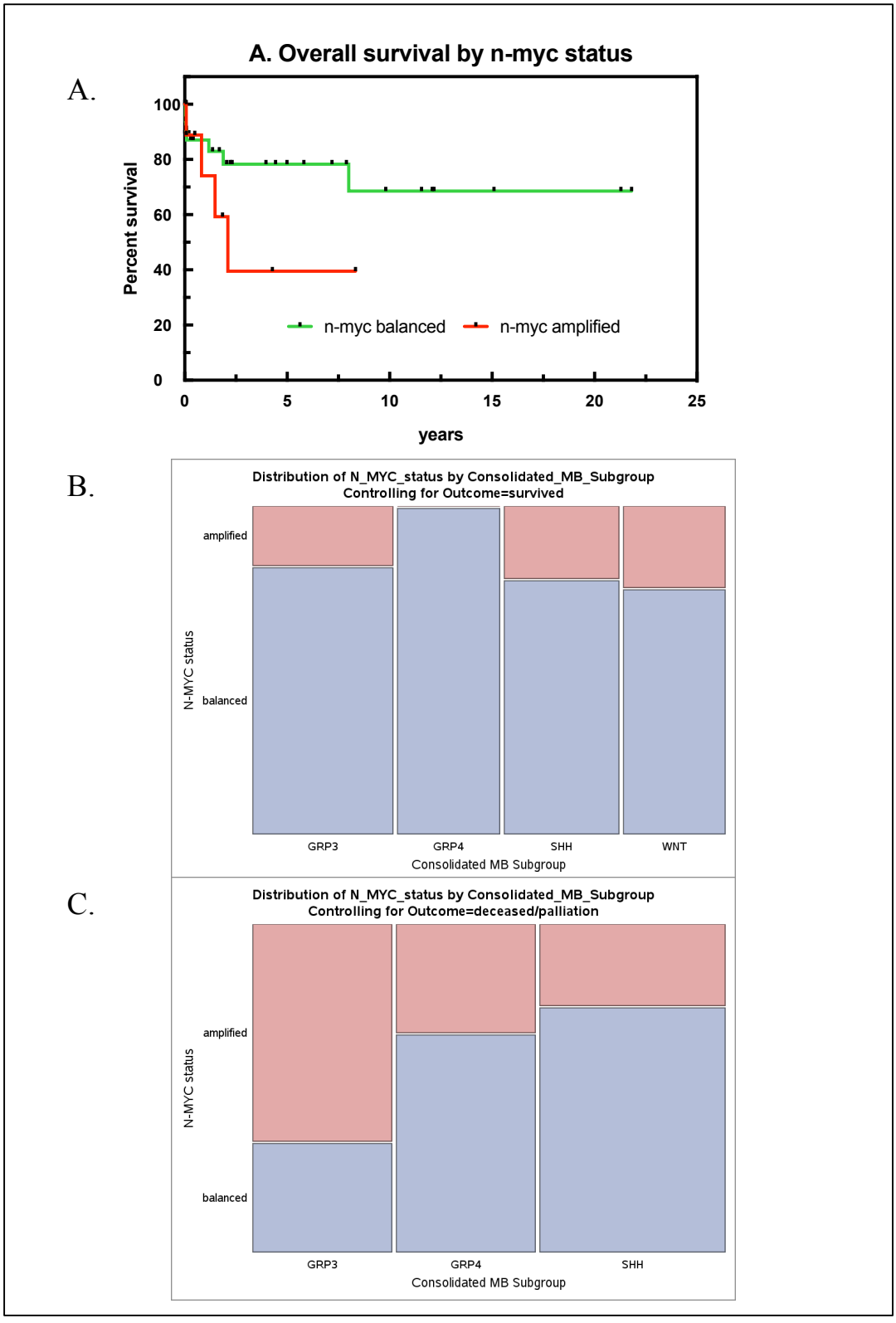

Figure 6.6: The distribution of N-MYC status by outcomes and subtype.

A - N-MYC status overall survival curves, dots represent last time point patients were seen or lost to follow up, follow up ranges were as follows, N-MYC balanced median 19 months (2 months – 21 years), N-MYC amplified median 14 months (2 months – 8 years), B - N-MYC status by those patients that have good outcome, C - N-MYC status for patients with poor outcome.

When looking at the performance of the IHC panel compared to the NS assay, there is a 34,5 % discordance rate between the subtypes predicted. The WNT types are most frequently miss-assigned to the SHH and Group 4 types by IHC, the SHH type is most frequently miss assigned to the Group 3 and Group 4 types while the Group 3 and Group 4 groups are most frequently miss assigned to each other respectively (Figure 6.7).

When we compare the RNA and protein levels of the same biomarker there is robust concordance and the subgroups predicted reflects the protein and RNA transcript abundances (Figure 6.8A). Furthermore, the FISH staining, IHC staining and morphological staining pattern have all performed robustly with the FISH and IHC probes showing consistency between and within the cohort and other published studies (Figure 6.8B, 6.8C and 6.8D).

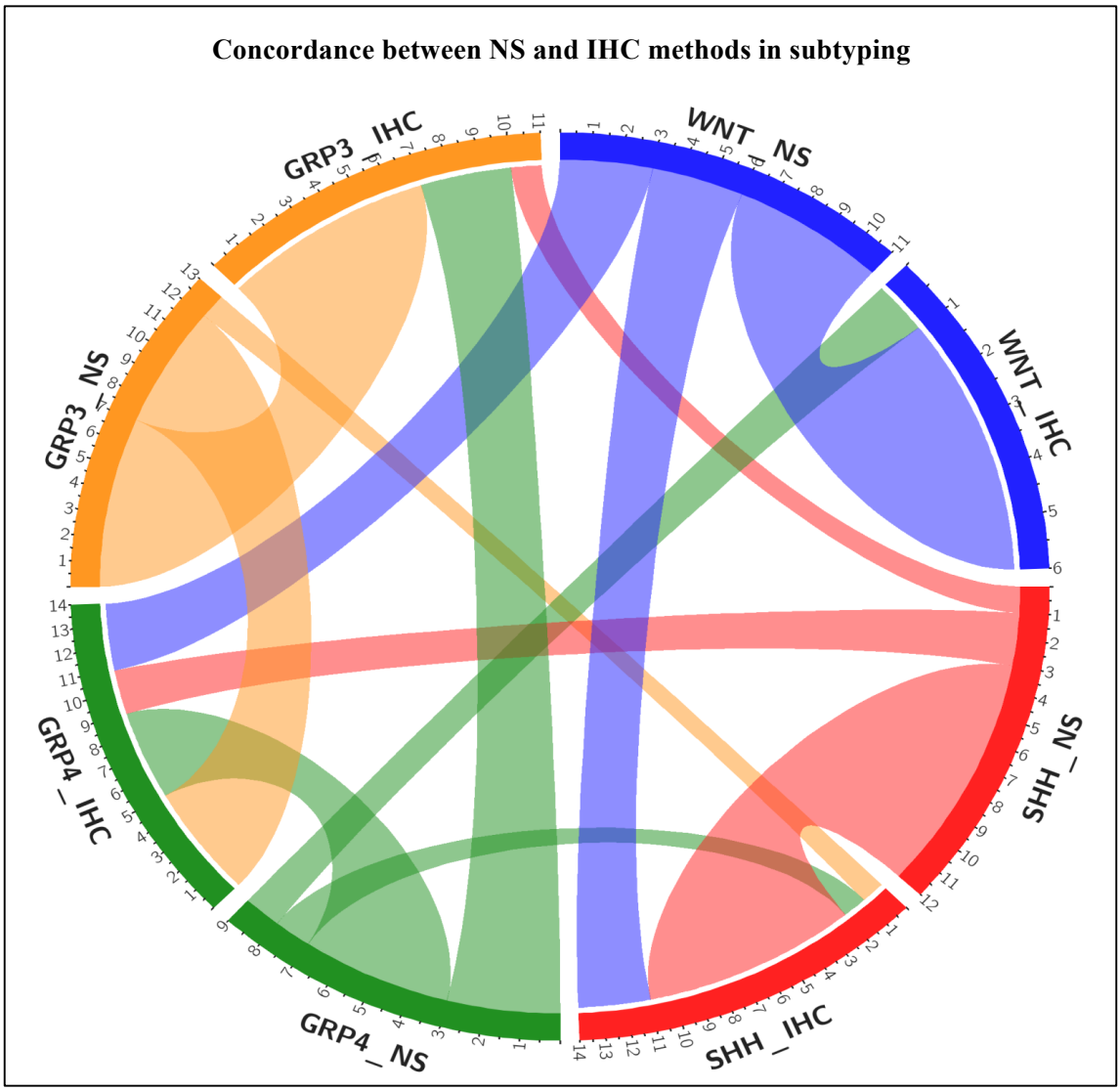

Figure 6.7: Chord diagram depicting the concordance between NS and IHC based subtype prediction differences. There is more variability with NS than there is with the IHC panel. Any disparity was later resolved by mass spectrometry based proteomic clustering (data in supplementary Figure s1).

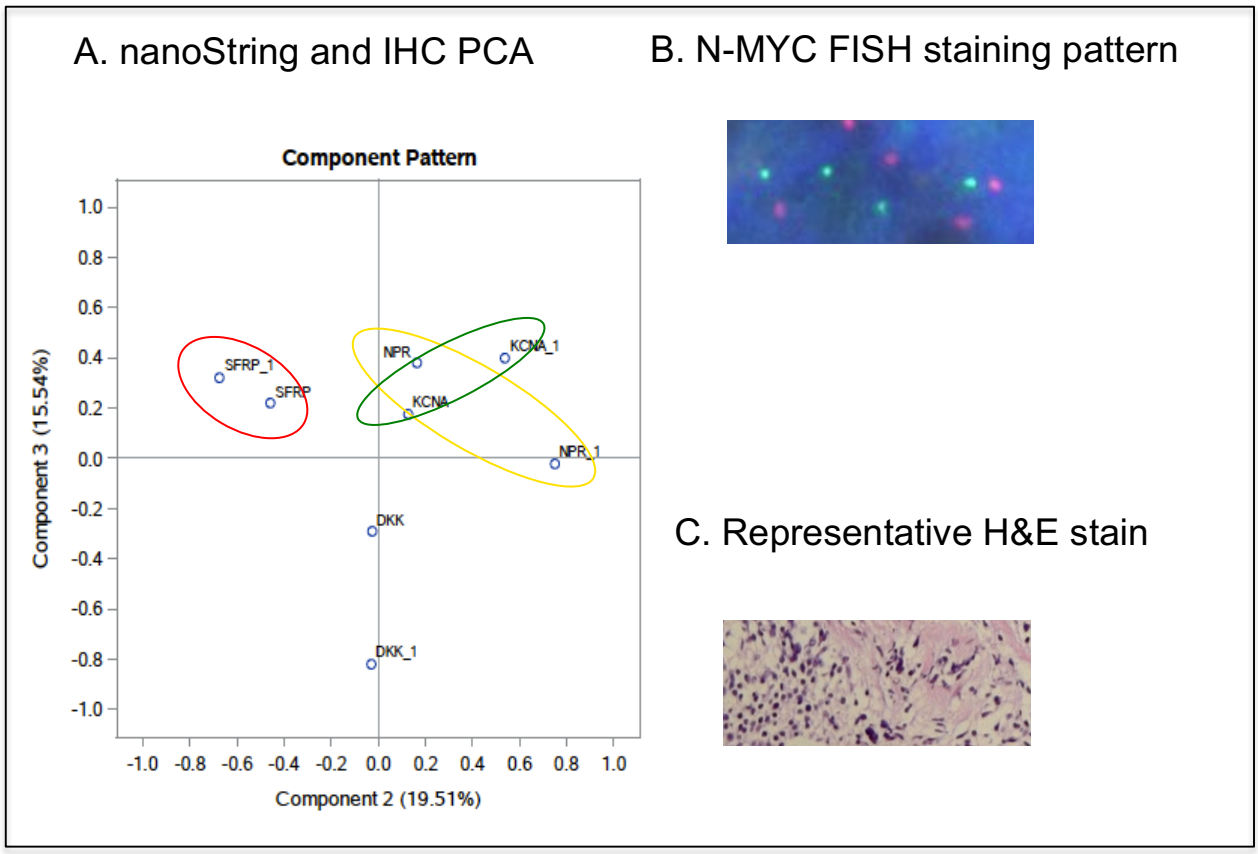

Figure 6.8: Utility of NS and IHC for MB subtyping, A - components plot showing concordance of biomarkers between the NS and IHC method, B - representative fluorescence image for N-MYC FISH staining, C - representative image for IHC staining showing the extent of nuclear positivity, representative H&E image used for histopathological classification.

Summary of MB subtypes and molecular markers with age, gender and outcome demographics

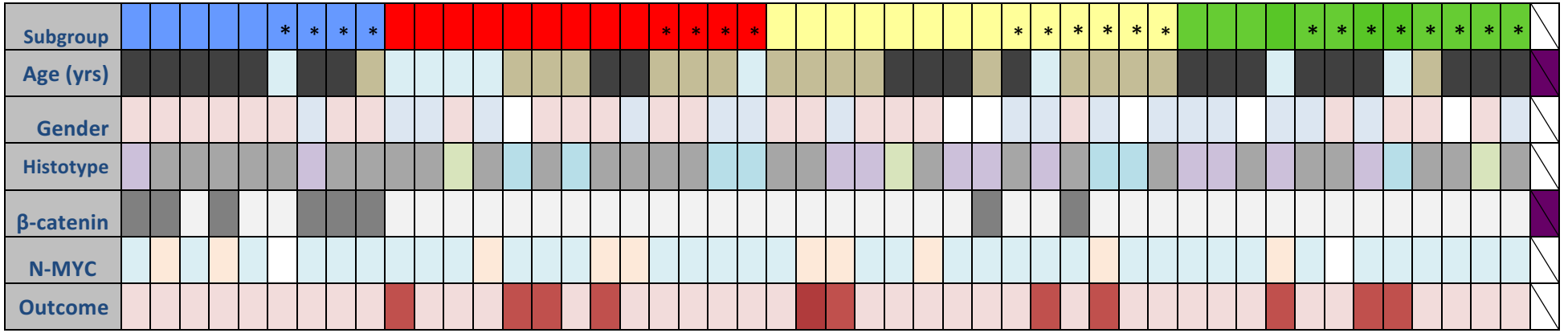

Key:

Subgroup	WNT	SHH	GROUP 3	GROUP 4
Age (yrs)	<3 yrs	3-5 yrs	>5 yrs	
Gender	Male	Female		
Histotype	Classic	LCA	Desmo/Nodular	MBEN
β-catenin	Positive	Negative		
N-MYC status	Amplified	Balanced		

Outcome	Good	Poor
Significant		***

More detailed subgrouping is presented in supplementary (Figure s1A), * represents conflicting subtyping between NS and IHC and was further resolved by MS based proteomic clustering (Figure s1B).

Age ***, P = 0.0096; with older patients > 5 years old over represented in WNT and Group 4 subtypes.

Sex, P = 0.1203; however, females more enriched in WNT subtype.

Histotype, P = 0.3563; with no LCA types corresponding to SHH subtype.

N-MYC, P=0.7980; with N-MYC amplification being subgroup independent and possibly lined to poorer outcomes.

β-catenin ***, P= 0.0011; enriched in WNT subtype and associated with favourable outcomes.

Significantly difference age distributions by Chi squared test, outcomes are defined as follows: Poor = deceased or under palliation, good = survived.

6.5 Discussion

The current genomic revolution in MB is increasingly unveiling novel features of this disease and is guiding new therapeutic strategies. The most recent WHO classification of MB indicates that it can be histologically classified into histotypes displaying classic, desmoplastic/nodular, large cell/anaplastic and MB with extensive nodularity morphological characteristics. Additionally, MB can be classified molecularly into 4 subgroups (WNT, SHH, Group 3, and Group 4) (Louis et al., 2016). It is therefore anticipated that identification of these subtypes will be required for entry into future clinical trials and will guide therapy recommendations. There is also now wide accord on risk stratification involving molecular subtypes (Ramaswamy et al., 2016). Both histotype and molecular subtype information are becoming more clinically important and this emphasises the relevance of subtyping MBs in the current molecular era.

Although there have been improvements in the treatments of this tumour, the overall survival has not been significantly improved in recent times. This further emphasises the complexity of this disease and our current understanding of the disease phenotype. In South Africa, and Africa at large, the data on MB incidence, prognosis, histological and molecular phenotypes has been lacking. This data is essential for MB molecular biology in Africa and for contemporary clinical trials and future targeted treatment protocols. Furthermore, this data is needed for ongoing international molecular biology driven insights into this complex disease and its presentation in a multitude of cohorts.

The current study shows data on the histological presentation, demographic profile and outcomes from a retrospective cohort of MB patients in a South African cohort as well as the molecular subtype and histotype associations to outcome and how this compares to international standards. While there is currently no standardisation in molecular subtype assignment there are other methodologies available such as the epigenetic arrays (Illumina 450k or MS Sequenom based subtyping methods) and RT-PCR based subtyping methods, particularly from FFPE archival material (Kaur et al., 2016; Edward C Schwalbe et al., 2013). It might be interesting to compare the different methods of subtyping and their sensitivities and robustness for future

standardisation in the MB field, as well as for accessibility in low-resource settings such as in Southern Africa. While the DNA methylation methods of subtyping are routine in international centres of excellence in Canada, Germany and the US, its availability and costs for studies from low-resource settings such as in South Africa is limited. Therefore, the lower cost more accessible methods of subtyping (NS and IHC, and conflicts resolved with MS based proteomic clustering) were employed in the current study, the data presented represents the consolidated subtype in each case. Some notable findings are discussed as follows.

Sex ratios in the current study seem to differ to cohorts in other studies which a male predominance reported at 1.5 times male to females overall, however subtype sex associations are known to exist as there are almost equal male to female ratios in WNT and SHH types and a male predominance in Group 3 and Group 4 subtypes (Kool et al., 2012). Furthermore, the sex distribution of the cohort investigated here is representative of the sex distribution in a larger South African MB cohort (data not shown).

The current study shows a balanced sex distribution 1:1, male/female ratio between the SHH and Group 3, while the WNT shows a predominantly female representation (0.2 male : female), and the Group 4 a predominant male representation (1,6 male : female) (Figure 6.2D). There are some disparities between the cohort presented here and others, with the WNT female predominance being the most prominent, with the SHH and Group 3 subtype gender distributions agreeing.

The overall predominance of females (1.3:1 ratio) in the current study is unexpected as primary brain tumours in general have a male predominance worldwide as reviewed (Sun, Warrington, & Rubin, 2012). However, it has been noted previously that there is a predominance of females in a Kenyan MB tumour cohort (1.8:1 ratio), however with a small sample size of 37 cases (Wanyoike, 2004) This difference is currently unexplained and future investigations will aid in the understanding of this finding, specifically for MB tumours.

The overall survival of MB at 10 years was 62,4% (Figure 6.1) in the current cohort, which has not significantly changed since the previously published data of 19 MB cases from Tygerberg Hospital in SA during 1983-1993 which showed an overall survival of >60% (Hesseling et al., 1995). The majority of MBs are reported in other international cohorts to be located predominantly in the midline of the cerebellum, with possible brain stem and fourth floor ventricular infiltration (Park et al., 1983). The current study is in agreement with this finding and 93,5% of cases have presented in the midline region in the cohort investigated (Table 6.3).

Historically, radical total resection of tumours was thought to do better that subtotal tumour resection (Park et al., 1983). However, more recent analyses suggest that there might be no additional benefit of gross total resection compared to near total resection when the likelihood of morbidity is high with removal of small remnants of tumour tissue during surgery (E. M. Thompson et al., 2016). Nevertheless, in our cohort patients with gross total resection had better outcomes (Figure 6.1B).

The incidence and proportion of molecular subtypes in the current study are largely in agreement with other international cohorts, with a slight enrichment for WNT and slight depletion in Group 4 subtypes. The finding of WNT subtypes having a good outlook is in agreement with other studies in international cohorts with Group 3 having the poorest outcomes, WNT subtype displayed the most favourable outcome, with the other groups showing a similar 10 year overall survival (WNT - 100 %, SHH - 67,5 %, Group 3 - 56,0 % and Group 4 - 77,0 %) (Ellison et al., 2005; Northcott, Korshunov, et al., 2011; E. M. Thompson et al., 2016). There is also an agreement with the expected subtype distribution as seen in previously published cohorts not from Africa (Figure 6.2C) (Northcott, Korshunov, et al., 2011).

The WNT subtype has been suggested to arise in older children, usually have a classic histology, with activating mutations in CTNNB1 (Kool et al., 2008; M. C. Thompson et al., 2006). Together with a nuclear positivity for β-catenin protein which tends to

yield better survival (Ellison et al., 2005). The current study cohort displays data that is in complete agreement with these findings in other cohorts (Figure 6.2).

Further delving into more details the age related incidence in SHH types tend to arise in young children <3 years old and the much older children (Kool et al., 2008). The data in the current study supports the notion that SHH types arise in younger children in this South African cohort, but cannot extend to the older children. However, the age range displayed in the current study extends up to 13 years old which may be excluding some of the older category.

SHH subtypes have been suggested to have large cell anaplastic or desmoplastic histology and usually have a poor prognosis (Kool et al., 2008; M. C. Thompson et al., 2006). The SHH subtypes in the current cohort display no LCA histotypes but do seem enriched in desmoplastic/nodular histotypes (Figure 6.3). The lack of LCA types in this cohort suggests that histotypes are variable and may be a less specific diversifier.

Group 3 has been reported to have a prevalence of classic and LCA histotypes, and overall survival of 33%, the poorest survival (Northcott, Korshunov, et al., 2011). The current study agrees with those previous findings but however report a survival of 64% (Figure 6.3). This might be explained by the case for a heterogeneous Group 3 as recent studies suggest a mix of standard risk and high risk groups within the Group 3 highlighted by MYC amplification (Shih et al., 2014). The current cohort indeed shows a mix of clinical risk in all subgroups including Group 3 (supplementary Figure s2).

The Group 4 subtypes have been reported to display a mostly classic histotype with a overall survival of 77% a better prognosis that for Group 3 (Northcott, Korshunov, et al., 2011). The current study broadly supports the findings and reports an overall survival of 61,1% in Group 4 subtypes (Figure 6.3).

Overall, in terms of histology this study shows a majority classic histotypes (Table 6.3), and a larger proportion of desmoplastic/nodular histotype associated with the SHH group (Figure 6.3). There has been reported majority classic histotypes and a significantly greater proportion of classic histotypes in Group 4 than in Group 3 and a greater proportion of LCA types in Group 3, with Group 3 subtypes with LCA histology have been reported to have an association with poorer prognosis (Northcott, Korshunov, et al., 2011). It has also been seen that there is an a greater proportion of desmoplastic/nodular histotypes associated with SHH types (Northcott, Korshunov, et al., 2011). Furthermore, the MBEN histotype has been suggested to be associated more strongly with infancy and the SHH subtype, the current study largely supports that finding (Gessi et al., 2016). However, some MBEN cases also appear as Group 3 and Group 4 (Figure 6.3).

NMYC amplifications were seen in 10/49 cases or 20,4% (Table 6.4) which is higher than seen in other cohorts with up to 10,6% of the cohort NMYC amplified (Ellison et al., 2010). The current study also shows that NMYC amplification has a link to poorer outcome with a hazard ratio of 2.2 (Figure 6.6). Given that the overall survival as well as the progression free survival in the current cohort is very good, this might suggest a bias in the NMYC amplification incidence. However, the fact that we have indeed seen association of NMYC amplification with poorer outcomes in the current cohort further emphasises the role of NMYC amplification status has on outcome. Studies on other cohorts have seen similar findings with NMYC amplifications resulting in early deaths in about half of those with NMYC amplifications (Ellison et al., 2010). Recent large cohort studies on NMYC amplifications suggest the link with poor outcome might have subtype specific effects with NMYC amplification in SHH types being convincingly linked with poor outcome even to consider a distinct high risk group within the SHH group (Shih et al., 2014). Indeed this heterogeneity in NMYC amplifications have been reported to have both good and poor outcomes in reported literature and while linked to SHH and Gli1/2 amplification with poor prognosis,

remains unclear as an independent marker of prognosis, or with other subtypes (Korshunov et al., 2012).

In terms of method of MB subtyping, RNA based techniques particularly from FFPE archival materials is not ideally suited for older specimens due to the longer term effects of crosslinking and RNA degradation resulting in decline of subtype prediction accuracy to less than 95% in specimens older than 8 years old (Northcott, Shih, et al., 2011). However, array based classification tools are move expensive (±450 USD for array based methods versus ±60 USD for NS based methods per sample respectively) In resource-constrained settings, as is in this case, these cost differences are important factors to consider. In the current study, the utility of a panel of IHC markers were also used to investigate subgroup as an aid to predict subtype particularly in older specimens.

Therefore, this study presented subtype distributions for the overall retrospective cohort, as well as the cohort stratified by age of the tissue blocks (Figures 6.2.1 and 6.2.2). The IHC panel for subtype prediction used in the current study more closely resembled the expected subtype distribution from international cohorts in the more recent, not older than 8 year tissue blocks (Ellison et al., 2005). However, there does appear to be WNT enrichment in this retrospective cohort using the NS method for subtype prediction. This could be consistent with the hypothesis that there might be slight WNT enrichment in this cohort. Future studies might aid in the clarification of this phenomena in this and other African cohorts.

Discordance rates have been suggested to be 20% between other array based subtyping methods compared to IHC panels, furthermore, it has been suggested that two or more molecular criteria be met to confirm a WNT or SHH grouping, including both an IHC and transcript level confirmation (Gottardo et al., 2014). In the current cohort, the discordance rate was 34,5% (Figure 7). The lower throughput molecular subgrouping strategies will have the disadvantage of seeking to consolidate those varying groupings by the different grouping technologies particularly the Group 3 and

Group 4 subtypes (Figure 8A). An area that requires further investigation is in the abundance of WNT subtypes, it was seen from nanoString that there is a higher proportion of the WNT type, but this was consolidated with the IHC (DKK and β-catenin staining) to a lower proportion in the cohort. However, this might not be a robust way of evaluating and validating subgroups in variable cohorts. The question of whether this represents the biology in suggesting there is indeed a higher proportion of WNT types as seen in some other cohorts showing up to 25% WNT subtypes (Ellison et al., 2005). One of the methods to more accurately circumvent this is do perform higher throughput molecular subgrouping using gene expression or methylation arrays (Remke et al., 2013). Therefore, future investigation is warranted into high throughput molecular profiles into this MB cohort with particular focus on WNT, Group 3 and Group 4.

6.6 Conclusion

MB, the leading cause of death in children with brain tumours, are also the most common malignant childhood brain tumour (S. Rutkowski et al., 2010). Mortality is high and survivors are often neurologically disabled (Packer & Vezina, 2008). Treatment of such disease optimally requires an experienced team of multidisciplinary health professionals and availability of resources to monitor progress and recurrence. The accessibility of such resources is limited in developing nations such as in South Africa. This study investigated MB molecular subtypes using two molecular factors, RNA transcripts (NS method of subtyping) and protein levels (IHC method). It can be concluded that this study cohort tends to be in agreement with other cohorts in terms of histotypes and their distributions with molecular subtype. The pathological presentation and outcome data also stands in agreement with international standards with better overall survival with gross total resections. However further investigations into comprehensive event free survivals are warranted to study functional outcomes in local cohorts. However, as the molecular and pathological presentations are consistent with international cohorts, it is suspected that functional and neurocognitive outcomes with also resemble international norms.

NMYC amplification status in general has a poorer outcome however there might be subgroup specific interplays that are to be further investigated into the molecular correlation to outcome. Due to the lower throughput nature and RNA crosslinking affecting stability of RNA, transcript based and IHC based subtyping show concordance differences with subtype prediction especially affecting the cases on the cohort with older aged specimens (> 8 years old archival blocks). A higher throughput approach considering a multitude of molecular markers is therefore warranted for a more comprehensive evaluation of subtypes. However, considering the cost intensive nature of this, multiple arms were used to more accurately assign subtypes in the current study and provide the first molecular with phenotypic data of its kind particularly in Sub-Saharan Africa.

7. Chapter 7 - Juvenile pilocytic astrocytoma molecular characteristics in cohort – Study 2

7.1 Introduction

Juvenile pilocytic astrocytoma (JPA) is the most common glial cell tumour of childhood, occurring mostly in the cerebellum, the optic pathways, hypothalamus or brainstem (Rodriguez et al., 2013). JPAs are mostly benign, slow growing, WHO grade I tumours (Louis et al., 2007). They are suggested to be a predominantly single pathway disease, with genetic abnormalities largely associated with the MAPK pathway (Jones et al., 2013).

Mutations are prominent in this growth promoting ERK-MAPK pathway (Schindler et al., 2011). There is also an association with extra-cerebellar occurrence. Several BRAF gene fusions have been reported such as the KIAA1549-BRAF fusions, the FAM131B fusions and the ARAF fusions. All of these result in the loss of the auto inhibitory signal in RAF which leads to constitutive kinase activity (Forshew et al., 2009). There are sporadic types associated with KIAA1549-BRAF fusion and these are likely to arise in cerebellar regions. Additionally, there are also the NF1-associated types that are more likely to arise in the optic pathway and brainstem (Louis et al., 2007).

MAPK pathway activation is evident by the presence of p-ERK (the activated form of ERK), and seems to be independent of any BRAF copy number changes or activating mutations or fusions (Jacob et al., 2009).

RB pathways in JPA P16

There have been reports of RB pathway dysregulation in more malignant nerve sheath tumours. Furthermore, p16 inactivation has been suggested as a mechanism of evasion of cell senescence and tumourigenesis (Tamayo-orrego et al., 2016).

7.2 Aims

The aims of this chapter are outlined in Study 2, which investigates the molecular characteristics of JPA in a retrospective cohort at our centre. Tumours are grouped in cerebellar and non-cerebellar locations. To characterise the tumours, we analysed the molecular expression of copy number of BRAF by FISH, and p-ERK and p16 protein expression markers by IHC. The molecular markers phenotypes were then correlated to clinical variables such as age, gender and survival.

7.3 Methods

The cohort investigated was retrieved from RCCH archives and met the inclusion criteria of having a clinical diagnosis of either cerebellar or non-cerebellar JPA, had sufficient tissue in blocks for analysis and had folders available for outcome determination. Outcomes are presented with follow up time medians and ranges. Outcome statuses are defined in this study as favourable, if patients are confirmed as alive and not confined to palliative care; and unfavourable, if patients are confirmed as deceased or are in relapse.

The FISH experiments were carried out as described in Chapter 6, using tissue digestion and uncrosslinking (Leica, Tissue digestion II), BRAF probing (BRAF spectrumGold, VY6N0920, Vysis) and visualisation with appropriate fluorescent filter set. IHC was performed as described in Chapter 6, with antibodies against p16 (CDKN2A, 6695248001, Ventana) and p-ERK (phospho p44-42, Thr202, Try 204, 9101, Cell signalling), visualised with haematoxylin counterstain nuclei and viewed under light microscopy as previously discussed.

Results are presented as mean, median, range and percentages of total patients in the cohort. Incidences are plotted by spline function, and survival curves are plotted using Kaplan-Meier curves both in GraphPad prism (version 7.0). Statistical significance

was determined by Chi-squared test for independent variables, a p-value less than 0.05 or 0.1 was deemed significant.

7.4 Results

The JPA cohort characteristics were as follows: there were 9 cerebellar JPA and 5 non-cerebellar cases (2 from the temporal region, 2 from the pineal region, and 1 from the parietal region), a total of 14 cases included in this cohort, with a median age of 6 years old. Metastasis (7%) and recurrence (14%) were infrequent (Table 7.1).

Table 7.1: Clinical and demographic variables in the JPA cohort presented in the current study

Clinical/Demographic variable	Measure	Number	Percentage
Age	Mean	5,1	
	Median	6	
	Range	4 months - 10 years	
Gender	Male	9	64%
	Female	5	36%
Location	Cerebellar	9	64%
	Non-cerebellar	5	36%
Year of Diagnosis	Range	1993 - 2011	
Metastasis		1	7%
Recurrence		2	14%
5 year Overall survival (13/14)			93%
5 year Progression-free survival (12/14)			86%

The JPA cases incidence by age shows an early (0-3 years) and later peak (around 9 years old) (Figure 7.1A). There is a favourable 5-year overall survival rate of 93%, and a progression free survival rate of 86% (Table 7.1, Figures 7.1B, 7.1C).

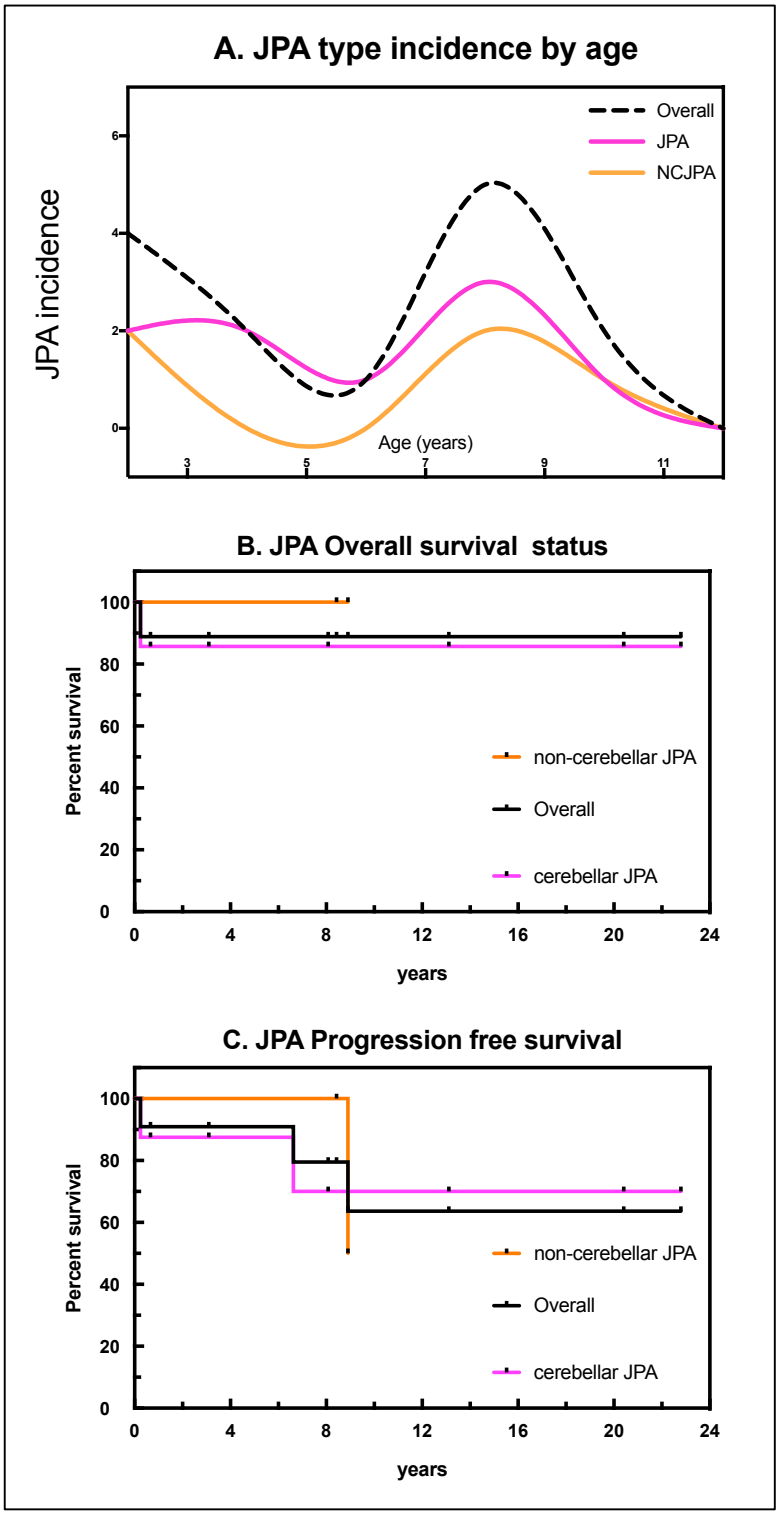

Figure 7.1: Plot showing age distribution of JPA locations

A – JPA incidences by age and location, B – Overall survival by JPA location, C – Progression free survival curves by location, dots represent last time point patients were seen

or lost to follow up, follow up median and ranges were as follows JPA: 96 months (3 months – 22 years), NC JPA: 101 months (3 months – 8 years).

The molecular phenotypes of JPA show that most (71%) were BRAF positive amplifications. This was more so for cerebellar JPA (P<0.001) than for non-cerebellar JPA. Most were either weakly or strongly positive for p16 and this was consistent across locations. Most also showed weakly or strongly positive P-ERK staining: most cerebellar tumours showed strong positivity and most non-cerebellar tumours showed weak positivity (Table 7.2).

Table 7.2: Results of molecular characterisation of the JPA cohort

		Overall	%	cerebellar JPA	%	non-cerebellar JPA	%
BRAF	Negative	4	29%	1	11%	3	60%
	Positive	10	71%	8	89%	2	40%
p16	Negative	1	7%	0	0%	1	20%
	Weak Positive	9	64%	7	78%	2	40%
	Strong Positive	4	29%	2	22%	2	40%
p-ERK	Negative	1	8%	0	0%	1	20%
	Weak Positive	6	46%	2	25%	4	80%
	Strong Positive	6	46%	6	75%	0	0%

7.4.1 Molecular data related to outcomes

Of the cohort of JPA patients, only 4 progressed or died. Of these patients; 1 non-cerebellar patient was negative for BRAF, p16 and p-ERK; 1 non-cerebellar patient was positive for BRAF, strongly positive for p16 and weakly positive for p-ERK; 1 cerebellar JPA patient was positive for BRAF, weakly positive for p16 and strongly positive for p-ERK; 1 cerebellar JPA patient was positive for BRAF and weakly positive for p16 and p-ERK, respectively (Figure 7.2). A summary of overall JPA data in this study is presented in Figure 7.3.

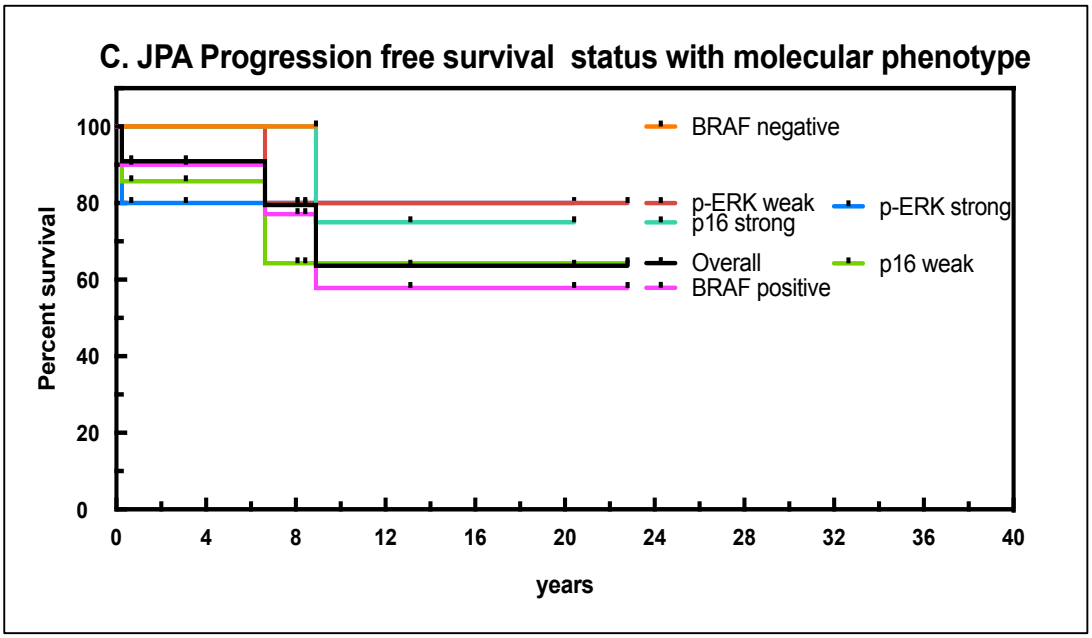

Figure 7.2: JPA Outcomes per location and molecular phenotype, dots represent last time point patients were seen or lost to follow up, follow up median and ranges were as follows BRAF negative: 54 months (3 months – 9 years), BRAF positive: 99 months (2 months – 22 years), pERK weak: 104 months (6 years – 8 years), pERK strong: 38 months (3 months – 22 years), p16 weak: 59 months (6 months – 22 years) and p16 strong: 133 months (2 months – 20 years).

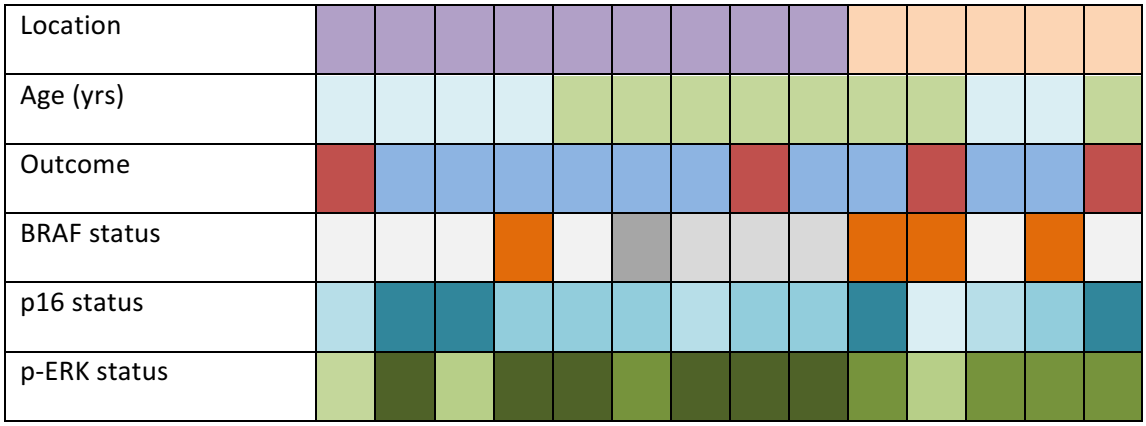

Key:

Location	Cerebellar	Non-cerebellar
Age (yrs)	<3 yrs	>3 yrs
Outcome	Poor outcome (death/unresectable tumour)	Favourable outcome
BRAF status	BRAF balanced	BRAF amplified
p16 status	p16 negative	p16 positive
p-ERK status	p-ERK negative	p-ERK positive

Figure 7.3: Overview of JPA molecular characteristics with outcomes and age demographics

Age, P = 0.8721; no difference in age between locations.

Outcomes, P = 0.4804; no difference in outcomes achieved between locations.

BRAF status, P = 0.0523; significant at P < 0.10, BRAF statistically more amplified in cerebellar JPA by chi squared test.

P16, P = 0.4978; no differences between locations.

p-ERK, P = 0.0157; significant at P < 0.10 more strongly positive in cerebellar JPA cases

7.5 Discussion

Although the cohort is relatively small with variable follow up, these represent the first data for JPA molecular analysis in a Sub-Saharan African cohort. Follow up times are presented in all cases to aid the translational interpretation of data presented herein.

The molecular characteristics of JPA in a retrospective cohort where patients were stratified based on tumour location, cerebellar JPA and non-cerebellar JPA, the median age of whom was 6 years old. As expected, metastasis and recurrence were infrequent. There is a favourable 5-year overall survival of 93%, and a progression free survival of 86% with follow up medians and ranges of 96 months (3 months – 22 years) for JPA cases and 101 months (3 months – 8 years) for NCJPA cases.

Most patients (71%) demonstrated BRAF positive amplifications; this association was statistically associated with cerebellar (P = 0.0523). Furthermore, BRAF amplified samples tended to have a poorer survival outcome as compared to the balanced BRAF samples, however, the sample size was very small to infer any significance. However, published studies have varying associations to outcome with some suggesting BRAF amplified (but KIAA1549:BRAF fusion positive) is associated with improved outcomes and others suggesting no significant associations (Colin et al., 2013; Horbinski, Nikiforova, Hagenkord, Hamilton, & Pollack, 2012; Jones et al., 2008; A. Lin et al., 2012). Possible future work could further investigate the BRAF fusions in this cohort and could provide the information on the extent of association to outcome if any.

Other studies have suggested a wider chromosomal amplification involving 7q34 which contains BRAF and HIPK2 amplified in extra-hemispheric JPA cases (Jacob et al., 2009). Our data support this finding in this local South African cohort.

Most stained weakly or strongly positive for P-ERK staining. Most cerebellar tumours showed strong positivity while non-cerebellar tumours variable positivity (P = 0.0157). This is consistent with findings in international cohorts, which report p-ERK

positivity (weakly and strongly positive) in all JPA cases irrespective of location and is indeed a hallmark of this tumour type as a reflection of MAPK pathway activation (Jacob et al., 2009).

With respect to outcomes, only 4 patients had disease progression or death, of these patients. Of note 1 non-cerebellar patient was negative for BRAF, p16 and p-ERK that interestingly had a poorer outcome. Another cerebellar JPA patient was positive for BRAF, weakly positive for p16 and strongly positive for p-ERK was also linked to a poorer outcome; 1 JPA patient was positive for BRAF and weakly positive for p16 and p-ERK, respectively had a poorer outcome. An interesting finding is that all these patients had poor or weakly positive p-ERK staining further implicating the weak staining phenotype of p-ERK as a marker of poor outcome.

Most cases stained weakly or strongly positive for p16 across both locations. Taken together low p16 had a trend toward association with poorer outcomes. This is also consistent with international studies where lack of p16 positivity predicted poorer outcome (Miettinen et al., 1999). It is also shown that astrocytomas with p16 gene deletions have a higher mitotic index and links to poor survivals (Ono et al., 1996). This study provides further evidence that p16 can be a predictor of outcomes, and p16 gene deletion studies on this cohort might be interesting to try delineating a possible mechanistic route of this phenomenon.

p16 inactivation was seen to be linked to poorer outcomes in JPA cases in this study. This finding is in agreement with other suggestions of p16 inactivation as a mechanism of tumourigenesis or malignancy (Tamayo-orrego et al., 2016).

7.6 Conclusion

In summary, this JPA cohort shows similar features to cohorts described elsewhere. The molecular characteristics shown in the current cohort are BRAF amplified by FISH and there is a strong association with cerebellar JPA cases. pERK positivity by IHC as a marker of MAPK pathway activation is consistent in this study. P16 also known as CDKN2A inactivation as determined by IHC weak staining trended towards

poorer prognosis and is also consistent with other international cohorts, thereby further implicating the lack of p16 protein in JPA pathogenesis.

8. Chapter 8 – Comprehensive proteomic profiles of Medulloblastoma and Juvenile Pilocytic Astrocytoma – Study 3 and Study 4

8.1 Introduction

There is a vast knowledge base of genomic data particularly related to paediatric brain cancers, but the proteomics knowledge is limited, and present the minority of cases in publically available proteomics repositories (Martens et al., 2006). While there is much genomic data available for MB much of the data is difficult to interpret in terms of the disease biology. For example, gene expression does not incorporate active signalling processes resulting from post-translational modifications in proteins. Furthermore, taking a combined gene profiling and proteomic approach may provide a more detailed characterisation of the pathophysiology giving biological systems level information.

8.2 MB markers

There have been previously reported biomarkers associated with MB subgroups, these include beta-catenin, ERBB2, TP53, TRKC and MYC amplifications, with more reported elsewhere (Northcott, Korshunov, et al., 2011)(Table 8.1). To interpret the massive data related to MB, enrichment pathways were constructed with statistical associations. These reveal biochemical pathways that are over represented and disease biology can then be better inferred.

Furthermore, cytogenetic data relating to MB can be represented in karyotype mapping of proteomic data thus helping interpret and validate findings for DNA changes such as chromosomal deletions or amplifications (Table 8.2). Transcript variants and gene fusion products can also be inferred by proteomic experiments. Although this is not the focus of this study, it is however a likely avenue for further proteomic investigations.

Table 8.1: Genetic biomarkers and pathways associated to MB subtypes (Northcott, Korshunov, et al., 2011)

Pathway associated		P value	Molecular marker
WNT	Axonal guidance signalling	<0.001	EPHA7, FZD10, BMP4, WNT16, EPHA4, NFATC4, SLIT2, EPHA3, ADAM12, PRKCD, FZD6, ADAM19, PLCB1, SEMA3B
	WNT/β-catenin signalling	<0.001	FZD10, AXIN2, WIF1, FZD6, DKK4, WNT16, DKK2, LEF1, KREMEN1, DKK1
	Angiogenesis	0.0033	FZD10, BMP4, PRKCD, FZD6, LEF1, DKK1
	O-glycan synthesis	0.0417	GLT8D2, GALNT7, GALNT14, GALNT12, GALNTL2
	Basal cell carcinoma signalling	0.0077	FZD10, BMP4, FZD6, WNT16, LEF1
SHH	SHH signalling	<0.001	DYRK1B, ARRB2, GLI2, GLI3, HHIP, GLI1, PTCH2
	Basal cell carcinoma signalling	<0.001	TP53, GLI2, GLI3, LEF1, HHIP, GLI1, BMP5, FZD7, PTCH2
	WNT/β-catenin signalling	<0.001	TP53, SFRP4, TCF4, HDAC1, SOX2, SOX9, RARB, TGFB2, SFRP5, PPP2R2C, LEF1, SFRP1, TCF7L2 (includes EG: 6934), FZD7
	Axonal guidance signalling	<0.001	GLI2, PLXNC1, CXCR4, SEMA6A, GNG3, HHIP, NFATC4, BMP5, ROBO1, PTCH2, PLCB4, GLI3, SRGAP1, SDC2, NTRK3, NGFR, EFNA5, ABLIM3, PDGFD, GLI1, PRKD1, FZD7, UNC5C
	Human embryonic stem-cell pluripotency	0.0029	SOX2, NTRK3, PDGFRA, SPHK1, TGFB2, LEF1, PDGFD, BMP5, FZD7
Group 3	Phototransduction pathway	<0.001	GNB3, GNGT1, RCVRN, PDE6H
	WNT/β-catenin signalling	0.0093	MYC, NLK, TGFB1, TGFBR3, PPP2R2B
	Glutamate receptor signalling	0.0112	GNB3, SLC17A7, SLC1A7
	Thyroid cancer signalling	0.0407	MYC, RXRG
	P38 MAPK signalling	0.042	MYC, TGFB1, EEF2K
Group 4	Semaphorin signalling in neurons	<0.001	ARHGEF12, RND1, RHOT1, DPYSL4, DIRAS3, FNBP1
	cAMP-mediated signalling	0.0027	GRK4, GRM8, RGS7, ADCY1, STAT3, PDE4B, AKAP9, CHRM3, PDE1C
	G-Protein-	0.0049	HTR2C, GRK4, GPR12, GRM8, RGS7, ADCY1, STAT3,

coupled receptor signalling		PDE4B, CHRM3, PDE1C
P53 signalling	0.0060	KAT2B, CCND2, GADD45G, C12ORF5, HIPK2, TP53
Cardiac β-adrenergic signalling	0.0061	ADCY1, CACNA1C, PDE4B, GNG2, AKAP9, CACNA1A, PDE1C

Table 8.2: Genomic aberrations previously reported (Kagawa et al., 2006)

Frequency seen in MB	Type of genomic aberration
	MSH2 gene amp
60%	NMYC gene amp
	AKT3 gene amp
	EGFR gene amp
	SNRPN gene amp
	MYB gene amp
	PTEN gene amp
	17q gain
	7q gain
	17p loss
	1p minor loss
	8p and 8q minor loss
	11p minor loss
10-40%	10p and 10q minor loss
	13q minor loss
30%	16q minor loss
20%	Xp and Xq
	Iso chromosome 17

8.3 JPA markers

It has been suggested that JPA tumours genetically reflect the brain location from which their non-malignant cells originated (M. K. Sharma et al., 2007). There is differential gene expression between the supratentorial JPAs and those in the posterior fossa (Jensen et al., 2005; M. K. Sharma et al., 2007). Several markers have been reported by genomic investigations and are specific for the pathophysiology (Table 8.3). There have also been reported low and high-grade JPA markers possibly linked to tumour aggressiveness and outcome (Table 8.4).

Table 8.3: Genomic markers associated with JPA locations adapted (Zakrzewski, Pfeifer, Oczko-wojciechowska, & Jarz, 2015)

Cerebellar JPA associated genes	**Reported p-value**	**Non-cerebellar JPA associated genes**	**Reported p-value**
IRX1, 2, 5	<1e-07	SIX1, 3, 6	<1e-07
PAX3	<1e-07	LHX2	<1e-07
RNF182	<1e-07	GPR98	<1e-07
CNTN1, 3	<1e-07	TMEM30B	<1e-07
SUSD5	<1e-07	FOXG1	<1e-07
CRNDE	<1e-07	SLIT1	<1e-07
FAM89A	<1e-07	ARX	<1e-07

Table 8.4: Low and high-grade JPA proteins published as adapted (Odreman et al., 2005)

	Genes associated
Low-grade JPA	GFAP, CCT5, PDIA3, PRKACA, QDPR, UCHL1
High-grade JPA	INA, PRDX1,6, APOA1, ANXA5, CRYAB

Furthermore, TIMP3 and bFGF have been suggested markers for JPA diagnosis systemically in urine (Fehnel et al., 2016).

A possible reason for brain region-selective JPAs is the region-specific gene expression profiles of astrocytes. Such associations are interesting and as yet inconclusive. However the JPA cell of origin and region specific expression hypotheses might be related to additional microenvironment responses in these tumours (Y.-H. Chen & Gutmann, 2014).

8.4 Technological advancements in mass spectrometry-based proteomics for clinical samples

There has been great improvement in the proteomics fields, with the technology becoming robust, reproducible, quantitative and more accessible for clinical research. While the technology can provide much systems level information, its use in the brain tumour field has been under-utilised and there is much potential for its use in discovering disease biomarkers and elucidation of pathophysiology and biological mechanisms of disease (Tian, Sangar, & Price, 2015). While proteomics-based studies are promising, the technology is limited in that it does not provide complete coverage, rather a snapshot of the proteome. There have been improvements in separations with nanoflow liquid chromatography separation, which allows analysis of very small amounts of samples, such as in FFPE sections. The resulting nanoflow system technology provides good separation and a high sensitivity (Sest´ak, Moravcov´a, & Kahle, 2015). However, even with such technological improvements, clinical samples are particularly challenging for proteomic analysis due to their complexity. In such samples, there is usually a small number of highly abundant (endogenous contaminating) proteins such as structural proteins and chromatin proteins that may be supressing the signals produced by low abundant proteins that might more useful in answering biological questions (Camerini & Mauri, 2014). Therefore, strategies have been employed to reduce the interference and improve the signal produced by the few high abundant proteins using gel-based fractionation, gel-free fractionation and depletion approaches as reviewed elsewhere (Camerini & Mauri, 2014). Each of these strategies has advantages and limitations and the choice of separation needs to be tailored to the application and the given resources in a setting. Given that FFPE material in a clinical cohort is variably cross-linked, in relation to tissue thickness, fixation times and sample storage issues, intactness of proteins is likely highly variable in FFPE tissues. Therefore, to counteract this variability peptide level fractionation is said to be more appropriate for FFPE clinical samples in this cohort. Peptide level fractionation has been reported to provide larger sequence coverage in clinical samples (Veelen & Palmblad, 2013).

Fractionation chemistry targets peptides physicochemical properties range, such as isoelectric point, ionisation, hydrophobicity, etc. High pH reverse phase fractionation is one of these techniques: it employs peptide separation based on hydrophobicity in interacting with an immobilised chemical substrate and flowing mobile phases with differing polarity of the solvent. It allows faster partitioning and is salt free. Compared to other techniques, this allows robust, economical solvent flow and no need for salt removal prior to MS analysis (Shen & Smith, 2012). Following fractionation, pooling is used to collect non-adjacent fractions to utilise the full MS experimental time. This study, therefore, employed high pH reverse peptide fractionation to gauge the proteomic coverage achieved in the analysis of these cohorts.

Previous proteomic studies have the major limitations of using cell culture models, pooling any available tissue samples or gauging only certain fractions of tumour tissue such as acid soluble fractions, and not applying effective quantitative strategies for extensive analysis (Martelli et al., 2016)(Peyrl et al., 2003)(Martelli et al., 2015). Therefore, to gauge a comprehensive proteomic profile of MB and JPA cutting edge proteomic techniques and analysis pipelines were uniquely assembled to give such insight.

8.5 Study 3 and Study 4 Aims

Study 3 Aims

The initial aim of proteomic profiling of MB formed Study 3, which investigated

1) The profiles of these tumours, as well as
2) The utility of single sample runs,
3) The methodology was tested against a more complex and extensive fractionation run.

The coverage and power of the proteomic study has to be interpreted taking the level of coverage into account, similar to genomic studies where genome coverage is considered.

The MB samples have been characterised into the established 4 subgroups by a gene expression technique using Nanostring RNA technology and a panel of immunohistochemistry markers (Chapter 6). We used the subgrouping and outcomes as classifiers to determine specific proteomic markers respectively. The investigative samples used are paediatric brain tumour specimens from the retrospective cohort previously described. Further validation work proceeded with a targeted proteomic approach on an additional smaller cohort of samples collected in the prospective cohort.

Study 4 Aims

Study 4A investigated proteomic profiles of cerebellar and non-cerebellar JPA tumours. A discovery proteomic workflow was performed on a training set cohort of JPA cases (n=14) and subsequently validated using a targeted proteomic approach (n=5) on a test set validation cohort.

JPA proteomic profiles were investigated comparing cerebellar JPA and non-cerebellar JPA in the JPA retrospective cohort. Furthermore, proteomic profiles were determined to investigate 1) proteins that are specifically associated with cerebellar JPA versus non-cerebellar JPA tumours, and 2) those that are linked to molecular data (Chapter 6). Malignancy-associated proteins were then investigated by comparing MB to the generally less aggressive JPA. These findings were validated taking a targeted proteomic approach in the prospective cohort. Biomarkers were statistically verified and select markers were used to generate an inclusion list for targeted proteomic experiments.

8.6 Study 3 and Study 4 Methods

8.6.1 Cohort and study design

Both the investigative cohort and validation cohort were used in this study. MB and JPA samples were randomised and subject to sample processing and mass spectrometric analysis. Further cohort characteristics and study designs have been discussed previously in this thesis.

8.6.2 Cohort inclusion criteria

For samples to be included in this study, they had to meet minimal criteria in order to proceed to the statistical analysis. Firstly, samples included here had to have available tissue blocks that passed staining with routine H&E tissue architecture stains. Furthermore, samples had to produce a discernible mass spectrogram free of technical spikes and with the machine passing a reference test at regular intervals.

8.6.3 Mass spectrometry methods

8.6.3.1 Sample preparation

All methods were done in duplicates with 7.5 µg starting proteomic material. Trypsination was carried out using sequencing-grade modified trypsin (Trypsin Ultra, New England Biolabs) at a ratio of 1:50 enzyme to proteomic material. All reagents obtained were of mass spectrometric grade (Sigma-Aldrich).

Filter-aided sample preparation (FASP) was performed by adding 7.5 µg of total protein. All buffer exchanges were carried out by centrifugation at a speed of 14 000 g for 15 min. Protein extract was transferred into a 500 µL Ultracel 30 000 MWCO centrifugal unit (Amicon Ultra, Merck). Protein extracts were buffer-exchanged with three rounds of 200 µL UT buffer (8 M urea, 0.1 M Tris, pH 8.5). Reduction with UT containing 10mM 1,4-dithiothreitol (DTT) was carried out and buffer exchanged with two rounds of UT, alkylation of cysteine bonds was carried out by incubation in the dark for 20 min in 200 µL UT buffer containing 0.05 M

Iodacetamide (IAA). Two 200 µL UT buffer exchanges were used to remove the alkylating agent, followed by three buffer exchanges with 100 µL of ABC buffer containing $CaCl_2$ (50 mM ammonium bicarbonate buffer, 20 mM $CaCl_2$, pH 8). Trypsin (New England Biolabs) was added to the retentate at a ratio of 1: 50 trypsin to proteomic material. Proteolysis was carried out at 37 °C for 18 h in a wet chamber. Three rounds of 40 µL of ABC buffer were used to elute the peptide-rich solution.

8.6.3.2 Desalting of tryptic digests

Peptide-rich eluates were desalted using a homemade stage tip containing Empore Octadecyl C18 solid-phase extraction disk (Supelco) (Rappsilber, Ishihama, & Mann, 2003). Activation, equilibration, and peptide wash and elution were all carried out using centrifugation at a speed of 5000G for 5 min with varying concentrations of acetonitrile (ACN) solutions containing 0.1% formic acid (FA) final concentration. Briefly, activation and equilibration of the C18 disk was carried out using three rinses with 80% ACN, followed by three rinses with 2% ACN, respectively. Approximately 10 µg of trypsinised peptides solution was loaded onto the disk and centrifuged. Desalting was carried out using three washes of 2% ACN. Elution of desalted peptides into glass capillary tubes was carried out using three rounds of 100 µL of 60% ACN. Peptides were dried in a vacuum and resuspended in 2% ACN at 200 ng/µl concentration.

8.6.3.3 LC MS/MS analysis

Liquid chromatography separation was done with a home-packed 100 µM ID × 20 mm precolumn connected to a 75 µM × 200 mm analytical column packed with C18 Luna beads (5 µm diameter, 100 Å pore size; Phenomenex 04A-5452). The columns were connected to an Ultimate 3500 RS nano UPLC system (Dionex). Approximately 200ng of peptide solution was loaded for each analysis; this amount was adjusted to

match the total ion currents of others in the cohort to allow more effective quantitation. Peptides were eluted with the following gradient of 10 min at 2% ACN, increase to 25% ACN for 115 min, to 35% ACN over 5 min, to 80% ACN over 5 min, followed by a column wash of 85% for 20 min at a constant flow rate of 300 µL/ min. Typical backpressure values during separation were <350 bar. Mass spectra were acquired with an Orbitrap Q Exactive mass spectrometer (Thermo Scientific) in a data-dependent manner for discovery experiments and targeted mode for validation experiments, with automatic switching between MS and MS/MS scans using a top-10 method. MS spectra were acquired at a resolution of 70 000 with a target value of 3×10^6 ions or a maximum integration time of 250 ms. The scan range was limited from 300 to 1750 m/z. Peptide fragmentation was performed via higher-energy collision dissociation with the energy set at 25 Normalised Collision Energy. Intensity threshold for ions selection was set at $1.7e^4$ with charge exclusion of $z = 1$ and $z > 5$. The MS/MS spectra were acquired at a resolution of 17 500, with a target value of $2 \times 10e^5$ ions or a maximum integration time of 120 ms and the isolation window was set at 4.0 m/z.

8.6.3.4 Bioinformatics analysis

MaxQuant version 1.5.3.12 was used to process the raw data resulting in peptide and protein group identification. Andromeda search engine used Uniprot human proteome (UP000005640) with 70 236 proteins as the target decoy database. MS/MS search was done using the default parameters with a MS/MS mass tolerance of 20ppm. Fixed modification was set to *Cysteine Carbamidomethylation* and variable modification was set to *Methionine oxidation* and *acetylation of the protein n-terminus*. Trypsin/P was set as the protease with up to 3 missed cleavages allowed. Results were filtered based on 0.01 false discovery rates at both the peptide and protein levels, with the minimum peptide length set to 7 amino acids. Gene ontology was assigned to proteins using Panther and Comparative GO (Fruzangohar et al., 2013; Mi, Poudel, Muruganujan, Casagrande, & Thomas, 2016). Plots generated using Perseus software and statistical analysis was performed using ANOVA with Bonferroni correction for

multiple comparisons using GraphPad Prisms (version 6, GraphPad Software, La Jolla California USA). For targeted MS validation analysis, Skyline (version 3.6) was using the Uniprot human proteome (UP000005640) as background. Reproducible high-confidence peptide transitions were selected for the targeted runs.

8.6.3.5 Statistical analysis

Label Free Quantitation (LFQ) intensities from MaxQuant were used to normalise data using total ion intensities for all samples. Such normalisation have been suggested to be effective in clinical samples provided the chromatogram and the total ion intensities in the cohort are similar (Moulder, Goo, & Goodlett, 2016). These values were used for downstream analysis of fold changes prior to statistical analysis. All potential contaminating protein and protein groups with PEP scores above 0.01 were discarded from downstream analysis. Representative protein group lists were subject to gene list enrichment analysis using List2Networks and Enrichr (E. Y. Chen et al., 2013). Further biological pathway analysis was performed using Reactome and statistical pathways with p-values < 0.01 were deemed significant (Gillespie, Vastrik, Eustachio, Schmidt, & Bono, 2005). Data normality was investigated using the Shapiro-Wilk normality test. Cytoscape and Panther platforms were used for data analysis and protein pathway analysis visualisations. Statistical measures were generated in all above and were used to infer the statistical significance and likelihood of dysregulation and enrichment of specific pathways and processes.

8.7 Study 3 Results

8.7.1 Validation cohort characteristics:

The clinical characteristics of the validation cohort are as follows, the MB molecular subtypes, age, gender and outcome information presented below (Table 8.0). This was collected on a prospective basis and patients were included based on the extent and availability of latest comprehensive outcome data.

Table 8.0: Clinical and molecular characteristics of the test and validation cohort.

Proteomic MB test cohort		**Number**	**Percentage**
Total cohort size		26	
Age	Mean	6,4	
	Median	0	
	Range	1 - 12 years old	
Gender	Male	9	35%
	Female	17	66%
Year of Diagnosis	Range	1989 - 2014	
MB subtype	WNT	6	
	SHH	9	
	Group 3	5	
	Group 4	6	

Proteomic JPA test cohort		**Number**	**Percentage**
Age	Mean	5,1	
	Median	6	
	Range	4 months - 10 years	
Gender	Male	9	64%
	Female	5	36%
Location	Cerebellar	9	64%
	Non-cerebellar	5	36%
Year of Diagnosis	Range	1993 - 2011	

Validation cohort clinical and demographic characteristics				
Year		2014-2016		
Age range (years)		2,8-12		
Gender	Males		4	40%
	Females		6	60%
MB	**Total**		**7**	
WNT subtype			2	29%
SHH subtype			1	14%
Group 3 subtype			2	29%
Group 4 subtype			2	29%
MB Outcomes	Progression free survival		4	57%
	Relapsed		3	43%
JPA	**Total**		**4**	
Cerebellar JPA			2	50%
Non-cerebellar JPA			2	50%
JPA Outcomes	Progression free survival		2	50%
	Relapsed		2	50%

8.7 Pre-Study 3 – Fractionation and level of proteomic depth of coverage in this study

Peptide level fractionation was performed on 3 patient samples and a reference cell culture sample (data not shown) to assess the level of proteome coverage achieved in this study. Matched samples from the same biopsy were split into 2, one treated with high pH reverse phase fractionation yielding 11 fractions and concatenated into 3 fraction runs, and the other non-fractionated. The fractionated sample produced a mean of 783,3 ± 148.8 proteins more than the non-fractionated samples. This is an increase yield of 1,46 times the coverage (Figure 8.1A). Additionally, looking at the distribution of peptide intensities, it is seen that peptides identified in fractionated samples are represented in the lower range of signal intensity, less than $1e^9$ (Figure 8.1B).

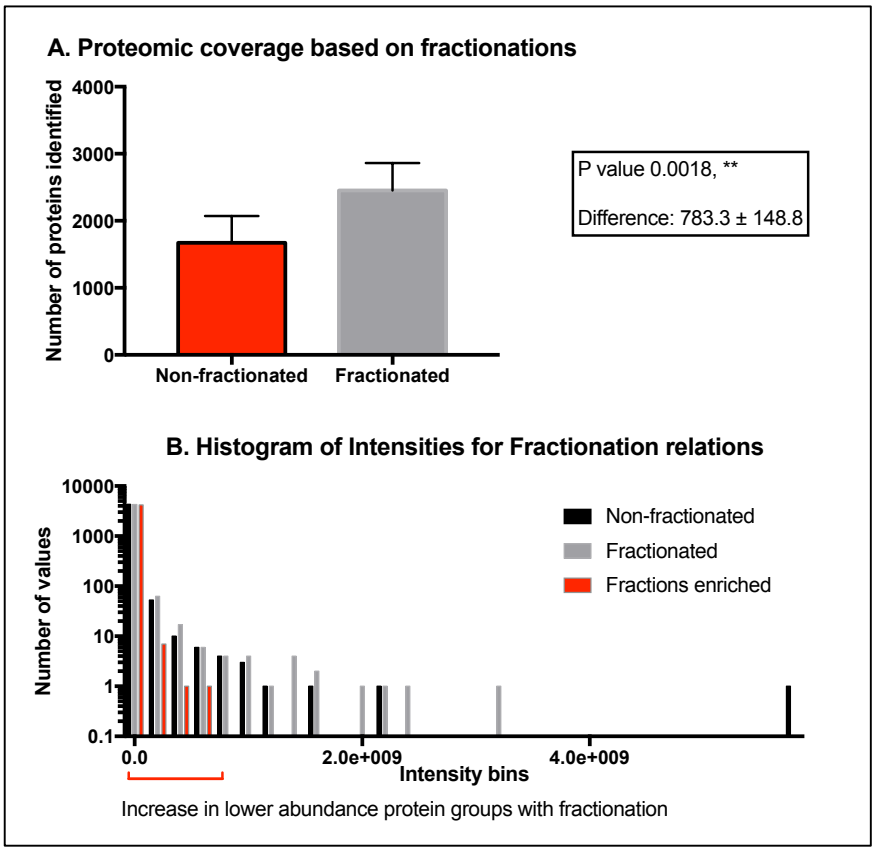

Figure 8.1 Proteomic data in this study in context of proteome coverage achieved, n=3

A – The number of protein groups identified using matched fractionated and non-fractionated samples. There is a statistically significant difference in the number of proteins identified, with a mean difference of 783.3 ± 148.8, suggesting that without extensive fractionations in these samples, a mean of 783.3 proteins are not being identified. Proteomic data from the current study has to be interpreted with this in consideration. B – Histogram showing spread over m/z signal intensities produced, there is an enrichment in fractionated samples for less intense signals, indicating that fractionation gives rise to more, less-intense peptides.

Pre-Study 3 Discussion

This study aimed to determine the level of proteome coverage achieved in the current study design. Shotgun proteomic experiments usually only present a snapshot of the proteome, with the resulting proteins identified giving a representative sampling of the total proteins. The proteins identified therefore provide a pool of candidate protein

markers, which can be further investigated for utility as a guide for disease mechanisms or usefulness as a diagnostic or prognostic marker. Furthermore, limited and small samples from biopsies usually lead to the decision to perform single shotgun proteomic experiments on these types of samples. However, the lower abundance protein groups are often missed in unfractionated experiments, and all results in shotgun type experiments should be interpreted in this light.

The current study therefore determined the coverage achieved in this experiment. There is an increase in lower abundance protein groups and about 800 more protein groups with high-pH reverse phase fractionation.

There are however, 20 197 curated protein-coding genes in the human reference map and additional splice isoforms, with about 10 000 proteins and neuropeptides suggested to be found in brain tissues in human diseased or animal model brain tissue (Klose et al., 2002; Y. Li et al., 2016). So, coverage in this study reveals up to 2000 proteins without extensive fractionation and about 800 more with fractionation. Therefore, the utility if single MS runs represents a snapshot of the proteome representing 20% of the total theoretical proteome. Furthermore, the use of advanced high resolution MS allows for great sensitivity, scope and dynamic range which enables shotgun proteomic experiments to quantitate differences between clinical samples for robust biomarker discoveries (Mcdonald & Yates, 2002).

8.7.1 Study 3A – Subgroup specific proteins in MB

This study examined the subgroup-specific proteins identified in the MB retrospective cohort. A total of 1452, 1934, 1850 and 1481 protein groups were identified across the WNT, SHH, Group 3 and the Group 4 subtype, respectively. To better understand the multitude of proteins identified, gene ontology (GO) enrichment analysis was employed in a parallel analysis for comparative enrichments using Bonferroni multiple testing correction and all results have a p value of $p < 0.05$. This analysis revealed cellular component enrichment of endoplasmic reticulum, immunoglobulin, and ribonuclear complex associations in the WNT subtype; excitatory synapse, SWI/SNF and membrane vesicle in SHH; ATPase degradation complexes, ribonuclear and DNA replication associations in Group 3; protein folding, splicing and motor protein association in Group 4 MB in this cohort (Table 8.2).

8.7.3.1 Results Study 3A

Table 8.2: GO cellular component enrichment for MB subgroups

Cellular component enrichment			
WNT (n=6)	**SHH (n=9)**	**Group 3 (n=5)**	**Group 4 (n=6)**
endoplasmic reticulum-Golgi intermediate compartment	CRD-mediated mRNA stability complex	VCP-NPL4-UFD1 AAA ATPase complex	prefoldin complex
endoplasmic reticulum part	excitatory synapse	preribosome	U6 snRNP
I band	cell-cell junction	aminoacyl-tRNA synthetase multienzyme complex	banded collagen fibril
Z disc	vacuolar membrane	preribosome, large subunit precursor	fibrillar collagen trimer
rough endoplasmic reticulum	SWI/SNF superfamily-type complex	small nucleolar ribonucleoprotein complex	dynactin complex
F-actin capping protein complex	actin-based cell projection	DNA replication factor A complex	microtubule organizing center
SMN-Sm protein complex	eukaryotic 48S preinitiation complex	mitochondrial proton-transporting ATP synthase complex, catalytic core F(1)	sarcoplasm
COPI vesicle coat	basal lamina	proton-transporting ATP synthase complex, catalytic core F(1)	cytoplasmic side of plasma membrane
fascia adherens	translation preinitiation complex		Lsm1-7-Pat1 complex

immunoglobulin complex, circulating	eukaryotic translation initiation factor 3 complex	cytoplasmic dynein complex
cell surface	mitochondrial intermembrane space	
secretory IgA immunoglobulin complex	clathrin-coated pit	
polymeric IgA immunoglobulin complex	proton-transporting ATP synthase complex, coupling factor F(o)	
IgA immunoglobulin complex, circulating	mitochondrial respiratory chain complex III	
GAIT complex	endocytic vesicle	
monomeric IgA immunoglobulin complex	podosome	
IgA immunoglobulin complex	cell-cell adherens junction	
ER to Golgi transport vesicle	organelle envelope lumen	
	respiratory chain complex III	
	flotillin complex	

Molecular function enrichment in this dataset revealed immunoglobulin binding, glycation product binding and disulphide bond activity in WNT; NADH quinone, protein translation regulation and GTPase activity in SHH; only NFκB binding and ATP synthase in Group 3; dopamine, protein and amino acid binding, as well as G-protein related serotonin binding in Group 4 MB (Table 8.3)

Table 8.3: GO molecular function enrichment for MB subgroups

Molecular function enrichment			
WNT	SHH	Group 3	Group 4
5S rRNA binding	beta-tubulin binding	NF-kappaB binding	molecular function regulator
immunoglobulin receptor binding	mRNA 5'-UTR binding	proton-transporting ATP synthase activity, rotational mechanism	G-protein beta/gamma-subunit complex binding
extracellular matrix bindi	RNA helicase activity		G-protein coupled serotonin receptor binding
RAGE receptor binding	oxidoreductase activity, acting on NAD(P)H, quinone or similar compound as acceptor		amino acid binding
translation initiation factor binding	NADH dehydrogenase activity		poly(U) RNA binding
Ran GTPase binding	NADH dehydrogenase		ATPase activator activity

	(quinone) activity	
disulfide oxidoreductase activity	NADH dehydrogenase (ubiquinone) activity	pyrimidine nucleotide binding
steroid binding	Rac GTPase binding	protein binding involved in protein folding
TBP-class protein binding	translation regulator activity	modified amino acid binding
protein disulfide isomerase activity	GTPase binding	dopamine receptor binding
intramolecular oxidoreductase activity, transposing S-S bonds		magnesium ion binding
monosaccharide binding		

The biological process enrichment profile of MBs in this cohort revealed vesicle-related processes, oxidative stress and protein folding processes in WNT; DNA replication, epigenetic regulation, cell growth and differentiation in SHH; mis-folded protein responses, gene silencing, DNA repair and protein sumoylation in Group 3; and ATPase function, synapse and cell development processes in Group 4 MBs in this cohort (Table 8.4).

Table 8.4: GO biological process enrichment for MB subgroups

biological process enrichment			
WNT	SHH	Group 3	Group 4
vesicle coating	positive regulation of substrate adhesion-dependent cell spreading	purine-containing compound biosynthetic process	modulation of synaptic transmission
COPII-coated vesicle budding	aspartate family amino acid metabolic process	protein heterotrimerization	regulation of dendrite development
endoplasmic reticulum unfolded protein response	glutamine metabolic process	ERAD pathway	positive regulation of ATPase activity
vesicle targeting, rough ER to cis-Golgi	DNA unwinding involved in DNA replication	nucleotide-excision repair	regulation of ATPase activity
protein export from nucleus	actin filament bundle assembly	gene silencing	extracellular matrix disassembly
ossification	neuron projection extension	acute-phase response	regulation of synaptic vesicle transport
response to lipid	regulation of viral life cycle	DNA repair	ATP hydrolysis coupled transmembrane transport
vesicle targeting, to, from or within Golgi	substrate adhesion-dependent cell spreading	ribose phosphate biosynthetic process	positive regulation of intrinsic apoptotic signaling pathway
cellular response to unfolded protein	hexose biosynthetic process	protein sumoylation	regulation of neurogenesis
IRE1-mediated unfolded protein response	regulation of multi-organism process	maturation of LSU-rRNA	cellular response to oxygen radical
positive regulation of cell-substrate adhesion	establishment or maintenance of cell	acute inflammatory response	cellular response to superoxide

	polarity		
COPII vesicle coating	nucleobase metabolic process	purine nucleotide biosynthetic process	positive regulation of dendritic spine development
retrograde vesicle-mediated transport, Golgi to ER	positive regulation of cytoskeleton organization	2-oxoglutarate metabolic process	nucleus organization
maintenance of location in cell	Fc receptor mediated stimulatory signaling pathway	purine ribonucleotide biosynthetic process	positive regulation of dendrite development
cell death in response to oxidative stress	muscle system process	ER-associated ubiquitin-dependent protein catabolic process	cellular chemical homeostasis
vesicle targeting	actin filament bundle organization	cellular response to DNA damage stimulus	glyceraldehyde-3-phosphate metabolic process
cellular response to topologically incorrect protein	regulation of symbiosis, encompassing mutualism through parasitism	chaperone-mediated protein complex assembly	regulation of synaptic plasticity
response to alcohol	morphogenesis of an epithelium		regulation of DNA replication
maintenance of location	endosomal transport		gene silencing by RNA
regeneration	protein targeting to mitochondrion		rRNA-containing ribonucleoprotein complex export from nucleus
cap-independent translational initiation	positive regulation of multi-organism process		glyoxylate metabolic process
regulation of vacuolar transport	IMP metabolic process		protein localization to cytoplasmic stress granule
glycogen catabolic process	gluconeogenesis		negative regulation of hydrolase activity
	Fc-gamma receptor signaling pathway		oxaloacetate metabolic process
	monocarboxylic acid catabolic process		tRNA metabolic process
	positive regulation of cell development		
	response to insulin		
	vacuolar transport		
	positive regulation of cysteine-type endopeptidase activity involved in apoptotic process		
	fibril organization		
	negative regulation of neuron apoptotic process		
	cellular amino acid catabolic process		
	dendritic spine development		
	tissue morphogenesis		
	lamellipodium organization, Ephrin receptor signalling		

The individual highly abundant protein groups statistically associated with subgroups (FDR 0.1%, ANOVA with multiple testing correction, $p<0.05$). WNT associated protein groups include VIM, DKK factors, COLA and RNA elongation factors; SHH contains PDLIMs, GAB, heat shock proteins and NEFM neurofilament proteins; Group 3 proteins include ribonuclear proteins, mitochondrial proteins COX, PYCR1 and sumoylation proteins; and Group 4 contains serine proteases RELN and serine protease inhibitors PEBP1, neurodevelopment proteins, TNIK and VAT1 (Table 8.5).

Table 8.5: Individual proteins associated with subgroup

MB Subtype	Statistically associated proteins
WNT	VIM, FN1, LDHA, EEF2, COL6A2, P4HB, ATP5D, FBLN1, EIF5A;EIF5AL1, SRSF6, ALDH1A1, MYH11, SH3BGRL3, PYGL, CTSZ, LAMP1, CST3, SCGN, CDK5RAP2, PGM5, HSPA2, S100A4, DES, HLA-DRA, MTPN, B2M, GPNMB, TPM1, PCSK9, TNC, LAMP2, NAGA, MYDGF, PNPO, IGLV1-47, MAPK3, SFN, CPXM1, MDK, ADAMTSL1, CENPP, P4HA2, ERAP1, PLBD2, IGHV4-59, MMP2, SRPRB, MGP, CES1, AOC3, COL7A1, CDH2, CNPY4, SERPINB6, GYPA, ALCAM, DSP, ALPL, CASP3, LAMTOR3, ITPR1, P4HA1, SEC61A1, PIN4, EPHA7, IGFBP7, FBLN2, EIF4E, VAMP3, DKK4
SHH	PDLIM3, HIST1H1D, HIST2H2BD, TUBAL3, SORCS3, , HBG2, KATNAL2, PGAM2, ALDH1A3, TANC2, SNCB, ADD3, METTL7A, GAB1, ADD2, ACTB, HEPACAM, NEFM, HSPA12A, IGLC2, CNTN2, PLD3, SHROOM2, HBA2, DCX, PEPD, COL21A1, FDPS, RPL21, PDYN, NLN, HSP90AB2P, HYDIN, EHD1, USP10, SLC2A1, TMEM97, CISD2, NDUFS2, SUGT1, ATP1B3, EBF3, MAPK1IP1L, MAP1LC3A, NDUFA10, SYT1, PACSIN2, MAPT, PGM2L1, RPS27, TMEM109, FERMT2, CLIP2, NDUFS4, CSK, CAMK2B, AK4, GNPDA1
Group 3	HIST1H2AJ, HNRNPR, PYCR1, ISOC1, SRM, CPSF7, CSNK2A1, ACADM, HIST1H1C, PRSS1, HIST2H2BE, SUMO3, HSPA6, TMSB10, FAU, TUBB2A, HSPA8, RPL29, HNRNPK, FCGBP, COX5B, HMGN5, HIST2H2AB, C2orf80, LTF, TOMM6, LIN7A, PCK2, CCAR1, COX4I1, DNAH8, SAA1, MAL2, NUCKS1, SNRPC, NDUFA4, MYL9, SAA2, CTRC, KRT81, RAD23A, RPRD1A, FUBP3, COX6C, IGKV1-5, PPM1A, COX7A2, BCAP31, MACROD1, TPD52, EML1, UBE2M, GUK1, CELA3B, MAGOHB, HMGN3, LAGE3, ERICH3, PPBP, SPON1, NDRG1, LETM1, FAF1, GNG5, TOMM20, EEF1E1, CFAP99
Group 4	H3F3B, FKBP1A, PEBP1, HIST1H3A, PDXP, VAT1, MYH4, PADI2, TNIK, COL5A1, ATP1B2, PBXIP1, NPTN, TRIO, DCC, CTSG, FAM171A2, AIPL1, PRNP, SEZ6, KIF12, IGSF8, HAGH, CDIPT, MAPRE2, CELSR3, CLSTN1, HP, AMPH, NT5C, PTGDS, PFDN1, RAB4A, GPC2, SLC44A2, ENGASE, ELANE, HSPA4L, CLIC6, PLXNA2, DDI2, LSM7, NSUN2, RHO, NQO2, MYO18A, LYPLA2, HSP90AB4P, MSI2, IRF2BPL, WDR37, COL11A1, RELN, BAZ1B, SYNJ1, SYNE2, DFNA5, HIST1H2AC, PANK4, RRAS2, SREK1, GSK3A, SRR, EFNB3, S100A16, KIAA1468

Table 8.6: Validated peptide results showing MB group specific peptides, Green – extent of overrepresentation abundances, Red – extent of underrepresentation abundances.

WNT				SHH				GROUP 3				GROUP 4			
Protein	Peptide	Intensity in WNT	other groups	**Protein**	Peptide	Intensity in SHH	other groups	**Protein**	Peptide	Group3	other groups	**Protein**	Peptide	Group 4	other groups
HSPA5	IEIESFYEGEDFSETLTR			**DPYSL2**	DIGAIAQVHAENGDIIAEEQQR			**TGFBI**	TLFELAAESDVSTAIDLFR			**RHOA**	DQFPEVYVPTVFENYVADIEVDGK		
	SQIFSTASDNQPTVTIK				AITIANQTNCPLYITK			**ARAP1**	AFVPPLAEDLLAR			**FRY**	LELIDLLAR		
DAD1	FLEEYLSSTPQR			**DPYSL5**	IPHGVSGVQDR				LGSVSLIPLR			**HAGH**	ALLEVLGR		
	SASVVSVISR				TISASTQVQGGDFNLYENMR			**DDA1**	EYPSEQIIVTEK						
FNB1	TNDDQTMCLDINECER			**DPYSL3**	AALAGGTTMIIDHVVPEPESSLTEAYEK				DQEQVELEGESSAPPR						
	TCVDINECLLEPR				AITIASQTNCPLYVTK			**LUC7L2**	LAETQEEISAEVAAK						
INA	HSAEVAGYQDSIGQLENDLR			**DPYSL4**	MDENEFVAVTSTNAAK				VEQLGAEGNVEESQK						
	SFGSEHYLCSSSSYR				GAPAVVISQGR			**LUC7L3**	MISAAQLLDELMG						

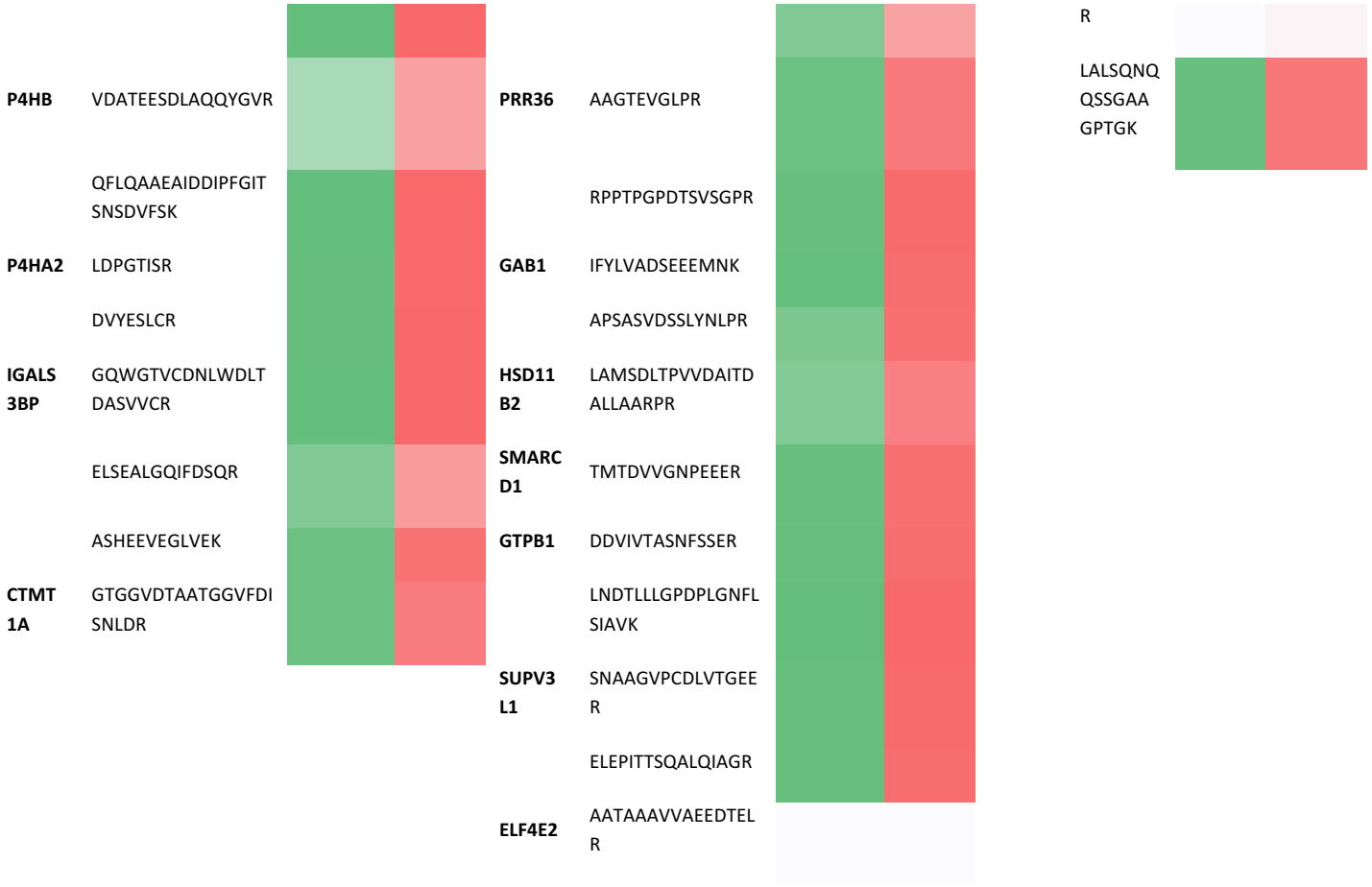
P4HB
VDATEESDLAQQYGVR
QFLQAAEAIDDIPFGITSNSDVFSK
P4HA2
LDPGTISR
DVYESLCR
IGALS3BP
GQWGTVCDNLWDLTDASVVCR
ELSEALGQIFDSQR
ASHEEVEGLVEK
CTMT1A
GTGGVDTAATGGVFDISNLDR
PRR36
AAGTEVGLPR
RPPTPGPDTSVSGPR
GAB1
IFYLVADSEEEMNK
APSASVDSSLYNLPR
HSD11B2
LAMSDLTPVVDAITDALLAARPR
SMARCD1
TMTDVVGNPEEER
GTPB1
DDVIVTASNFSSER
LNDTLLLGPDPLGNFLSIAVK
SUPV3L1
SNAAGVPCDLVTGEER
ELEPITTSQALQIAGR
ELF4E2
AATAAAVVAEEDTELR
R
LALSQNQQSSGAAGPTGK

MS validated peptides associated with MB subgroups show that peptides linked to HSPA5, DAD1, FBN1 and INA protein groups are specific to WNT subtype. Similarly, peptides for DPSY2-5, PRR36 and GAB1 are specific in SHH. While peptides for TGFBI, ARAP1 and LUC peptides specifically link to Group 3. Finally, peptides for RHOA, FRY and HAGH are specifically linked to Group 4 subgroups (Table 8.6).

8.7.1.2 Study 3 Discussion and conclusions

While there have been proteomic investigations into MB, most of the previous published studies have been performed on cell lines, there is limited available patient specific MB proteomic data available. While cell lines do provide insight into the proteome of MB, there are issues with confirmation of cellular identity and lack of surrounding extracellular matrix; therefore, tumour tissue proteomics, while limited by minimal patient sampling, can provide a more comprehensive view of the native proteomic environment. The current study investigated the MB subgroup-specific proteins as identified by MS based proteomics from patient tumour tissue. The tumour tissues were sub-grouped by NS assay and an IHC panel and represented earlier tissue blocks, less than 8 years old (Chapter 6). The subgroup characteristics were used as a proteomic classifier in the current chapter. Proteomic validation in this context means peptides that have been statistically associated in the discovery-based proteomic studies looking at the snapshot of all proteins, have been further validated in a targeted proteomic experiment looking at a fewer number of peptides. Looking at a fewer number of peptides allows for more robust confidence that the peptides are present in those samples and are substantiate the associations by comparing to their representative controls.

Study 3A determined the MB subgroup-specific proteins in the MB retrospective cohort. MS identified more than 1400 proteins in each of the subgroups respectively.

GO enrichment analysis was employed in a parallel analysis for comparative enrichments to gauge biological meaning related to MB subgroups.

The proteins and GO analysis revealed that the WNT subtype were enriched for endoplasmic reticulum, immunoglobulin, together with immunoglobulin binding, glycation product binding and disulphide bond activity; vesicle related processes, oxidative stress and protein folding processes in the WNT subtype.

Excitatory synapse, SWI/SNF and membrane vesicle together with molecular function enrichment of NADH quinone, protein translation regulation and GTPase activity with DNA replication, epigenetic regulation, cell growth and differentiation in were enriched in SHH.

ATPase degradation complexes, ribonuclear, DNA replication associations with only NFkB binding and ATP synthase and mis-folded protein responses, gene silencing, DNA repair and protein sumoylation were enriched in Group 3.

Protein folding, splicing and motor protein association with dopamine, protein and amino acid binding, as well as G-protein related serotonin binding and ATPase function, synapse and cell development processes were enriched in Group 4 MBs in this cohort.

WNT-specific enrichment

Previously reported DDX3X mutations has been previously associated with a loss-of-function phenotype in WNT subtype (Jones et al., 2012). This protein was enriched in the WNT subtype in the current study at the protein level, as well as in the SHH subtype. However, functionality of the enriched protein would have to be further investigated in further experiments. OTX2, a regulator of neurodevelopment and pluripotency marker was also enriched in the WNT subtype. Previous studies have shown that OTX2 gene expression is upregulated in the groups other that SHH, silenced in normal cerebellum, and controls dopamine progenitors (Adamson et al., 2010; Omodei et al., 2008). Given that OTX2, a regulator of dopamine progenitors, is

enriched in WNT subtype, dopamine is seen in the WNT subtype but is however more enriched in the Group 4 subtype in the current study, particularly dopamine receptor binding proteins.

An interesting finding in the current study was the specific enrichment of CD14 in the WNT subtype. CD14 has been implicated as the predominant leukocyte (CD34, CD14 positive monocytes) in primary blood mononuclear cells from MB patients (Nair et al., 2015).

Additionally, the fibrillin proteins (FBN1) have been previously associated with MB in general but is not present in healthy brain tissues (Haeberle, Dudley, Liu, & Butte, 2012). FBN1 is strongly associated with MB in this study, particularly validated with the WNT subtype in the current study. Here HSPA5 was highly specific and validated for the WNT subtype at the protein level. Other proteomic studies have reported high levels of HSPA5 in SHH stem-like cells; however, the WNT subtype was not further investigated (Ronci et al., 2015). Interestingly HSPA5 has also been reported in cultured MB cell line extracellular vesicles (Bisaro et al., 2015). DAD1 is also validated in the current cohort, specific for WNT types. DAD1 functions as an anti-apoptotic role player and is suggested to be inhibited by some miRNAs particularly miR-466 under oxidative stress and glucose deprivation (J. He & Jiang, 2016). The overrepresentation of DAD1 in WNT subtypes suggests possible roles in pathogenesis of this subtype, as it indicates the cell biology within the tumour tissues are adapting to possible proliferative signals. INA has been previously shown to be expressed in most MB and some AT/RTs, and is an indicator of neuronal differentiation (Kaya, Mena, Miettinen, & Rushing, 2003). INA is shown in the current study to be specific for WNT subtype MB and therefore might be some indication that WNT tumours possibly exhibit more neuronal differentiation that the other subtypes at the molecular level. P4H proteins (P4HB and P4HA2) were validated at the peptide level for WNT subgroups in the current study. Previous gene expression studies in multiple large cohorts have also supported this finding and link specifically P4HA2 to WNT subtypes (Edward Carl Schwalbe, 2011).

Taken together there is a panel of peptide candidates reported in the current study and supported by prior evidences in the literature to be specific for the WNT subtype. There are opportunities to delineate WNT MB tumour pathobiology from biochemical pathways and specific proteins identified. There is also further utility in the creation of a custom WNT-specific targeted proteomic experiment possibly to subtype tumours for further clinical proteomic applications.

SHH-specific enrichment

The chromatin remodelling factors previously reported from genomic studies have suggested that methyltransferases and alterations of these are involved in MB pathogenesis (Northcott et al., 2009). In the current study, there was upregulation of chromatin remodelling factors such as SMARC family proteins, histone deacetylases and YY1 proteins that direct chromatin modifications, particularly enriched in SHH MB in the current cohort. These results are consistent with findings that suggest the SWI/SNF remodelling complexes have a regulatory role in SHH target genes in SHH altered signalling cancers (Shi et al., 2014). Therefore, the specific overrepresentation of SMARC proteins but not Gli1 in SHH further implicates these factors in SHH pathogenesis at the protein level *in vivo*. This is consistent with discoveries that SMARC proteins are key regulators of the SHH pathways and consistent with findings in mouse models that suggest SHH MBs can form in mice independent of Gli1, 2 (Jagani et al., 2010; Weiner et al., 2002).

Prominent SHH-specific peptides revealed in this study include the DPYSL proteins (DPSY2-5). These peptides correspond to DPSY proteins that are involved in semophorin signalling and nervous system development, and have been implicated in neuropsychiatric diseases as well as ischemic stroke (Arai & Itokawa, 2010). Furthermore, this protein family has a dynamic turnover state possibly linked to pathobiology and so further investigations into time-linked prognostic associations may be valuable (Turck et al., 2016).

HSD11B2 is specific for SHH tumours in the current study. This protein has been implicated to be upregulated at the transcript level in CNS neurocytomas, and converts the stress hormone cortisol to the inactive metabolite cortisone (Vasiljevic et al., 2012).

The SHH-associated gene GAB1 as previously reported associated specifically with SHH tumours are supported by data in this study, which showed peptides for GAB1 to be highly specific for SHH tumours. GAB1 is a suggested predictor of SHH types and is involved in cellular processes such as proliferation, cell motility in its role as an adapter protein (Ellison et al., 2011).

SUPV3L1, a component of the mitochondrial degradozome is enriched in SHH tumours in this study. It functions in the degradation of aberrantly formed RNA and may therefore have an anti-apoptotic role (Pereira et al., 2007). Investigating which RNA transcripts are targeted by this protein specifically might provide information on genetic events linked to these tumours, such as those leading to chromothripsis and gene fusions. In all, the chromatin remodelling factors as well as the SWI/SNF, DPYSL protein, cell motility proteins and RNA transcript degradation pathways have been suggested in this study to be implicated in SHH-specific tumours in the cohort investigated.

Group 3 specific protein and peptide enrichment

In the current study ribonuclear proteins (HNRNPR, HNRNPK) are associated with Group 3 MB. These types of proteins have been previously associated with classic and desmoplastic/nodular histotypes and indeed with Group 3 MB, particularly those with MYC amplifications (Peyrl et al., 2003; Staal et al., 2015; Zanini et al., 2011).

SUMO3 was also linked to Group 3 MB. Sumoylation proteins (sumo conjugating enzyme UBC9) have been previously reported in DAOY cell lines by proteomic experiments; DAOY is likely linked to desmoplastic MB (Martelli et al., 2016). Furthermore, the previously uncharacterised protein group C2orf80 has been linked to

Group 3; it is found on chromosome 2 and has been implicated in MB at a genomic and gene expression level (Birks et al., 2013). Additionally, FOX protein (FOXM1) is shown enriched in Group 3 MB in the current study. FOX proteins have been suggested to lead to mesenchymal to epithelial transition, thus leading to tumour formation by disruption of e-cadherin and loss of cell-cell adhesion, possibly enabling cells to metastasise (Martirosian et al., 2016). The findings in the current study where it is shown that there are 4 cases associated with metastasis in Group 3 MB which were also enriched for FOX proteins is consistent with the hypothesis that FOX proteins might contribute to metastasis and tissue invasion, however it is not seen with all of the Group 3 cases.

TGFBI peptides were also enriched in this Group 3. This protein has been implicated in WNT subtypes previously (Kool et al., 2008). Their enrichment and dysregulation at the transcript level in Group 3 MB has been reported in other studies (Aref et al., 2013; Northcott, Korshunov, et al., 2011).

ARAP1 peptides were strongly associated with Group 3 MB in this study. This protein functions as a point of convergence in the Arf and Rho molecular signalling pathways and is postulated to have anti cell motility roles (Miura et al., 2002). Therefore, its association with Group 3 MB here could suggest its effects as part of negative feedback paths and its overrepresentation possibly representing anti-tumour adaptations. Furthermore, DDA1 peptides have a similar enrichment profile in the current study. DDA1 proteins form part of the E2 ligase CUL4A system that has been suggested as a candidate anti-cancer drug target for cancers and other diseases (P. Sharma & Nag, 2014).

Peptides corresponding to LUC7L2 and 3 were enriched in Group 3 MB. This protein family has been shown to have copy number gains in JPA cases and are involved in truncations in sodium gated voltage gated channels with implications for cardiac functioning (Gao et al., 2011; Harding, Busse, Tooke, & Biegel, 2014). Data from these peptides and corresponding proteins in the current study support them as possible new candidate markers for Group 3 MB.

In summary, ribonuclear proteins, SUMO-related protein modification, Rho signalling and the LUC7L proteins have been implicated in Group 3 specific tumours in the current study.

Group 4 specific protein and peptide enrichment

Protein folding, splicing and motor protein association with dopamine, protein and amino acid binding, as well as G-protein related serotonin binding and ATPase function, synapse and cell development processes were enriched in Group 4 MBs in this cohort.

Dopamine binding proteins were highly enriched in the Group 4 subtype. Dopamine receptors stimulate the ERK1/2 pathway, leading to cellular proliferation, and have been shown to be repressed in the majority of MB as well as in other paediatric CNS tumours (Unland et al., 2014).

Furthermore, RHOA peptides were specific for Group 4 MB in this study. This protein is not surprisingly linked to KCNA2, a protein previously reported to be highly specific to Group 4 MB and included as a marker in the MB subtyping Nanostring panel (Northcott, Shih, et al., 2011). RHOA mediates KCNA channels by modulating the channel re-uptake into the cell by endocytosis (Stirling, Williams, & Morielli, 2009). Its overrepresentation in Group 4 MB is therefore postulated to result from the upregulation of KCNA, and the need to modulate its function to reach homeostasis within the local environment.

FRY peptides are also specific for Group 4 MB in this study. FRY protein functions in spindle organisation in early mitosis and has been shown in previous studies to bind to Aurora kinases (AURA) and to modulate its activity, thus maintaining mitotic spindle polarity during early mitosis (Ikeda, Chiba, Ohashi, & Mizuno, 2012). The utility of FRY is further supported by Aurora inhibitors under investigation as a new therapeutic anticancer agent for MB (Cicenas, 2016).

HAGH peptides also show enrichment in Group 4 MB in the current study. This protein is a mitochondrial protein involved in the metabolism of glutathione (Pettinati, Brem, Lee, Mchugh, & Scho, 2016). Glutathione metabolism in MB has been implicated in treatment resistance, including resistance to ionising radiation conferring cyto-protection in tumour cells, as well as binding metals and metabolising chemotherapeutic agents (Backos, Franklin, & Reigan, 2012; T. W. Miller et al., 2015).

As interim conclusions from this study, there are a several specific protein and peptide associations to MB subtypes that may be useful as subgroup-specific predictors and also infer biological information. The clinical associations of these identified markers and others are investigated in further studies in this chapter.

8.7.2 Study 3B – Prognosis associated proteins in MB

This study investigated prognosis-related protein groups enriched in the MB test cohort. A total of 30 patients were included in this study, all of whom had clinical, outcome and subtype data from less than 8 year old tissue blocks. There were 5 WNT patients, 9 SHH, 10 Group 3 and 6 Group 4 patients. All of the WNT identified patients had a favourable outcome (Figure 8.2). Overall, the proteins associated with poor outcome were the collagens, GFAP, CRB, and hypoxia proteins. Some of these could be related to late stage disease, such as collagens-associated necrosis and hypoxic stress in tumour interiors. Therefore, more detailed analysis of subgroup specific prognosis markers should follow, and statistical significance can be set to $p < 0.1$ ($1x10^{-1}$), and further validated using additional targeted MS methods. Some of the proteins associated with favourable outcome include VARS a valine-tRNA ligase, co-chaperones FKBP4, CCT7 and growth inhibitors RTN4 (Figure 8.2).

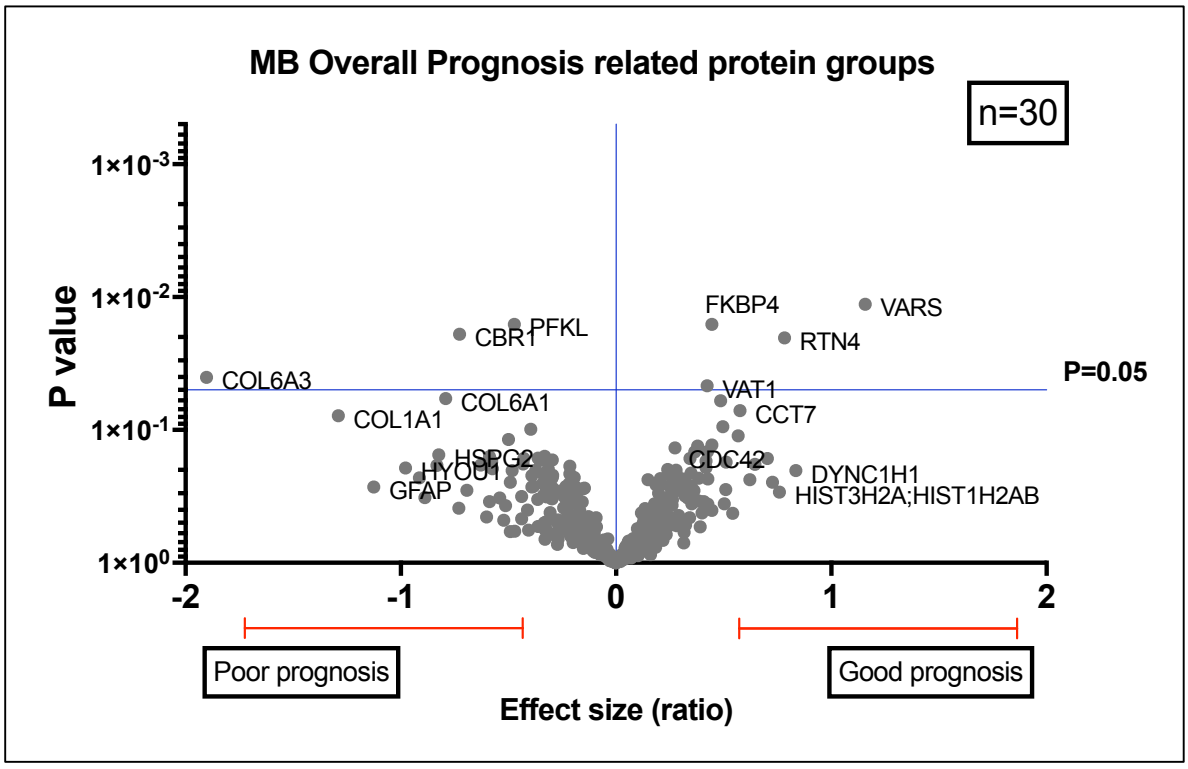

Figure 8.2: Overall MB proteins linked to outcome, the overall prognosis related protein groups identified in the retrospective cohort proteomic investigations. Solid lines represent a P value threshold of P = 0.05. The overall sample size for this analysis included 30 patients.

Investigating WNT-specific prognosis was challenging in the current study because WNT patients had good outcomes; therefore, all identified WNT subtype specific protein groups were linked to a favourable prognosis (see Study 3A).

For SHH patients, some subgroup specific prognosis candidate proteins for poor prognosis include GFAP, CKB, SPTAN1, DHX9, SRI, RPSX4; while those associated with favourable prognosis include A2M, FGB, HIST1, RAB1B, PDIA6, ST13, PRDX5 and YWHAZ protein groups (Figure 8.3A).

Those associated with Group 3 favourable prognosis include RAB5A, ANP32A, DDX5, RPS13, CCT2 and DYNC1H1, while those associated with poor outcomes include VIM, LAMC1, IGKCs, NCAM and GSN protein groups (Figure 8.3B)

Proteins associated with Group 4 MB favourable outcomes include RPL13, SERPINA3, RPS12 and C1QBP, while those associated with a poorer outcome in include HIST1, PDXP, IDH2, AKR1B1 and C14orf166 protein groups (Figure 8.3C).

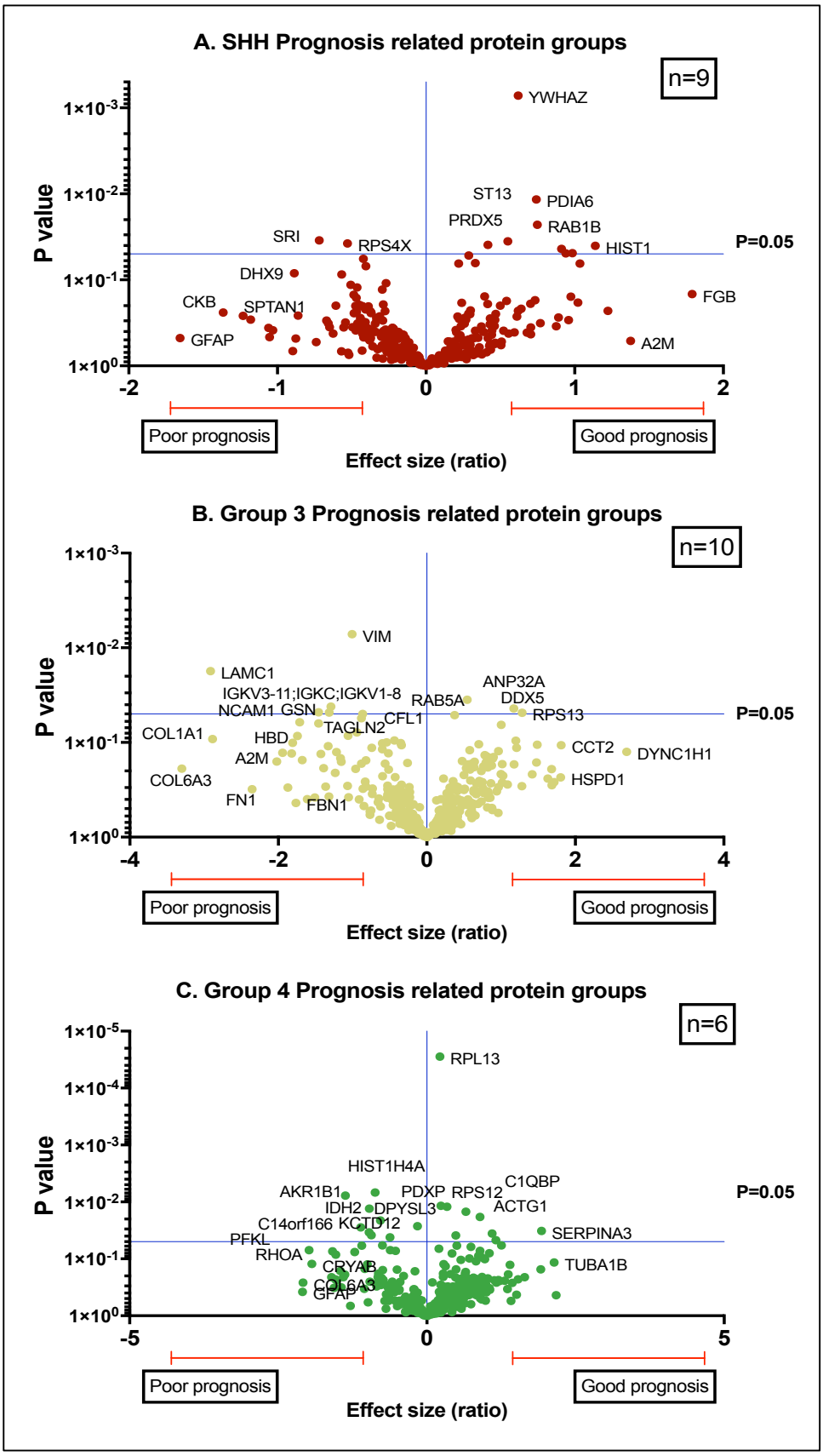

Figure 8.3: MB subgroup specific proteins linked with outcome

A - SHH subtype specific outcome linked protein groups, B - Group 3 MB protein groups linked with outcome, C - Group 4 proteins linked with outcome

The high abundance proteins linked with outcome can be partially explained by time of presentation and extent of necrosis processes. The presence of high abundance collagen proteins and GFAP protein support this notion. Therefore, focussing only on the high abundance protein groups might bias the analysis; so, lower abundance proteins groups should also be examined.

Chromosomal location of outcome associated protein groups

To examine whether these associations have similar chromosomal links the significant proteins related to outcome are displayed based on chromosomal location (Figure 8.4). A region on chromosome 6p appears enriched for VARS, RPS12 and HIST1H3A, and are associated with good outcomes in MB overall and Group 4 and SHH more specifically.

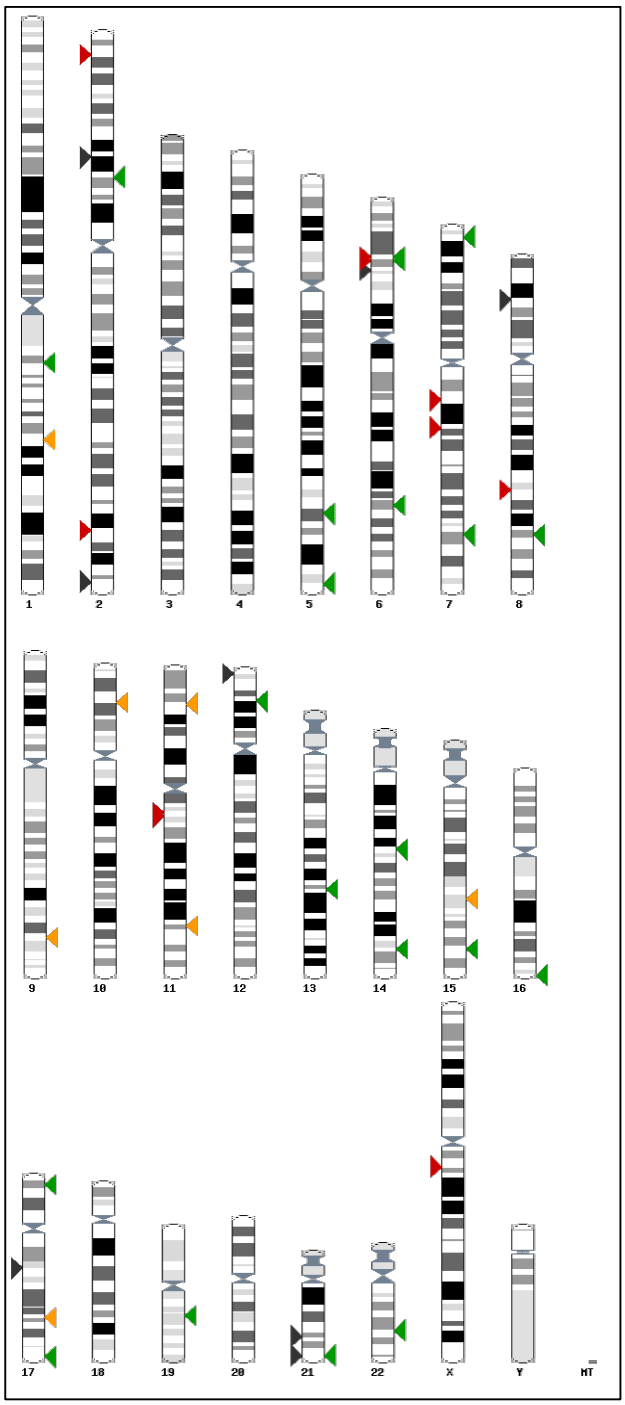

Figure 8.4: Significant outcome associated protein groups based on chromosomal location

Black – Overall MB prognosis associated proteins, Red – SHH subtype prognosis associated proteins, Yellow – Group 3, Green – Group4

Peptides associated with outcomes

Table 8.7: Validated MB prognosis related peptides, Green represents a good outcome, and Red presents a poorer outcome status.

Protein	Peptide	Good outcome	Poor outcome	Significance
DPSYL2	DIGAIAQVHAENGDIIAEEQQR - 1189.0908++			
	AITIANQTNCPLYITK - 910.9824++			*
GAB1	IFYLVADSEEEMNK - 844.3978++			
	APSASVDSSLYNLPR - 526.2704+++			****
ARAP1	AFVPPLAEDLLAR - 471.2696+++			***
	LGSVSLIPLR - 352.2255+++			
DDA1	EYPSEQIIVTEK - 479.2487+++			
	DQEQVELEGESSAPPR - 590.9429+++			*
RHOA	DQFPEVYVPTVFENYVADIEVDGK - 925.1130+++			*
	IGAFGYMECSAK - 445.2020+++			*
FRY	LELIDLLAR - 352.5535+++			
	EDVLFGFTNFLLR - 524.2803+++			***
DKK3	EVEELMEDTQHK - 744.3378++			*
	LLDLITWELEPDGALDR - 985.0175++			
TNC	LPVGSQCSVDLESASGEK - 931.9437++			
	VPGDQTSTIIQELEPGVEYFIR - 1246.1394++			

	VSQTDNSITLEWR - 774.8863++			**
UNC119	QVGATVEFTVGDKPVNNFR - 693.3604+++			*
	NTCEHIYDFPPLSEELISEMIR - 898.4244+++			
	HPYETQSDSFYFVDDR - 1003.4318++			
TPD52L2	MDSAGQDINLNSPNK - 535.2509+++			*
	TPAVEGLTEAEEEELR - 591.6231+++			
ILF3	HSSVYPTQEELEAVQNMVSHTER - 891.0854+++			
	AVSDWIDEQEK - 440.5420+++			***
ACTB	KDLYANTVLSGGTTMYPGIADR - 781.7265+++			***
GAPDH	WGDAGAEYVVESTGVFTTMEK - 759.6842+++			*

Two peptides for DPSYL2 and GAB1 respectively are validated in this study as linked to prognosis in both cohorts studied here by MS-based proteomics (Table 8.7). The higher peptide levels of DPSYL2 are linked to a favourable outcome in SHH tumours and the higher peptide expression of GAB1 is shown statistically associated with poorer outcomes in the same tumour subtypes.

Furthermore, high levels of two peptides each for ARAP1 and DDA1 were associated with favourable outcomes in Group 3 MB in the current study (Table 8.7).

Additionally, peptides for RHOA and FRY proteins are significantly associated with outcomes in Group 4 MB in the current study (Table 8.7). Higher RHOA peptide expressions are correlated with favourable outcomes and higher levels of FRY peptides are correlated with poorer outcomes in this subtype.

Moreover, peptides not specifically associated with any particular subtype also show associations of outcomes, these include peptides for TPD52L2, ILF3, ACTB and GAPDH (Table 8.7). Higher levels of TPD52L2 peptides are shown associated with favourable outcomes while higher levels of ILF3 are seen associated with poorer outcomes in a subtype independent manner. Interestingly, higher levels of peptides for ACTB, usually a structural housekeeping gene in many studies, are shown here associated with favourable outcomes. While higher levels of peptides for GAPDH, a key cellular metabolism protein is shown here associated with poorer outcomes, again in a MB subtype independent relation.

8.7.2.2 Study 3B Discussion

This study investigated MB tumours and their proteomic links to clinical outcome variables.

Subtype independent protein markers linked to prognosis

When investigating overall MB samples, the proteins associated with poor outcome are the collagens, GFAP, CBR1 and hypoxia-related proteins. Indeed, these markers could be indicative of late stage disease. Collagens can be associated with necrosis and hypoxic stress in tumour interiors. However, it has been reported that type I collagens are highly up-regulated in MB, particularly linked to the vascular microenvironment but not in normal brain parenchyma, and a mechanism linked to vascularisation is postulated to be linked to MB as it is a highly vascular tumour type (Liang, Diehn, Bollen, Israel, & Gupta, 2008). The current findings are contrary to reports suggesting gene expression of type I collagens are linked to favourable outcomes in international cohorts (Pomeroy et al., 2002). However, using outcome predictors in MB is a complex task, requiring rigorous validations for effective clinical utility. GFAP is also enriched in the poor outcome group; this possibly links glial differentiation to poorer outcome in this cohort. It has been long reported that high GFAP expression positivity in MB is associated with poor outcome irrespective of histological defined glial differentiation (Janss et al., 1996). Noting results that are expected in such a cohort adds molecular integrity to the findings of this study. Therefore, interpreting the data presented in this study takes into account expected and previously linked proteins and indicates the utility of this cohort in understanding the molecular and clinical significance of MB. Additionally, CBR1 protein is seen enriched in poor outcome patients. This protein has been implicated in poor outcomes, particularly SNPs in these proteins show links to late chemotherapy-induced cardiomyopathy in MB cases (Armenian, Landier, Hudson, Robison, & Bhatia, 2013). Notwithstanding, while this phenomenon was not directly investigated in the current study, it is still linked to a generally poorer outcome. Lastly, hypoxia-

associated proteins (HYOU1) are linked with poor outcomes. This protein has been previously reported in proteomic experiments on DAOY MB cell lines, with its role unaltered by HDAC inhibitors (Pham et al., 2013). A common feature in many solid tumours, including MB, is hypoxia. This can be chronic or intermittent with changing vascularisation and tumour growth. Indeed it has been suggested that hypoxia induces angiogenesis, metastasis, and even resistance to radio and chemotherapy by reducing the facilitated performance of free reactive oxygen species (Michiels, Tellier, & Feron, 2016). There is also a marked dynamic effect on gene and protein expression in tumour cells experiencing hypoxic conditions and could lead to possible immune tolerance and evasion of anti-tumour immunity (Chouaid, Messai, Escudier, Hasmim, & Noman, 2012).

Moreover, peptides for TPD52L2, ILF3, ACTB and GAPDH are discussed and validated in the current study in the prospective cohort. Higher levels of TPD52L2 peptides were associated with favourable outcomes. This is known to be involved with tumour cells. In particular it has been seen over expressed in GBM patients and is shown to contain splice variants in oligodendrocytes, with a suggested role in cellular proliferation regulation (Jain, Kulkarni, Dhali, Rapole, & Srivastava, 2014; Tavares et al., 2016).

Higher levels of ILF3 were associated with poorer outcomes in a subtype-independent manner in the current study. Elevations of this protein has been seen in other cancers such as ovarian cancers (Guo et al., 2012). It is from a gene that can yield two isoforms by alternative splicing, the ILF3 and NF90 proteins, both of which will have overlapping peptides (Duchange, Pidoux, Camus, & Sauvaget, 2000). The current study has identified peptides that are unique for ILF3 in this context. There is also a link of this protein to Tau protein targeting in axons, which may be of interest for neurodegenerative diseases (Larcher, Gasmi, Viranaïcken, & Eddé, 2004). The link and validation of these peptides to MB subtype independent prognosis is a novel finding in this study. It will also be of further interest to determine the quality of life outcomes of surviving patients with moderate to high levels of this protein in relation to its links with neurodegenerative diseases.

Interestingly, peptides from two constitutively present proteins for ACTB and GAPDH are shown here associated with outcomes. While these proteins are usually present at high levels and may be considered interfering proteins in common MS based proteomic workflows, it is worthwhile considering their roles for MB in this context.

Higher levels of ACTB are seen associated with favourable outcomes. This protein may be expressed ubiquitously in all cells; therefore, its prognostic association might reflect cell number or tissue structure.

Higher levels of peptides for GAPDH, a key cellular metabolism protein was associated with poorer outcomes in a MB subtype independent manner. GAPDH is a protein associated with cellular respiration and the glycolysis process. It also has a suggested role in cell structure in microtubule dynamics (Tisdale, 2002).

Taken together, the validated findings of peptides for glial proteins, hypoxic stress related proteins, neurodegenerative proteins and the common structural proteins add to our understanding of MB pathogenesis across all subgroups.

Subtype-specific proteins associated with prognosis

A further more detailed analysis followed, looking at subgroup specific prognosis markers with statistical significance at $p < 0.1$.

Recently, certain XRCC1 SNPs have been previously reported as a conferring a decreased risk for paediatric astrocytomas, while XRCC4 haplotypes confer a decreased risk for non-astrocytic brain tumours (Fahmideh et al., 2016).

SHH specific prognosis related protein markers

SHH subgroup specific prognosis indicative protein groups displayed in the current study include GFAP, CKB, SPTAN1, DHX9, SRI, RPSX4; while those associated with good outcomes include A2M, FGB, HIST1, RAB1B, PDIA6, ST13, PRDX5 and YWHAZ protein groups.

Poor prognosis: CKB, a protein linked to metabolic and energy metabolism, was associated with outcome in SHH tumours. This protein has been implicated in previous studies on SHH cancer stem cells and could be as a result of SHH pathway associated metabolism to sustain tumour cell growth (Ronci et al., 2015; Tech & Gershon, 2015).

GFAP peptides showing links towards poor outcomes in SHH tumours in the current study is interesting. GFAP positivity is usually a marker of astrocytes; in MB it might suggest that the MB cells are differentiating to a glial appearance or could mean there is an influx of astrocytic cells into the local tumour environment (Kumanishi, Washiyama, Watabe, & Sekiguchi, 1985). While there is no histological evidence of increased asctrocytes in the tumour specimens, the likelihood is that these cells are in the process of differentiating into a glial appearance. The links of GFAP positivity to outcome have varied in the published literature, with some authors suggesting a link to favourable outcomes and others suggesting no link (Goldberg-stern, Gadoth, & Stern, 1991; Woodburn, Azzarelli, Montebello, & Goss, 2001). However, prior studies of GFAP links have not taken subtype stratification into consideration. The results of this study therefore support GFAP being a prognostic marker for poorer outcome, albeit only in SHH. Furthermore, GFAP peptide identification using a sensitive technique such as mass spectrometry-based proteomics could indeed provide insight on early transformation of MB cells to more glial differentiated MB with links to outcome.

SPTAN1, a protein implicated in calcium dependent movement of the cytoskeleton at the membrane, was linked to poorer outcomes in SHH tumours in the current study. This protein has been implicated in cell cycle control in MB via the CUX1 pathway

interaction partners. This pathway is suggested to play a role in MB pathogenesis as it is seen highly expressed in MB granule neural precursor cells and not in healthy cerebellum and might be linked to the cancer stem cell of origin for SHH MB (Topka, Glassmann, Weisheit, Schüller, & Schilling, 2014).

DHX9 is shown in the current study to be linked to prognosis in SHH tumours. This protein has been previously shown in genomic and expression studies on high risk MBs to be highly over expressed in Group 3 and 4 MB, possibly playing role in ribosome biogenesis; however, no links to prognosis have been suggested (Staal et al., 2015).

SRI is a protein linked to modulation of ion channels and is linked to SHH prognosis in the current study. Interestingly, this is also associated with multidrug resistance and is linked to poorer outcomes by testing for levels of SRI in pre-treatment biopsies for MB (Pomeroy et al., 2002). It is therefore not surprising that SRI peptides are evident in the current study; however, interestingly associated specifically with SHH tumour prognosis.

RAB1B is also associated with poor outcomes in SHH specific tumours in this cohort. It has been recently reported that RAB21, a related protein, is linked to outcome (Changjun Cao, Wang, & Jiang, 2016). Similarly reported gene transcripts RAB2A and RAB7A are seen enriched in SHH tumours with a poor outcome in the current study at the protein and peptide level, but were not statistically significant. It is suggested that a closely related RAB21 protein correlates with outcome when investigating gene expression in MB tumours (Changjun Cao et al., 2016).

Favourable: Proteins linked to a more favourable outcome in SHH tumours include A2M, FGB, HIST1, RAB1B, PDIA6, STI3, PRDX5 and YWHAZ. A2M protein is a known proteinase inhibitor. It also shown binds to to and influences the glucocorticoid and JUN receptors, leading to transcriptional activity, provided STAT3 is present (Darnell, 2002). It might be of interest to determine the levels of STAT3 in this context for possible future studies. FGB is a protein component of blood clots; it is the precursor for the insoluble polymeric fibrin. This might indicate the presence of

blood components in the tumour environment, possibly linked to micro-haemorrhage from the extensive vasculature often seen in MB. It has been recently reported that tumour thrombosis might be seen at the molecular level in MB irrespective of clinical evidence of thrombosis, and these coagulant and anti-coagulant proteins are unregulated in SHH in agreement with the findings in the current study (D'Asti, Kool, Pfister, & Rak, 2014). The association with HIST1, a histone protein subunit, might be as a result of chromosomal changes associated with this subtype, or chromosomal amplifications or ploidy-related affects. RAB1B – a small protein GTPase is a protein that has been linked to cancer cell secretion of pro-invasive and pro-angiogenic factors (Halberg et al., 2016). However, its role in secretion is dependent on location to the golgi; therefore, it may be of useful for studies to investigate this protein in terms of intra-cellular location in MB tumours, and their profile in the different subtype. The mechanism of association with favourable prognosis in SHH is unclear. PDIA6 has a speculated function of inhibiting the aggregation of mis-folded proteins in cells, a possible chaperone function (Jordan et al., 2016). It is therefore unsurprising that this would confer a beneficial effect in tumour cells where there is dysregulated protein sequence and translation effects leading to mis-folded proteins in supressing the unfolded protein response (Reste, Avril, Morandi, & Chevet, 2016). ST13 is a protein with a protein chaperone inferred function which has been reported as highly abundant in SHH MB stem-like cells and its link to prognosis is supported by the current study (Ronci et al., 2015).

PRDX5 has a physiological role in reduction reactions of peroxides, having antioxidant effects. Furthermore, it plays a role in redox signalling, and inhibition of this protein can lead to increased radiosensitivity in some cancers (J. He & Jiang, 2016). It has been suggested that the redox and antioxidant protein are downregulated in MBs and even in peripheral blood (Pohanka, Hynek, Kracmarova, Kruseova, & Ruttkay-, 2012; Pu et al., 1996). The current study data suggests that this protein is highly represented in SHH tumours and confers a beneficial effect in SHH tumours. This could be as a result of its antioxidant role in reducing the oncogenic properties of reactive oxygen species, implicating the reactive oxygen species role in SHH MB as an interesting metabolite with relation to prognostication.

YWHAZ protein is a known adapter protein that interacts as part of many signalling pathways. It has been previously reported to be highly expressed in SHH stem-like cells and is suggested as a candidate marker as a house keeping gene for cancer stem cells as its expression is robustly stable in these cell types (Lemma, Avnet, Salerno, Chano, & Baldini, 2016; Ronci et al., 2015). This could suggest that there is a predominance of the cancer-related stem cells in SHH tumours and is an interesting link to favourable prognosis.

Additionally, 2 peptides for DPSYL2 and GAB1 respectively are validated at the peptide level by targeted MS in this study as linked to prognosis in both cohorts studied here. DPSYL2 is associated with favourable outcome and GAB1 is shown with poorer outcomes in SHH. These protein roles have been discussed previously in relation to their specific roles as SHH-specific markers.

The SHH pathway is an area of growing interest in MB pathogenesis research. Recent studies have suggested that targeting dysregulated or mutated smoothened receptors could be a SHH specific pathway target in treatment of the SHH type tumours. While promising, only temporary responses in patients treated with these type of targeted drugs have been reported (Lou et al., 2016). Further work, such as in the current study, to identify more appropriate targets or target agents may add greater insight into the SHH pathway and its pathogenesis.

Group 3-specific protein prognosis markers

There is little that specifically defines the Group 3 protein profile from Group 4. The proteins identified in the current study implicate RAB5A, ANP32A, DDX5, RPS13, CCT2 and DYNC1H1 with favourable outcome, and VIM, LAMC1, IGKCs, NCAM and GSN protein groups with poor outcome.

Favourable outcome: RAB5A is a protein linked to growth factor modulation by regulation of endocytosis of membrane bound growth factor receptors (Chia & Tang,

2009). The link to favourable outcomes in the current study is possibly evidence of innate response to decrease the proliferative signalling (Goumnerova, 1996).

ANP32A is a protein associated with tumour suppression shown to be the target of miRNA-21 in CNS tumour pathogenesis. This tumour suppression role supports its association with favourable prognosis in Group 3 (Stoicea et al., 2016).

DDX5 has a RNA helicase function, and has been suggested to synergise with the TP53 tumour suppressor protein to stimulate gene expression from p53 target genes (Bates et al., 2005). It has been shown to interact with DHX9 and AKAP9, both implicated in Group 4 MB in the previous study (Study 3A). Taken together, the link to favourable outcomes in Group 3 MB is interesting and could suggest a tumour co-suppressor effect in combination with TP53 with effects in both Group 3 and Group 4 MB.

RPS13 is a ribosomal protein component. Interestingly, this specific protein has been suggested to have a role in RNA processing, splicing and cell growth regulation from studies in colorectal cancer (Bhavsar, Makley, & Tsonis, 2010). The current data suggests a possible link between this ribosomal protein and a tumour specific role in Group 3 MB.

CCT2 is a protein-folding chaperone known to be involved in cytoskeletal protein folding. It has also been implicated in copy number gains in many cancer types at the DNA level (Beroukhim et al., 2010).

DYNC1H1 is a motor protein involved in moving vesicles and in neural development and maintenance of the cellular primary cilium (Lalonde et al., 2011). These motors have been suggested to play a role in MB pathogenesis linked to the stabilisation this primary cilium for which there is antitumor evidence in this region, which play a role during Aurora kinase inhibition (Han et al., 2009).

Poor outcome: VIM is a protein normally associated with mesenchymal and glial cells and is therefore a common marker of epithelial to mesenchymal transitions in cancer cell progression (Schiffer et al., 1986). The mechanism is suggested to be

associated to the change in composition of intermediate filaments with an increased representation of VIM protein. This alters the filament polarity signals, misaligning anchorage proteins leading to increased cell motility (Lamouille, Xu, & Derynck, 2014). The current data suggests the cells might be experiencing epithelial to mesenchymal transition-like events that are associated with a poorer outcome. Another possibility here is that the Group 3 MB cells are recapitulating their protein expression from their cell of origin or have gained the molecular characteristics of stem-ness and increased motility.

LAMC1 is also associated with cell motility and adhesion; it plays a role in cellular attachment via interactions with the extracellular matrix components (Merve et al., 2014). It has been reported that inhibiting LAMC1 enhances stem cell traits and cell invasiveness in glioma cells (Xia et al., 2012). Therefore, the link to prognosis in Group 3 MB is unsurprising.

IGKCs are immunoglobulin proteins that may suggest the presence of tumour infiltrating plasma cell types and related immunity. In contrast, it is associated with favourable prognosis in some other solid tumour types (M. Schmidt et al., 2012). The tumour immune relation is a complex phenomenon, particularly in the immune privileged CNS region where tumour growth can be favoured under pro-inflammatory conditions (Fridman, Pagès, & Sautès-fridman, 2012). The current study supports the hypothesis that in Group 3 MB there is a link between immunoglobulin κC proteins over representation to poorer outcomes in patients.

NCAM is a cell adhesion protein highly expressed in brain cancer cells. Specifically, it is post translationally modified by polysialic acids in relation to pathogenesis, neurite outgrowth and axon guidance signal transduction (Schmid & Maness, 2008). The association with poorer outcome in Group 3 MB suggests that NCAM over representation is a characteristic feature of awry cell adhesion processes; however, further investigations into the post-translational status of these proteins are needed. Interestingly, this protein has also been seen in serum in brain tumour patients and might provide insight into cancer progression in the peripheral blood (Todaro et al., 2007).

GSN was also associated with poorer outcomes in Group 3 MB in the current study. It is a regulator of actin filaments and is a well-known mediator of cancer cell invasion. Little is known about its mechanism; however, it may interact with superoxide dismutase proteins, increasing the reactive oxygen species in the local tumour environment (Tochhawng et al., 2016).

High levels of two peptides each for ARAP1 and DDA1 are shown associated and validated for in patients with favourable outcomes in Group 3 MB. These peptides have links to proteins that have been reported and discussed relating to their specific roles in Group 3 MB in this thesis (Study 3).

Taken together, the proteins associated with poor outcomes in Group 3 MB in the current cohort are mostly linked with cell adhesion, invasion and immunity related functions. Proteins associated with a favourable outcome included functions involved in tumour suppression and growth factor receptor shielding or withdrawal.

Group 4 specific protein prognosis markers

Favourable outcome: Proteins associated with Group 4 MB favourable outcomes include RPL13, SERPINA3, RPS12 and C1QBP. RPL13 is a component of the 60S ribosomal structure, and has been implicated in cancer-related regulation of protein translation, promoting stress tolerance and cell growth in cancer cells (H. W. Yang et al., 2014). Interestingly, it is also one of the genes regulated by the MYC oncogene (M. K. H. Kim et al., 2003). RPL13 has also been implicated SHH-specific tumour cell types in MB, however its association here to Group 4 subtypes is currently unexplained and further investigations might be more revealing to this phenomena (Ronci et al., 2015). Taken together, the association with favourable outcome for the ribosomal proteins likely reflects the cellular phenotype, with increased protein translation being driven by other factors related to pathogenesis.

SERPINA3 is a protein produced in the liver as part of the acute phase inflammatory response. In the brain it is highly expressed in the CSF of glioma patients (Shalaby, Achini, & Grotzer, 2016). Its role in cancer remains unclear: it is reported to be upregulated in cervical cancers but downregulated in breast cancer tissues, and it is also implicated in neurodegenerative diseases (Khalil, 2007; Shaikhibrahim, Lindstrot, Ellinger, & Rogenhofer, 2011). Therefore, its link to favourable prognosis is novel in MB molecular biology and may provide an avenue for further investigations.

C1QBP is a complement-related protein that has functions in RNA splicing and coagulation enhancement (Vriend & Marzban, 2016). It may play a beneficial role in glioma cells, with Stathmin pathway involvement (Kazue et al., 2016). The current data suggest C1QBP as a prognostic marker for favourable outcomes in Group 4 MB. Its mechanism of action may be its interaction with the Stathmin pathway or a pro coagulant effect in reducing the inflammatory effects of cerebellar micro-haemorrhage commonly associated with MBs.

Poor outcome: Poor outcome in Group 4 tumours was associated with HIST1, PDXP, IDH2, AKR1B1 and C14orf166 protein groups. The over-representation of histone proteins may reflect chromosomal gains or polyploidy effects, which may suggest genomic instability within this group. This is supported by studies finding that accumulation of genetic aberrations relates to poor prognosis (Korshunov et al., 2008).

PDXP is a mitosis regulating protein involved in actin reorganisation in cytokinesis. It also appears to be involved in cancer in cell invasion and proliferation in gliomas, possibly through epigenetic methylation effects (Schulze et al., 2015)(Leblanc & Marra, 2016).

IDH2 is a protein implicated in many brain cancers. Its mutation status is thought to be a predictor of favourable prognosis as well as response to Temozolamide in low grade gliomas (Houillier et al., 2010). Indeed, this protein has been suggested by the WHO as a molecular marker for paediatric CNS glial tumours in the latest update on

CNS tumour classification (Louis et al., 2016). Current data further support IDH2 as a prognostic marker in Group 4 MB patients in our cohort.

AKR1B1 is a detoxifying enzyme that reduces carbonyls to alcohols for further drug metabolism and excretion in cells. It also correlates with poor patient survival in a number of cancers and has been suggested as a candidate drug target for cancer therapeutics (Laffin & Petrash, 2012). Recently, it has been implicated in mechanisms of cancer drug resistance (Penning, 2016). This protein is therefore particularly interesting in MB as a potential drug target, with further data supporting its utility as a prognostic marker in Group 4 MB from the current study.

C14orf166 may be an interaction partner for Cux1. This pathway and its interaction partners is suggested to play a role in MB pathogenesis and is linked to the cancer stem cell of origin for SHH MB and is supported by data in the current study (Topka et al., 2014). Of note, this protein has been implicated in many other cancers as a prognostic marker of poor outcomes (most recently in bladder, cervical and breast cancers) (Cheang et al., 2016; M. Chen et al., 2016; Zhang, Ou, Lei, Hou, & Wu, 2016).

Higher levels of RHOA peptide expressions are correlated with favourable outcomes and higher levels of FRY peptides are correlated and validated against Group 4 MB patients with poorer outcomes in this study. These peptides have links to proteins that have been reported and discussed relating to their specific roles in Group 4 MB in this thesis (Study 3).

In summary, the protein groups related to favourable prognosis in Group 4 MB are ribosomal and protein translation linked together with pro-coagulation proteins and inflammatory related factors. The proteins linked to poorer outcomes are histone and ploidy-related, mitosis, IDH oncometabolite-related and chemotherapy resistant-related proteins. Interestingly, these proteins provide a description of the molecular mechanisms that are at play in this tumour subtype that can be a validation of new and previously implicated molecular pathways in Group 4 MB.

8.7.3 Study 4 Results

Study 4A investigated proteomic profiles of cerebellar and non-cerebellar JPA tumours. A discovery proteomic workflow was performed on a training set cohort of JPA cases (n=14) and subsequently validated using a targeted proteomic approach (n=5) on a test set validation cohort.

A total of 1587 and 1068 protein groups were identified in 9 cerebellar JPA and 5 NCJPA samples respectively. The proteins identified were mapped to gene families and biological pathways (Table 8.6). JPAs were enriched for Coronins and various CD molecule gene families, while the enriched pathways include MAPK integrin, complement signalling and adaptive immune processes.

Furthermore, the NC JPA samples were specifically enriched for dopamine, GABA and serotonin-associated proteins and Rho cell motility processes. Interestingly, chemo-osmotic and vasopressin associated water reabsorption protein groups were overrepresented in these cases.

Table 8.6: JPA enriched gene families, and biological pathways

Biomolecular association	JPA_GeneSet
Coronins	CORO1A,CORO1B,CORO1C,CORO2B
CD molecules	ADAM10,ATP1B3,BSG,CD44,CD47,CD59,CD74,CD81,CD99,CDH2,IGLL1,IGSF8,ITGAM,ITGAV,JAM2,L1CAM,LRP1,PTGFRN,SLC4A1,THY1
Gap junction degradation	AP2M1,CLTA,CLTB,CLTC,DNM1,DNM2,GJA1,MYO6
Membrane Trafficking	AP1B1,AP1M1,AP2M1,ARCN1,CHMP4B,CHMP6,CLTA,CLTB,CLTC,COPA,COPB1,COPB2,COPE,COPG1,CTSZ,DNASE2,DNM1,DNM2,FTH1,FTL,GJA1,HIP1R,HSPA8,MYO6,NAPA,PICALM,RAB10,RAB5C,RALA,SEC13,SEC23A,SEC24C,SEC31A,SH3GL2,SNAP23,SNAPIN,SNX5,SRC,TJP1,TXNDC5,VAMP2,VTA1,YWHAB,YWHAE,YWHAG,YWHAH,YWHAQ,YWHAZ
Complement cascade	C1QA,C1QB,C3,C4A,C4BPA,C6,C7,C8B,C9,CD59,CFB,CFH,CFI,IGHG1,IGHG2,IGHG3,IGHG4,IGKC,IGKV1D-33,IGKV3-20,IGKV4-1,VTN
Regulation of Complement cascade	C3,C4A,C4BPA,C6,C7,C8B,C9,CD59,CFB,CFH,CFI,VTN
Bacterial invasion of epithelial cells	ACTG1,ARPC1A,ARPC2,ARPC5L,CDC42,CLTA,CLTB,CLTC,CRK,CRKL,CTNNA1,CTNNA2,CTNNB1,CTTN,DNM1,DNM2,DNM3,FN1,RHOA,RHOG,SRC,VCL,WASF2,WASL
Cytosolic tRNA aminoacylation	AARS,DARS,FARSA,FARSB,KARS,LARS,NARS,PPA1,QARS,RARS,SARS,TARS,VARS,WARS
Prion diseases	BAX,C1QA,C1QB,C6,C7,C8B,C9,HSPA5,LAMC1,MAPK1,MAPK3,NCAM1,NCAM2,SOD1,STIP1
Opioid	GNAI2,GNAI3,GNAO1,GNB1,GNB2,GNG10,GNG12,GNG2,GNG4,GNG7,SNAP23,SNAP25,VA

proopiomelanocortin and prodynorphin pathway	MP2,VAMP3
S1P4 pathway	CDC42,GNA13,GNAI2,GNAI3,GNAO1,GNAZ,MAPK1,MAPK3,RHOA
Complement and Coagulation Cascades	A2M,APOA2,C1QA,C1QB,C3,C6,C7,C9,F12,F2,FGB,KNG1,PLG,SERPINA1,SERPINC1,SERPIND1, SERPINF2,SERPING1
Citric Acid Cycle	ACO2,CS,DLST,FH,IDH3A,MDH2,OGDH,PC,PDHA1,PDHB
Thrombin signalling through proteinase activated receptors (PARs)	F2,GNA11,GNA13,GNAQ,GNB1,GNB2,GNG10,GNG12,GNG2,GNG4,GNG7,MAPK1,MAPK3,SRC
Clathrin derived vesicle budding	AP1B1,AP1M1,CLTA,CLTC,CTSZ,DNASE2,DNM2,FTH1,FTL,HIP1R,HSPA8,NAPA,PICALM,RAB5C,SH3GL2,SNAP23,SNAPIN,SNX5,TXNDC5,VAMP2
trans-Golgi Network Vesicle Budding	AP1B1,AP1M1,CLTA,CLTC,CTSZ,DNASE2,DNM2,FTH1,FTL,HIP1R,HSPA8,NAPA,PICALM,RAB5C,SH3GL2,SNAP23,SNAPIN,SNX5,TXNDC5,VAMP2
Cortocotropin releasing factor receptor signaling pathway	GNA11,GNAQ,GNB1,GNB2,GNG10,GNG12,GNG2,GNG4,GNG7,SNAP23,SNAP25,VAMP2,VAMP3
Formation of annular gap junctions	AP2M1,CLTA,CLTB,CLTC,DNM1,DNM2,GJA1
p130Cas linkage to MAPK signaling for integrins	CRK,FGA,FGB,FGG,FN1,RAP1A,RAP1B,SRC,TLN1
GRB2:SOS provides linkage to MAPK signaling for Intergrins	FGA,FGB,FGG,FN1,GRB2,RAP1A,RAP1B,SRC,TLN1
2-Hydroxyglutric Aciduria (D And L Form)	ABAT,ACAT1,ACSM1,ALDH2,ALDH5A1,ILVBL,OXCT1,PDHA1,PDHB
Mitotic Metaphase, Anaphase	BANF1,CKAP5,CLASP2,KIF2A,LMNA,LMNB1,MAPRE1,PAFAH1B1,PPP1CC,PPP2R1A,PPP2R2A,PSMA2,PSMA3,PSMA5,PSMA6,PSMB1,PSMB2,PSMB3,PSMB4,PSMB5,PSMB6,PSMB9,PSMC1,PSMC2,PSMC3,PSMC4,PSMC5,PSMD1,PSMD11,PSMD2,PSMD3,PSMD5,PSMD6,PSME1,PSME2,PSMF1,SEC13,TMPO,XPO1
Neurofascin interactions	ANK1,CNTN1,CNTNAP1,DCX,NFASC,NRCAM
Nef Mediated CD8 Down-regulation	AP2A1,AP2A2,AP2B1,AP2M1,AP2S1,ATP6V1H
TCA cycle	ACO2,CS,DLD,DLST,FH,IDH3A,MDH2,OGDH,SUCLG2
Shigellosis	ACTG1,ARPC1A,ARPC2,ARPC5L,CD44,CDC42,CRK,CRKL,CTTN,MAPK1,MAPK3,PFN1,PFN2,RELA,RHOG,SRC,VCL,WASF2,WASL
Opioid proenkephalin pathway	GNAI2,GNAI3,GNB1,GNB2,GNG10,GNG12,GNG2,GNG4,GNG7,SNAP23,SNAP25,VAMP2,VAMP3
S1P3 pathway	GNA11,GNA13,GNAI2,GNAI3,GNAO1,GNAQ,GNAZ,ITGAV,MAPK1,MAPK3,RHOA,SRC
Uptake of Oxygen and Release of Carbon Dioxide	AQP1,CA1,CA2,HBA1,HBB,HBD,SLC4A1

by Erythrocytes	
Uptake of Carbon Dioxide and Release of Oxygen by Erythrocytes	AQP1,CA1,CA2,HBA1,HBB,HBD,SLC4A1
O2/CO2 exchange in erythrocytes	AQP1,CA1,CA2,HBA1,HBB,HBD,SLC4A1
Adaptive Immune System	ACTR1A,ACTR1B,AP1B1,AP1M1,AP2A1,AP2A2,AP2B1,AP2M1,AP2S1,C3,CALR,CANX,CD74,CD81,CDC42,CLTA,etc.
Synthesis of DNA	PSMA2,PSMA3,PSMA5,PSMA6,PSMB1,PSMB2,PSMB3,PSMB4,PSMB5,PSMB6,PSMB9,PSMC1,PSMC2,PSMC3,PSMC4,PSMC5,PSMD1,PSMD11,PSMD2,PSMD3,PSMD5,PSMD6,PSME1,PSME2,PSMF1
Chylomicron-mediated lipid transport	APOA1,APOA2,APOA4,APOA5,APOB,APOC3,APOE,HSPG2,P4HB
Complement Activation, Classical Pathway	C1QA,C1QB,C3,C4A,C4B,C6,C7,C8B,C9

NCJPA enrichments

Dopamine Neurotransmitter Release Cycle	RAB3A,SNAP25,STX1A,STXBP1,SYN1,SYN2,SYT1,VAMP2
Serotonin Neurotransmitter Release Cycle	RAB3A,SNAP25,STX1A,STXBP1,SYN1,SYN2,SYT1,VAMP2
Ensemble of genes encoding core extracellular matrix	ACAN,AGRN,BCAN,BGN,COL14A1,COL18A1,COL1A1,COL1A2,COL3A1,COL4A2,COL5A2,COL6A1,COL6A2,COL6A3,DCN,DPT,EFEMP1,EMILIN1,FBLN5,FBN1,FGA,etc.
Formation of ATP by chemiosmotic coupling	ATP5A1,ATP5B,ATP5C1,ATP5D,ATP5F1,ATP5H,ATP5I,ATP5J,ATP5O
Selenium Pathway	ALB,APOA1,CAT,F2,GPX1,HBA1,HBB,ICAM1,MPO,PLG,PNPO,PRDX1,PRDX2,PRDX3,PRDX4,PRDX5,SERPINA3,SOD1,SOD2,SOD3,TXN
Mitochondrial Electron Transport Chain	ATP5A1,ATP5B,ATP5C1,ATP5D,ATP5F1,GAPDH,GPD1,GPD2,UQCRC1
GABA synthesis, release, reuptake and degradation	ABAT,ALDH5A1,HSPA8,RAB3A,SNAP25,STX1A,STXBP1,SYT1,VAMP2
Post-chaperonin tubulin folding pathway	TBCA,TBCB,TUBA1B,TUBA4A,TUBB2B,TUBB3,TUBB4A,TUBB4B,TUBB6
oxidative phosphorylation	ATP5A1,ATP5C1,ATP5F1,ATP5J,ATP6V0D1,ATP6V1B2,COX4I1,CYC1,NDUFA6,NDUFAB1,NDUFB10,NDUFB8,NDUFS3,NDUFV2,UQCRH
Citrate cycle, first carbon oxidation, oxaloacetate =>	ACO1,ACO2,CS,IDH1,IDH2,IDH3A

2-oxoglutarate	
Genes encoding proteoglycans	ACAN,BCAN,BGN,DCN,HAPLN1,HAPLN2,HSPG2,LUM,NCAN,OGN,PRELP,VCAN
Transmission across Chemical Synapses	ABAT,ACHE,ALDH2,ALDH5A1,AP2A1,AP2A2,AP2B1,AP2S1,CACNA2D1,CAMK2A,CAMK2B,etc.
Caspase-mediated cleavage	ADD1,DBNL,GSN,MAPT,PLEC,SPTAN1,VIM
Focal Adhesion	ACTG1,ACTN1,CAPN1,CDC42,COL1A1,COL1A2,COL3A1,COL4A2,COL5A2,COL6A2,CRK,FLNA,FN1,GRB2,ITGAV,ITGB8,LAMA2,LAMA4,LAMB1,LAMB2,LAMC1,MAPK1,MYL6,RAP1B,RHOA,THBS1,TLN1,TNC,TNR,VCL,VTN,ZYX
Cytoskeletal regulation by Rho GTPase	ACTG1,ARHGAP1,ARPC2,ARPC5,CDC42,CFL1,MYH10,MYH9,PFN1,PFN2,STMN1,TUBB2B,TUBB3,TUBB4A,TUBB4B,TUBB6,TUBB8
NCAM signaling for neurite out-growth	AGRN,COL4A2,COL6A1,COL6A2,COL6A3,GRB2,MAPK1,NCAM1,NCAN,NRAS,SPTA1,SPTAN1,SPTB,SPTBN1,SPTBN2,YWHAB
Rho cell motility signaling pathway	ACTR2,ACTR3,ARHGAP1,ARPC2,ARPC5,CFL1,GSN,PFN1,RHOA,TLN1,VCL
2-Oxocarboxylic acid metabolism	ACO1,ACO2,CS,GOT1,GOT2,IDH1,IDH2,IDH3A
Gluconeogenesis, oxaloacetate => fructose-6P	ALDOA,ALDOC,ENO1,ENO2,GAPDH,PGAM1,PGK1,TPI1
Vasopressin-regulated water reabsorption	AQP4,ARHGDIA,DCTN2,DYNC1H1,DYNC1I1,DYNC1LI2,GNAS,NSF,RAB11B,RAB5A,RAB5B,RAB5C,VAMP2
Respiratory electron transport	COX4I1,COX5A,COX6B1,CYC1,ETFA,ETFB,MT-CO2,NDUFA13,NDUFA6,NDUFAB1,NDUFB10,NDUFB8,NDUFS1,NDUFS3,NDUFV2,UQCRC1,UQCRC2,UQCRH

Individual proteins specifically associated with JPAs were FBN1, ANXA1, MARCKS, SNRPD, PRDX1 and GFAP, while NCJPA specific proteins included NUMA1, VGF, RPS20, etc. (Figure 8.5).

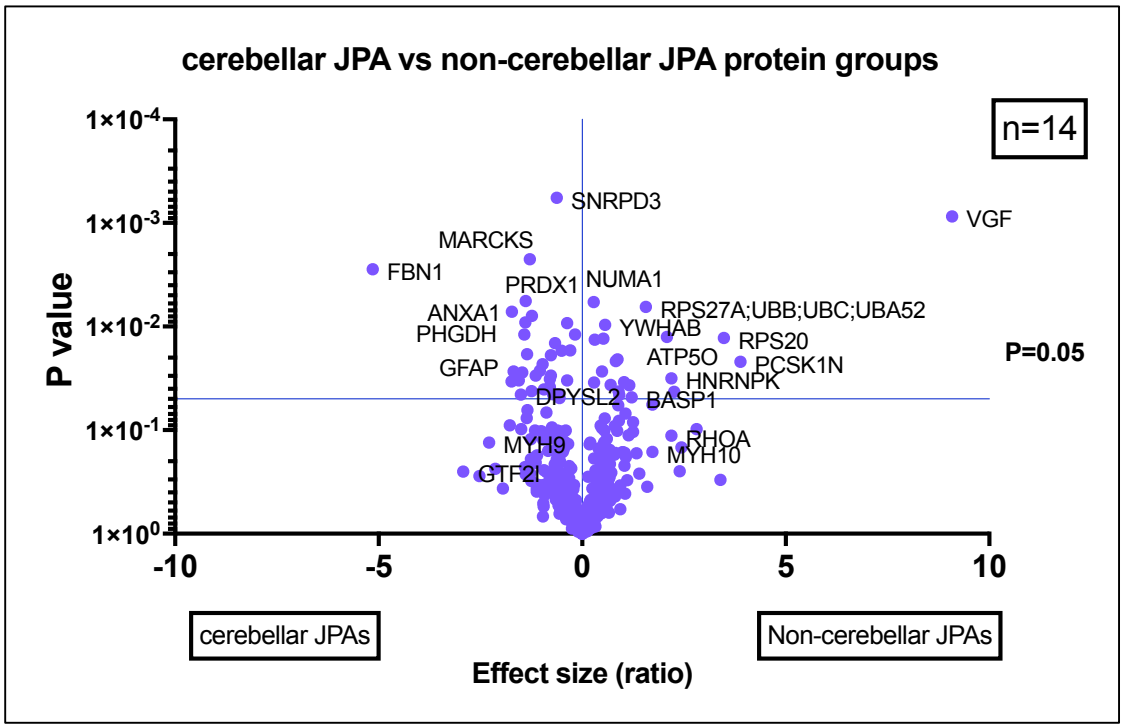

Figure 8.5: Cerebellar and non-cerebellar supratentorial JPA tumour specific protein groups

8.7.3.2 Study 4 Discussion and conclusions

This study aimed to investigate proteomic profiles of cerebellar and non-cerebellar JPA tumours respectively. Data from this study represent subtle and distinct molecular associations to each of these tumour types.

Cerebellar JPA-specific proteins and pathways

Coronin proteins, particularly Coronins 1 and 2 (type I and II), are over represented in our studied cases. These have been suggested to have an actin binding function and also play a roles in immunity with links to T cell and NK cell formation and activations (Uetrecht & Bear, 2006). Furthermore, Coronin 1 protein has been a suggested marker for the presence and activation of CNS microglia; it is seen highly expressed in these cell types and are linked to cytoskeletal rearrangements during

their activation (Ahmed et al., 2007). However, it is uncertain whether the tumour tissue in JPA cases are enriched for microglia or whether the astrocytic or other cellular components themselves take on coronin 1 expression. It has been suggested that up to 30% of low-grade gliomas do indeed contain microglia and tumour associated macrophages (Hambardzumyan, Gutmann, & Kettenmann, 2016).

CD44 has been of interest in cancer as it shown to be involved in cell proliferation, migration and angiogenesis. However, there is contradicting evidences in the literature on whether this protein correlates with prognosis (Naor, Nedvetzki, Golan, Melnik, & Faitelson, 2002). The current study implicates this protein in cerebellar specific JPA. CD47 has been shown to be an angiogenesis regulatory factor and, more importantly, they provide an anti-apoptosis signal to retard immune phagocytosis in many cancer cells and so is the target of much investigation (Chao et al., 2010; Lee, Han, Bai, & Kim, 2009).

The gene for CD59 has been suggested by other studies to be upregulated by hypomethylation in JPAs, and inhibits complement mediated cell killing (Maenpaa, Junnikkala, Hakulinen, Timonen, & Meri, 1996).

ADAM10 is a metalloproteinase that cleaves off many cell surface proteins involved in cancer processes. It is also implicated in triggering inflammation by cleaving off and solubilising pro-inflammatory cytokines (Pruessmeyer & Ludwig, 2009).

Proteins GRB2 and RAP1 were highly evident in the association with outcome of the MAPK integrin pathways in cerebellar JPA patients. There is wide consensus in the literature that the MAPK pathway is important in JPA pathogenesis. More specifically, GRB2 is an adapter protein that is part of the GRB2/SOS complex that can activate the MAPK pathway with activation of Ras protein leading to enhanced tumorigenesis (Kleihues & Ohgaki, 2000).

Complement and coagulation signalling involving proteins were specifically overrepresented in JPA cases, with proteins such as SERPINA1, SERPINC1 and SERPIND1 being highly associated. It is known that in the highly vascular MB tumours coagulation proteins can provide a prognostic benefit as reported in the

previous study. Its implications for JPA pathogenesis are unclear. The coagulome of genes and proteins in cancers have been of interest in the literature, as both targets and possible inducers of tumour progression. This is proposed to occur indirectly by initiation of malignant processes within cancer cells or by the reactivation of dormant tumour cells (Magnus, Asti, Meehan, Garnier, & Rak, 2014)

Adaptive immune processes, including CD74, 81 and RELA, were more specifically associated with cerebellar JPA. It is known that the native and adaptive immune responses has an effect on immune-surveillance in cancer cells, but the roles are less well defined as immune relations can be tumour supressing as well as inflammatory tumour promoting (Vesely, Kershaw, Schreiber, & Smyth, 2011). There are also cooperative mechanisms proposed to link the innate and adaptive immune responses in the tumour environment (Marie et al., 2002). Furthermore, this is supported by findings here of neural innate immune proteins such as GFAP and ANX1 which are overrepresented in these JPAs. Proteins specifically associated with JPAs were FBN1, MARCKS, SNRPD and PRDX1; structural and metabolic protein groups are also seen overrepresented in these cases. The structural protein component is suggestive of cell and tissue reorganisations that are processes of tumour development and growth.

In summary, the current study highlights adaptive immune related markers with specific relation to cerebellar JPA cases using MS based proteomics.

Non-cerebellar JPA specific proteins and pathways

In non-cerebellar JPA cases, the samples were specifically enriched for dopamine, GABA and serotonin associated proteins and Rho cell motility processes. Chemo-osmotic and vasopressin associated water reabsorption protein groups were also overrepresented.

The overrepresentation of neurotransmitter receptors and their pathways such as dopamine, GABA and serotonin may reflect increased neural cells present in these tumours, or of the beginnings of neural differentiation. Furthermore, it could reflect

the pathobiology of non-cerebellar JPA, as it has been reported that some of these tumour cells indeed do have high levels of RNA transcripts for certain neurotransmitters (Entschladen, Lang, Drell, Joseph, & Zaenker, 2002). There have also been reports of alternative roles for neurotransmitters such as those involved in in migration signalling of both leukocytes and tumour cells (Entschladen et al., 2002). This might be suggestive of the clinical role of neurotransmitters in non-cerebellar JPA. However, it is worth considering that this may also suggest location-based artefacts, where brain regions are enriched for these types of neurotransmitters, such as the serotonin and GABA producing Raphe nuclei group of neurons in the brainstem (Weissbourd, Ren, Deloach, Guenthner, & Miyamichi, 2014).

There is also an association with Rho cell motility processes in these tumours. This is supported by recent proteomic findings in smaller cohorts that Rho GTPases are highly associated with astrocytomas and oligodendrogliomas (S. Lin, Wang, & Feng, 2016). It is further supported by more speculative investigative treatments involving recombinant toxins targeting these cell motility pathways in treating aggressive astrocytomas (Al-dimassi et al., 2016). It is noteworthy that the expressions of the protein in these pathways have been suggested to be inversely related to IDH1 mutation status in other cohorts (Hara et al., 2016).

The association of vasopressin and water reabsorption protein groups to non-cerebellar JPA in the current study is interesting. These proteins were formerly targets for older palliative treatments with diuretics. The most likely association is with the tumour vasculature becoming more permeable as a result of blood-brain-barrier breakdown in glioma pathophysiology processes of vasogenic edema, which is hypothesised to allow for better flow of fluids that contain metabolites of importance for the cancer cells' survival (Maugeri et al., 2016). This is also further supported by the overrepresentation of VGF protein in these JPAs which is associated with vasopressin by co-localisation and fluid homeostasis functional regulation (Toshinai & Nakazato, 2009). Therefore, the overrepresentation of these proteins and pathways

are descriptive of the molecular pathology and selective processes that allow for these tumours to survive and grow.

8.7.4 Study 4B – JPA cerebellar and non-cerebellar links to outcome

This study investigated the specific proteomic associations of both JPA and NCJPA to outcomes. As most JPAs are a low grade and have a good outcome, the inclusion criteria for the current study included patients that relapsed or had metastasis or succumbed to disease-related deaths. There were 2 out of 9 cerebellar JPA patients who have presented with poor outcome and 2 of 5 in the NC JPA patients. The main limitation of this analysis was the small sample size. Therefore, the results should be viewed as exploratory.

MYH9, RPL7A, PDIA6 and other proteins were associated with poor outcomes, while CDC42, YWHAG, CCT5, TRA2B and others were associated with favourable outcomes (Figure 8.6A).

For cerebellar JPA cases, MYH10, RPS8, 4X, PRDX were associated with poor outcome, while PCBP1, RAB10, IDH2 and others were associated with favourable outcomes (Figure 8.6B)

The NC JPA cases associated with poorer outcome included MYH9, PSMC1, RPL7A and other proteins, while those associated with good outcomes were PCSK1N, CDC42, YWHAG and other proteins (Figure 8.6C).

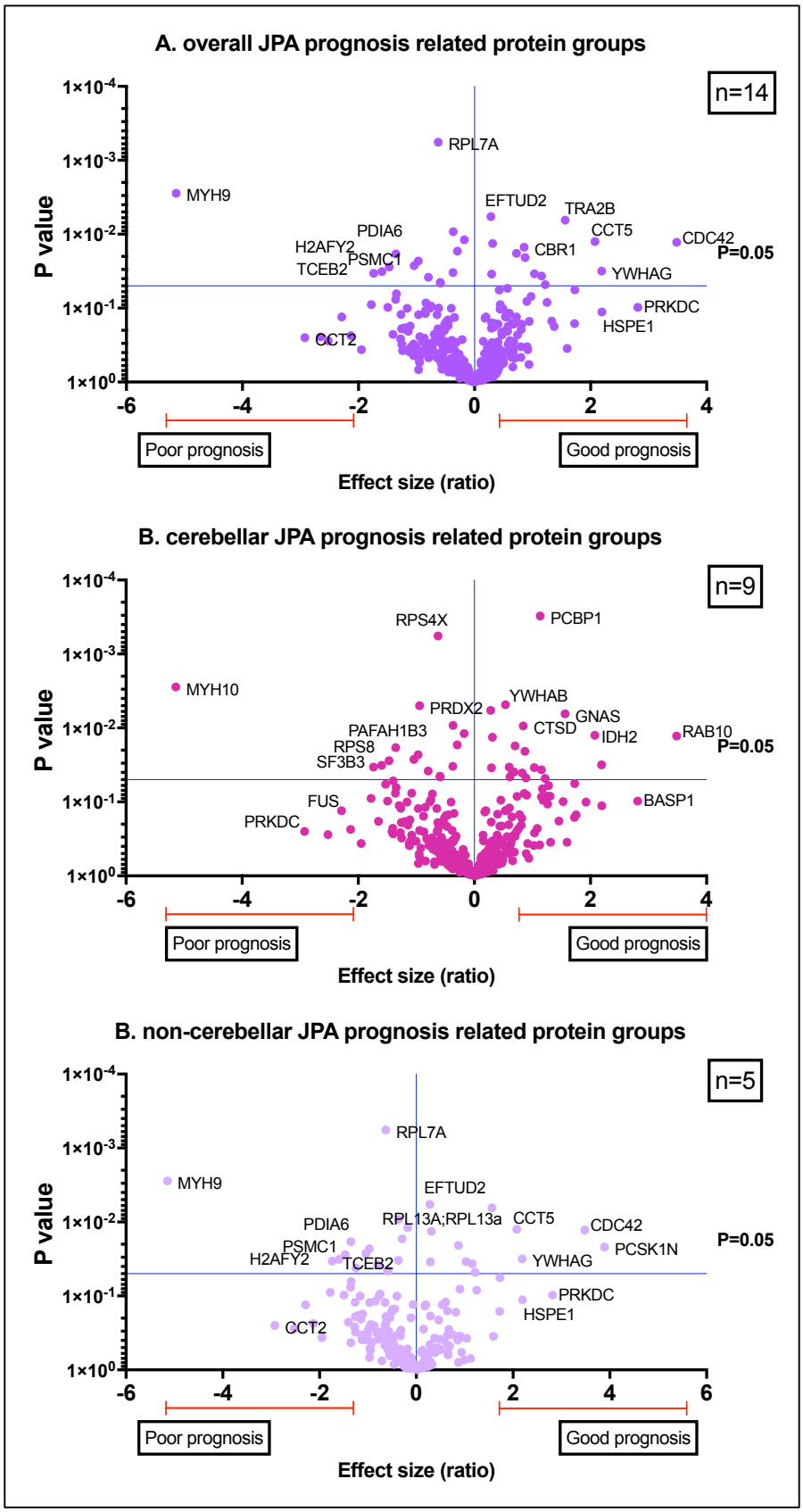

Figure 8.6: JPA outcome related protein markers

A – Overall JPA outcome linked protein groups, B – Cerebellar JPA specific outcome related protein groups, C – Non-cerebellar supratentorial JPA outcome related protein groups

The validated peptides and proteins corresponding to a more favourable prognosis in JPA cases are outlined and these include CELF2, PLLP, DTNA, XRCC5/6, ILF3, EPN2 and ANXA2.

Table 8.8: Peptides upregulated in JPAs with favourable outcomes

Protein	Peptide transition	JPA poor outcome	JPA favourable outcome
CELF2	ELFEPYGAVYQINVLR - 637.6719+++		
	VMFSPFGQIEECR - 533.9147+++		
PLLP	TSSPAQGAEASVSALRPDLGFVR - 772.7363+++		
	GVGSNAATSQMAGGYA - 481.2174+++		
DTNA	LAAESSSSQPPQQR - 495.9146+++		
	NDLLVAADSITNTMSSLVK - 664.6821+++		
EPN2	NIVNNYSEAEIK - 465.2368+++		
	TGAPLGQSEELQPLSQR - 604.3146+++		
XRCC5	IQPGSQQADFLDALIVSMDVIQHETIGK - 1018.5253+++		
	TEQGGAHFSVSSLAEGSVTSVGSVNPAENFR - 1041.1656+++		
ILF3	HSSVYPTQEELEAVQNMVSHTER - 891.0854+++		
	AVSDWIDEQEK - 440.5420+++		
XRCC6	DIISIAEDEDLR - 463.5683+++		
ANXA2	RAEDGSVIDYELIDQDAR - 688.9993+++		
ITIH2	IYGNQDTSSQLK - 451.8930+++		

	LDQIESVITATSANTQLVLETLAQMDDLQDFLSK - 1250.9713+++		

8.7.4.2 Study 4B Discussion

This study investigated the specific proteomic associations of both the cerebellar JPA and non-cerebellar JPA to prognosis. As most JPAs are a low grade and have a good outcome, the inclusion criteria for unfavourable outcomes in the current study included patients that relapsed or had metastasis or succumbed to disease-related deaths.

Overall protein characteristics of JPA

Unfavourable outcome: MYH9, is a structural protein that plays a role in cellular reorganisation, it has also been suggested to be overrepresented in glioma cell lines which is likely a result of protease activation during tumour growth (Alzate et al., 2006). RPL7A is a component of the ribosomal machinery; its role in cancer is suggestive of stimulated protein synthesis which represent increased cellular growth and proliferation (Polisetty, Gautam, & Gupta, 2016). PDIA6 is a protein folding chaperone, but has roles in tumorigenesis linked to the ADAM proteins by modulating disulphide-bond ADAM substrates (Murphy, 2008). This is supported by findings suggesting PDIA6 inhibition might be a target for EGFR mediated cell migration in glioblastoma cells (T. Kim et al., 2016). This finding is novel in suggesting the association of this protein to JPA cases with a poorer outcome.

Favourable outcome: CDC42 is a protein part of the Rho GTPase family and is an important of cell motility processes (Hara et al., 2016). Similarly, YWHAG is a motility related protein, they are found significantly associated with high motility astrocytoma cell lines (Shin, Sun, Jin, Jeong, & Kang, 2007). It is therefore interesting that these are associated with favourable outcome in JPA cases in the current study. It might be counter-intuitive as these are linked with high cell motility. CCT5 is a protein chaperone involved in folding many proteins, including actin and tubulin

proteins. It is also found up-regulated at the RNA level in other studies in gliomas (Malzkorn et al., 2010).

TRA2B is a specific RNA splicing protein that is upregulated in gliomas and knocking down expression was shown to inhibit cell migration and proliferation (L. Yang et al., 2015). Furthermore, this protein has also been implicated in aberrant splicing disorder in tumour cells (Ritchie, Granjeaud, Puthier, & Gautheret, 2008). The current study therefore supports the finding that this protein is important in glial tumour processes, but is confounded by being associated to favourable outcomes.

The validated peptides and proteins corresponding to a more favourable prognosis in JPA cases include CELF2, which is a protein involved in RNA splicing, translation and stability, its functional role is suggested to be implicated in translational control of COX2 and protection from UV irradiation damage pathways (Barreau, Paillard, Méreau, & Osborne, 2006). PLLP is a protein involved in myelination that has been shown to be highly associated with astrocytes and oligodendrocytes (Oldham et al., 2008). As such it may be a descriptive biomarker of glial overrepresentation in these tumours. DTNA has a suggested function involving clustering of nicotinic receptors and stability of synapses; the expression of these have been previously shown in other studies and have been implicated in a rare splice variant in some glial tumours (French et al., 2007). XRCC6 is involved in DNA repair mechanisms, there is also an association with glioma risk in patients presenting with particular SNPs in this protein coding sequence (Tsai & Wu, 2011). XRCC5/6 have likely tumour suppressor roles; furthermore, these two proteins can function as a dimer which might play a role in DNA damage repair (Deimling et al., 1992). Data from this study suggest the XRCC6 is roughly ten times more abundant than XRCC5, so dimers are likely probable, although the study design in the current study cannot directly determine protein interactions (data in supplementary).

ILF3 protein may play a role in post-transcriptional RNA regulation and has also been shown to be expressed at the protein level in glioma cell lines (Meyer, 2014). EPN2

protein plays a role in endocytosis; its activity is known to be phosphorylation dependent where the phosphor form of the protein is suggested to be involved in vesicle endocytosis blocking during mitosis (H. Chen, Slepnev, Di Fiore, & De Camilli, 1999). There are therefore hypothesis-generating questions involving their phosphorylation status during JPA pathogenesis.

Lastly, ANXA2 is a calcium binding protein with other functions related to cancer tumour microenvironment and metastasis in some cancers (Lokman, Ween, Oehler, & Ricciardelli, 2011).

Cerebellar JPA proteomic links

Unfavourable outcome: MYH10, a cellular myosin protein, has been implicated in actin cytoskeletal signalling and cell growth has also been shown to be secreted by highly mitotic glioblastoma cell lines (M. K. Gupta et al., 2013). RPS8 and RPS4X are both components of the 40S ribosomal subunit, these were shown to be upregulated at the RNA level in JPA cases in other studies (Macdonald, Pollack, Okada, Bhattacharya, & Lyons-weiler, 2004). PRDX is a protein previously found associated with high grade astrocytomas; it has a peroxide regulation function which implies its role in reactive oxygen species detoxifications (Odreman et al., 2005). It is therefore novel but unsurprising that there is a significant proteomic link of this protein to poor prognosis in JPA cases.

Favourable outcomes: PCBP1 is a protein that binds to DNA sequences, specifically oligo dC. It has been shown to have an interaction with miRNA-21, an anti-apoptotic factor (Xue et al., 2016). Its overrepresentation suggests upregulation at the protein level and implies its counter action to anti-apoptosis in tumour cells, thereby giving a protective or is suggestive of favourable outcome links. RAB10 is present in extracellular vesicles in GBM cases, and has been suggested to be dysregulated in other cancers (Mallawaaratchy et al., 2016; H. Wang et al., 2014). The link of this protein to favourable prognosis in JPA cases is a novel finding in this context.

IDH2, has been discussed in this thesis with respect to its links with molecular mutation status in the latest classification of CNS tumours (Louis et al., 2016). It is seen in the current study overrepresented in JPA tumours that have a favourable outcome. While the design of this study is not suited to determine mutation status it does provide a foundation for further investigation.

Non-cerebellar JPA proteomic links

Unfavourable outcome: MYH9 and RPL7A were discussed in relation to associations with poor outcomes in overall JPA. PSMC1 appeared significantly associated with poorer outcomes specifically with NC JPA cases. This is a protease regulatory protein. Protease regulation is essential in maintaining normal cellular function. Protease functions have also been implicated in cell cycle progression, angiogenesis and apoptosis, which are particularly important for tumour growth and progression (Pajonk, Mcbride, Pajonk, & Mcbride, 2001).

Favourable outcomes: CDC42 and YWHAG have been discussed previously with links to overall JPA. PCSK1N protein has a proposed function in neuroendocrine secretion; however, its role in cancer cells is unclear. In contrast to the current study, it has been shown in GBM patients with particularly poor outcomes that the RNA abundance of PCSK1N is downregulated (Xiong, Bing, Su, Deng, & Peng, 2014).

Taken together, neuroendocrine secretion proteins as well as CDC42 and YWHAG are shown related to favourable prognosis. This may add molecular insights that correlate with outcomes in JPA cases.

8.7.5 Study 4C – Results: MB and JPA proteomes possible proteomic drivers of malignancy

This study investigated the proteomic associations between the generally lower-grade JPA and the higher-grade MB with the aim of identifying malignancy associated proteins. Proteins associated with malignancy included ST13, RPL13, LMNB2, CCT proteins, GNAS and FN1. Conversely, proteins associated with lower grade tumours include ITI proteins, C4B, ANXA, SPTAN1, VCAN, ALDOC and other proteins (Figure 8.8).

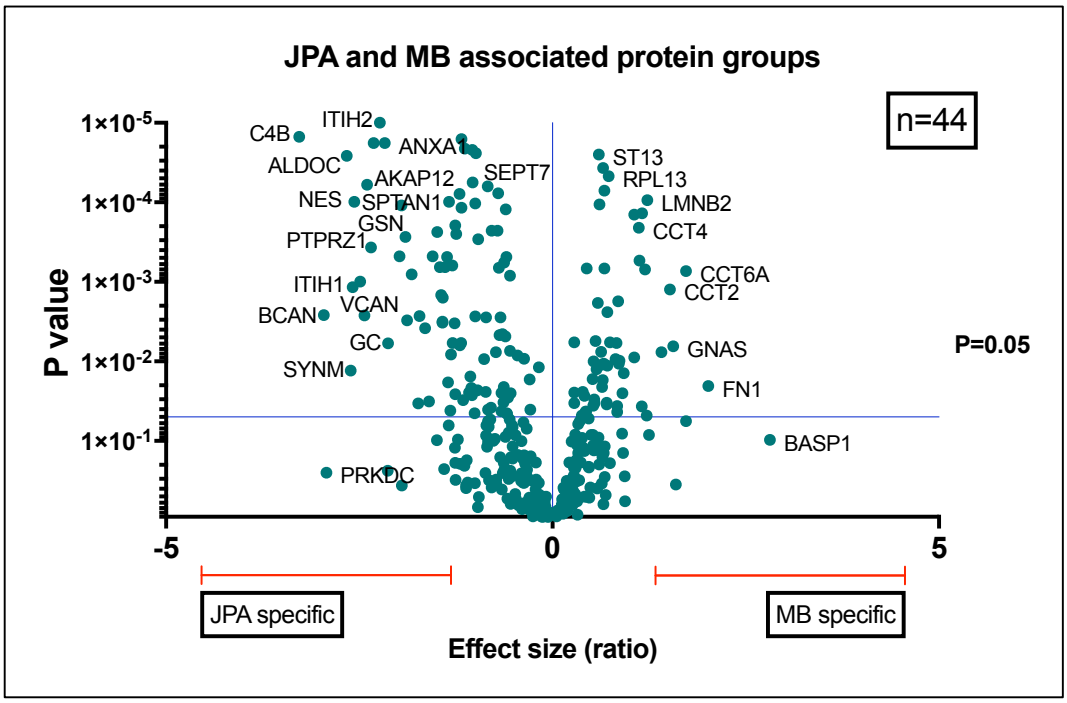

Figure 8.8: Proteomic associations of JPA and MB in this cohort

Study 4C Discussion

The current study investigated the proteomic associations in the lower grade JPA and MB more generally to identify malignancy associations or associations that are specific to their respective tumour biology.

Malignancy-associated proteins groups showed here included ST13, which is a protein with a possible protein chaperone function. It has been previously reported as highly abundant in SHH MB stem-like cells and its link to MB prognosis is supported by current data (Ronci et al., 2015). This protein has also been used in some experimental oncolytic viral treatments, where it has been shown to have tumour supressing activity (Boisgerault, Tangy, & Gregoire, 2010). RPL13, is a component of the 60S ribosomal structure, this protein has been implicated in cancer related regulation of protein translation promoting stress tolerance and cell growth in cancer cells and is also one of the genes regulated by the MYC oncogene (M. K. H. Kim et al., 2003; H. W. Yang et al., 2014). LMNB2, is a lamin protein with functions such as DNA replication, transcription and mitosis, as well as being implicated in breast, pancreatic and hepatocellular carcinomas (Hutchison, 2014). The utility of lamins as cancer biomarkers is interesting but complicated by the variability of lamins between and within tumour subtypes (Foster, Przyborski, Wilson, & Hutchison, 2010). Therefore, further examination of the patterns of expression and abundance are required to further validate these proteins and their utility as cancer biomarkers. CCT proteins are molecular protein folding chaperone proteins that are involved in correcting misfolded proteins. The dysregulation of these proteins have been implicated in neurodegenerative diseases and autism spectrum disorder (Yoo, Kim, Cairns, Fountoulakis, & Lubec, 2001). It might be worthwhile to investigate in further studies the possible link to quality of life outcomes, particularly the effects of neurodegeneration.

GNAS are transducer proteins involved in GPCR signalling. These are suggested to be downregulated in tumours that arise in younger children and upregulated in tumours arising in older children such as oligodendrogliomas (Johansson, Go, & Westermark, 2005).

FN1 are proteins that bind to cell surfaces and are involved in cancer processes such as cell adhesion and cell motility. It is known to be a target gene for hypoxic stress-related proteins in cancer cells (Semenza, 2003). MB is a solid tumour that may have areas that experience intra-tumour hypoxic conditions.

The proteins associated with lower grade tumours include ITI proteins, ITIH2 peptides. These are validated and discussed in the JPA cases in the previous study.

C4B, is a complement and inflammation related protein, for which there is much interest in relation to inflammation and cancer interactions, with inhibitors of this protein resulting in decreases in cell migration in some cancer cells (M. J. Rutkowski, Sughrue, Kane, Mills, & Parsa, 2010). This protein is therefore likely a descriptor of pathogenesis.

SPTAN1, is involved in cytoskeletal movements and is dependent on calcium, it is shown to be involved in GBM pathogenesis and there is evidence of its secretion in GBM cell lines (M. K. Gupta et al., 2013). VCAN, is suggested to play role in cell-extracellular connections, and the expression of this proteoglycan in GBMs have been shown to be altered with relation to promoting tumour cell invasion (Wade et al., 2013). This is indeed interesting as the proteoglycans have been shown to promote signalling in cancers and are might be promising biomarkers of cancer prognosis.

ALDOC is a metabolic enzyme which has been shown to be significantly upregulated in subependymal giant cell astrocytomas (Tyburczy et al., 2010). It might be a useful target for JPA treatment as targets that alter the cellular metabolism usually highly active in cancer exhibiting the Warburg effect, where cancer cells produce high levels

of energy through increases in metabolism through the glycolysis and lactic acid fermentation pathways (Scatena, Bottoni, Pontoglio, & Mastrototaro, 2008).

In summary, specific malignancy-associated proteins such as the protein folding chaperones and cell adhesion and motility are suggested in the current study. Proteins involved with immunity, cell motility and cellular metabolism are implicated with lower grade tumours.

9. Chapter 9-Overall discussion and further work

Brain tumours in children are one of the most challenging diseases to treat, and so outcomes are variable and often lacking. Mortality is high and survivors are often experience poor quality of life due to neurologic disability. Existing treatments require an experienced team of multidisciplinary health professionals and availability of resources to monitor progress and recurrence. Current research in molecular biology of brain tumours is exciting and yields promise of clinically useful results, but this is limited in under-resourced areas.

There are currently no reliable data of brain tumours in children in South Africa. We have no data on the presentation of disease, the spectrum of tumours treated, how these are treated, and what the outcomes are. Importantly there are also no existing molecular biology programs of research. Absence of this data restricts our understanding of the burden of childhood brain tumours in South African children, how we compare with international standards and so what needs to be addressed, and our involvement in international trials of novel therapies and protocols of treatment.

This thesis investigated the two commonest types of childhood brain tumour, MB and the generally less aggressive and slower growing JPA with relation to their molecular biology and their clinical correlates in a local Southern African cohort.

The study design in this thesis takes a systematic approach to determine clinical and molecular data from the respective patient cohorts. This dissertation is structured into MB characterisation followed by JPA characterisation, and thereafter 4 studies on their respective proteomic profiles. Study 1 and 2 characterise the demographics and molecular profiles of the MB and JPA clinical cohorts. Study 3 and 4 undertake examine and validate proteomic profiles of MB and JPA with specific sub-aims. The study designs were conceptualised by creating appropriate cohorts and estimating the sample characteristics and sample size required to achieve adequate statistical power and to aid in interpretation of the results.

9.1 MB cohort characterisation

This study determined the molecular characteristics of a retrospective cohort of MB patients in a South African cohort and presents the first molecular subgrouping for medulloblastoma in an African setting. There were 13% WNT, 33% SHH, 24% Group 3 and 30% Group 4 subtypes presented in this cohort of 48 cases between 1988 - 2014 with follow up until 2016. Demographic and phenotypic data is consistent with data from other international cohorts, with the exception of a greater proportion of female patients and greater proportion of NMYC amplified cases - 20% in the current cohort. The 5-year overall survival was 74% and 10-year overall survival was 62%.

9.2 JPA cohort characteristics

The JPA cohort investigated in this thesis showed a median age of 6 years old with expected low rates of metastasis and recurrent disease. There is a favourable 5-year overall survival of 93%, similarly a progression-free survival of 86%.

The molecular characteristics shown in the current cohorts are BRAF amplification as determined by FISH where there is a strong association with cerebellar JPA cases and showed a trend towards poorer outcomes. pERK positivity by IHC as a marker of MAPK pathway activation is consistent in most patients. P16 inactivation, also known as CDKN2A inactivation, was shown by IHC weak staining patterns trended towards poorer prognosis.

Study 1 and Study 2 limitations

Limitations of the characterisation analysis of Studies 1 and 2 are to be considered in the interpretation of the statistical significance of the data. These studies are designed as cohort studies and not as population-based studies. They have limited sample sizes and data has to be interpreted in this context. Furthermore, clinical associations to outcomes are interpreted with some patients having limited follow-up. This loss to follow-up is a significant challenge for clinical research in a developing world setting.

Furthermore, censoring early loss to follow up patients could be considered informative censoring and lead to bias in the dataset. This means that if we encode early cases of loss to follow as having an unfavourable outcome we are informing the dataset and suggesting that those that are early loss to follow up have differing odds of poor outcome compared to those that are not censored, a factor that is as yet indeterminate in the case of MB and JPA pathology. Therefore, it has been suggested that to produce unbiased survival data from varying follow-up times, that the arms of comparison need to have approximately the same ranges of follow up (Clark, Bradburn, Love, & Altman, 2003). For example, if we make informative censoring decisions of early loss to follow up cases in this study, we would be making the assumption that a WNT subtype that was loss to follow up at 3 months has similar odds of surviving as a more aggressive SHH, Group 3 or Group 4 case. This is an unlikely event especially if we make this assumption across diseases, like assuming similar odds of Group 3 having similar odds of surviving at early stages compared to the less aggressive JPA cases. Therefore, every effort was made to follow up the cases in these cohorts, with early loss to follow up together with follow up ranges detailed in all cases to support minimally unbiased survival estimates. This is a challenge as some of the cases presented were not local to the region and thus extensive follow up is challenging in a investigating retrospective cohorts in a developing world context. It is less challenging for the more recent the patients but becomes increasingly complex to delineate outcomes in the much older cases.

Additionally, the confounding factors of subtyping in the MB characterisation of Study 1 represent a conflict in methodology of subtyping. To resolve this, proteomic-clustering analysis was performed to confirm assigned subgroups in those cases of conflicting assignments. The methods of subtyping were chosen due to its applicability to FFPE material and physical and cost accessibility for a limited resource setting in Southern Africa. There is currently no consensus on the methodology for subtyping and the WHO guidelines do not advocate for specific methods and could represent a limitation in subtyping studies (Louis et al., 2016).

9.3 Proteomic profiles

There is a vast knowledge base of genomic data related to paediatric brain cancers. However, in contrast to this, the availability of proteomics knowledge is limited in brain tumour studies, and present the minority of cases in publically available proteomics repositories (Martens et al., 2006). While there is much genomic data available for MB, much of the data is difficult to interpret in terms of the disease biology. For example, gene expression does not incorporate active signalling processes resulting from post-translational modifications in proteins. It therefore seems likely that taking a combined gene profiling and proteomic approach may provide a more detailed characterisation of the pathophysiology giving biological systems level information as well as validated genomic markers at the protein level.

Proteomic work in this thesis involved ascertaining oncoproteomic profile of the retrospective cohorts of MB and JPA using a discovery proteomic approach. Thereafter, a subsequent targeted proteomic approach validated the findings in a prospective cohort. Samples that were subject to proteomic characterisation were a subset of the retrospective cohorts described above. The samples included in the proteomic analysis were required to produce a discernible mass spectrogram, free of contaminants and produce quantifiable proteins and peptides by label-free quantitation.

Study 3 and Study 4 limitations

Limitations in the proteomic investigations of Studies 3 and 4 include the investigation in a smaller subset of the entire MB and JPA cohorts. This was due to the effects of FFPE fixation and tissue block age on producing comparable mass spectrograms. There are also limitations in associations to outcomes as some patients represent limited follow up or were loss to follow up, and is a significant limitation to outcome based studies in a developing world setting. However, any links that was statistically associated in the discovery based proteomic investigations was further validated at the peptide level using a targeted proteomic approach. The targeted MS approach investigates a smaller number of peptides and compares their associations against representative cases. Namely, the associations were validated in cases that had

favourable outcomes against those that had poor outcomes. Furthermore, subtype specific associations were validated using the targeted MS based investigation and compared to all other subtypes. The IHC panel determined the specific subtypes assigned to the validation cohort. This method of assigning subtype is sub-optimal and could be considered a limitation. However, to address this, the targeted data produced from the validation cohort is interpreted as enrichment profiles. This makes the assumption that even with sub-optimal subtype prediction, the assigned group categories of WNT, SHH, Group 3 and Group 4 will have more of the true subtype cases and is likely enriched with those true subtypes. Notwithstanding, the targeted MS validation data is presented here as likely candidate markers with proteomic evidences within the limitations as stated. These will require comprehensive verification by the wider research community for any future utility as clinical biomarkers.

Understanding protein prognosis links is complex; studies such as the ones presented in this work provide only an insight into the nature of these prognosis links. Further mechanistic hypothesis can be generated and tested from this study and provide a comprehensive understanding of the biology of these associations. Determining proteomic associations such as those presented here might provide more mechanistic insights into brain cancer pathogenesis.

Only peptides that were overrepresented in specific subtypes were reported. Similarly, only peptides overrepresented in specific outcomes and validated at the peptide level were reported. Lastly, given the limitations stated here, the data was interpreted as enrichment profiles which suggests that the comparison groups between subtypes, pathologies and prognosis groups were enriched for the true groups and the data is interpreted in the light of adequate statistical power achieved in each study.

MB proteomic profiles

WNT specific associations

MB gene ontology analysis revealed enrichment of endoplasmic reticulum, immunoglobulin, and ribonuclear complex associations in the WNT subtype. Molecular function enrichment in this dataset revealed immunoglobulin binding, glycation product binding and disulphide bond activity here. Biological process enrichment profile of MBs in this cohort demonstrated vesicle-related processes, oxidative stress and protein folding processes. The individual highly abundant protein groups statistically associated with WNT subgroups show VIM, DKK factors, COLA and RNA elongation factors. Validated peptides linked to WNT were HSPA5, DAD1, FBN1 and INA protein groups were all specific to this subtype.

Taken together, there is a panel of peptide candidates reported in the current study and supported by prior evidences in the literature to be specific for the WNT subtype. There are opportunities to delineate WNT MB tumour pathobiology from biochemical pathways and specific proteins identified. There is also further utility in the creation of a custom WNT specific targeted proteomic experiment possibly to subtype tumours for further clinical proteomic applications.

Investigating WNT specific prognosis was challenging in this thesis, as there were very few patients with WNT MB that displayed poor clinical outcomes; therefore, all identified WNT subtype specific protein groups were linked to a favourable prognosis.

SHH-specific associations

Cellular component enrichment revealed proteins associated with the excitatory synapse, SWI/SNF and membrane vesicle in SHH. Molecular function enrichment in this subtype included NADH quinone, protein translation regulation and GTPase activity. Biological process enrichment showed DNA replication, epigenetic regulation, cell growth and differentiation. SHH contained PDLIMs, GAB, heat shock

proteins and NEFM neurofilament proteins. Similarly, peptides for DPSY2-5, PRR36 and GAB1 are specific in SHH.

In all, the chromatin remodelling factors, as well as the SWI/SNF, DPYSL protein, cell motility proteins and RNA transcript degradation pathways have been suggested in this thesis to be implicated in SHH-specific tumours in the cohort investigated.

Some subgroup-specific candidate proteins for poor prognosis in SHH patients include GFAP, CKB, SPTAN1, DHX9, SRI, RPSX4; while those associated with good outcomes include A2M, FGB, HIST1, RAB1B, PDIA6, ST13, PRDX5 and YWHAZ protein groups.

Recent studies have described dysregulated or mutated smoothened receptors as a SHH pathway target. While promising, only temporary responses in patients treated with these type of targeted drugs have been reported (Lou et al., 2016). Further work, such as in the current study to identify more appropriate targets or target agents may add more insight into the SHH pathway and its mechanisms of pathogenesis.

Group 3 specific associations

Cellular component enrichment in Group 3 MB revealed ATPase degradation complexes, ribonuclear and DNA replication associations. Only NFκB binding and ATP synthase was enriched as a molecular function in this subtype. Mis-folded protein responses, gene silencing, DNA repair and protein sumoylation were biological processes implicated in Group 3. Proteins for ribonuclear complexes, mitochondrial proteins, COX, PYCR1 and sumoylation proteins were significantly associated in this subtype. Peptides for TGFBI, ARAP1 and LUC peptides specifically link to Group 3.

In all, ribonuclear proteins, SUMO related protein modification, Rho signalling and the LUC7L proteins have been implicated in Group 3 specific tumours in the current study.

The protein groups associated with Group 3 favourable prognosis included RAB5A, ANP32A, DDX5, RPS13, CCT2 and DYNC1H1, while those associated with poor outcomes included VIM, LAMC1, IGKCs, NCAM and GSN protein groups.

Taken together, the proteins associated with poor outcomes in Group 3 MB in the cohorts studied are mostly linked with cell adhesion, invasion and immunity-related functions, proteins associated with a favourable outcome included functions involved in tumour suppression and growth factor receptor shielding or withdrawal.

Group 4 specific associations

Protein folding, splicing and motor protein associations were revealed as cellular component enrichments in Group 4 MB in this cohort. Dopamine, protein and amino acid binding, as well as G-protein related serotonin binding were enriched as a molecular function in this subtype. ATPase function, synapse and cell development processes are enriched as a biological process in this group. Group 4 contains serine proteases RELN and serine protease inhibitors PEBP1, neurodevelopment proteins, TNIK and VAT1. Specific peptides associated with this group include markers for RHOA, FRY and HAGH are specifically linked to Group 4 subgroups.

Protein folding, splicing and motor protein association with dopamine, protein and amino acid binding, as well as G-protein related serotonin binding and ATPase function, synapse and cell development processes were enriched in Group 4 MBs in this cohort.

Proteins associated with Group 4 MB favourable outcomes include RPL13, SERPINA3, RPS12 and C1QBP, while those associated with a poorer outcome in Group 4 tumours include HIST1, PDXP, IDH2, AKR1B1 and C14orf166 protein groups.

Taken together the protein groups related to favourable prognosis in Group 4 MB are ribosomal and protein translation linked with pro-coagulation proteins and inflammatory-related while the proteins linked to poorer outcomes are histone and ploidy-related, mitosis, IDH oncometabolite-related and chemotherapy resistant-related proteins.

Overall the proteins associated with poor outcome in MB are the collagens, GFAP, CRB, hypoxia proteins. Some of these could be related to late stage disease such as collagens associated necrosis and hypoxic stress in tumour interiors. Therefore, a further more detailed analysis should follow to examine subgroup-specific prognosis markers and lowering the statistical significance to $p < 0.1$. Additionally, some of the proteins associated with favourable outcome include, VARS a valine-tRNA ligase, co-chaperones FKBP4, CCT7 and growth inhibitors RTN4.

Chromosomal links for the significant proteins related to outcome are displayed based on chromosomal location (Figure 9.4). A region on chromosome 6p seems to be enriched for VARS, RPS12 and HIST1H3A. All were associated with good outcomes in MB overall, Group 4 and SHH respectively.

Cerebellar JPA specific protein

Data from this thesis suggest adaptive immune related markers are more specifically related to cerebellar JPA cases using MS based proteomics. MYH10, RPS8, RPS4X, PRDX and more are associated with poor outcome in cerebellar JPA cases.

Non-cerebellar specific protein

In non-cerebellar JPA cases, the samples were specifically enriched for dopamine, GABA and serotonin associated proteins and Rho cell motility processes. Chemo-osmotic and vasopressin associated water reabsorption protein groups being

overrepresented in these cases. Poorer outcome was associated with MYH9, PSMC1 and RPL7A.

Malignancy associated proteins

The current study investigated the proteomic associations in the lower grade JPA and MB more generally to identify malignancy associations. Malignancy associated proteins included ST13, RPL13, LMNB2, CCT proteins, GNAS and FN1. The proteins associated with lower grade tumours include ITI proteins, C4B, ANXA, SPTAN1, VCAN and ALDOC.

Taken together, there are specific malignancy associated proteins such as the protein folding chaperones and cell adhesion and motility are suggested in the current study. Proteins involved with immunity, cell motility and cellular metabolism are implicated with lower grade tumours.

9.4 Statistical power achieved in this thesis

The statistical power achieved in the characterisation investigations of Study 1 and 2, which investigated a quantitative low-mid throughput panel of markers. The actual power of these studies is outlined and lies between 0,95 – 0,99 (Table 9.1).

Table 9.1 Statistical power achieved by the characterisation investigations of Studies 1 and 2

Study	Experiment	Effect size	Power achieved
Study 1 MB characterisation	Nanostring	0,57	0,95
	IHC	4,02	0,99
	FISH	0,89	>0,95
Study 2 JPA characterisation	IHC	0,28	0,95
	FISH	2,87	0,99

In general, the FISH panels have a larger effect size compared to the Nanostring or IHC panels, which suggests that the associations determined by FISH are more pronounced in effect.

The statistical power achieved in the molecular proteomic investigations was guided by the proteomic coverage achieved. There are however, 20 197 curated protein-coding genes in the human reference map and additional splice isoforms, with about 10 000 proteins and neuropeptides suggested to be found in brain tissues in human diseased or animal model brain tissue (Klose et al., 2002; Y. Li et al., 2016). Coverage in this study reveals up to 2000 proteins without extensive fractionation and about 800 more with fractionation. The trade off in reaching higher coverage is therefore taken into consideration, as this representation is about 20-28% of the total predicted proteome. Furthermore, the use of advanced high resolution MS allows for great sensitivity, scope and dynamic range which enables shotgun proteomic experiments to quantitate differences between clinical samples for robust biomarker discoveries (Mcdonald & Yates, 2002).

Previously published biological and technical total variations in similar proteomics study designs were in the range of 18-40% or greater (Levin, 2011). Therefore estimating the variation from previously reported simulations is in that range; the number of samples in each group should be greater that 5 with a minimum of 2 fold difference for a power greater than 0.8.

Table 9.2: Statistical power achieved by the proteomic investigations of Studies 3 and 4

Study	Group	N	Fold	CV	Power
Study 3 - MB subgroup specific proteins	WNT	6	>3	6,82	0,90
	SHH	9	>3	6,35	1,00
	Group 3	5	>3	6,48	0,95
	Group 4	6	>3	6,54	1,00
Study 4A - JPA location specific proteins	Cerebellar	9	>2	7,18	1,00
	Non-cerebellar	5	>2	6,77	0,95
Study 4B - JPA proteomic associations to outcomes	Cerebellar	2	>3	6,53	0,40
	Non-cerebellar	3	>1,5	6,69	0,70

The results of this thesis are to be interpreted with relation to the statistical power estimated to be achieved utilising power prediction for quantitative proteomic calculations (Levin, 2011)(Table 9.1). Overall, a high statistical power is seen across all the studies presented here, with the exception of the JPA prognosis related protein studies. However, the sample size has been the limiting factor, as patients with the lower grade JPA tend to have a generally favourable outcome.

It is noteworthy that this thesis aimed to systematically investigate the molecular biochemical profile of paediatric brain tumours namely, MB and JPA. The study design utilised molecular profiles and comparisons between and within the diseased cases. In this regard, the controls used for the more highly malignant MB was the lower grade JPAs and vice versa. This type of study design is likely robust in comparisons of this nature as it reveals a wide snapshot of the most overtly abundant markers as well as the more-subtle markers. Other studies utilising a case-control study designs with relative controls such as matched peritumoural surrounding normal cells or unmatched tissue from other minor surgical accessible pathologies such as during epilepsy and even neurodevelopmental abnormalities such as fatty filum tissue samples have yielded few differentiated proteins (Lemée et al., 2013). This is likely due to:

1) Molecular tumour microenvironmental effects in peritumoural tissues,

2) Poor correlation with brain and other CNS tissues (such as spinal cord tissue) and

3) Lastly, epilepsy or other pathologically related proteomic expression resembling tumoural processes.

Therefore, this thesis provides novel insight from a study design perspective and expands interpretation of the results.

9.5 Further work

Taking the molecular profiles further, incorporating newer techniques such as metabolite profiling of astrocytoma and MB can provide evidence for specific pathways by determining their stable metabolic end products (Morales, Martinetto, Calvar, & Sevlever, 2010). Such studies are interesting validation tools in implicating markers from other biomolecules. They also provide more accessible sampling as stable metabolites are usually in solution and can be investigated by minimal sampling or by non-invasive spectroscopy. Going forward, the molecular era provides laboratory tools that are translatable to clinical studies with the goal of providing a more comprehensive multi-omic profile of tumour pathology. This work paves the way for using such biomarkers as potential targets for treatment based on either traditional therapies or repurposed therapies for more inexpensive treatment with direct applicability for a low resource setting such as Southern Africa.

Discovery-based studies such as those presented in this thesis are inherently hypothesis generating. Other possible insights should be more specifically investigated using suggestions from this work as well as other lines of evidences for a robust validation and possible translational applications. Therefore, further large-scale validation efforts using discovery studies is needed to move the field forward in applying modern molecular findings in the clinical setting. Validations from diverse cohorts such as the ones used in this thesis also further support the wide applicability of biomarkers in genetically diverse populations.

While this work presents novel data there are still other under-investigated areas in brain tumour proteomics. Such research areas include the vast array of important post-translational modifications that reveal the molecular state of cells and tissues. Another interesting application of this type of research is investigations into neuropeptides, which the study design in the current thesis limited. Neuropeptides have been suggested to be an independent marker of tumour behaviour in some brain cancers (Fleshman, Shimada, & Dorisio, 1992). This type of investigations might be useful to

delineate tumour and regional brain responses as well as more peripheral responses to brain tumours.

Peripheral markers and their utility and applicability are also important to consider. Markers including serum biomarkers, autoantigens and circulating cell/vesicles/proteins and others could provide candidates for useful aspects of modern brain tumour care including subtyping and predicting aggressiveness.

Sampling from CSF, blood, urine etc. and minimally invasive sampling such as the modern microdialysis, markers intra-operatively (thermal and ultrasonic by-product sampling) or non-invasive MRI, CT or PET imaging spectroscopy all provide biological sample material pools on which to investigate and validate candidate biomarkers.

Furthermore, it might also be interesting to examine molecular associations using (omic-based) technologies into quality of life in survivors of brain tumours. However, the complexity involving surgical, chemo- and radiotherapy interplays with molecular factors and are likely a summation of all these factors associated with quality of life measures.

9.6 A South African context

Of interest in the South African context is the high prevalence of infectious diseases such as HIV and Tuberculosis. There have been reports of HIV associated cerebral lymphomas and astrocytomas (Tacconi, Stapleton, Signorelli, & Thomas, 1996).

The rare cases of HIV associated brain tumours might provide for novel insights into brain tumour pathology. This thesis provides a molecular basis on which to build other important aspects of brain tumour research in the local context. This type of

crossover research can provide unique research findings in places where there might be significantly more cases of these rare tumours.

Socio-economic effects of brain tumour clinical trials have been recently investigated in developed countries. It has been suggested that while there is proportional representation of ethnic groups in phase I clinical trials, there are some underrepresented groups, particularly in CNS tumour trials (Nooka, Behera, Lonial, & Dixon, 2016). This has further implications for low and middle-income countries such as South Africa that are generally under-represented in international multicentre clinical trials for new treatments for childhood brain cancers. Work such as the studies presented in this thesis provide some molecular basis for local research and increases capacity for future work to be conducted to support inclusion in possible trials. Beyond this, there are also aspects of access to clinical care that remain relevant. Recent evidence suggests that even in developed nations such as Switzerland there are socio-economic effects on paediatric CNS tumour mortality (Adam et al., 2016). Countries with larger inequalities likely demonstrate more pronounced socio-economic disparities in the outcomes of these patients. Such phenomena are still under-investigated in an African context, where other more immediate health challenges persist and non-communicable disease research lags behind the developed world in many regards.

Furthermore, comprehensive epidemiological studies on brain tumours in African countries are very rare and countries such as Morocco have provided some insight to the profile of brain tumours in the region (Karkouri et al., 2010). Such epidemiological studies can serve to guide national health initiatives to tackle the challenge more appropriately even in their resource constrained settings.

9.7 Conclusions

This thesis provides a systematic analysis of MB and JPA brain tumours in a South African paediatric cohort. The clinical and molecular profiles of these tumours are largely consistent with other international cohorts with some exceptions.

Data from the proteomic profiles of MB and JPA suggest that there are specific malignancy-associated proteins such as the protein folding chaperones and cell adhesion and motility. Proteins involved with immunity, cell motility and cellular metabolism are implicated with lower grade tumours in this study. The proteomic profiles of both MB and JPA describe their respective pathologic processes.

The individual highly abundant protein groups statistically associated with subgroups show VIM, DKK factors, COLA and RNA elongation factors. Validated peptides associated with MB subgroups show that peptides linked to HSPA5, DAD1, FBN1 and INA protein groups are specific to WNT subtype.

Some subgroup specific prognosis candidate proteins include those for SHH with poor outcomes include GFAP, CKB, SPTAN1, DHX9, SRI, RPSX4; while those associated with good outlook include A2M, FGB, HIST1, RAB1B, PDIA6, ST13, PRDX5 and YWHAZ protein groups.

The protein groups associated with Group 3 favourable prognosis include RAB5A, ANP32A, DDX5, RPS13, CCT2 and DYNC1H1, while those associated with poor outcomes include VIM, LAMC1, IGKCs, NCAM and GSN protein groups.

Taken together the proteins associated with poor outcomes in Group 3 MB in the cohorts studied are mostly linked with cell adhesion, invasion and immunity related functions.

Proteins associated with Group 4 MB favourable outcomes include RPL13, SERPINA3, RPS12 and C1QBP, while those associated with a poorer outcome in Group 4 tumours include HIST1, PDXP, IDH2, AKR1B1 and C14orf166 protein groups.

Taken together the protein groups related to favourable prognosis in Group 4 MB are ribosomal and protein translation linked with pro-coagulation proteins and inflammatory related while the proteins linked to poorer outcomes are histone and ploidy related, mitosis, IDH oncometabolite related and chemotherapy resistant related proteins.

The cerebellar JPA cases showed more specific prognostic links, it was seen that MYH10, RPS8, RPS4X, PRDX and more are associated with poor outcome.

The non-cerebellar JPA cases were specifically enriched for dopamine, GABA and serotonin associated proteins and Rho cell motility processes. With chemo-osmotic and vasopressin associated water reabsorption protein groups being overrepresented in these cases.

Overall, a high statistical power is seen across all the studies presented here, with the least power achieved in JPA prognosis related protein studies due to the generally favourable outcomes with this tumour type.

Molecular proteomic profiles of MB and JPA cases in this thesis provide evidence for some novel molecular pathways, proteins and peptides associated with pathogenesis. This work therefore provides data that is hypothesis generating for further studies in a South African and larger African context.

Bibliography

Adam, M., Rueegg, C. S., Schmidlin, K., Spoerri, A., Niggli, F., Grotzer, M., … Kuehni, C. E. (2016). Socioeconomic disparities in childhood cancer survival in Switzerland. *International Journal of Cancer*, *138*, 2856–2866. http://doi.org/10.1002/ijc.30029

Adamson, D. C., Shi, Q., Wortham, M., Northcott, P. A., Di, C., Duncan, C. G., … Yan, H. (2010). OTX2 Is Critical for the Maintenance and Progression of Shh-Independent Medulloblastomas. *Molecular and Cellular Pathobiology*, *70*(1), 181–191. http://doi.org/10.1158/0008-5472.CAN-09-2331

Ahmed, Z., Shaw, G., Sharma, V. P., Yang, C., Mcgowan, E., & Dickson, D. W. (2007). Actin-binding Proteins Coronin-1a and IBA-1 Are Effective Microglial Markers for Immunohistochemistry. *Journal of Histochemistry and Cytochemistry*, *55*(7), 687–700. http://doi.org/10.1369/jhc.6A7156.2007

Al-dimassi, S., Salloum, G., Saykali, B., Khoury, O., Liu, S., H.Leppla, S., … El-Sibai, M. (2016). Targeting the MAP kinase pathway in astrocytoma cells using a recombinant anthrax lethal toxin as a way to inhibit cell motility and invasion. *International Journal of Oncology*, (48), 1913–1920. http://doi.org/10.3892/ijo.2016.3431

Albright, A. L. (1993). Pediatric Brain Tumours. *CA: A Cancer Journal for Clinicians*, *43*(5), 272–288.

Aldosari, N., Bigner, S. H., Burger, P. C., Becker, L., Kepner, J. L., Friedman, H. S., & Mclendon, R. E. (2002). MYCC and MYCN Oncogene Amplification in A Fluorescence In Situ Hybridization Study on Paraffin Sections From the Children's Oncology Group. *Archives of Pathology & Laboratory Medicine*, *126*, 540–544.

Alzate, Ó., Osorio, C., Herbstreith, M. H., Hjelmeland, M., Buechler, R., He, D. N., … Rich, J. N. (2006). TGF- b and a specific TGF- b inhibitor regulate pericentrin B and MYH9 in glioma cell lines TGF- b y un inhibidor específico de TGF- b regulan pericentrina B y MYH9 en células de glioma. *Rev. Colomb Biotecnol*, *VIII*(1), 48–56.

April, C., Klotzle, B., Royce, T., Wickham-garcia, E., Boyaniwsky, T., Izzo, J., … Fan, J. (2009). Whole-Genome Gene Expression Profiling of Formalin-Fixed, Paraffin-Embedded Tissue Samples. *PloS One*, *4*(12), 1–10. http://doi.org/10.1371/journal.pone.0008162

Arai, M., & Itokawa, M. (2010). A hard road in psychiatric genetics : schizophrenia. *Journal*

of Human Genetics, *55*, 397–399. http://doi.org/10.1038/jhg.2010.66

Aref, D., Moffatt, C. J., Agnihotri, S., Ramaswamy, V., Dubuc, A. M., Northcott, P. A., … Croul, S. E. (2013). Canonical TGF-beta Pathway Activity Is a Predictor of SHH-Driven Medulloblastoma Survival and Delineates Putative Precursors in Cerebellar Development. *Brain Pathology*, *23*, 178–191. http://doi.org/10.1111/j.1750-3639.2012.00631.x

Armenian, S. H., Landier, W., Hudson, M. M., Robison, L. L., & Bhatia, S. (2013). Children's Oncology Group's 2013 Blueprint for Research: Survivorship and Outcomes. *Pediatric Blood Cancer*, 1–6. http://doi.org/10.1002/pbc

Attard, T. M., Giglio, P., Koppula, S., Snyder, C., & Lynch, H. T. (2007). Brain Tumors in Individuals With Familial Adenomatous Polyposis A Cancer Registry Experience and Pooled Case Report Analysis. *Cancer*, *109*(4), 761–766. http://doi.org/10.1002/cncr.22475

Backos, D. S., Franklin, C. C., & Reigan, P. (2012). The role of glutathione in brain tumor drug resistance. *Biochemical Pharmacology*, *83*(8), 1005–1012. http://doi.org/10.1016/j.bcp.2011.11.016

Bandopadhayay, P., Bergthold, G., Nguyen, B., Schubert, S., Gholamin, S., Tang, Y., … Cho, Y.-J. (2015). BET-bromodomain inhibition of MYC-amplified medulloblastoma. *Clinical Cancer Research*, *20*(4), 912–925. http://doi.org/10.1158/1078-0432.CCR-13-2281.BET-bromodomain

Barreau, C., Paillard, L., Méreau, A., & Osborne, H. B. (2006). Mammalian CELF/Bruno-like RNA-binding proteins: molecular characteristics and biological functions. *Biochimie*, *88*, 515–525. http://doi.org/10.1016/j.biochi.2005.10.011

Baryawno, N., Rahbar, A., Wolmer-solberg, N., Taher, C., Odeberg, J., Darabi, A., … Söderberg-nauclér, C. (2011). Detection of human cytomegalovirus in medulloblastomas reveals a potential therapeutic target. *Journal of Clinical Investigation*, *121*(10), 4043–4055. http://doi.org/10.1172/JCI57147.colon

Basta, N. O., James, P. W., Craft, A. W., & McNally, R. J. Q. (2010). Season of birth and diagnosis for childhood cancer in Northern England, 1968-2005. *Paediatric and Perinatal Epidemiology*, *24*(3), 309–18. http://doi.org/10.1111/j.1365-3016.2010.01112.x

Bates, G. J., Nicol, S. M., Wilson, B. J., Jacobs, A. F., Bourdon, J., Wardrop, J., … Fuller-Pace, F. V. (2005). The DEAD box protein p68 : a novel transcriptional coactivator of the p53 tumour suppressor. *The EMBO Journal*, *24*(3), 543–553. http://doi.org/10.1038/sj.emboj.7600550

Becker, A. P., Scapulatempo-neto, C., Neder, L., Chimelli, L., & Reis, R. M. (2013). Pilocytic Astrocytoma : Anatomic , Pathological and Molecular Aspects. In *Clinical management and evolving novel theraputic strategies for patients with brain tumours* (pp. 127–144). InTech Drug Discovery.

Beroukhim, R., Mermel, C. H., Porter, D., Wei, G., Raychaudhuri, S., Donovan, J., … Meyerson, M. (2010). The landscape of somatic copy-number alteration across human cancers. *Nature*, *463*, 899–905. http://doi.org/10.1038/nature08822

Bhavsar, R. B., Makley, L. N., & Tsonis, P. A. (2010). The other lives of ribosomal proteins. *Human Genomics*, *4*(5), 327–334.

Birks, D. K., Donson, A. M., Patel, P. R., Sufit, A., Algar, E. M., Dunham, C., … Foreman, N. K. (2013). Pediatric Rhabdoid Tumors of Kidney and Brain Show Many Differences in Gene Expression But Share Dysregulation of Cell Cycle and Epigenetic Effector Genes. *Pediatric Blood Cancer*, *60*, 1095–1102. http://doi.org/10.1002/pbc

Bisaro, B., Mandili, G., Poli, A., Piolatto, A., Papa, V., Novelli, F., … Zanini, C. (2015). Proteomic analysis of extracellular vesicles from medullospheres reveals a role for iron in the cancer progression of medulloblastoma. *Molecular and Cellular Therapies*, *3*(8). http://doi.org/10.1186/s40591-015-0045-3

Blüml, S., Margol, A. S., Sposto, R., Kennedy, R. J., Robison, N. J., Vali, M., … Asgharzadeh, S. (2015). Molecular subgroups of medulloblastoma identification using noninvasive magnetic resonance spectroscopy. *Neuro-Oncology*, *18*(1), 126–131. http://doi.org/10.1093/neuonc/nov097

Boisgerault, N., Tangy, F., & Gregoire, M. (2010). New perspectives in cancer virotherapy : bringing the immune system into play. *Immunotherapy*, *2*(2), 185–199.

Boots-Sprenger, S. H. E., Sijben, A., Rijntjes, J., Tops, B. B. J., Idema, A. J., Rivera, A. L., … Jeuken, J. W. M. (2013). Significance of complete 1p/19q co-deletion, IDH1 mutation and MGMT promoter methylation in gliomas: use with caution. *Modern Pathology*, *26*(7), 922–929. http://doi.org/10.1038/modpathol.2012.166

Brain tumors. (2016). Retrieved September 19, 2016, from http://www.chw.org/medical-care/macc-fund-center/conditions/oncology/brain-tumors/

Brenner, D. J., Elliston, C. D., Hall, E. J., & Berdon, W. E. (2001). Estimated Risks of Radiation- Induced Fatal Cancer from Pediatric CT. *American Journal of Roentgenology*, *176*, 289–296.

Bunin, G. (2000). What Causes Childhood Brain Tumors? Limited Knowledge, Many Clues. *Pediatric Neurosurgery*, *32*, 321–326.

Camerini, S., & Mauri, P. (2014). The role of protein and peptide separation before mass spectrometry analysis in clinical proteomics. *Journal of Chromatography A*, *1381*, 1–26. http://doi.org/10.1016/j.chroma.2014.12.035

Cancer Facts and Figures 2016. (2016). *American cancer society*.

Cao, C., Shen, Y., Wang, J., Li, L., & Liang, G. (2013). Controlled intracellular self-assembly of gadolinium nanoparticles as smart molecular MR contrast agents. *Scientific Reports*, *3*(1024), 1–9. http://doi.org/10.1038/srep01024

Cao, C., Wang, W., & Jiang, P. (2016). Identification of prognostic genes in paediatric medulloblastoma from mRNA expression profiles. *International Journal of Clinical and Experimental Medicine*, *9*(10), 19925–19929.

Chao, M. P., Jaiswal, S., Weissman-tsukamoto, R., Alizadeh, A. A., Park, C. Y., Majeti, R., & Weissman, I. L. (2010). Calreticulin Is the Dominant Pro-Phagocytic Signal on Multiple Human Cancers and Is Counterbalanced by CD47. *Science Translational Medicine 2*, *2*(63), 1–9. http://doi.org/10.1126/scitranslmed.3001375

Cheang, T., Zhou, H., Chen, W., Zhang, B., Liu, L., Yang, J., … Li, H. (2016). C14orf166 overexpression correlates with tumor progression and poor prognosis of breast cancer. *Journal of Translational Medicine*, *14*(54), 1–9. http://doi.org/10.1186/s12967-016-0805-0

Chen, E. Y., Tan, C. M., Kou, Y., Duan, Q., Wang, Z., Meirelles, G. V., … Ma'ayan, A. (2013). Enrichr : interactive and collaborative HTML5 gene list enrichment analysis tool. *BMC Bioinformatics*, *14*(128).

Chen, H., Slepnev, V. I., Di Fiore, P. P., & De Camilli, P. (1999). The Interaction of Epsin and Eps15 with the Clathrin Adaptor AP-2 Is Inhibited by Mitotic Phosphorylation and Enhanced by Stimulation- dependent Dephosphorylation in Nerve Terminals. *The*

Journal of Biological Chemistry, *274*(6), 3257–3261.

Chen, M., Ye, Y., Zou, B., Guo, S., Zhou, F., Lu, K., … Qin, Z. (2016). C14orf166 is a high‐risk biomarker for bladder cancer and promotes bladder cancer cell proliferation. *Journal of Translational Medicine*, *14*(55), 1–10. http://doi.org/10.1186/s12967-016-0801-4

Chen, Y.-H., & Gutmann, D. H. (2014). The molecular and cell biology of pediatric low-grade gliomas. *Oncogene*, (33), 2019–2026. http://doi.org/10.1038/onc.2013.148

Chia, W. J., & Tang, B. L. (2009). Emerging roles for Rab family GTPases in human cancer. *Biochimica et Biophysica Acta*, *1795*(2), 110–116. http://doi.org/10.1016/j.bbcan.2008.10.001

Chiang, J. C. H., & Ellison, D. W. (2017). Molecular pathology of paediatric central nervous system tumours. *Journal of Pathology*, *241*, 159–172. http://doi.org/10.1002/path.4813

Chiarle, R., Voena, C., Ambrogio, C., Piva, R., & Inghirami, G. (2008). The anaplastic lymphoma kinase in the pathogenesis of cancer. *Nature Reviews Cancer*, *8*, 11–23. http://doi.org/10.1038/nrc2291

Childhood Astrocytomas Treatment. (2015). Retrieved from https://www.cancer.gov/types/brain/hp/child-astrocytoma-treament-pdq

Cho, Y. J., Tsherniak, A., Tamayo, P., Santagata, S., Ligon, A., Greulich, H., … Pomeroy, S. L. (2011). Integrative genomic analysis of medulloblastoma identifies a molecular subgroup that drives poor clinical outcome. *Journal of Clinical Oncology*, *29*(11), 1424–1430. http://doi.org/10.1200/JCO.2010.28.5148

Chouaid, S., Messai, Y., Escudier, S., Hasmim, M., & Noman, M. Z. (2012). Hypoxia promotes tumor growth in linking angiogenesis to immune escape. *Frontiers in Immunology*, *3*, 1–10. http://doi.org/10.3389/fimmu.2012.00021

Cicenas, J. (2016). The Aurora kinase inhibitors in cancer research and therapy. *Journal of Cancer Research and Clinical Oncology*. http://doi.org/10.1007/s00432-016-2136-1

Clark, T. G., Bradburn, M. J., Love, S. B., & Altman, D. G. (2003). Survival Analysis Part I: Basic concepts and first analyses. *British Journal of Cancer*, *89*, 232–238. http://doi.org/10.1038/sj.bjc.6601118

Cloughesy, T. F., Cavenee, W. K., & Mischel, P. S. (2014). Glioblastoma: from molecular pathology to targeted treatment. *Annual Review of Pathology*, *9*, 1–25.

http://doi.org/10.1146/annurev-pathol-011110-130324

Colin, C., Padovani, L., Chappé, C., Mercurio, S., Scavarda, D., Loundou, A., … Figarella-Branger, D. (2013). Outcome analysis of childhood pilocytic astrocytomas : a retrospective study of 148 cases at a single institution. *Neuropath and Applied Neurobiology*, *39*(6), 693–705. http://doi.org/10.1111/nan.12013

Collins, V. P., Jones, D. T. W., & Giannini, C. (2015). Pilocytic astrocytoma : pathology , molecular mechanisms and markers. *Acta Neuropathologica*, *129*, 775–788. http://doi.org/10.1007/s00401-015-1410-7

D'Asti, E., Kool, M., Pfister, S. M., & Rak, J. (2014). Coagulation and angiogenic gene expression profiles are defined by molecular subgroups of medulloblastoma : evidence for growth factor-thrombin cross-talk. *Journal of Thrombosis and Haemostasis*, *12*, 1838–1849. http://doi.org/10.1111/jth.12715

Darnell, J. E. (2002). TRANSCRIPTION FACTORS AS TARGETS FOR CANCER THERAPY. *Nature Reviews*, *2*, 740–749. http://doi.org/10.1038/nrc906

Deimling, A. Von, Louis, D. N., Ammon, K. Von, Petersen, I., Wiestier, O. D., & Seizinger, B. R. (1992). Evidence for a Tumor Suppressor Gene on Chromosome 19q Associated with human astrocytomas, oligodendroglioma and mixed gliomas. *Cancer Research*, *52*, 4277–4279.

Dhurgsharma, S., Walker, D., Liu, J., & Wilne, S. (2015). HeadSmart : are you brain tumour aware ? *Paediatrics and Child Health*, *26*(2), 81–86. http://doi.org/10.1016/j.paed.2015.10.006

Duchange, N., Pidoux, J., Camus, E., & Sauvaget, D. (2000). Alternative splicing in the human interleukin enhancer binding factor 3 (ILF3) gene. *Gene*, *261*, 345–353.

Duffner, P. K., Horowitz, M. E., Krischer, J. P., Friedman, H. S., Burger, P. C., Cohen, M. E., … Kun, L. E. (1993). Postoperative chemotherapy and delayed radiation in children less than three years of age with malignant brain tumours. *The New England Journal of Medicine*, *328*(24), 1725–1731.

Ellison, D. W., Dalton, J., Kocak, M., Nicholson, S. L., Fraga, C., Neale, G., … Gilbertson, R. J. (2011). Medulloblastoma: Clinicopathological correlates of SHH, WNT, and non-SHH/WNT molecular subgroups. *Acta Neuropathologica*, *1*, 1–16. http://doi.org/10.1007/s00401-011-0800-8

Ellison, D. W., Kocak, M., Dalton, J., Megahed, H., Lusher, M. E., Ryan, S. L., … Clifford, S. C. (2010). Definition of Disease-Risk Stratification Groups in Childhood Medulloblastoma Using Combined Clinical, Pathologic, and Molecular Variables. *Journal of Clinical Oncology*, 1–12. http://doi.org/10.1200/JCO.2010.30.2810

Ellison, D. W., Onilude, O. E., Lindsey, J. C., Lusher, M. E., Weston, C. L., Taylor, R. E., … Clifford, S. C. (2005). B-Catenin Status Predicts a Favorable Outcome in Childhood Medulloblastoma: The United Kingdom Children's Cancer Study Group Brain Tumour Committee. *Journal of Clinical Oncology*, *23*(31), 7951–7957. http://doi.org/10.1200/JCO.2005.01.5479

Entschladen, F., Lang, Æ. K., Drell, Æ. T. L., Joseph, J., & Zaenker, Æ. K. S. (2002). Neurotransmitters are regulators for the migration of tumor cells and leukocytes. *Cancer Immunology and Immunitherapy*, *51*, 467–482. http://doi.org/10.1007/s00262-002-0300-8

Erkek, S., Kawauchi, D., Shih, D. J. H., Northcott, P. A., Lee, C., Zichner, T., … Gilbertson, R. J. (2014). Enhancer hijacking activates GFI1 family oncogenes in medulloblastoma. *Nature*, *511*, 428–434. http://doi.org/10.1038/nature13379

Fahmideh, M. A., Lavebratt, C., Schüz, J., Röösli, M., Tynes, T., Grotzer, M. A., … Feychting, M. (2016). Common genetic variations in cell cycle and DNA repair pathways associated with pediatric brain tumor susceptibility. *Oncotarget*, *7*(39).

Farwell, J. R., Dohrmann, G. J., & Flannery, J. T. (1984). Medulloblastoma in childhood: an epidemiological study. *Journal of Neurosurgery*, *61*(4), 657–64. http://doi.org/10.3171/jns.1984.61.4.0657

Fattet, S., Christine, H., Patricia, L., Pascale, V., Arielle, L.-T., Severine, L., … Delattre, O. (2010). Beta-catenin status in paediatric medulloblastomas: correlation of immunohistochemical expression with mutational status, genetic profiles, and clinical characteristics. *The Journal of Pathology*, *220*(September), 114–125. http://doi.org/10.1002/path

Faul, F., Erdfelder, E., Lang, A. G., & Buchner, A. (2007). G * Power 3 : A flexible statistical power analysis program for the social , behavioral , and biomedical sciences. *Behavior Research Methods*, *39*(2), 175–191.

Fehnel, K. P., Duggins-warf, M., Zurakowski, D., Mckee-proctor, M., Majumder, R., Raber,

M., … Smith, E. R. (2016). Using urinary bFGF and TIMP3 levels to predict the presence of juvenile pilocytic astrocytoma and establish a distinct biomarker signature. *JNS Pediatrics*, *6*, 1–12. http://doi.org/10.3171/2015.12.PEDS15448.

Fink, J. R., Muzi, M., Peck, M., & Krohn, K. A. (2015). Multimodality Brain Tumor Imaging: MR Imaging, PET, and PET/MR Imaging. *Journal of Nuclear Medicine*, *56*(10), 1554–1562. http://doi.org/10.2967/jnumed.113.131516

Fleshman, D. J., Shimada, H., & Dorisio, T. M. O. (1992). Neuroblastoma Correlation of Neuropeptide Expression in Tumor Tissue with Other Prognostic Factors. *Cancer*, *20*(7), 2005–2012.

Forshew, T., Tatevossian, R. G., Lawson, A. R. J., Ma, J., Neale, G., Ogunkolade, W., … Sheer, D. (2009). Activation of the ERK / MAPK pathway : a signature genetic defect in posterior fossa pilocytic astrocytomas. *Journal of Pathology*, (218), 172–181. http://doi.org/10.1002/path

Foster, C. R., Przyborski, S. A., Wilson, R. G., & Hutchison, C. J. (2010). Lamins as cancer biomarkers. *Biochemistry Society Transactions*, *38*, 297–300. http://doi.org/10.1042/BST0380297

Frappart, P., & Mckinnon, P. J. (2006). Ataxia-Telangiectasia and Related Diseases. *Neuromolecular Medicine*, *8*, 495–511. http://doi.org/10.1385/NMM

French, P. J., Peeters, J., Horsman, S., Duijm, E., Siccama, I., Bent, M. J. Van Den, … Smitt, P. A. S. (2007). Identification of Differentially Regulated Splice Variants and Novel Exons in Glial Brain Tumors Using Exon Expression Arrays. *Cancer Research*, *67*(12), 5635–5642. http://doi.org/10.1158/0008-5472.CAN-06-2869

Fridman, W. H., Pagès, F., & Sautès-fridman, C. (2012). The immune contexture in human tumours : impact on clinical outcome. *Nature Publishing Group*, *12*(4), 298–306. http://doi.org/10.1038/nrc3245

Fruzangohar, M., Ebrahimie, E., Ogunniyi, A. D., Mahdi, L. K., Paton, J. C., & Adelson, D. L. (2013). Comparative GO : A Web Application for Comparative Gene Ontology and Gene Ontology-Based Gene Selection in Bacteria. *PloS One*, *8*(3), 1–8. http://doi.org/10.1371/journal.pone.0058759

Gajjar, A., Bowers, D. C., Karajannis, M. A., Leary, S., Witt, H., & Gottardo, N. G. (2015). Pediatric Brain Tumors: Innovative Genomic Information Is Transforming the

Diagnostic and Clinical Landscape. *Journal of Clinical Oncology*, *33*(27), 2986–2998. http://doi.org/10.1200/JCO.2014.59.9217

Gajjar, A., & Robinson, G. W. (2014). Medulloblastoma—translating discoveries from the bench to the bedside. *Nature Reviews Clinical Oncology*, *11*(12), 714–722. http://doi.org/10.1038/nrclinonc.2014.181

Gao, G., Xie, A., Huang, S., Zhou, A., Zhang, J., Herman, A. M., … Dudley, S. C. (2011). Role of RBM25/LUC7L3 in Abnormal Cardiac Sodium Channel Splicing Regulation in Human Heart Failure. *Circulation Research*, 1124–1131. http://doi.org/10.1161/CIRCULATIONAHA.111.044495

Gerber, N. U., Mynarek, M., von Hoff, K., Friedrich, C., Resch, a, & Rutkowski, S. (2014). Recent developments and current concepts in medulloblastoma. *Cancer Treatment Reviews*, *40*(3), 356–65. http://doi.org/10.1016/j.ctrv.2013.11.010

Gessi, M., Goschzik, T., Dorner, E., Soldner, K., Schupp, C., & Pietsch, T. (2016). Medulloblastoma with extensive nodularity: a tumour exclusively of infancy? *Neuropath and Applied Neurobiology*, *1*, 1–4. http://doi.org/10.1111/nan.12322

Gibson, P., Tong, Y., Robinson, G., Thompson, M. C., Currle, D. S., Eden, C., … Gilbertson, R. J. (2010). Subtypes of medulloblastoma have distinct developmental origins. *Nature*, *468*(7327), 1095–1099. http://doi.org/10.1038/nature09587

Gillespie, M., Vastrik, I., Eustachio, P. D., Schmidt, E., & Bono, B. De. (2005). Reactome: a knowledgebase of biological pathways. *Nucleic Acids Research*, *33*, 428–432. http://doi.org/10.1093/nar/gki072

Goldberg-stern, H., Gadoth, N., & Stern, S. (1991). The Prognostic Significance of Glial Fibrillary Acidic Protein Staining in Medulloblastoma. *Cancer*, *3*, 568–573.

Gottardo, N. G., & Gajjar, A. (2009). Chemotherapy for malignant brain tumors of childhood. *Journal of Child Neurology*, *23*(10), 1149–1159. http://doi.org/10.1177/0883073808321765.Chemotherapy

Gottardo, N. G., Hansford, J. R., McGlade, J. P., Alvaro, F., Ashley, D. M., Bailey, S., … Gajjar, A. (2014). Medulloblastoma Down Under 2013: a report from the third annual meeting of the International Medulloblastoma Working Group. *Acta Neuropathologica*, *127*(2), 189–201. http://doi.org/10.1007/s00401-013-1213-7

Goumnerova, L. C. (1996). Growth factor receptors and medulloblastoma. *Journal of Neuro-*

Oncology, *29*, 85–89.

Guerit, S., & Liebner, S. (2016). Blood-Brain Barrier Breakdown Determines Differential Therapeutic Outcome in Genetically Diverse Forms of Medulloblastoma. *Cancer Cell*, *29*(4), 427–429. http://doi.org/10.1016/j.ccell.2016.03.024

Guo, Y. I., Fu, P., Zhu, H., Reed, E., Remick, S. C., Petros, W., … Yu, J. J. I. E. (2012). Correlations among ERCC1 , XPB , UBE2I , EGF , TAL2 and ILF3 revealed by gene signatures of histological subtypes of patients with epithelial ovarian cancer. *Oncology Reports*, *27*, 286–292. http://doi.org/10.3892/or.2011.1483

Gupta, M. K., Polisetty, R. V., Ramamoorthy, K., Tiwary, S., Kaur, N., Uppin, M. S., … Sirdeshmukh, R. (2013). Secretome analysis of Glioblastoma cell line - HNGC-2. *Molecular BioSystems*, *9*, 1390–1400. http://doi.org/10.1039/c3mb25383j

Gupta, T., Krishnatry, R., Kannan, S., Kurkure, P., Deopujari, C., Shetty, P., … Shirsat, N. V. (2013). Real-time PCR assay based on the differential expression of microRNAs and protein-coding genes for molecular classification of formalin-fixed paraffin embedded medulloblastomas. *Neuro-Oncology*, *15*(12), 1644–1651.

Haeberle, H., Dudley, J. T., Liu, J. T. C., & Butte, A. J. (2012). Identification of Cell Surface Targets through Meta-analysis of Microarray Data. *Neoplasia*, *14*(7), 666–669. http://doi.org/10.1593/neo.12634

Halberg, N., Sengelaub, C. A., Navrazhina, K., Molina, H., Uryu, K., Tavazoie, S. F., … Tavazoie, S. F. (2016). Drive Malignant Secretion Article PITPNC1 Recruits RAB1B to the Golgi Network to Drive Malignant Secretion. *Cancer Cell*, *29*(3), 339–353. http://doi.org/10.1016/j.ccell.2016.02.013

Hambardzumyan, D., Gutmann, D. H., & Kettenmann, H. (2016). The role of microglia and macrophages in glioma maintenance and progression. *Nature Neuroscience*, *19*(1), 20–27. http://doi.org/10.1038/nn.4185

Hamou, M., Tribolet, N. De, Weller, M., Kros, J. M., Hainfellner, J. A., Mason, W., … Stupp, R. (2005). Gene Silencing and Benefit from Temozolomide in Glioblastoma. *The New England Journal of Medicine*, *352*, 997–1003.

Han, Y., Kim, H. J., Dlugosz, A. A., Ellison, D. W., Gilbertson, R. J., & Alvarez-buylla, A. (2009). Dual and opposing roles of primary cilia in medulloblastoma development. *Nature Medicine*, *1*(August), 1–5. http://doi.org/10.1038/nm.2020

Hara, A., Hashimura, M., Tsutsumi, K., Akiya, M., Inukai, M., Ohta, Y., & Saegusa, M. (2016). The role of FilGAP, a Rac- specific Rho-GTPase-activating protein, in tumor progression and behavior of astrocytomas. *Cancer Medicine*, 1–14. http://doi.org/10.1002/cam4.937

Harding, B. N., Busse, T. M., Tooke, L. S., & Biegel, J. A. (2014). Diagnostic application of high resolution single nucleotide polymorphism array analysis for children with brain tumors. *Cancer Genetics*, 1–13. http://doi.org/10.1016/j.cancergen.2014.03.002

He, J., & Jiang, B. (2016). Interplay Between Reactive Oxygen Species and MicroRNAs in Cancer. *Current Pharmaceutical Design*, *2*, 82–90. http://doi.org/10.1007/s40495-016-0051-4

He, X., Zhang, L., Chen, Y., Remke, M., Shih, D., Lu, F., … Lu, Q. R. (2014). The G protein αlpha subunit G αlpha-s is a tumor suppressor in Sonic hedgehog−driven medulloblastoma. *Nature Medicine*, *20*(9), 1035–1044. http://doi.org/10.1038/nm.3666

Hemmati, H. D., Nakano, I., Lazareff, J. A., Masterman-smith, M., Geschwind, D. H., Bronner-fraser, M., & Kornblum, H. I. (2003). Cancerous stem cells can arise from pediatric brain tumors. *Proceedings of the National Academy of Sciences*, *100*(25), 15178–15183.

Hesseling, P. B., Wessels, G., & Riet, F. A. Van. (1995). The Tygerberg Hospital Children's Tumour Registry 1983-1993. *European Journal of Biochemistry / FEBS*, *31*(9), 1471–1475.

Horbinski, C., Nikiforova, M. N., Hagenkord, J. M., Hamilton, R. L., & Pollack, I. F. (2012). Interplay among BRAF, p16, p53, and MIB1 in pediatric low-grade gliomas. *Neuro-Oncology*, *14*(6), 777–789.

Houillier, C., Wang, X., Kaloshi, G., Mokhtari, K., Guillevin, R., Laffaire, J., … Delattre, J. Y. (2010). IDH1 or IDH2 mutations predict longer survival and response to temozolomide in low-grade gliomas. *Neurology*, *75*, 1560–1566.

Huang, H., Mahler-araujo, B. M., Sankila, A., Chimelli, L., Yonekawa, Y., Kleihues, P., & Ohgaki, H. (2000). APC Mutations in Sporadic Medulloblastomas. *The American Journal of Pathology*, *156*(2), 433–437. http://doi.org/10.1016/S0002-9440(10)64747-5

Hutchison, C. J. (2014). B-type lamins in health and disease. *Seminars in Cell and Developmental Biology*, *29*, 158–163. http://doi.org/10.1016/j.semcdb.2013.12.012

Idowu, O., Akang, E., & Malomo, A. (2007). Symptomatic primary intracranial neoplasms in Nigeria, West Africa. *Journal of Neurological Sciences*, *24*(3), 212–218.

Ikeda, M., Chiba, S., Ohashi, K., & Mizuno, K. (2012). Furry Protein Promotes Aurora A-mediated Polo-like Kinase 1. *The Journal of Biological Chemistry*, *287*(33), 27670–27681. http://doi.org/10.1074/jbc.M112.378968

Jacob, K., Albrecht, S., Sollier, C., Faury, D., Sader, E., Montpetit, A., … Jabado, N. (2009). Duplication of 7q34 is specific to juvenile pilocytic astrocytomas and a hallmark of cerebellar and optic pathway tumours. *British Journal of Cancer*, *101*(4), 722–733. http://doi.org/10.1038/sj.bjc.6605179

Jagani, Z., Mora-blanco, E. L., Sansam, C. G., Mckenna, E. S., Wilson, B., Chen, D., … Dorsch, M. (2010). Loss of the tumor suppressor Snf5 leads to aberrant activation of the Hedgehog-Gli pathway. *Nature Medicine*, *16*(12), 1–6. http://doi.org/10.1038/nm.2251

Jain, R., Kulkarni, P., Dhali, S., Rapole, S., & Srivastava, S. (2014). Quantitative proteomic analysis of global effect of LLL12 on U87 cell's proteome: An insight into the molecular mechanism of LLL12. *Journal of Proteomics*, *113*, 127–142. http://doi.org/10.1016/j.jprot.2014.09.020

Janss, A. J., Yachnis, A. T., Silber, J. H., Trojanowski, J. Q., Lee, V. M., Sutton, L. N., … Lb, R. (1996). Glial Differentiation Predicts Poor Clinical Outcome in Primitive Neuroectodermal Brain Tumors. *Annals of Neurology*, *39*, 481–489.

Jensen, P., Macdonald, T. J., Taylor, M. D., Poppleton, H., Fuller, C., Su, X., … Gilbertson, R. J. (2005). Radial glia cells are candidate stem cells of ependymoma Radial glia cells are candidate stem cells of ependymoma. *Cancer Cell*, *8*, 323–335. http://doi.org/10.1016/j.ccr.2005.09.001

Johansson, F. K., Go, H., & Westermark, B. (2005). Expression analysis of genes involved in brain tumor progression driven by retroviral insertional mutagenesis in mice. *Oncogene*, *24*, 3896–3905. http://doi.org/10.1038/sj.onc.1208553

Johnson, D., McCabe, M. A., Nicholson, H. S., Joseph, A. L., Getson, P. R., Byrne, J., … Raeman, G. (1994). Quality of long-term survival in young children with medulloblastoma. *Journal of Neurosurgery*, *80*, 1004–1010.

Jones, D. T. W., Hutter, B., Jäger, N., Korshunov, A., Kool, M., Warnatz, H., … Felsberg, J. (2013). Recurrent somatic alterations of FGFR1 and NTRK2 in pilocytic astrocytoma.

Nature Genetics, *45*(8), 927–932. http://doi.org/10.1038/ng.2682

Jones, D. T. W., Jager, N., Kool, M., Zichner, T., Hutter, B., Sultan, M., … Lichter, P. (2012). Dissecting the genomic complexity underlying medulloblastoma. *Nature*, *488*, 100–105. http://doi.org/10.1038/nature11284

Jones, D. T. W., Kocialkowski, S., Liu, L., Pearson, D. M., Ba, L. M., Ichimura, K., & Collins, V. P. (2008). Tandem Duplication Producing a Novel Oncogenic BRAF Fusion Gene Defines the Majority of Pilocytic Astrocytomas. *Cancer Research*, *68*(21), 8673–8678. http://doi.org/10.1158/0008-5472.CAN-08-2097

Jordan, P. A., Stevens, J. M., Hubbard, G. P., Barrett, N. E., Sage, T., Authi, K. S., & Gibbins, J. M. (2016). A role for the thiol isomerase protein ERP5 in platelet function. *Hemostasis, Thrombosis and Vascular Biology*, *105*(4), 1500–1508. http://doi.org/10.1182/blood-2004-02-0608.Supported

Kagawa, N., Maruno, M., Suzuki, T., Hashiba, T., Hashimoto, N., Izumoto, S., & Yoshimine, T. (2006). Detection of genetic and chromosomal aberrations in medulloblastomas and primitive neuroectodermal tumors with DNA microarrays. *Brain Tumor Pathology*, *23*(1), 41–47. http://doi.org/10.1007/s10014-006-0201-1

Kaloshi, G., Diakite, F., Taillibert, S., Lejeune, J., Iraqi, W., Idbaih, A., … Sanson, M. (2007). Temozolomide for low-grade gliomas Predictive impact of 1p/19q loss on response and outcome. *Neurology*, *68*, 1831–1836.

Karajannis, M., & Allen, J. C. (2008). Treatment of Pediatric Brain Tumors. *Journal of Cellular Physiology*, 584–589. http://doi.org/10.1002/jcp.21544

Karkouri, M., Zafad, S., Khattab, M., & Benjaafar, N. (2010). Epidemiologic profile of pediatric brain tumors in Morocco. *Childs Nervous System*, *26*, 1021–1027. http://doi.org/10.1007/s00381-010-1097-y

Kaur, K., Kakkar, A., Kumar, A., Mallick, S., & Julka, P. K. (2016). Integrating Molecular Subclassification of Medulloblastomas into Routine Clinical Practice: A Simplified Approach. *Brain Pathology*, *26*, 334–343. http://doi.org/10.1111/bpa.12293

Kaya, B., Mena, H., Miettinen, M., & Rushing, E. (2003). Alpha-internexin expression in medulloblastomas and atypical teratoid-rhabdoid tumors. *Clinical Neuropathology*, *22*(5), 215–221.

Kazue, S., Marie, N., Oba-shinjo, S. M., Silva, R., Gimenez, M., Reis, G. N., … Uno, M.

(2016). Stathmin involvement in the maternal embryonic leucine zipper kinase pathway in glioblastoma. *Proteome Science*, *14*(6), 1–15. http://doi.org/10.1186/s12953-016-0094-9

Khalil, A. A. (2007). Biomarker discovery : A proteomic approach for brain cancer profiling. *Cancer Science*, *98*(2), 201–213. http://doi.org/10.1111/j.1349-7006.2007.00374.x

Khuong-quang, D., Buczkowicz, P., Rakopoulos, P., Liu, X.-Y., Fontebasso, A. M., Bouffet, E., … Hawkins, C. (2012). K27M mutation in histone H3.3 defines clinically and biologically distinct subgroups of pediatric diffuse intrinsic pontine gliomas. *Acta Neuropathologica*, *124*, 439–447. http://doi.org/10.1007/s00401-012-0998-0

Kim, J. Y. H., Koralnik, I. J., Lefave, M., Segal, R. A., Luz-andrea, P., & Pomeroy, S. L. (2002). Medulloblastomas and primitive neuroectodermal tumors rarely contain polyomavirus DNA sequences. *Neuro-Oncology*, 165–170.

Kim, M. K. H., Moos, P., Ph, D., Carlson, M., Bruggers, C., Hooper, D. K., … Carroll, W. L. (2003). Identification of Genes that Are Regulated Transcriptionally by Myc in Childhood Tumors. *Cancer*, *98*(4), 841–853. http://doi.org/10.1002/cncr.11584

Kim, T., Ryu, H., Li, S., Li, C., Lim, S., Jang, W., & Jung, S. (2016). PDIA6 regulation of ADAM17 shedding activity and EGFR-mediated migration and invasion of glioblastoma cells. *Journal of Neurosurgery*, 1–10. http://doi.org/10.3171/2016.5.JNS152831.

Kleihues, P., & Ohgaki, H. (2000). Phenotype vs Genotype in the Evolution of Astrocytic Brain Tumors. *Cellular and Molecular Neurocarcinogenesis*, *28*, 164–170.

Klose, J., Nock, C., Herrmann, M., Stühler, K., Marcus, K., Blüggel, M., … Lehrach, H. (2002). Genetic analysis of the mouse brain proteome. *Nature Gene*, *30*, 385–393. http://doi.org/10.1038/ng861

Kool, M., Korshunov, A., Remke, M., Jones, D. T. W., Schlanstein, M., Northcott, P. a, … Pfister, S. M. (2012). Molecular subgroups of medulloblastoma: an international meta-analysis of transcriptome, genetic aberrations, and clinical data of WNT, SHH, Group 3, and Group 4 medulloblastomas. *Acta Neuropathologica*, *123*(4), 473–484. http://doi.org/10.1007/s00401-012-0958-8

Kool, M., Koster, J., Bunt, J., Hasselt, N. E., Lakeman, A., van Sluis, P., … Versteeg, R. (2008). Integrated genomics identifies five medulloblastoma subtypes with distinct

genetic profiles, pathway signatures and clinicopathological features. *PloS One*, *3*(8), e3088. http://doi.org/10.1371/journal.pone.0003088

Korshunov, A., Benner, A., Remke, M., Lichter, P., Deimling, A., & Pfister, S. (2008). Accumulation of genomic aberrations during clinical progression of medulloblastoma. *Acta Neuropathologica*, *116*(4), 383–390. http://doi.org/10.1007/s00401-008-0422-y

Korshunov, A., Remke, M., Kool, M., Hielscher, T., Northcott, P. A., Westermann, F., … Pfister, S. M. (2012). Biological and clinical heterogeneity of MYCN -amplified medulloblastoma. *Acta Neuropathologica*, *123*, 515–527. http://doi.org/10.1007/s00401-011-0918-8

Krzywinski, M., Schein, J., Birol, I., Connors, J., Gascoyne, R., Jones, S. J., & Marra, M. A. (2009). Circos: an Information Aesthetic for Comparative Genomics. *Genome Research*, 1–25.

Kuijten, R. R., Strom, S. S., Rorke, L. B., Boesel, C. P., Buckley, J. D., Meadows, A. T., & Bunin, G. R. (1993). Family history of cancer and seizures in young children with brain tumors: a report from the Childrens Cancer Group (United States and Canada). *Cancer Causes and Control*, *4*, 455–464.

Kumanishi, T., Washiyama, K., Watabe, K., & Sekiguchi, K. (1985). Glial Fibrillary Acidic Protein in Medulloblastomas. *Acta Neuropathologica*, *67*, 1–5.

Laffin, B., & Petrash, J. M. (2012). Expression of the aldo-ketoreductases AKR1B1 and AKR1B10 in human cancers. *Frontiers in Pharmacy*, *3*, 1–7. http://doi.org/10.3389/fphar.2012.00104

Lalonde, R., Strazielle, C., Rouen, U. De, Sciences, F., Psychologie, D., Cedex, M., … Médecine, F. De. (2011). Brain regions and genes affecting limb-clasping responses. *Brain Research Reviews*, *67*(1–2), 252–259. http://doi.org/10.1016/j.brainresrev.2011.02.005

Lamouille, S., Xu, J., & Derynck, R. (2014). Molecular mechanisms of epithelial–mesenchymal transition. *Nature Reviews Molecular Cell Biology*, *15*(3), 178–196. http://doi.org/10.1038/nrm3758.Molecular

Larcher, J., Gasmi, L., Viranaïcken, W., & Eddé, B. (2004). Ilf3 and NF90 associate with the axonal targeting element of Tau mRNA. *The FASEB Journal*, *24*, 1–24.

Laughton, S. J., Merchant, T. E., Sklar, C. A., Kun, L. E., Fouladi, M., Broniscer, A., …

Wallace, D. (2008). Endocrine Outcomes for Children With Embryonal Brain Tumors After Risk-Adapted Craniospinal and Conformal Primary-Site Irradiation and High-Dose Chemotherapy With Stem-Cell Rescue on the SJMB-96 Trial. *Journal of Clinical Oncology*, *26*(7), 1112–1118. http://doi.org/10.1200/JCO.2008.13.5293

Leblanc, V. G., & Marra, M. A. (2016). DNA methylation in adult diffuse gliomas. *Briefings in Functional Genomics*, 1–10. http://doi.org/10.1093/bfgp/elw019

Lee, H. S., Han, J., Bai, H., & Kim, K. (2009). Brain angiogenesis in developmental and pathological processes : regulation , molecular and cellular communication at the neurovascular interface. *The FEBS Journal*, *276*, 4622–4635. http://doi.org/10.1111/j.1742-4658.2009.07174.x

Lemée, J., Com, E., Clavreul, A., Avril, T., Quillien, V., Tayrac, M. De, … Menei, P. (2013). Proteomic analysis of glioblastomas: What is the best brain control sample? *Journal of Proteomics*, 1–9. http://doi.org/10.1016/j.jprot.2013.04.031

Lemma, S., Avnet, S., Salerno, M., Chano, T., & Baldini, N. (2016). Identification and Validation of Housekeeping Genes for Gene Expression Analysis of Cancer Stem Cells. *PloS One*, 1–19. http://doi.org/10.1371/journal.pone.0149481

Levin, Y. (2011). The role of statistical power analysis in quantitative proteomics. *Proteomics*, *11*, 2565–2567. http://doi.org/10.1002/pmic.201100033

Li, M., Lee, K. F., Lu, Y., Clarke, I., Shih, D., Eberhart, C., … Huang, A. (n.d.). Frequent Amplification of a chr19q13 . 41 MicroRNA Polycistron in Aggressive Primitive Neuroectodermal Brain Tumors. *Cancer Cell*, *16*(6), 533–546. http://doi.org/10.1016/j.ccr.2009.10.025

Li, Y., Wang, X., Cho, J., Shaw, T. I., Wu, Z., Bai, B., … Peng, J. (2016). JUMPg: an Integrative Proteogenomics Pipeline Identifying Unannotated Proteins in Human Brain and Cancer Cells. *Journal of Proteome Research*, *1*, 1–30. http://doi.org/10.1021/acs.jproteome.6b00344

Liang, Y., Diehn, Æ. M., Bollen, Æ. A. W., Israel, M. A., & Gupta, Æ. N. (2008). Type I collagen is overexpressed in medulloblastoma as a component of tumor microenvironment. *Journal of Neuro-Oncology*, *86*, 133–141. http://doi.org/10.1007/s11060-007-9457-5

Lin, A., Rodriguez, F. J., Karajannis, M. A., Williams, S. C., Legault, G., Zagzag, D., … Bar,

E. E. (2012). BRAF Alterations in Primary Glial and Glioneuronal Neoplasms of the Central Nervous System With Identification of 2 Novel KIAA1549 : BRAF Fusion Variants. *Journal of Neuropathology and Experimental Neurology*, *71*(1), 66–72.

Lin, C. Y., Erkek, S., Tong, Y., Yin, L., Federation, A. J., Zapatka, M., … Victor, V. (2016). Active medulloblastoma enhancers reveal subgroup-specific cellular origins. *Nature*, 1–20. http://doi.org/10.1038/nature16546

Lin, S., Wang, P., & Feng, F. (2016). Differential proteomics analysis of oligodendrogliomas and astrocytomas using iTRAQ quantification Differential Proteomics analysis of Oligodendroglioma and Astrocytoma using iTRAQ quantifiction. *PeerJ Preprints*.

Lokman, N. A., Ween, M. P., Oehler, M. K., & Ricciardelli, C. (2011). The Role of Annexin A2 in Tumorigenesis and Cancer Progression. *Cancer Microenvironment*, *4*, 199–208. http://doi.org/10.1007/s12307-011-0064-9

Lou, E., Schomaker, M., Wilson, J. D., Ahrens, M., Dolan, M., Nelson, A. C., … Dolan, M. (2016). Complete and sustained response of adult medulloblastoma to first-line sonic hedgehog inhibition with vismodegib. *Cancer Biology & Therapy*, *1*, 1–7. http://doi.org/10.1080/15384047.2016.1220453

Louis, D. N., Ohgaki, H., Wiestler, O. D., Cavenee, W. K., Burger, P. C., Jouvet, A., … Kleihues, P. (2007). The 2007 WHO classification of tumours of the central nervous system. *Acta Neuropathologica*, *114*(2), 97–109. http://doi.org/10.1007/s00401-007-0243-4

Louis, D. N., Perry, A., Reifenberger, G., Deimling, A. Von, Figarella, D., Webster, B., … Ellison, D. W. (2016). The 2016 World Health Organization Classification of Tumors of the Central Nervous System : a summary. *Acta Neuropathologica*, *131*(6), 803–820. http://doi.org/10.1007/s00401-016-1545-1

Macdonald, T. J., Pollack, I. F., Okada, H., Bhattacharya, S., & Lyons-weiler, J. (2004). Progression-Associated Genes in Astrocytoma Identified by Novel Microarray Gene Expression Data Reanalysis. In *Methods in Molecular Biology* (Vol. 377, pp. 203–221).

Maenpaa, A., Junnikkala, S., Hakulinen, J., Timonen, T., & Meri, S. (1996). Expression of Complement Membrane Regulators Membrane Cofactor Protein (CD46), Decay Accelerating Factor (CD55), and Protectin (CD59) in Human Malignant Gliomas. *American Journal of Pathology*, *148*(4), 1139–1152.

Magdeldin, S., & Yamamoto, T. (2012). Toward deciphering proteomes of formalin-fixed paraffin-embedded (FFPE) tissues. *Proteomics*, *12*, 1045–1058. http://doi.org/10.1002/pmic.201100550

Magnus, N., Asti, E. D., Meehan, B., Garnier, D., & Rak, J. (2014). Oncogenes and the coagulation system – forces that modulate dormant and aggressive states in cancer. *Thrombosis Research*, *133*, S1–S9. http://doi.org/10.1016/S0049-3848(14)50001-1

Mallawaaratchy, D. M., Hallal, S., Russell, B., Ly, L., Ebrahimkhani, S., Wei, H., & Christopherson, R. I. (2016). Comprehensive proteome profiling of glioblastoma-derived extracellular vesicles identifies markers for more aggressive disease. *Journal of Neuro-Oncology*, 1–12. http://doi.org/10.1007/s11060-016-2298-3

Malzkorn, B., Wolter, M., Liesenberg, F., Grzendowski, M., Stühler, K., Meyer, H. E., & Reifenberger, G. (2010). Identification and Functional Characterization of microRNAs Involved in the Malignant Progression of Gliomas. *Brain Pathogy (Zurich, Switzerland)*, *20*(13), 539–550. http://doi.org/10.1111/j.1750-3639.2009.00328.x

Mamelak, A., Prados, M., Obana, W., Cogen, P., & Edwards, M. (1994). Treatment options and prognosis for multicentric juvenile pilocytic astrocytoma. *Journal of Neurosurgery*, *81*, 24–30.

Marie, J. C., Astier, A. L., Rivailler, P., Rabourdin-combe, C., Wild, T. F., & Horvat, B. (2002). Linking innate and acquired immunity : divergent role of CD46 cytoplasmic domains in T cell – induced inflammation. *Nature Immunology*, *3*(7), 659–666. http://doi.org/10.1038/ni810

Martelli, C., Angelo, L. D., Barba, M., Baranzini, M., Inserra, I., Iavarone, F., … Desiderio, C. (2016). Proteomics Top-down proteomic characterization of DAOY medulloblastoma tumor cell line. *EUPROT*, *12*, 13–21. http://doi.org/10.1016/j.euprot.2016.03.015

Martelli, C., Iavarone, F., Angelo, L. D., Arba, M., Vincenzoni, F., Inserra, I., … Sanna, T. (2015). Integrated proteomic platforms for the comparative characterization of medulloblastoma and pilocytic astrocytoma pediatric brain tumors : a preliminary study. *Molecular BioSystems*. http://doi.org/10.1039/C5MB00076A

Martens, L., Quinn, A. F., Taylor, C. F., Jones, P., Co, R. G., Derache, W., … Apweiler, R. (2006). PRIDE: a public repository of protein and peptide identifications for the proteomics community. *Nucleic Acids Research*, *34*, 659–663.

http://doi.org/10.1093/nar/gkj138

Martirosian, V., Chen, T. C., Lin, M., & Neman, J. (2016). Medulloblastoma Initiation and Spread: Where Neurodevelopment, Microenvironment and Cancer Cross Pathways. *Journal of Neuroscience Research*, *94*, 1511–1519. http://doi.org/10.1002/jnr.23917

Maugeri, R., Schiera, G., Maria, C., Liegro, D., Fricano, A., Iacopino, D. G., & Liegro, I. Di. (2016). Aquaporins and Brain Tumors. *International Journal of Molecular Sciences*, *17*(1029), 1–18. http://doi.org/10.3390/ijms17071029

Mcdonald, W. H., & Yates, J. R. (2002). Shotgun proteomics and biomarker discovery. *Disease Markers*, *18*, 99–105.

Mcneill, R. S., Vitucci, M., Wu, J., & Miller, C. R. (2015). Contemporary murine models in preclinical astrocytoma drug development. *Neuro-Oncology*, *17*(1), 12–28. http://doi.org/10.1093/neuonc/nou288

Merve, A., Dubuc, A. M., Zhang, X., Remke, M., Baxter, P. A., Li, X., … Marino, S. (2014). Polycomb group gene BMI1 controls invasion of medulloblastoma cells and inhibits BMP-regulated cell adhesion. *Acta Neuropathologica Communications*, *2*(10), 1–18.

Meyer, M. A. (2014). Highly expressed genes in human high grade gliomas : immunohistochemical analysis of data from the Human Protein Atlas. *Neurology International*, *6*(5348), 29–31. http://doi.org/10.4081/ni.2014.5348

Mi, H., Poudel, S., Muruganujan, A., Casagrande, J. T., & Thomas, P. D. (2016). PANTHER version 10: expanded protein families and functions, and analysis tools. *Nucleic Acids Research*, *44*, 336–342. http://doi.org/10.1093/nar/gkv1194

Michiels, C., Tellier, C., & Feron, O. (2016). Cycling hypoxia: A key feature of the tumor microenvironment. *Biochemica et Biophysica Acta*, *1866*, 76–86. http://doi.org/10.1016/j.bbcan.2016.06.004

Miettinen, H., Kononen, J., Sallinen, P., Alho, H., Helen, P., Helin, H., … Palj, L. (1999). CDKN2/p16 predicts survival in oligodendrogliomas: comparison with astrocytomas. *Journal of Neuro-Oncology*, *41*, 205–211.

Milker-zabel, S. (2006). Radiosensitizers in Brain Cancer Clinical Experience to Date. *American Journal of Cancer Research*, *5*(6), 363–370.

Miller, R. W., & Rubinstein, J. H. (1995). Tumors in Rubinstein-Taybi Syndrome. *American Journal of Medical Genetics*, *115*, 112–115.

Miller, T. W., Soto-pantoja, D. R., Schwartz, A. L., Sipes, J. M., Degraff, W. G., Ridnour, L. A., … Roberts, X. D. D. (2015). CD47 Receptor Globally Regulates Metabolic Pathways That Control Resistance to Ionizing Radiation. *Journal of Biological Chemistry*, *290*(41), 24858–24874. http://doi.org/10.1074/jbc.M115.665752

Miura, K., Jacques, K. M., Stauffer, S., Kubosaki, A., Zhu, K., Hirsch, D. S., … Randazzo, P. A. (2002). ARAP1: A Point of Convergence for Arf and Rho Signaling. *Molecular Cell*, *9*, 109–119.

Morales, J. M., Martinetto, H., Calvar, J., & Sevlever, G. (2010). Comparative metabolic profiling of paediatric ependymoma, medulloblastoma and pilocytic astrocytoma. *Journal of Molecular Medicine*, *26*, 941–948. http://doi.org/10.3892/ijmm

Moulder, R., Goo, Y. A., & Goodlett, D. R. (2016). Label-Free Quantitation for Clinical Proteomics. In *Quantitative Proteomics by Mass Spectrometry* (Vol. 1410, pp. 65–76). http://doi.org/10.1007/978-1-4939-3524-6

Müller, K., Mynarek, M., Zwiener, I., Siegler, N., Zimmermann, M., Christiansen, H., … Tippelt, S. (2014). Postponed Is Not Canceled: Role of Craniospinal Radiation Therapy in the Management of Recurrent Infant Medulloblastoma—An Experience From the HIT-REZ 1997 & 2005 Studies. *International Journal of Radiation Oncology*, *88*(5), 1019–1024. http://doi.org/10.1016/j.ijrobp.2014.01.013

Murphy, G. (2008). The ADAMs: signalling scissors in the tumour microenvironment. *Nature Reviews*, *8*, 929–941. http://doi.org/10.1038/nrc2459

Nair, S. K., Driscoll, T., Boczkowski, D., Schmittling, R., Bigner, D. D., Sampson, J. H., … Mitchell, D. A. (2015). Ex vivo generation of dendritic cells from cryopreserved, post-induction chemotherapy, mobilized leukapheresis from pediatric patients with medulloblastoma. *Journal of Neuro-Oncology*, *125*(1), 65–74. http://doi.org/10.1007/s11060-015-1890-2

Naor, D., Nedvetzki, S., Golan, I., Melnik, L., & Faitelson, Y. (2002). CD44 in Cancer. *Critical Reviews in Clinical Laboratory Sciences*, *39*(6), 527–579.

NCI, GDC Data portal. (2016). Retrieved from https://gdc-portal.nci.nih.gov/#

Nooka, A. K., Behera, M., Lonial, S., & Dixon, M. D. (2016). Access to Children's Oncology Group and Pediatric Brain Tumor Consortium Phase 1 Clinical Trials: Racial/Ethnic Dissimilarities in Participation. *Cancer*, 1–8. http://doi.org/10.1002/cncr.30090

Northcott, P. A., Jones, D. T. W., Kool, M., Robinson, G. W., Gilbertson, R. J., Cho, Y. J., … Pfister, S. M. (2014). Medulloblastomics: The End of the Beginning. *Nature Reviews Cancer*, *12*(12), 818–834. http://doi.org/10.1038/nrc3410.Medulloblastomics

Northcott, P. A., Korshunov, A., Witt, H., Hielscher, T., Eberhart, C. G., Mack, S., … Taylor, M. D. (2011). Medulloblastoma comprises four distinct molecular variants. *Journal of Clinical Oncology*, *29*(11), 1408–14. http://doi.org/10.1200/JCO.2009.27.4324

Northcott, P. A., Nakahara, Y., Wu, X., Feuk, L., Ellison, D. W., Croul, S., … Taylor, M. D. (2009). Multiple recurrent genetic events converge on control of histone lysine methylation in medulloblastoma. *Nature Genetics*, *41*(4), 465–472. http://doi.org/10.1038/ng.336

Northcott, P. A., Shih, D. J. H., Peacock, J., Garzia, L., Morrissy, a S., Zichner, T., … Taylor, M. D. (2012). Subgroup-specific structural variation across 1,000 medulloblastoma genomes. *Nature*, *488*(7409), 49–56. http://doi.org/10.1038/nature11327

Northcott, P. A., Shih, D. J. H., Remke, M., Cho, Y.-J., Kool, M., Hawkins, C., … Taylor, M. D. (2011). Rapid, reliable, and reproducible molecular sub-grouping of clinical medulloblastoma samples. *Acta Neuropathologica*, *123*(4), 615–26. http://doi.org/10.1007/s00401-011-0899-7

Odreman, F., Vindigni, M., Gonzales, M. L., Niccolini, B., Candiano, G., Zanotti, B., … Vindigni, A. (2005). Proteomic Studies on Low- and High-Grade Human Brain Astrocytomas. *Journal of Proteome Research*, *4*, 698–708.

Offit, K., Levran, O., Mullaney, B., Mah, K., Deffenbaugh, A., Scholl, T., … Auerbach, A. D. (2003). Shared genetic susceptibility to Breast Cancer , Brain Tumors , and Fanconi Anemia. *Journal of the National Cancer Institute*, *95*(20), 1548–1552. http://doi.org/10.1093/jnci/djg072

Okamoto, H., Mineta, T., Ueda, S., Nakahara, Y., Shiraishi, T., Tamiya, T., & Tabuchi, K. (2005). Detection of JC virus DNA sequences in brain tumors in pediatric patients. *Journal of Neurosurgery*, *102*(Pediatrics 3), 294–298.

Okota, N. Y., Ishizawa, S. N., Hta, S. O., Ate, H. D., Ugimura, H. S., Amba, H. N., & Aekawa, M. M. (2002). Role of WNT pathway in Medulloblastoma Oncogenesis. *International Journal of Cancer*, *201*, 198–201. http://doi.org/10.1002/ijc.10559

Oldham, M. C., Konopka, G., Iwamoto, K., Langfelder, P., Kato, T., Horvath, S., & Geschwind, D. H. (2008). Functional organization of the transcriptome in human brain. *Nature Neuroscience*, *11*(11), 1271–1282. http://doi.org/10.1038/nn.2207

Omodei, D., Acampora, D., Mancuso, P., Prakash, N., Giovanni, L., Giovannantonio, D., … Simeone, A. (2008). Anterior-posterior graded response to Otx2 controls proliferation and differentiation of dopaminergic progenitors in the ventral mesencephalon. *Development*, *135*, 3459–3470. http://doi.org/10.1242/dev.027003

Ono, Y., Tamiya, T., Ichikawa, T., Kunishio, K., Matsumoto, K., Furuta, T., … Louis, D. N. (1996). Malignant astrocytomas with homozygous CDKN2/p16 Gene duplications have a higer Ki-67 proliferation indices. *Journal of Neuropathology and Experimental Neurology*, *55*(10), 1026–1031.

Packer, R. J., Friedman, H. S., Kun, L. E., & Fuller, G. N. (2002). Tumors Of The Brain Stem, Cerebellum, and Fourth Ventricle. In *Primary Central Nervous System tumours* (pp. 171–192).

Packer, R. J., Macdonald, T., & Verzina, G. (2010). Central Nervous System Tumors. *Hematology/Oncology Clinics of NA*, *24*(1), 87–108. http://doi.org/10.1016/j.hoc.2009.11.012

Packer, R. J., & Vezina, G. (2008). Management of and Prognosis With Medulloblastoma. *Journal of the American Medical Association*, *65*(11), 1419–1424.

Packer, R. J., Zhou, T., Holmes, E., Vezina, G., & Gajjar, A. (2013). Survival and secondary tumors in children with medulloblastoma receiving radiotherapy and adjuvant chemotherapy: results of Children's Oncology Group trial A9961. *Neuro-Oncology*, *15*(1), 97–103.

Pajonk, F., Mcbride, W. H., Pajonk, F., & Mcbride, W. H. (2001). The Proteasome in Cancer Biology and Treatment The Proteasome in Cancer Biology and Treatment. *Radiation Research*, *156*(5), 447–459.

Pajtler, K. W., Witt, H., Kool, M., Pfister, S. M., Pajtler, K. W., Witt, H., … Kratochwil, F. (2015). Molecular Classification of Ependymal Tumors across All CNS Compartments, Histopathological Grades, and Age Groups. *Cancer Cell*, *27*, 728–743. http://doi.org/10.1016/j.ccell.2015.04.002

Park, T. S., Hoffman, H. J., Hendrick, E. B., Humphreys, R. P., & Becker, L. E. (1983).

Medulloblastoma: clinical presentation and management. *Journal of Neurosurgery*, *58*, 543–552.

Penning, T. M. (2016). Ado-Keto Reductase Regulation by the Nrf2-System: Implications for Stress Response, Chemotherapy Drug Resistance and Carcinogenesis. *Chemical Research in Toxicology*, 1–46. http://doi.org/10.1021/acs.chemrestox.6b00319

Pereira, M., Mason, P., Szczesny, R. J., Maddukuri, L., Dziwura, S., Jedrzejczak, R., … Stepien, P. P. (2007). Interaction of human SUV3 RNA/DNA helicase with BLM helicase; loss of the SUV3 gene results in mouse embryonic lethality. *Mechanisms of Aging and Development*, *128*, 609–617. http://doi.org/10.1016/j.mad.2007.09.001

Perreault, S., Ramaswamy, V., Achrol, A. S., Chao, K., Liu, T. T., Shih, D., … Yeom, K. W. (2014). MRI Surrogates for Molecular Subgroups of Medulloblastoma. *American Journal of Neuroradiology*, *35*, 1263–1269.

Pettinati, I., Brem, J., Lee, S. Y., Mchugh, P. J., & Scho, C. J. (2016). The Chemical Biology of Human Metallo-beta-Lactamase Fold Proteins. *Trends in Biochemical Sciences*, *41*(4), 338–355. http://doi.org/10.1016/j.tibs.2015.12.007

Peyrl, A., Krapfenbauer, K., Slavc, I., Yang, J., Strobel, T., & Lubec, G. (2003). Protein profiles of medulloblastoma cell lines DAOY and D283: Identification of tumor-related proteins. *Proteomics*, *3*, 1781–1800. http://doi.org/10.1002/pmic.200300460

Pfister, S., Hartmann, C., & Korshunov, A. (2009). Histology and molecular pathology of pediatric brain tumors. *Journal of Child Neurology*, *24*(11), 1375–1386. http://doi.org/10.1177/0883073809339213

Pfister, S., Remke, M., Benner, A., Mendrzyk, F., Toedt, G., Devens, F., … Korshunov, A. (2009). Outcome Prediction in Pediatric Medulloblastoma Based on DNA Copy-Number Aberrations of Chromosomes 6q and 17q and the MYC and MYCN Loci. *Journal of Clinical Oncology*, *27*(10), 1627–1636. http://doi.org/10.1200/JCO.2008.17.9432

Pham, T. T., Scharf, C., Hammer, E., Gesell, M., Sonnemann, J., Beck, J., & Völker, U. (2013). Investigation of the Effects of the Histone Deacetylase Inhibitor Saha on the Medulloblastoma Cell Line Daoy Using Gel-Based Proteomics. In *International conference on biomedical engineering* (pp. 201–204).

Piehowski, P. D., Petyuk, V. A., Orton, D. J., Xie, F., Ramirez-, M., Engel, A., … Myers, A.

J. (2013). Sources of Technical Variability in Quantitative LC-MS Proteomics: Human Brain Tissue Sample Analysis. *Journal of Proteome Research*, *12*(5), 2128–2137. http://doi.org/10.1021/pr301146m.Sources

Pohanka, M., Hynek, D., Kracmarova, A., Kruseova, J., & Ruttkay-, B. (2012). Voltammetry Assay for Assessment of Oxidative Stress linked Pathologies in Brain Tumor suffered Childhood Patients. *International Journal of Electrochemical Science*, *7*, 11978–11992.

Polisetty, R. V., Gautam, P., & Gupta, M. K. (2016). Microsomal membrane proteome of low grade diffuse astrocytomas: Differentially expressed proteins and candidate surveillance biomarkers. *Scientific Reports*, *6*, 1–10. http://doi.org/10.1038/srep26882

Pollack, I. F., & Jakacki, R. I. (2011). Childhood brain tumours: epidemiology, current management and future directions. *Nature Reviews Neurology*, *7*(9), 495–506. http://doi.org/10.1038/nrneurol.2011.110

Pomeroy, S. L., Tamayo, P., Gaasenbeek, M., Sturla, L. M., Angelo, M., Mclaughlin, M. E., … Ii, T. R. G. (2002). Prediction of central nervous system embryonal tumour outcome based on gene expression. *Nature*, *415*, 436–442.

Pöschl, J., Koch, A., & Schüller, U. (2015). Histological subtype of medulloblastoma frequently changes upon recurrence. *Acta Neuropathologica*, *129*, 459–461. http://doi.org/10.1007/s00401-015-1397-0

Pruessmeyer, J., & Ludwig, A. (2009). The good, the bad and the ugly substrates for ADAM10 and ADAM17 in brain pathology, inflammation and cancer. *Seminars in Cell and Developmental Biology*, *20*, 164–174. http://doi.org/10.1016/j.semcdb.2008.09.005

Pu, P., Lan, J., Shan, S., Huang, E., Bai, Y., Guo, Y., & Jiang, D. (1996). Study of the antioxidant enzymes in human brain tumors. *Journal of Neuro-Oncology*, *29*, 121–128.

Qaddoumi, I., Sultan, I., & Broniscer, A. (2016). Pediatric low-grade gliomas and the need for new options for therapy: why and how? *Cancer Biology and Therapy*, *40*(1), 1–7. http://doi.org/10.4161/cbt.8.1.7237

Ramaswamy, V., Northcott, P. a, & Taylor, M. D. (2011). FISH and chips: the recipe for improved prognostication and outcomes for children with medulloblastoma. *Cancer Genetics*, *204*(11), 577–88. http://doi.org/10.1016/j.cancergen.2011.11.001

Ramaswamy, V., Remke, M., Bouffet, E., Bailey, S., Clifford, S. C., Doz, F., … Dufour, C. (2016). Risk stratification of childhood medulloblastoma in the molecular era: the

current consensus. *Acta Neuropathologica*, *4*, 1–11. http://doi.org/10.1007/s00401-016-1569-6

Rappsilber, J., Ishihama, Y., & Mann, M. (2003). Stop and Go Extraction Tips for Matrix-Assisted Laser Desorption/Ionization, Nanoelectrospray, and LC/MS Sample Pretreatment in Proteomics. *Analytical Chemistry*, *75*(3), 663–670.

Read, T., Hegedus, B., Wechsler-reya, R., & Gutmann, D. H. (2006). The Neurobiology of Neurooncology. *Neurological Progress*, *1*, 3–11. http://doi.org/10.1002/ana.20912

Rees, J. (2003). Advances in magnetic resonance imaging of brain tumours. *Current Opinion in Neurology*, *16*, 643–650. http://doi.org/10.1097/01.wco.0000102626.38669.b9

Remke, M., Kool, M., Northcott, P., Hovestadt, V., Remke, M., Kool, M., … Jones, D. T. W. (2013). Robust molecular subgrouping and copy- number profiling of medulloblastoma from small amounts of archival tumour material using high-density DNA methylation arrays Robust molecular subgrouping and copy‐number profiling of medulloblastoma from small amou. *Acta Neuropathologica*, *125*, 913–916. http://doi.org/10.1007/s00401-013-1126-5

Reste, P. Le, Avril, T., Morandi, X., & Chevet, E. (2016). Signaling the unfolded protein response in primary brain cancers. *Brain Research*, *16*, 1–28. http://doi.org/10.1016/j.brainres.2016.03.015

Ritchie, W., Granjeaud, S., Puthier, D., & Gautheret, D. (2008). Entropy Measures Quantify Global Splicing Disorders in Cancer. *PLoS Computational Biology*, *4*(3), 1–9. http://doi.org/10.1371/journal.pcbi.1000011

Rodriguez, F. J., Lim, K. S., Bowers, D., & Eberhart, C. G. (2013). Pathological and Molecular Advances in Pediatric Low-Grade Astrocytoma. *Annual Review of Pathology*, *8*, 361–379. http://doi.org/10.1146/annurev-pathol-020712-164009

Ronci, M., Catanzaro, G., Pieroni, L., Po, A., Besharat, Z. M., Greco, V., … Urbani, A. (2015). Proteomic analysis of human sonic hedgehog (SHH) medulloblastoma stem-like cells. *Molecular BioSystems*, 1–9. http://doi.org/10.1039/C5MB00034C

Rutkowski, M. J., Sughrue, M. E., Kane, A. J., Mills, S. A., & Parsa, A. T. (2010). Cancer and the Complement Cascade. *Molecular Cancer Research*, *8*(11), 1453–1465. http://doi.org/10.1158/1541-7786.MCR-10-0225

Rutkowski, S., Gerber, N. U., Hoff, K. Von, Gnekow, A., Bode, U., Graf, N., … Kuehl, J.

(2008). Treatment of early childhood medulloblastoma by postoperative chemotherapy and deferred radiotherapy. *Neuro-Oncology*, 201–210. http://doi.org/10.1215/15228517-2008-084

Rutkowski, S., von Hoff, K., Emser, A., Zwiener, I., Pietsch, T., Figarella-Branger, D., … Grill, J. (2010). Survival and prognostic factors of early childhood medulloblastoma: an international meta-analysis. *Journal of Clinical Oncology*, *28*(33), 4961–8. http://doi.org/10.1200/JCO.2010.30.2299

Sajjad, J., Kaliaperumal, C., Yousaf, I., Bhatti, R. J., & Sullivan, M. O. (2016). A Prospective Analysis of Complications of Intracranial Tumor Surgery. *Journal of Neurological Surgery*, *8*, 1–7.

Sardi, I., Lucchesi, M., Becciani, S., Facchini, L., Guidi, M., Maria, A., … De, M. (2015). Absence of human cytomegalovirus infection in childhood brain tumors. *American Journal of Cancer Research*, *5*(8), 2476–2483.

Scatena, R., Bottoni, P., Pontoglio, A., & Mastrototaro, L. (2008). Glycolytic enzyme inhibitors in cancer treatment. *Expert Opinion on Investigational Drugs*, *17*(10), 1533–1545.

Schiffer, D., Giordana, M. T., Mauro, A., Migheli, A., Germano, I., & Giaccone, G. (1986). Immunohistoehemical Demonstration of Vimentin in Human Cerebral Tumors. *Acta Neuropathologica Communications*, *70*, 209–219.

Schiffman, J. D., Hodgson, J. G., Vandenberg, S. R., Flaherty, P., Polley, M. C., Yu, M., … James, C. D. (2010). Oncogenic BRAF Mutation with CDKN2A Inactivation Is Characteristic of a Subset of Pediatric Malignant Astrocytomas. *Cancer Research*, *70*(2), 512–519. http://doi.org/10.1158/0008-5472.CAN-09-1851

Schindler, G., Capper, D., Meyer, J., Janzarik, W., Omran, H., Kirsten, C. H., … Deimling, A. Von. (2011). Analysis of BRAF V600E mutation in 1320 nervous system tumors reveals high mutation frequencies in pleomorphic xanthoastrocytoma, ganglioglioma and extra-cerebellar pilocytic astrocytoma. *Acta Neuropathologica*, *121*, 397–405. http://doi.org/10.1007/s00401-011-0802-6

Schmandt, S. M., Packer, J., Gilbert, L., & Jane, J. (2000). Spontaneous Regression of Low-Grade Astrocytomas in Childhood. *Pediatric Neurosurgery*, *32*, 132–136.

Schmid, R. S., & Maness, P. F. (2008). L1 and NCAM adhesion molecules as signaling

coreceptors in neuronal migration and process outgrowth. *Current Opinion in Neurobiology*, *18*, 245–250. http://doi.org/10.1016/j.conb.2008.07.015

Schmidt, L. S., Grell, K., Frederiksen, K., Johansen, C., Schmiegelow, K., & Schüz, J. (2009). Seasonality of birth in children with central nervous system tumours in Denmark, 1970-2003. *British Journal of Cancer*, *100*(1), 185–187. http://doi.org/10.1038/sj.bjc.6604813

Schmidt, M., Hellwig, B., Hammad, S., Othman, A., Lohr, M., Chen, Z., … Marchan, R. (2012). A Comprehensive Analysis of Human Gene Expression Profiles Identifies Stromal Immunoglobulin k C as a Compatible Prognostic Marker in Human Solid Tumors. *Clinical Cancer Research*, *18*(3), 2695–2703. http://doi.org/10.1158/1078-0432.CCR-11-2210

Schu, U., Heine, V. M., Mao, J., Kho, A. T., Dillon, A. K., Han, Y., … Alvarez-buylla, A. (2008). Acquisition of Granule Neuron Precursor Identity Is a Critical Determinant of Progenitor Cell Competence to Form Shh-Induced Medulloblastoma. *Cancer Cell*, *14*, 123–134. http://doi.org/10.1016/j.ccr.2008.07.005

Schulze, M., Fedorchenko, O., Zink, T. G., Knobbe-thomsen, C. B., Kraus, S., Schwinn, S., … Reifenberger, G. (2015). Chronophin is a glial tumor modifier involved in the regulation of glioblastoma growth and invasiveness. *Oncogene*, 1–15. http://doi.org/10.1038/onc.2015.376

Schwalbe, E. C. (2011). *Molecular subclassification of medulloblastoma and its utility for disease prognostication*. Newcastle University.

Schwalbe, E. C., Williamson, D., Lindsey, J. C., Hamilton, D., Ryan, S. L., Northcott, P. A., … Clifford, S. C. (2013). DNA methylation profiling of medulloblastoma allows robust subclassification and improved outcome prediction using formalin-fixed biopsies. *Acta Neuropathologica*, 359–371. http://doi.org/10.1007/s00401-012-1077-2

Schwalbe, E. C., Williamson, D., Lindsey, J. C., Hamilton, D., Sarra, L., Megahed, H., … Clifford, S. C. (2015). DNA methylation profiling of medulloblastoma allows robust sub-classification and improved outcome prediction using formalin-fixed biopsies. *Acta Neuropathologica*, *125*(3), 359–371. http://doi.org/10.1007/s00401-012-1077-2.DNA

Scott, J. N., Brasher, P. M. A., Sevick, R. J., Rewcastle, N. B., & Forsyth, P. A. (2002). How often are nonenhancing supratentorial gliomas malignant? A population study.

Neurology, *1*, 947–949.

Searles, S., Beth, N., Susan, A. M., Holly, E. A., Little, J., Bracci, P. M., … Flora, F. (2008). Family cancer history and risk of brain tumors in children: results of the SEARCH international brain tumor study. *Cancer Causes and Control*, *19*, 641–648. http://doi.org/10.1007/s10552-008-9128-7

Semenza, G. L. (2003). Targeting HIF-1 for Cancer Therapy. *Nature Reviews Cancer*, *3*, 721–732. http://doi.org/10.1038/nrc1187

Sest´ak, J., Moravcov´a, D., & Kahle, V. (2015). Instrument platforms for nano liquid chromatography. *Journal of Chromatography A*, 1–72. http://doi.org/10.1016/j.chroma.2015.07.090

Shaikhibrahim, Z., Lindstrot, A., Ellinger, J., & Rogenhofer, S. (2011). Identification of immunity-related genes in prostate cancer and potential role of the ETS family of transcription factors in their regulation. *International Journal of Molecular Medicine*, (10), 799–807. http://doi.org/10.3892/ijmm.2011.771

Shalaby, T., Achini, F., & Grotzer, M. A. (2016). Targeting cerebrospinal fluid for discovery of brain cancer biomarkers. *Journal of Cancer Metastasis and Treatment*, *2*, 176–187. http://doi.org/10.20517/2394-4722.2016.12

Sharma, M. K., Mansur, D. B., Reifenberger, G., Perry, A., Leonard, J. R., Aldape, K. D., … Gutmann, D. H. (2007). Distinct Genetic Signatures among Pilocytic Astrocytomas Relate to Their Brain Region Origin. *Cancer Research*, *67*(3), 890–900. http://doi.org/10.1158/0008-5472.CAN-06-0973

Sharma, P., & Nag, A. (2014). CUL4A ubiquitin ligase: a promising drug target for cancer and other human diseases. *Open Biology*, *4*(130217), 1–14.

Shen, Y., & Smith, R. D. (2012). High-pH reverse-phase chromatography with fraction concatenation for 2D proteomic analysis. *Expert Review of Proteomics*, *9*(2), 129–134.

Shi, X., Zhang, Z., Zhan, X., Cao, M., Satoh, T., Akira, S., … Wu, J. (2014). An epigenetic switch induced by Shh signalling regulates gene activation during development and medulloblastoma growth Xuanming. *Nature Communications*, *5*(May), 1–12. http://doi.org/10.1038/ncomms6425

Shih, D. J. H., Northcott, P. A., Remke, M., Korshunov, A., Ramaswamy, V., Kool, M., … Taylor, M. D. (2014). Cytogenetic Prognostication Within Medulloblastoma Subgroups.

Journal of Clinical Oncology, *32*(9), 886–896. http://doi.org/10.1200/JCO.2013.50.9539

Shin, H. R. Æ., Sun, J. Æ. H., Jin, S. J. Æ. Y., Jeong, Æ. I. K. Æ. Y., & Kang, S. (2007). Screening for motility-associated genes in malignant astrocytoma cell lines. *Journal of Neuro-Oncology*, *82*, 125–131. http://doi.org/10.1007/s11060-006-9262-6

Skeie, B. S., Eide, G. E., Flatebø, M., Heggdal, J. I., Larsen, E., & Bragstad, S. (2016). Quality of life is maintained using Gamma Knife radiosurgery: a prospective study of a brain metastases patient cohort. *Journal of Neurosurgery*, 1–18. http://doi.org/10.3171/2015.10.JNS15801

Smit, S., Hoefsloot, H. C. J., & Smilde, A. K. (2008). Statistical data processing in clinical proteomics. *Journal of Chromatography B*, *866*, 77–88. http://doi.org/10.1016/j.jchromb.2007.10.042

Smoll, N. R., & Drummond, K. J. (2012). The incidence of medulloblastomas and primitive neurectodermal tumours in adults and children. *Journal of Clinical Neuroscience*, *19*(11), 1541–1544. http://doi.org/10.1016/j.jocn.2012.04.009

Songtao, Q., Lei, Y., Si, G., Yanqing, D., Huixia, H., Xuelin, Z., … Fei, Y. (2012). IDH mutations predict longer survival and response to temozolomide in secondary glioblastoma. *Cancer Science*, *103*(2), 269–273. http://doi.org/10.1111/j.1349-7006.2011.02134.x

Souweidane, M. M., Edgar, M. A., Morgenstern, P. F., Christos, P. J., Khakoo, Y., Rutka, J. T., & Dunkel, I. J. (2009). Intraoperative Arachnoid and Cerebrospinal fluid sampling in Children with Posterior Fossa Brain Tumours. *Neurosurgery*, *65*(1), 72–78. http://doi.org/10.1227/01.NEU.0000348011.98625.43

Srinivasan, M., & Sedmak, D. (2002). Content and Integrity of Nucleic Acids. *The American Journal of Pathology*, *161*(6), 1961–1971. http://doi.org/10.1016/S0002-9440(10)64472-0

Srivastava, V., Pandey, V., Rn, M., Ag, S., Rk, M., & Op, S. (2016). Impact of Brain Tumour Treatment on Quality of Life in Children: A Health Perspective. *Neuro-Oncology*, *2*(14), 1–6.

Staal, J. A., Lau, L. S., Zhang, H., Ingram, W. J., Andrew, R., Northcott, P. A., … Rood, B. R. (2015). Proteomic profiling of high risk medulloblastoma reveals functional biology. *Oncotarget*, *6*(16), 1–12.

Stirling, L., Williams, M. R., & Morielli, A. D. (2009). Dual Roles for RHOA/RHO-Kinase In the Regulated Trafficking of a Voltage-sensitive Potassium Channel. *Molecular Biology of the Cell*, *20*, 2991–3002. http://doi.org/10.1091/mbc.E08

Stoicea, N., Du, A., Lakis, D. C., Tipton, C., Arias-morales, C. E., & Bergese, S. D. (2016). The MiRNA Journey from Theory to Practice as a CNS Biomarker. *Frontiers in Genetics*, *7*, 1–8. http://doi.org/10.3389/fgene.2016.00011

Strother, D. R., Lafay-cousin, L., Boyett, J. M., Burger, P., Aronin, P., Constine, L., … Tennessee, J. M. B. (2014). Benefit from prolonged dose-intensive chemotherapy for infants with malignant brain tumors is restricted to patients with ependymoma: a report of the Pediatric Oncology Group randomized controlled trial 9233/34. *Neuro-Oncology*, *16*(3), 457–465. http://doi.org/10.1093/neuonc/not163

Sun, T., Warrington, N. M., & Rubin, J. B. (2012). Why does Jack, and not Jill, break his crown? Sex disparity in brain tumors. *Biology of Sex Differences*, *3*(3), 1–10. http://doi.org/10.1186/2042-6410-3-3

Tacconi, L., Stapleton, S., Signorelli, F., & Thomas, D. G. T. (1996). Acquired immune deficiency syndrome (AIDS) and cerebral astrocytoma. *Clinical Neurology and Neurosurgery*, *98*, 149–151.

Tamayo-orrego, L., Wu, C., Bouchard, N., Skowron, P., Taylor, M. D., Tamayo-orrego, L., … Remke, M. (2016). Evasion of Cell Senescence Leads to Medulloblastoma Progression Article Evasion of Cell Senescence Leads to Medulloblastoma Progression. *Cell Reports*, *14*, 2925–2937. http://doi.org/10.1016/j.celrep.2016.02.061

Tanca, A., Pagnozzi, D., & Addis, M. F. (2012). Setting proteins free: Progresses and achievements in proteomics of formalin-fixed, paraffin-embedded tissues. *Proteomics - Clinical Applications*, *6*(1–2), 7–21. http://doi.org/10.1002/prca.201100044

Tavares, R., Wajnberg, G., Scherer, N. D. M., Pauletti, A., Cassoli, J. S., Ferreira, C. G., … Fabio, P. (2016). Unveiling alterative splice diversity from human oligodendrocyte proteome data. *Journal of Proteomics*, 1–37. http://doi.org/10.1016/j.jprot.2016.05.023

Taylor, M. D., Northcott, P. A., Korshunov, A., Remke, M., Cho, Y.-J., Clifford, S. C., … Pfister, S. M. (2012). Molecular subgroups of medulloblastoma: the current consensus. *Acta Neuropathologica*, *123*(4), 465–472. http://doi.org/10.1007/s00401-011-0922-z

Tech, K., & Gershon, T. R. (2015). Energy metabolism in neurodevelopment and

medulloblastoma. *Translational Pediatrics*, *4*(1), 12–19. http://doi.org/10.3978/j.issn.2224-4336.2015.01.03

Thompson, E. M., Hielscher, T., Bouff, E., Remke, M., Luu, B., Gururangan, S., … Olson, J. J. (2016). Prognostic value of medulloblastoma extent of resection after accounting for molecular subgroup : a retrospective integrated clinical and molecular analysis. *Lancet Oncology*, *1*(April), 1–12. http://doi.org/10.1016/S1470-2045(15)00581-1

Thompson, M. C., Fuller, C., Hogg, T. L., Dalton, J., Finkelstein, D., Lau, C. C., … Gilbertson, R. J. (2006). Genomics Identifies Medulloblastoma Subgroups That Are Enriched for Specific Genetic Alterations. *Journal of Clinical Oncology*, *24*(12), 1924–31. http://doi.org/10.1200/JCO.2005.04.4974

Tian, Q., Sangar, V., & Price, N. D. (2015). Emerging proteomic technologies provide enormous and underutilized potential for brain cancer research. *Molecular and Cellular Proteomics*.

Tisdale, E. J. (2002). Glyceraldehyde-3-phosphate Dehydrogenase Is Phosphorylated by Protein Kinase C and Plays a Role in Microtubule Dynamics in the Early Secretory Pathway. *Journal of Biological Chemistry*, *277*(5), 3334–3341. http://doi.org/10.1074/jbc.M109744200

Tochhawng, L., Deng, S., Pugalenthi, G., Kumar, A. P., Lim, K. H., Yang, H., … Yap, C. T. (2016). Gelsolin-Cu/ZnSOD interaction alters intracellular reactive oxygen species levels to promote cancer cell invasion. *Oncotarget*, *6*, 1–18. http://doi.org/10.18632/oncotarget.10451

Todaro, L., Christiansen, S., Varela, M., Eugenia, L., Lustig, S. De, & Puricelli, L. (2007). Alteration of serum and tumoral neural cell adhesion molecule (NCAM) isoforms in patients with brain tumors. *Journal of Neuro-Oncology*, *83*, 135–144. http://doi.org/10.1007/s11060-006-9312-0

Topka, S., Glassmann, A., Weisheit, G., Schüller, U., & Schilling, K. (2014). The Transcription Factor Cux1 in Cerebellar Granule Cell Development and Medulloblastoma Pathogenesis. *Cerebellum*, *13*, 698–712. http://doi.org/10.1007/s12311-014-0588-x

Toshinai, K., & Nakazato, M. (2009). Neuroendocrine regulatory peptide-1 and -2: Novel bioactive peptides processed from VGF. *Cellular and Molecular Life Sciences*, *66*,

1939–1945. http://doi.org/10.1007/s00018-009-8796-0

Tsai, C., & Wu, C. (2011). Role of the XRCC5/XRCC6 dimer in carcinogenesis and pharmacogenomics. *Future Medicine*, *12*(4), 515–534.

Turck, C. W., Webhofer, C., Nussbaumer, M., Teplyska, L., Chen, A., Maccarrone, G., & Filiou, M. D. (2016). Stable isotope metabolic labeling suggests differential turnover of the DPYSL protein family. *Proteomics*, *1*, 1–12. http://doi.org/10.1002/prca.201600078.This

Turner, M. C., Mckean-cowdin, R., Fisher, J. L., & Philip, J. (2014). Childhood Brain Tumor Epidemiology: A Brain Tumor Epidemiology Consortium Review. *American Journal of Cancer Research*, *1*, 1–46. http://doi.org/10.1158/1055-9965.EPI-14-0207

Tyburczy, M. E., Kotulska, K., Pokarowski, P., Mieczkowski, J., Kucharska, J., Grajkowska, W., … Jozwiak, S. (2010). Novel Proteins Regulated by mTOR in Subependymal Giant Cell Astrocytomas of Patients with Tuberous Sclerosis Complex and New Therapeutic Implications. *The American Journal of Pathology*, *176*(4), 1878–1890. http://doi.org/10.2353/ajpath.2010.090950

Uetrecht, A. C., & Bear, J. E. (2006). Coronins: the return of the crown. *Trends in Biology*, *16*(8), 421–426. http://doi.org/10.1016/j.tcb.2006.06.002

Unland, R., Kerl, K., Schlosser, S., Farwick, N., Plagemann, T., Lechtape, B., … Frühwald, M. C. (2014). Epigenetic repression of the dopamine receptor D4 in pediatric tumors of the central nervous system. *Journal of Neuro-Oncology*, *116*(2), 237–49. http://doi.org/10.1007/s11060-013-1313-1

Vasiljevic, A., Champier, J., Figarella-branger, D., Wierinckx, A., Jouvet, A., & Fèvre-montange, M. (2012). Molecular characterization of central neurocytomas: Potential markers for tumor typing and progression. *Neuropathology*, *1*, 1–13. http://doi.org/10.1111/j.1440-1789.2012.01338.x

Veelen, P. A. Van, & Palmblad, M. (2013). Comparison of peptide and protein fractionation methods in proteomics. *EUPROT*, *1*, 30–37. http://doi.org/10.1016/j.euprot.2013.09.001

Vesely, M. D., Kershaw, M. H., Schreiber, R. D., & Smyth, M. J. (2011). Natural Innate and Adaptive Immunity to Cancer. *Annual Review of Immunology*, *29*, 235–271. http://doi.org/10.1146/annurev-immunol-031210-101324

Vriend, J., & Marzban, H. (2016). The ubiquitin-proteasome system and chromosome 17 in

cerebellar granule cells and medulloblastoma subgroups. *Cellular and Molecular Life Sciences*, *1*, 1–19. http://doi.org/10.1007/s00018-016-2354-3

Wade, A., Robinson, A. E., Engler, J. R., Petritsch, C., James, C. D., & Phillips, J. J. (2013). Proteoglycans and their roles in brain cancer. *The FEBS Journal*, *280*, 2399–2417. http://doi.org/10.1111/febs.12109

Walter, T., Shattuck, D. W., Baldock, R., Bastin, M. E., Carpenter, A. E., Duce, S., … Hériché, J. (2010). Visualization of image data from cells to organisms. *Nature Methods Supplement*, *7*(3), 26–41. http://doi.org/10.1038/NMETH.1431

Wang, H., Zhao, Y., Zhang, C., Li, M., Jiang, C., & Li, Y. (2014). Rab27a Was Identified as a Prognostic Biomaker by mRNA Profiling, Correlated with Malignant Progression and Subtype Preference in Gliomas. *PloS One*, *9*(2), 1–8. http://doi.org/10.1371/journal.pone.0089782

Wang, X., Dubuc, A. M., Ramaswamy, V., Mack, S., Gendoo, D. M. A., Remke, M., … Taylor, M. D. (2015). Medulloblastoma subgroups remain stable across primary and metastatic compartments. *Acta Neuropathologica*, *129*, 449–457. http://doi.org/10.1007/s00401-015-1389-0

Wanyoike, P. (2004). Posterior cranial fossa tumours in children at Kenyatta National Hospital, Nairobi. *East African Medical Journal*, *81*(5), 258–260.

Warren, K. E., Goldman, S., Pollack, I. F., Fangusaro, J., Schaiquevich, P., Stewart, C. F., … Kun, L. E. (2011). Phase I Trial of Lenalidomide in Pediatric Patients With Recurrent, Refractory, or Progressive Primary CNS Tumors: Pediatric Brain Tumor Consortium Study PBTC-018. *Journal of Clinical Oncology*, *29*(3), 324–329. http://doi.org/10.1200/JCO.2010.31.3601

Weiner, H. L., Bakst, R., Hurlbert, M. S., Ruggiero, J., Ahn, E., Lee, W. S., … Turnbull, D. H. (2002). Induction of Medulloblastomas in Mice by Sonic Hedgehog, Independent of Gli1. *Cancer Research*, *62*, 6385–6389.

Weissbourd, B., Ren, J., Deloach, K. E., Guenthner, C. J., & Miyamichi, K. (2014). Presynaptic Partners of Dorsal Raphe Serotonergic and GABAergic Neurons. *Neuron*, *83*(3), 645–662. http://doi.org/10.1016/j.neuron.2014.06.024

Wiestler, B., Capper, D., Holland, T., Korshunov, A., Deimling, A. Von, Michael, S., … Wick, W. (2013). ATRX loss refines the classification of anaplastic gliomas and

identifies a subgroup of IDH mutant astrocytic tumors with better prognosis. *Acta Neuropathologica*, *1*, 1–9. http://doi.org/10.1007/s00401-013-1156-z

Włodarski, P., Grajkowska, W., Łojek, M., Rainko, K., & Jóźwiak, J. (2006). Activation of Akt and Erk pathways in medulloblastoma. *Folia Neuropathologica*, *44*(3), 214–220.

Woodburn, R. T., Azzarelli, B., Montebello, J. F., & Goss, I. E. (2001). Intense p53 staining is a valuable prognostic indicator for poor prognosis in medulloblastoma/central nervous system primitive neuroectodermal tumors. *Journal of Neuro-Oncology*, *52*, 57–62.

Xia, H., Cheung, W. K. C., Ng, S. S., Jiang, X., Jiang, S., Sze, J., … Lin, M. C. (2012). Loss of Brain-enriched miR-124 MicroRNA Enhances Stem-like Traits and Invasiveness of Glioma Cells. *Journal of Biological Chemistry*, *287*(13), 9962–9971. http://doi.org/10.1074/jbc.M111.332627

Xiong, J., Bing, Z., Su, Y., Deng, D., & Peng, X. (2014). An Integrated mRNA and microRNA Expression Signature for Glioblastoma Multiforme Prognosis. *PloS One*, *9*(5), 1–8. http://doi.org/10.1371/journal.pone.0098419

Xue, L., Xu, Z., Wang, K., Wang, N., Zhang, X., & Wang, S. (2016). Network analysis of microRNAs, transcription factors, target genes and host genes in human anaplastic astrocytoma. *Experimental and Therapeutic Medicine*, *12*, 437–444. http://doi.org/10.3892/etm.2016.3272

Yang, H. W., Kim, T., Song, S. S., Menon, L., Jiang, X., Huang, W., … Carroll, R. S. (2014). A small subunit processome protein promotes cancer by altering translation. *Oncogene*, *1*, 1–11. http://doi.org/10.1038/onc.2014.376

Yang, L., Tao, T., Wang, Y., Bao, Z., He, X., & Cui, G. (2015). Knocking down the expression of TRA2β inhibits the proliferation and migration of human glioma cells. *Pathology-Research and Practice*, *1*, 1–9. http://doi.org/10.1016/j.prp.2015.04.014

Yang, Z., Ellis, T., Markant, S. L., Read, T., Kessler, J. D., Bourboulas, M., … Wainwright, B. J. (2008). Medulloblastoma Can Be Initiated by Deletion of Patched in Lineage-Restricted Progenitors or Stem Cells. *Cancer Cell*, *14*, 135–145. http://doi.org/10.1016/j.ccr.2008.07.003

Yoo, B. C., Kim, S. H., Cairns, N., Fountoulakis, M., & Lubec, G. (2001). Deranged Expression of Molecular Chaperones in Brains of Patients with Alzheimer's Disease. *Biochemical and Biophysical Research Communications*, *280*, 249–258.

http://doi.org/10.1006/bbrc.2000.4109

Zakrzewski, K., Pfeifer, A., Oczko-wojciechowska, M., & Jarz, B. (2015). Transcriptional profiles of pilocytic astrocytoma are related to their three different locations, but not to radiological tumor features. *BMC Cancer*, *15*(778), 1–16. http://doi.org/10.1186/s12885-015-1810-z

Zanini, C., Mandili, G., Bertin, D., Cerutti, F., Baci, D., Leone, M., … Forni, M. (2011). Analysis of different medulloblastoma histotypes by two-dimensional gel and MALDI-TOF. *Childs Nervous System*, *27*, 2077–2085. http://doi.org/10.1007/s00381-011-1515-9

Zhang, W., Ou, J., Lei, F., Hou, T., & Wu, S. (2016). C14ORF166 overexpression is associated with pelvic lymph node metastasis and poor prognosis in uterine cervical cancer. *Tumor Biology*, *37*(651), 369–379. http://doi.org/10.1007/s13277-015-3806-3

Zimmer, L., & Luxen, A. (2011). PET radiotracers for molecular imaging in the brain: Past, present and future. *Neuroimage*, *1*, 363–368. http://doi.org/10.1016/j.neuroimage.2011.12.037

Supplementary

MB subtype disparity resolution by mass spectrometry based clustering

A

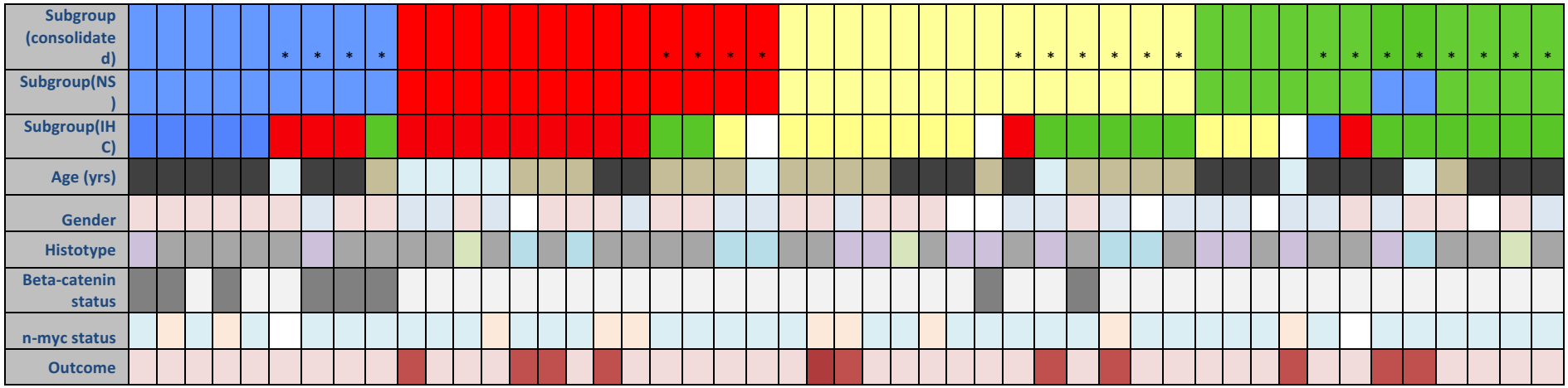

B

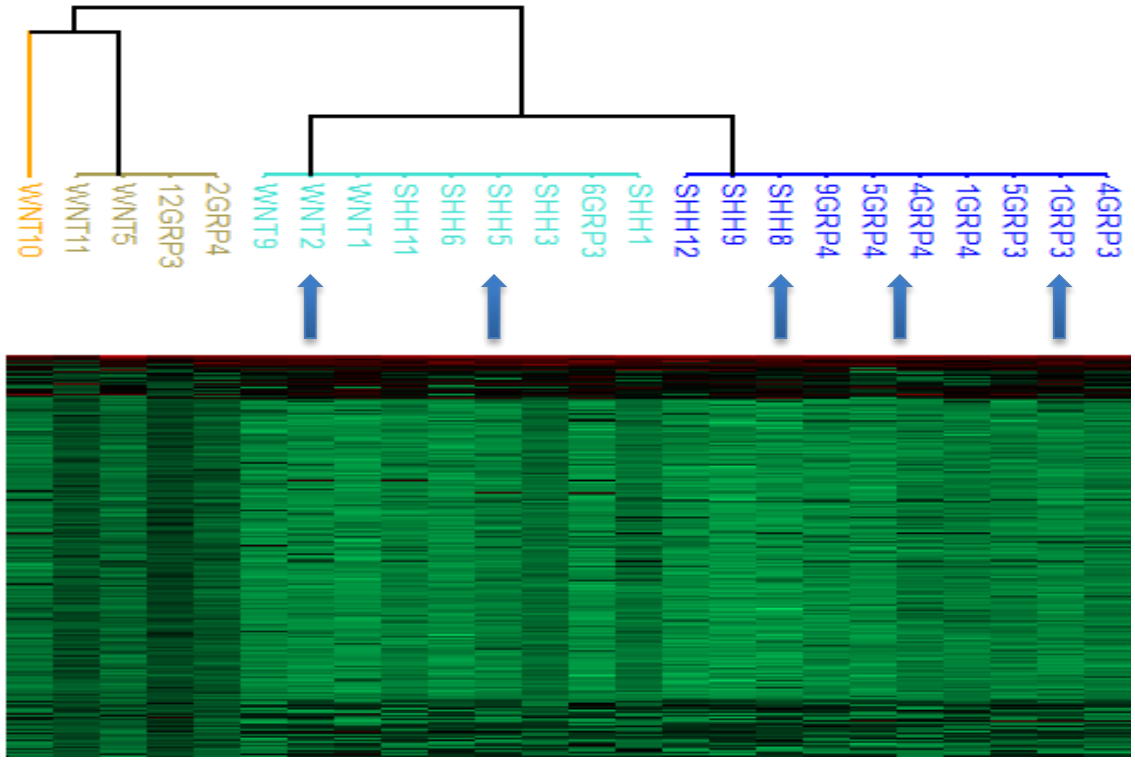

Figure s1: Overall summary of NS and IHC based subtyping and the mass spectrometry based proteomic resolving of any disparities or conflict in subtyping.

A – Summary of the patient subtype and molecular data that aided in resolution of any conflicts in subtyping by NS and IHC, conflicting subtypes are indicated by *. B – Any conflicting subtypes were clustered against the proteomic data of the wider cohort. Conflicted subtypes by NS and IHC are indicated by arrows and are thus assigned to subtype based on proteomic clustering using k-nearest neighbour clustering.

Key:

Subgroup	WNT	SHH	GROUP 3	GROUP 4
Age (yrs)	<3 yrs	3-5 yrs	>5 yrs	
Gender	Male	Female		
Histotype	Classic	LCA	Desmo/Nodular	MBEN
β-catenin	Positive	Negative		
N-MYC status	Amplified	Balanced		
Outcome	Good	Poor		
Significant		***		

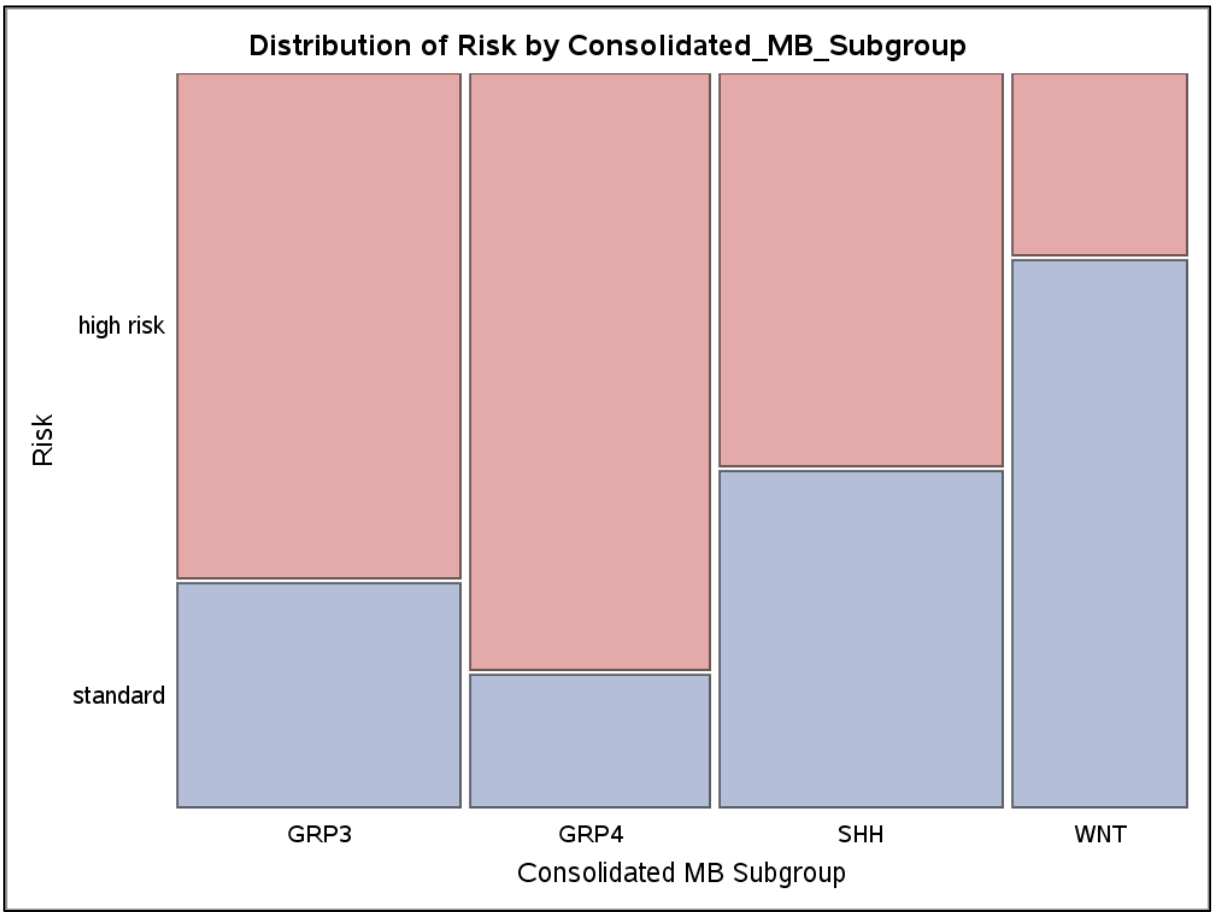

Figure s2: Distribution of clinical risk by consolidated molecular subtype

MB associations

Cellular component	
Title (or Source) cell component	wnt_GeneSet
endoplasmic reticulum-Golgi intermediate compartment	COL7A1,COPB1,CTSZ,ERP44,FN1,GOLGA2,HMGB1,HSPA5,LMAN1,LMAN2,MYDGF,NUCB1,NUCB2,P4HB,PDIA6,RAB1B,RAB2A,SEC22B,SERPINA1,SERPINH1,SURF4,TMED10,TMED3,TMED9,UGGT1
endoplasmic reticulum part	ADAMTSL1,AHCYL1,ALDH3A2,APOA1,APOA2,APOA4,ARCN1,ARL6IP5,ASNA1,ASPH,ATL1,ATP2A2,B2M,BAX,CALR,CALU,CANX,CAPN2,CDC42,CDS2,CES1,CKAP4,COL12A1,COL14A1,COL16A1,COL18A1,COL1A1,COL1A2,COL26A1,COL4A1,COL4A2,COL6A1,COL6A2,COL6A3,COL7A1,COPA,COPB1,COPB2,COPG1,COPZ1,CTSZ,CYB5A,CYB5R3,DAD1,DDOST,DDRGK1,DNAJA1,DNAJB11,DPM3,EIF5A,EMC1,EPHX1,ERAP1,ERLIN2,ERO1A,ERP29,ERP44,ESD,ESYT1,F2,FKBP1A,FKBP3,FKBP4,GANAB,HACD3,HLA-A,HLA-DRA,HSP90B1,HSPA5,HYOU1,ITPR1,KPNB1,KTN1,LMAN1,LMAN2,LRRC59,MBOAT7,MLEC,MTDH,MYDGF,NOTCH1,OSBP,P3H1,P4HA1,P4HA2,P4HB,PDCD6,PDCD6IP,PDIA2,PDIA3,PDIA4,PDIA6,PGRMC1,PLOD1,PPIB,PRKCSH,RAB10,RAB18,RAB1B,RAB21,RAB2A,RAB6A,RCN2,RHOA,RNF170,RRBP1,RTCB,RTN1,RTN4,SACM1L,SCFD1,SEC13,SEC22B,SEC23A,SEC24C,SEC31A,SEC61A1,SEC61B,SEC62,SERPINA1,SERPINH1,SEZ6L,SLC18A1,SPCS2,SRI,SRP9,SRPRA,SRPRB,SSR1,SSR4,STT3B,SURF4,THBS1,TMED10,TMED3,TMED4,TMED9,TMEM43,TMPO,TXNDC5,UBA1,UBXN1,UCHL1,UGGT1,VAPA,VCP,VTN
I band	ACTC1,ACTN1,ACTN4,ALDOA,ANK2,ANXA5,ATP2B4,CAPZB,CFL2,CRYAB,CTNNB1,DES,FKBP1A,FLNB,FLNC,GLRX3,HSPB1,MYL12A,PDLIM5,PGM5,PPP3CB,SLC4A1,SORBS2,SPTAN1,SRI,SYNM,VCL
Z disc	ACTN1,ACTN4,ANK2,ANXA5,ATP2B4,CAPZB,CRYAB,CTNNB1,DES,FKBP1A,FLNB,FLNC,GLRX3,HSPB1,MYL12A,PDLIM5,PGM5,PPP3CB,SLC4A1,SORBS2,SPTAN1,SRI,SYNM,VCL
rough endoplasmic reticulum	CANX,EPHA5,FGA,GLUL,HSPD1,MAP2,NUCB1,PCSK9,PEBP1,PLOD1,SEC61A1,SEC61B,SEC62,SRP9,SRPRA,SRPRB,SSR4,UBA1,VDAC3,VTN
F-actin capping protein complex	ADD1,CAPG,CAPZA1,CAPZA2,CAPZB,MTPN
SMN-Sm protein complex	SNRPB,SNRPD1,SNRPD2,SNRPD3,SNRPE,SNRPF,SNRPG,STRAP
COPI vesicle coat	ARCN1,COPA,COPB1,COPB2,COPG1,COPZ1,TMED3
fascia adherens	ACTN1,CDH2,CTNNB1,DES,DSP,SPTAN1,VCL
immunoglobulin complex, circulating	IGHA1,IGHA2,IGHG1,IGHG2,IGHG3,IGHM,IGKV3-20,IGLL5,JCHAIN
cell surface	AGRN,ALCAM,ANXA1,ANXA2,ANXA5,AOC3,APMAP,APOA1,APOA4,APOE,APOH,AQP4,ATP5B,B2M,BGN,C1QBP,CALR,CD14,CD276,CD44,CDH13,CKAP4,CLU,CRYAB,CSPG4,CTSB,CXADR,CXCR4,EPHA5,ERP29,ERP44,FCER1G,FGA,FGB,FGG,GFRA1,GOT2,GSR,HLA-A,HLA-DRA,HMGB1,HNRNPM,HNRNPU,HSP90AA1,HSP90AB1,HSPA2,HSPA5,HSPA8,HSPD1,IGHA1,IGHA2,IGHG1,IGHG2,IGHG3,IGHM,IGLL5,ITGB1,L1CAM,LAMP1,LGALS1,LGALS3,LMAN2,MBL2,MSN,MYH10,MYH9,NCAM1,NID2,NOTCH1,NRCAM,P4HB,PCSK9,PDIA3,PDIA4,PDXP,PEBP1,PHB,PHB2,PLG,PPP1CC,PTN,RAB21,RALA,RDX,RHOA,RHOB,RNPEP,SLC1A3,SLC3A2,SLC4A1,THBS1,THY1,TLN1,TPM3,TYROBP,USP14,VAMP3,VC

	AN
secretory IgA immunoglobulin complex	IGHA1,IGHA2,IGKV3-20,JCHAIN
polymeric IgA immunoglobulin complex	IGHA1,IGHA2,IGKV3-20,JCHAIN
IgA immunoglobulin complex, circulating	IGHA1,IGHA2,IGKV3-20,JCHAIN
GAIT complex	EPRS,GAPDH,RPL13A,SYNCRIP
monomeric IgA immunoglobulin complex	IGHA1,IGHA2,IGKV3-20,JCHAIN
IgA immunoglobulin complex	IGHA1,IGHA2,IGKV3-20,JCHAIN
ER to Golgi transport vesicle	B2M,COL7A1,CTSZ,GOLGA2,HLA-A,HLA-DRA,LMAN1,PCSK9,SEC13,SEC22B,SEC23A,SEC24C,SEC31A,SERPINA1,TMED10,USO1

Title (or Source)	shh_GeneSet
CRD-mediated mRNA stability complex	CSDE1,DHX9,HNRNPU,IGF2BP1,SYNCRIP,YBX1
excitatory synapse	ACTB,ACTR3,ADD1,ADD2,ADD3,ANK2,ARF1,ARHGEF2,BAIAP2,CALD1,CAMK2B,CNN3,CRYAB,CTNNA2,CTNND2,DBN1,DBNL,DCLK1,DNM2,EPB41L1,EPB41L3,FMR1,GAP43,GSK3B,HNRNPK,HSPA8,MACF1,MAP1A,MAP1B,MAP2,MAP4,MAPT,NEFM,NGFR,NSF,PAK1,PALM,PICALM,PPP2CA,RIMS1,RTN4,SLC17A7,SORCS3,SPTBN1,SRC,STX1B,SYN1,SYN2,SYP,SYT1,SYT11,VPS35,YWHAZ
cell-cell junction	ABI2,ACTN1,ACTN4,ACTR3,ADD3,AHNAK,AKR1B1,ANK2,ANXA5,ANXA6,APP,AQP4,ARHGEF2,ATP1A2,ATP1B1,ATP2A2,CADM1,CALB2,CAMK2D,CAPZA1,CAPZB,CASK,CD200,CDC42,CFL1,CLIC4,CORO1A,CSK,CTNNA1,CTNNA2,CTNNB1,CTNND1,CXADR,CXCR4,DBN1,EPB41L3,FABP7,FLNA,FLOT1,FLOT2,FSCN1,GRB2,HEPACAM,ILK,IQGAP1,LAMA1,MTDH,MYADM,MYH9,MYLK,NCAM1,NECTIN3,NGFR,PACSIN2,PAK1,PDXP,PNN,RAP1B,RAP2B,RDX,RHOA,SCRIB,SHROOM2,SLC2A1,SLC4A1,SORBS1,SPTAN1,SV2A,TBCD,TLN1,UBA1,VAPA,VCL,YWHAH,ZYX
vacuolar membrane	AHNAK,ANKFY1,ANXA1,ANXA2,ANXA6,AP1B1,AP1G1,AP2A1,AP2A2,AP2B1,AP2M1,AP2S1,ARF6,ARL8A,ATP6V0A1,ATP6V0D1,ATP6V1A,ATP6V1B2,ATP6V1D,ATP6V1E1,ATP6V1F,ATP6V1G2,ATP6V1H,CD14,CLN5,CLTA,CLTC,COL6A1,CP,EEF1A1,EEF1A2,EHD1,FLOT1,GAA,GABARAPL2,GFAP,GNA11,GNAI3,GNAQ,GNB1,GNB2,GNB4,HLA-A,HSP90AB1,HSPA8,LAMTOR1,LRP1,MAP1LC3A,MAP1LC3B,MVB12A,MYO1B,NAPA,NSF,PACSIN2,PLIN3,PRAF2,PSAP,RAB10,RAB11B,RAB14,RAB21,RAB2A,RAB35,RAB5A,RAB5B,RAB5C,RAB7A,RAP2B,RCC2,RHOB,RPS27A,SCARB2,SH3GL1,SH3GLB1,SNX2,SNX3,SORT1,STX12,STX7,SUN2,TFRC,TMEM192,TSG101,UBA1,VPS25,VPS28,VPS29,VPS33A,VPS35,VPS37B,VPS45,VPS4A,VPS4B,VTA1,WASH6P
SWI/SNF superfamily-type complex	ACTL6A,ANP32E,CHD4,CSNK2A1,DPF3,GATAD2B,HDAC2,MBD3,MTA1,MTA2,PBRM1,RBBP4,RSF1,RUVBL1,RUVBL2,SMARCA4,SMARCA5,SMARCB1,SMARCC2,SMARCD1,SMARCE1,YY1
actin-based cell projection	ABI2,ACTA2,ACTC1,AKR1B1,AP2A1,APBB1,APP,ARF6,ATP6V1A,ATP6V1B2,ATP6V1E1,BAIAP2,CA2,CBR1,CDC42,CLCA1,CLIC4,CTNNB1,CXADR,DBN1,DCXR,DYNC1H1,ENAH,EZR,FARP1,FMR1,FSCN1,GAP43,GPM6A,IGF2BP1,LCP1,MSN,MYO1B,MYO5A,PALM,PLS3,PTPRZ1,RDX,RUFY3,SLC9A3R1,SNAP25,TWF2,UBE2K
eukaryotic 48S preinitiation complex	EIF2S1,EIF3B,EIF3C,EIF3E,EIF3F,EIF3G,EIF3I,EIF3L,EIF3M

basal lamina	AGRN,FN1,HSPG2,LAMA1,LAMA2,LAMA4,LAMA5,LAMB1,LAMB2,LAMC1,NID1
translation preinitiation complex	EIF2S1,EIF3B,EIF3C,EIF3E,EIF3F,EIF3G,EIF3I,EIF3L,EIF3M
eukaryotic translation initiation factor 3 complex	DDX3X,EIF3B,EIF3C,EIF3E,EIF3F,EIF3G,EIF3I,EIF3L,EIF3M
mitochondrial intermembrane space	AIFM1,AK2,CAT,CIAPIN1,COX6B1,CYCS,DIABLO,DTYMK,HTRA2,NDUFA8,NDUFS1,NLN,OPA1,PARK7,PDIA3,SHMT2,SOD1,STOML2,THOP1,TIMM13,TIMM8A,TIMM8B
clathrin-coated pit	AP2A1,AP2A2,AP2B1,AP2M1,AP2S1,APP,ATAT1,CLTA,CLTB,CLTC,CTTN,DNM1L,DNM2,EPN1,HSPD1,LRP1,PICALM,RAB35,SORT1,TFRC
proton-transporting ATP synthase complex, coupling factor F(o)	ATP5F1,ATP5H,ATP5I,ATP5J,ATP5J2,ATP5L,ATP5O,MT-ATP6
mitochondrial respiratory chain complex III	BCS1L,UQCR10,UQCRB,UQCRC1,UQCRC2,UQCRFS1,UQCRH
endocytic vesicle	AP1B1,AP1G1,AP2A1,AP2A2,AP2B1,AP2M1,AP2S1,APOA1,APOE,ARF6,ATP6V0A1,ATP6V0D1,CALR,CAMK2B,CAMK2D,CLTC,CORO1A,DNM2,EHD1,FLOT2,HBA1,HBA2,HBB,HLA-A,HP,HPX,HSP90AA1,HSP90B1,HSPH1,HYOU1,KIAA0368,KIF5B,LRP1,NGFR,PICALM,RAB10,RAB11B,RAB14,RAB35,RAB5A,RAB5B,RAB5C,RAB7A,RALA,RPS27A,SH3GL2,SNX3,STX12,STX7
podosome	ACTR3,CTTN,DBNL,FSCN1,GSN,HNRNPK,LCP1,SH3GL1,TPM3,TPM4,WDR1
cell-cell adherens junction	ABI2,ACTN1,CADM1,CD200,CTNNA1,CTNNA2,CTNNB1,CTNND1,FLOT1,FLOT2,MYH9,NECTIN3,RDX,SCRIB,SHROOM2,SORBS1,SPTAN1,VCL,ZYX
organelle envelope lumen	AIFM1,AK2,APP,CAT,CIAPIN1,COX6B1,CYCS,DIABLO,DTYMK,HTRA2,NDUFA8,NDUFS1,NLN,OPA1,PARK7,PDIA3,SHMT2,SOD1,STOML2,THOP1,TIMM13,TIMM8A,TIMM8B
respiratory chain complex III	BCS1L,UQCR10,UQCRB,UQCRC1,UQCRC2,UQCRFS1,UQCRH
flotillin complex	CORO1C,CTNNA1,CTNNB1,CTNND1,FLOT1,FLOT2,SORBS1
proton-transporting two-sector ATPase complex, proton-transporting domain	ATP5F1,ATP5H,ATP5I,ATP5J,ATP5J2,ATP5L,ATP5O,ATP6V0A1,ATP6V0D1,MT-ATP6
eukaryotic 43S preinitiation complex	EIF3B,EIF3C,EIF3E,EIF3F,EIF3G,EIF3I,EIF3L,EIF3M
clathrin-coated vesicle membrane	AP1B1,AP1G1,AP2A1,AP2A2,AP2B1,AP2M1,AP2S1,AP3B2,CLTA,CLTB,CLTC,DBNL,HSPA8,NCALD,PICALM,RAB3A,SH3GL2,SLC17A7,SLC18A1,SYT1,VAMP2
clathrin-coated vesicle	AP1B1,AP1G1,AP2A1,AP2A2,AP2B1,AP2M1,AP2S1,AP3B2,CLINT1,CLTA,CLTB,CLTC,DBNL,DNM2,HSPA8,LRP1,NCALD,NGFR,PICALM,RAB14,RAB35,RAB3A,SH3GL2,SLC17A7,SLC18A1,SNX3,SORT1,SYT1,TMED10,TMED9,VAMP2,VPS33A,VWF

Title (or Source)	Grp 3_GeneSet
VCP-NPL4-UFD1 AAA ATPase complex	FAF1,FAF2,NPLOC4,UBXN1,UBXN7,UFD1L,VCP
preribosome	BOP1,EBNA1BP2,EIF6,FBL,MAK16,MRTO4,NOP56,NOP58,PES1,RPLP0,RPLP1,RPLP2,RPS7,RPSA,RRP1,RRS1,RSL1D1,SNU13,TBL3,WDR3
aminoacyl-tRNA synthetase multienzyme complex	AIMP1,EEF1E1,EPRS,KARS,RARS,RPL5
preribosome, large subunit precursor	BOP1,EBNA1BP2,EIF6,MAK16,MRTO4,PES1,RPLP0,RPLP1,RPLP2,RRP1,RRS1
small nucleolar ribonucleoprotein complex	DKC1,FBL,LSM6,NHP2,NOP56,NOP58,SNRNP40,SNRPF,SNRPG,SNU13
DNA replication factor A complex	CDC5L,PLRG1,PRPF19,PURA,PURB,RPA1,RPA2,RPA3
mitochondrial proton-transporting ATP synthase complex, catalytic core F(1)	ATP5A1,ATP5B,ATP5C1,ATP5D,ATP5EP2

proton-transporting ATP synthase complex, catalytic core F(1)	ATP5A1,ATP5B,ATP5C1,ATP5D,ATP5EP2

Title (or Source)	Grp 4_GeneSet
prefoldin complex	PFDN1,PFDN2,PFDN4,PFDN5,PFDN6,VBP1
U6 snRNP	DDX39B,LSM2,LSM3,LSM4,LSM5,LSM7
banded collagen fibril	COL11A1,COL1A1,COL1A2,COL3A1,COL5A1,COL5A2,LUM
fibrillar collagen trimer	COL11A1,COL1A1,COL1A2,COL3A1,COL5A1,COL5A2,LUM
dynactin complex	ACTR1A,ACTR1B,DCTN1,DCTN2,DCTN3,DCTN4
microtubule organizing center	ACTR1A,ACTR1B,APEX1,ATP6V0D1,BCL2L1,C14orf166,CALM2,CAPG,CCT4,CCT5,CCT8,CDC42,CEP170,CEP41,CETN2,CHD4,CKAP5,CLASP2,CRMP1,CROCC,CTNNB1,DCTN1,DCTN2,DCTN3,DCTN4,DDAH2,DHX9,DYNC1H1,DYNC1I2,DYNC1LI1,DYNC1LI2,DYNLL2,DYNLRB1,EZR,FLOT1,FRY,GNAI1,GNAI2,GNAI3,H2AFY,HSPA1B,KIF12,KIF2A,KIF5B,MAPK1,MAPRE1,MARCKS,MCM3,MDH1,MLLT11,NDRG2,NME1,NPM1,NUDCD2,NUDT21,NUMA1,OLA1,PAFAH1B1,PCNA,PQBP1,PRKACB,PRKAR2A,PRKAR2B,PSMA1,PSMB5,RAB11B,RAN,RANBP1,RBM39,RPRD1B,RPS7,RUVBL1,SKP1,SLC9A3R1,STX1B,TCP1,TLN1,UNC119,VPS4A
sarcoplasm	AGL,ANK1,ATP2A2,CA4,CACNA2D1,CALR,CAMK2D,FKBP1A,GSN,GSTM2,NOL3,PLEC,PYGM,SAR1A,SRI,SYNE2,THBS1
cytoplasmic side of plasma membrane	ACP1,ATP2A2,ATP2B1,EZR,GM2A,GNA11,GNA13,GNAI1,GNAI2,GNAI3,GNAO1,GNAQ,GNAS,GNAT1,GNAZ,GNB1,GNB2,GNB3,GNG2,GNG4,GPHN,IQGAP1,MSN,RHOA,S100A6,SPTA1,SPTB,SRC,SRMS
Lsm1-7-Pat1 complex	LSM2,LSM3,LSM5,LSM7
cytoplasmic dynein complex	DCTN1,DCTN4,DYNC1H1,DYNC1I2,DYNC1LI1,DYNC1LI2,DYNLRB1,TPR

Molecular function	
GO Molecular function enrichment	wnt_GeneSet
5S rRNA binding	EEF2,RPL3,RPL4,RPL5,RPL7,TST
immunoglobulin receptor binding	FLNA,IGHA1,IGHA2,IGHG1,IGHG2,IGHG3,IGHM,IGKV3-20,IGLL5,JCHAIN,LGALS3
extracellular matrix binding	ADGRG1,AGRN,BGN,FBLN2,GPC1,ITGB1,LGALS1,LGALS3,NID1,RPSA,SMOC1,SPP1,TGFBI,THBS1,THBS4,VTN
RAGE receptor binding	HMGB1,HMGB2,S100A13,S100A4,S100A8,S100A9,S100B
translation initiation factor binding	DDX3X,EIF3B,EIF3C,EIF3F,EIF4E,EIF4EBP1,EIF4G1,OTX2,RBX1,RPS19,RPS24,RPS3A
Ran GTPase binding	CSE1L,IPO5,IPO7,IPO9,KPNB1,NUTF2,RANBP1,RANBP3,TNPO1,XPO1,XPO5,XPO7
disulfide oxidoreductase activity	CCS,ERO1A,GLRX,GLRX3,GSR,GSTO1,PDIA2,PDIA3,SH3BGRL3,TXN,TXNL1
steroid binding	ALDH1A1,ANXA6,APOA1,APOA2,APOA4,APOC3,APOD,APOE,ATP1A2,ATP1A3,ATP5O,CALB1,ERLIN2,GC,HSD17B10,OSBP,PDIA2,PGRMC1,PGRMC2,PYGL,TSPO
TBP-class protein binding	CAND1,DR1,HNRNPF,NACA,PSMC1,PSMC2,PSMC3,PSMC4,PSMC5
protein disulfide isomerase activity	ERO1A,ERP29,ERP44,P4HB,PDIA2,PDIA3,PDIA4,PDIA6,TXND

	C5
intramolecular oxidoreductase activity, transposing S-S bonds	ERO1A,ERP29,ERP44,P4HB,PDIA2,PDIA3,PDIA4,PDIA6,TXNDC5
monosaccharide binding	ALDOA,BSG,CLN5,GPI,GYG1,HK1,HK2,LGALS1,LGALS3,LMAN1,LMAN2,MBL2,P3H1,P4HA1,P4HA2,PFKL,PFKM,PGLS,PLOD1,PYGL,UGP2

Title (or Source)	shh_GeneSet
beta-tubulin binding	ADNP,AKAP1,ARL8A,BCAS3,CAPZB,CCT5,EMD,GABARAPL2,HDAC6,LRPPRC,MAP1S,PDCD5,SNCA,SNCB,TBCA,TBCD,VAPB
mRNA 5'-UTR binding	ACO1,DDX3X,FMR1,IGF2BP1,IGF2BP2,IGF2BP3,RPS14,SYNCRIP
RNA helicase activity	DDX1,DDX17,DDX18,DDX21,DDX39A,DDX39B,DDX3X,DDX42,DDX46,DDX5,DDX50,DDX6,DHX15,DHX30,DHX9,EIF4A1,EIF4A2,EIF4A3,G3BP1,SKIV2L2,SNRNP200,UPF1
oxidoreductase activity, acting on NAD(P)H, quinone or similar compound as acceptor	CBR1,CRYZ,DCXR,NDUFA10,NDUFA13,NDUFA5,NDUFA6,NDUFA8,NDUFA9,NDUFB4,NDUFB9,NDUFS1,NDUFS2,NDUFS3,NDUFS4,NDUFS6,NDUFS8,NDUFV1,NDUFV2
NADH dehydrogenase activity	NDUFA10,NDUFA13,NDUFA5,NDUFA6,NDUFA8,NDUFA9,NDUFB4,NDUFB9,NDUFS1,NDUFS2,NDUFS3,NDUFS4,NDUFS6,NDUFS8,NDUFV1,NDUFV2
NADH dehydrogenase (quinone) activity	NDUFA10,NDUFA13,NDUFA5,NDUFA6,NDUFA8,NDUFA9,NDUFB4,NDUFB9,NDUFS1,NDUFS2,NDUFS3,NDUFS4,NDUFS6,NDUFS8,NDUFV1,NDUFV2
NADH dehydrogenase (ubiquinone) activity	NDUFA10,NDUFA13,NDUFA5,NDUFA6,NDUFA8,NDUFA9,NDUFB4,NDUFB9,NDUFS1,NDUFS2,NDUFS3,NDUFS4,NDUFS6,NDUFS8,NDUFV1,NDUFV2
Rac GTPase binding	ABI2,ARHGDIB,ARHGEF2,BRK1,CORO1C,CYFIP1,FARP1,FLNA,IQGAP1,NCKAP1,RAB7A,RCC2,SOD1,SRGAP3,WASF1
translation regulator activity	ABCF1,CELF1,CIRBP,FMR1,IGF2BP1,IGF2BP2,IGF2BP3,PABPC1,PAIP1,PCBP1,PURA,PURB,RPS14,RPS27L,RPS9
GTPase binding	ABI2,ANKFY1,ANXA2,AP1G1,ARHGDIA,ARHGDIB,ARHGEF2,BRK1,CDC42EP4,CORO1C,CSE1L,CYFIP1,EHD1,ENO1,EPRS,FARP1,FLNA,GDI1,GDI2,GIT1,GNB1,GNB2,HSP90AA1,IARS,IPO5,IPO7,IPO9,IQGAP1,KPNB1,LCP1,LSM2,MICAL1,MYO5A,NCKAP1,NGFR,NSF,NUTF2,PFN1,RAB3A,RAB7A,RANBP1,RANBP2,RCC2,RIMS1,SH3GL1,SOD1,SPTBN1,SRGAP3,STOML2,TBC1D10B,TBC1D9B,TNPO1,VCL,VPS4A,WASF1,XPO1,XPO5,YBX1

Title (or Source)	Grp 3_GeneSet
NF-kappaB binding	ANXA4,APEX1,CPNE1,DNAJA3,FAF1,GSK3B,HDAC2,HSPA1B,MTDH,NPM1,PSMA6,RELA,RPS3
proton-transporting ATP synthase activity, rotational mechanism	ATP5A1,ATP5B,ATP5C1,ATP5D,ATP5EP2,ATP5F1,ATP5O

Title (or Source)	Grp 4_GeneSet
molecular function regulator	A2M,ADRM1,AGAP3,AGRN,AHSA1,AHSG,ALDH1A1,AMPH,ANP32E,ANXA1,ANXA2,ANXA4,ANXA5,APOA1,APOA2,APOA4,APOC3,APOE,ARF1,ARF4,ARHGAP1,ARHGDIA,ARHGEF2,ARPP19,ATP1B1,ATP1B2,ATP2B4,ATP6V1H,BAG3,BAG5,BAZ1B,BCL2L1,BCL2L13,BGN,C3,C4B,CALM2,CAMK2D,CCAR2,CDC37,CDC42EP4,CHN2,COL6A3,CSNK2A1,CSNK2B,CSTB,DBNL,DCN,DNAJB1,DNAJB6,DOCK7,DPEP1,DUT,ENSA,FAF2,FBLN1,FKBP1A,FN1,FN3K,FRY,GCN1,GDI1,GDI2,GM2A,GMFB,GNAQ,

	GNB2,GRB2,GSTP1,H2AFY,HACD3,HMGB1,HNRNPC,HSP90AA1,HSP90AB1,HSPB1,IPO5,IQGAP1,ITIH1,ITIH2,ITIH4,KNG1,LAMTOR2,NCAM1,NEFL,NOL3,NOTCH1,NPM1,NRG1,PARK7,PCNA,PCSK1N,PDC,PDCD5,PEBP1,PFN1,PFN2,PHPT1,PLAA,PPME1,PPP1R14B,PPP1R1A,PPP1R7,PPP2R1A,PRDX3,PRDX5,PRKAR2A,PRKAR2B,PRKRA,PRPSAP2,PRSS8,PSAP,PSMD1,PSMD14,PSMD2,PSMD3,PSME1,PSME2,PSMF1,PTPA,RAB3A,RAB4A,RAB6A,RACK1,RANBP1,RANGAP1,RAP1GDS1,RCAN1,RCC1,RCVRN,RGN,RING1,RNH1,RPLP1,SAE1,SERPINA1,SERPINA3,SERPINC1,SERPIND1,SERPINH1,SET,SLC9A3R1,SNCA,SPTA1,SPTAN1,SPTB,SPTBN1,SPTBN2,SRGAP3,SRI,STX7,TOR1AIP1,TRIO,UBA2,UBE2L3,USP14,VCP,YWHAE,YWHAG,YWHAH
G-protein beta/gamma-subunit complex binding	CETN2,GNA11,GNA13,GNAI1,GNAI2,GNAI3,GNAO1,GNAQ,GNAS,GNAT1,GNAZ
G-protein coupled serotonin receptor binding	GNA11,GNAI1,GNAI3,GNAO1,GNAQ,GNAZ
amino acid binding	AARS,AGXT,ASS1,CAD,CPNE1,CPNE6,DDAH1,DDAH2,GAP43,GLUD1,GLUL,GOT2,GSS,HMGB1,HSPA8,MARCKS,MAT2A,PIN1,RARS,SHMT2,SLC1A3,SRR,SYT4,THBS1,YWHAB,YWHAE
poly(U) RNA binding	FMR1,HNRNPC,HNRNPH1,KHDRBS1,KHDRBS2,MSI1,MSI2,PABPC1,RPS7
ATPase activator activity	AHSA1,ATP1B1,ATP1B2,DNAJB1,DNAJB6,RAB3A,RAB4A,RAB6A,TOR1AIP1
pyrimidine nucleotide binding	CAD,DCTPP1,DUT,HSP90AA1,HSP90AB1,NT5C,UGP2
protein binding involved in protein folding	CALR,CCT2,CCT3,CCT6A,DNAJB6,HSPA1B,PFDN1,PFDN2
modified amino acid binding	CPNE1,CPNE6,DPEP1,FASN,GAP43,GPX1,GPX4,GSR,GSS,GSTM2,GSTM3,GSTP1,HMGB1,HSPA8,LANCL1,MARCKS,SYT4,THBS1
dopamine receptor binding	ATP1A3,CLIC6,DNM1,GNA13,GNAS,NSF,PALM,PTPN11,SLC9A3R1
magnesium ion binding	ARF1,BPNT1,COMT,DCTPP1,DUT,ENO1,ENO2,ENOPH1,FARSB,FEN1,GLUL,GNAI1,GSS,HPRT1,IDH1,IDH2,IDH3A,IMPA1,MSH2,NME1,NUDT16,OXSR1,PDXK,PDXP,PGM1,PGM2,PKM,PPA1,PRKACB,PRPS1,PRPSAP2,SIK3,SNCA,SRR

biological process	
Title (or Source)	wnt_GeneSet
vesicle coating	AP1B1,AP2B1,AP2S1,COL7A1,CTSZ,CUL3,GOLGA2,LMAN1,NAPA,NSF,PICALM,RAB1B,SCFD1,SEC13,SEC22B,SEC23A,SEC24C,SEC31A,SERPINA1,TFG,TMED10,TMED9,TRAPPC5,USO1
COPII-coated vesicle budding	COL7A1,CTSZ,CUL3,GOLGA2,LMAN1,NAPA,NSF,RAB1B,SAR1A,SCFD1,SEC13,SEC22B,SEC23A,SEC24C,SEC31A,SERPINA1,TFG,TMED10,TRAPPC5,USO1,VAPA
endoplasmic reticulum unfolded protein response	AARS,ACADVL,ADD1,ASNA1,BAX,CALR,DCTN1,DNAJB11,EIF2S1,ERO1A,HDGF,HSP90B1,HSPA5,HYOU1,LMNA,MYDGF,PDIA6,RACK1,SEC31A,SEC61A1,SEC61B,SEC62,SRPRA,SRPRB,SSR1,TLN1,TPP1,VCP
vesicle targeting, rough ER to cis-Golgi	COL7A1,CTSZ,CUL3,GOLGA2,LMAN1,NAPA,NSF,RAB1B,SCFD1,SEC13,SEC22B,SEC23A,SEC24C,SEC31A,SERPINA1,TFG,TMED10,TRAPPC5,USO1
protein export from nucleus	ADAR,AHCYL1,CALR,CAMK4,CSE1L,EIF5A,EMD,HSPA9,NUTF2,PARK7,RAN,RANBP3,SFN,TPR,TXN,XPO1,XPO5,XPO7

ossification	ADAR,AHSG,ALPL,ALYREF,ATP5B,CAT,CBFB,CD276,CDK6,CLIC1,CLTC,COL1A1,COL6A1,CTNNB1,DDR2,DDX21,DDX5,DHX9,ERH,FASN,FBL,FGF2,GNAS,GPM6B,GPNMB,H3F3A,HNRNPC,HNRNPU,HSD17B4,HSPE1,HSPG2,LMNA,MAPK1,MAPK3,MGP,MMP2,NOTCH1,P3H1,PCP4,PDLIM7,PHB,PSMC2,PTN,RACK1,RBMX,RHOA,RPL38,RPS11,RPS15,RRBP1,SBDS,SMOC1,SND1,SNRNP200,SPP1,SYNCRIP,TMSB4X,TNC,TPM4,VCAN
response to lipid	ADD1,ADH5,AGXT,ALPL,ANXA1,APOA1,APOA2,APOC3,APOH,ATP1A2,ATP1A3,ATP2B1,B2M,BAX,BID,C3,CA2,CAD,CALM2,CALR,CASP3,CAT,CBX3,CD14,CDC73,CNP,COL1A1,COMT,CRYAB,CTNNA1,CTNNB1,DDRGK1,DDX17,DDX5,DEFA3,DNAJA1,DNMT3A,DTYMK,EEF2,EIF4E,EIF4EBP1,EPHA5,FABP3,FGA,FKBP4,FN1,GC,GLRX,GNAS,GNB1,GNG2,GOT1,GRN,GSTM3,GSTP1,HDAC2,HMGB1,HMGB2,HNRNPA0,HNRNPD,HNRNPK,HNRNPM,HNRNPU,HSP90AA1,IDH1,ITGB1,LDHA,LOX,LOXL1,MAOB,MAPK1,MAPK3,MDK,MECP2,MMP2,MPO,MSN,MTDH,NASP,NDUFA13,NME1,NOTCH1,NR5A1,PARK7,PARP1,PCNA,PDIA3,PELP1,PGRMC2,PHB,PHB2,POSTN,PRDX2,PRDX3,PRPF8,PTGES3,PTK7,PTN,RAB7A,RAN,RANBP1,RBBP7,RBM14,RELA,RHOA,RPL13A,RUVBL2,S100A8,S100B,SAFB,SCAMP3,SERPINF1,SPP1,THBS1,THRAP3,TNC,TSPO,UBE2I,UBE2L3,YWHAH
vesicle targeting, to, from or within Golgi	COL7A1,CTSZ,CUL3,GOLGA2,LMAN1,NAPA,NSF,RAB1B,SCFD1,SEC13,SEC22B,SEC23A,SEC24C,SEC31A,SERPINA1,TFG,TMED10,TMED9,TRAPPC5,USO1
cellular response to unfolded protein	AARS,ACADVL,ADD1,ASNA1,BAX,CALR,DCTN1,DNAJB11,EIF2S1,ERO1A,HDGF,HSP90B1,HSPA5,HYOU1,LMNA,MYDGF,PDIA6,RACK1,SEC31A,SEC61A1,SEC61B,SEC62,SRPRA,SRPRB,SSR1,TLN1,TPP1,VCP
IRE1-mediated unfolded protein response	ACADVL,ADD1,ASNA1,BAX,DCTN1,DNAJB11,HDGF,HSPA5,HYOU1,LMNA,MYDGF,PDIA6,SEC31A,SEC61A1,SEC61B,SEC62,SRPRA,SRPRB,SSR1,TLN1,TPP1
positive regulation of cell-substrate adhesion	APOA1,ARPC2,C1QBP,CALR,CDC42,CDH13,CDK6,COL16A1,COL26A1,DBN1,EMILIN1,FBLN1,FBLN2,FGA,FGB,FGG,FLNA,FN1,IQGAP1,ITGB1,NID1,PTN,SMOC1,SPP1,THBS1,VTN
COPII vesicle coating	COL7A1,CTSZ,CUL3,GOLGA2,LMAN1,NAPA,NSF,RAB1B,SCFD1,SEC13,SEC22B,SEC23A,SEC24C,SEC31A,SERPINA1,TFG,TMED10,TRAPPC5,USO1
retrograde vesicle-mediated transport, Golgi to ER	ARCN1,ARF4,ARF5,COPA,COPB1,COPB2,COPG1,COPZ1,KLC1,LMAN2,NAPA,NSF,RAB1B,RAB6A,SCFD1,SEC22B,SURF4,TMED10,TMED3,TMED9
maintenance of location in cell	ALB,APOE,DBN1,EPB41L3,EZR,FLNA,FLNB,FTH1,G3BP2,GAA,GSN,HK1,HK2,HSPA5,NR5A1,PDIA2,PDIA3,PFN1,POLR2M,PSMD10,SRI,TLN1,TSPO,YWHAB
cell death in response to oxidative stress	ARL6IP5,DIABLO,GLRX,GPX1,HSPB1,HSPH1,MAPT,NONO,P4HB,PARK7,PARP1,PDIA2,PSAP,PYCR1,RACK1,SFPQ,SOD1,TXN,UBQLN1
vesicle targeting	COL7A1,CTSZ,CUL3,GOLGA2,LMAN1,NAPA,NSF,RAB1B,SCFD1,SEC13,SEC22B,SEC23A,SEC24C,SEC31A,SERPINA1,TFG,TMED10,TMED9,TRAPPC5,USO1
cellular response to topologically incorrect protein	AARS,ACADVL,ADD1,ASNA1,BAX,CALR,DCTN1,DNAJB11,EIF2S1,ERO1A,HDGF,HSP90B1,HSPA5,HYOU1,LMNA,MYDGF,PDIA6,RACK1,SEC31A,SEC61A1,SEC61B,SEC62,SRPRA,SRPRB,SSR1,TLN1,TPP1,VCP
response to alcohol	ABAT,ACTC1,ALDH1A1,ALPL,ANXA1,ATP2B1,BAX,BID,C3,CAD,CALM2,CALR,CASP3,CAT,CBX3,CD14,CDK1,COL1A1,CRYAB,CTNNA1,CTNNB1,CTSB,DNMT3A,EEF1B2,EEF2,EIF4E,EIF4EBP1,FGA,GC,GLRX,GOT2,GRN,GSN,GSTP1,HDAC2,HNRNPD,HNRNPK,HNRNPU,ITGB1,MAOB,MECP2,MMP2,MSN,NASP,N

	ME1,OXCT1,PDIA3,POSTN,PSMD14,PTN,RUVBL2,S100A8,SERPINF1,SOD1,SPP1,TNC,TSPO
maintenance of location	ALB,ANK2,APOA1,APOE,ASPH,ATP1A2,BAX,C3,CALM2,CALR,CORO1A,DBN1,EPB41L3,ERO1A,EZR,F2,FBN1,FGF2,FKBP1A,FLNA,FLNB,FTH1,G3BP2,GAA,GSN,GSTM2,GSTO1,HK1,HK2,HSP90B1,HSPA5,ITPR1,LGALS1,LGALS3,NR5A1,PDIA2,PDIA3,PFN1,PLCG1,POLR2M,PSMD10,S100A8,S100A9,SRI,THY1,TLN1,TSPO,YWHAB
regeneration	ANXA1,APOA1,APOA2,APOA4,APOD,APOE,APOH,ATIC,CAD,CALU,CDK1,CTNNA1,EIF4A1,FGA,GAP43,GFAP,GPX1,GSN,GSTP1,LAMB2,MMP2,MTPN,NACA,NOTCH1,PKM,PLG,POSTN,PRMT5,PRPS1,RTN4,SPP1,SRSF5,TNC,TSPO,VTN
cap-independent translational initiation	DENR,EIF3B,EIF3F,EIF4EBP1,PCBP2,PTBP1,RBM4,SSB
regulation of vacuolar transport	ARF1,EHD2,EZR,MAPK1,MAPK3,MSN,RAB11B,RAB21,RDX,SNX3,VPS35
glycogen catabolic process	CALM2,GAA,GYG1,HMGB1,PFKM,PGM1,PGM2,PPP1CA,PPP1CB,PYGB,PYGL
Title (or Source)	shh_GeneSet
positive regulation of substrate adhesion-dependent cell spreading	APOA1,ARHGEF7,ARPC2,C1QBP,CALR,CDC42,DBN1,DNM2,FGA,FGB,FGG,FLNA,MYADM,PREX1
aspartate family amino acid metabolic process	AASDHPPT,AHCY,AHCYL1,ALDH7A1,ASNS,ASRGL1,ASS1,DLD,DLST,ENOPH1,GCDH,GOT1,GOT2,MTAP,MTHFD1,NIT2,OGDH,PHGDH,SMS
glutamine metabolic process	ALDH5A1,ASNS,CAD,CTPS1,GGH,GLS,GLUD1,GLUL,GMPS,MECP2,NIT2,PFAS,PHGDH,PPAT
DNA unwinding involved in DNA replication	HMGA1,MCM2,MCM4,MCM6,MCM7,PURA,TOP2A,TOP2B
actin filament bundle assembly	ACTN1,ACTN4,ADD1,ADD2,AIF1,APOA1,BAIAP2,CALD1,CDC42,CLASP1,CUL3,DBN1,DBNL,DPYSL3,ELN,EZR,FLNA,FSCN1,HSP90B1,KANK2,LCP1,MYO1B,PAK1,PDXP,PFN1,PFN2,PPM1E,PPM1F,RDX,RHOA,SERPINF2,SFRP1,SHROOM2,SORBS1,SRC,TPM1,ZYX
neuron projection extension	ADNP,APOE,CPNE1,CTTN,CYFIP1,DBN1,DCLK1,DCX,DNM2,DPYSL2,EIF4G2,FN1,GSK3B,HNRNPK,ILK,IQGAP1,L1CAM,LAMB2,MACF1,MAP1B,MAPT,NEDD4L,NRCAM,NRG1,OGN,PAFAH1B1,POSTN,RAB21,RIMS1,RPL4,RTN4,RUFY3,SYT1,TNR,TPBGL,TWF2,USP9X,VCL
regulation of viral life cycle	ADAR,DDB1,DDX3X,DDX5,EIF2AK2,FMR1,GSN,HACD3,HMGA2,ILF3,ISG15,LGALS1,MVB12A,NELFA,NELFB,NOTCH1,P4HB,PABPC1,PFN1,POLR2H,POLR2I,POLR2L,PPIA,PPIB,PPID,PPIH,RAD50,RSF1,SMARCA4,SMARCB1,SNW1,SNX3,STAU1,STOM,SUPT5H,TARDBP,TOP2A,TRIM28,TSG101,VAPA,VAPB,VPS25,VPS37B,VPS4A,VPS4B
substrate adhesion-dependent cell spreading	ACTN4,APOA1,ARHGEF7,ARPC2,C1QBP,CALR,CDC42,CORO1C,DBN1,DNM2,FBLN1,FERMT2,FGA,FGB,FGG,FLNA,FN1,ILK,LAMA5,LAMB1,LAMC1,MYADM,PARVA,POSTN,PREX1,PXN,RCC2,SFRP1,SRC
hexose biosynthetic process	ACADM,AKR1B1,ALDOA,ALDOC,BPGM,ENO1,ENO2,ENO3,GAPDH,GNPDA1,GOT1,GOT2,GPD2,GPI,MDH1,MDH2,NLN,PGAM1,PGAM2,PGK1,PGM1,PPP4R3A,RANBP2,SLC25A1,SLC25A11,SLC25A12,SLC25A13,SORD,TPI1
regulation of multi-organism process	ACIN1,ADAR,ANXA5,AP1B1,AP1G1,AP2A1,AP2A2,AP2B1,AP2M1,AP2S1,APOE,ARF1,ARHGDIB,ATP1B1,ATP6V1H,C1QBP,CFL1,CRNKL1,DDB1,DDX3X,DDX5,DERL1,DPF3,DYNLT1,EIF2AK2,EIF2S1,EXOC7,FBLN1,FMR1,GSN,HACD3,HIST1H3A,HLA-A,HMGA2,ILF3,ISG15,LGALS1,LSM4,MAP1A,MBL2,MDH1,M

	PO,MVB12A,MYLK,NELFA,NELFB,NOTCH1,NUP93,P4HB,PABPC1,PAK2,PCBP2,PFN1,POLR2H,POLR2I,POLR2L,PPIA,PPIB,PPID,PPIH,PPP2R1A,PRDX2,PRDX4,RAB7A,RAD50,RSF1,SLC1A3,SMARCA4,SMARCB1,SNRPB,SNRPD1,SNW1,SNX3,STAT1,STAU1,STOM,SUPT5H,TARDBP,TKFC,TOP2A,TRIM28,TSG101,VAPA,VAPB,VPS25,VPS37B,VPS4A,VPS4B
establishment or maintenance of cell polarity	ACTR2,ACTR3,ANK1,ARF4,ARF6,ARHGEF2,ARPC5,BCAS3,CDC42,CFL1,CKAP5,CLASP1,CLIC4,CTNNA1,DYNLT1,EZR,FLOT2,FSCN1,GSK3B,GSN,ILK,LAMA1,LMNA,MACF1,MAP1B,MAP2,MAP4,MSN,MYH9,NCKAP1,NUMA1,PAFAH1B1,PARVA,PAX6,RAB10,RACK1,RAP1B,RUFY3,SCRIB,SLC9A3R1,ZW10
nucleobase metabolic process	ALDH6A1,APRT,CAD,CMPK1,DPYS,GART,GMPS,HPRT1,KDM1A,MAPK1,PAICS,PPAT,PRPS1,PRTFDC1,RRM1,TYMP,UMPS
positive regulation of cytoskeleton organization	ABI2,ACTR2,ACTR3,APOA1,ARF1,ARF6,ARPC2,ARPC3,ARPC5,BAIAP2,BCAS3,BRK1,CDC42EP4,CFL1,CLASP1,CORO1A,CTTN,CYFIP1,DSTN,GMFB,GRB2,GSN,MAP1B,MAPT,NCKAP1,NES,NPM1,PAK1,PDXP,PFDN2,PFN1,PFN2,PPM1E,PPM1F,RANBP1,RCC2,RHOA,RPS3,SERPINF2,SFRP1,TPM1,VPS4B,WASF1,WASH6P,WDR1
Fc receptor mediated stimulatory signaling pathway	ACTB,ACTG1,ACTR2,ACTR3,ARPC2,ARPC3,ARPC5,BAIAP2,BRK1,CDC42,CRK,CSK,CYFIP1,CYFIP2,GRB2,HSP90AA1,HSP90AB1,IGHG1,IGHG2,IGHG3,IGKV1D-33,IGKV3-20,IGLC1,MAPK1,NCKAP1,PAK1,SRC
muscle system process	ABAT,ACTA2,ACTC1,ADK,AGRN,AIF1,AKAP1,ALDOA,ANK2,ANXA6,ATP1A2,ATP1A3,ATP1B1,ATP2A2,ATP2B4,CACNA2D1,CALD1,CALM2,CAMK2B,CAMK2D,COL14A1,CRYAB,CTTN,CXCR4,DBN1,DDX39B,EEF2,EMD,FDPS,FKBP1A,GAA,GLRX3,GNAO1,GRK2,GSK3B,GSN,GSTM2,GSTO1,GTF2I,HDAC2,HSBP1,HSP90AA1,KNG1,MAP2K6,MB,MGEA5,MYL12A,MYL6,MYLK,MYOF,NDUFS6,NEDD4L,NOL3,PABPN1,PARP1,PGAM2,PIN1,PPP3CA,PSMB9,PXN,RAP1GDS1,RHOA,RPS6KB1,SLC25A4,SOD1,SORBS1,SRI,SRSF1,SYNM,TBCE,TLN1,TPM1,TPM3,TPM4,TRPV1,VCL,VIM
actin filament bundle organization	ACTN1,ACTN4,ADD1,ADD2,AIF1,APOA1,BAIAP2,CALD1,CDC42,CLASP1,CUL3,DBN1,DBNL,DPYSL3,ELN,EZR,FLNA,FSCN1,HSP90B1,KANK2,LCP1,MYO1B,PAK1,PDXP,PFN1,PFN2,PPM1E,PPM1F,RDX,RHOA,SERPINF2,SFRP1,SHROOM2,SORBS1,SRC,TPM1,ZYX
regulation of symbiosis, encompassing mutualism through parasitism	ADAR,APOE,CFL1,DDB1,DDX3X,DDX5,DERL1,DYNLT1,EIF2AK2,EXOC7,FBLN1,FMR1,GSN,HACD3,HMGA2,ILF3,ISG15,LGALS1,MBL2,MPO,MVB12A,NELFA,NELFB,NOTCH1,P4HB,PABPC1,PFN1,POLR2H,POLR2I,POLR2L,PPIA,PPIB,PPID,PPIH,RAB7A,RAD50,RSF1,SMARCA4,SMARCB1,SNW1,SNX3,STAT1,STAU1,STOM,SUPT5H,TARDBP,TOP2A,TRIM28,TSG101,VAPA,VAPB,VPS25,VPS37B,VPS4A,VPS4B
morphogenesis of an epithelium	ALDH1A1,ALDH1A3,AP2A1,AP2A2,AP2B1,AP2M1,AP2S1,BAX,CA2,CD44,CDC42,CFL1,CLASP1,CLIC4,CLTC,COL4A1,CSNK2B,CTNNB1,CTNND1,CTSD,CXCR4,ENAH,ENG,EZR,FLNA,GRB2,GSN,HMGA2,ILK,KRAS,LAMA1,LAMA5,LCP1,MSN,MTHFD1,NCKAP1,NGFR,NOTCH1,OPA1,PAFAH1B1,PAK1,PFN1,PHB2,PLXNB2,PPP3R1,PRKACB,PSMA1,PSMA2,PSMA3,PSMA4,PSMA5,PSMA6,PSMA7,PSMB1,PSMB2,PSMB3,PSMB4,PSMB5,PSMB6,PSMB7,PSMB9,PSMC1,PSMC2,PSMC3,PSMC4,PSMC5,PSMC6,PSMD1,PSMD11,PSMD12,PSMD13,PSMD14,PSMD2,PSMD3,PSMD4,PSMD5,PSMD6,PSMD7,PSME1,PSME2,PSME3,PSMF1,PXN,RAB10,RALA,RBM15,RHOA,RHOB,RPS27A,RPS7,SCRIB,SFRP1,SLC9A3R1,SMAD4,SMARCA4,SRC,STAT1,TGM2,TMED2,TNC,TRIM28,VCL,ZIC5

endosomal transport	ANKFY1,AP1G1,AP2A1,ARF1,CDC42,CLTC,CORO1A,DCLK1,DCTN1,DPY30,EHD1,EZR,FLNA,LRBA,MAPK1,MSN,PICALM,RAB10,RAB11B,RAB14,RAB21,RAB35,RAB5A,RAB5B,RAB5C,RAB6A,RAB7A,RDX,RHOB,RPS27A,SNAP25,SNX12,SNX2,SNX3,SORT1,SRC,SURF4,TBC1D10B,TMED9,TOM1,TSG101,VPS25,VPS26B,VPS28,VPS29,VPS33A,VPS35,VPS37B,VPS4A,VPS4B,VPS51,VTA1,WASH6P
protein targeting to mitochondrion	ABLIM3,ACTL6A,AIP,BID,FIS1,HSP90AA1,HSPA4,HTRA2,HUWE1,MFF,MTX1,MTX2,NDUFA13,NOL3,NPEPPS,NRG1,PDCD5,PMPCA,PSMB7,RPL28,RUVBL1,SAE1,SH3GLB1,SLC25A6,TIMM13,TIMM44,TIMM50,TIMM8A,TIMM8B,TOMM22,TOMM70,TSPO,U2AF1,U2AF2,UBE2L3,YWHAZ
positive regulation of multi-organism process	ADAR,APOE,C1QBP,CFL1,DDB1,DDX3X,FMR1,HACD3,LGALS1,MVB12A,NELFA,NELFB,NOTCH1,P4HB,PABPC1,PFN1,POLR2H,POLR2I,POLR2L,PPIA,PPIB,PPID,PPIH,RAB7A,RSF1,SMARCA4,SMARCB1,SNW1,STAU1,STOM,SUPT5H,TOP2A,TSG101,VAPA,VAPB,VPS37B,VPS4A,VPS4B
IMP metabolic process	ADSL,ATIC,GART,HPRT1,NT5C2,PAICS,PFAS,PPAT,PRTFDC1
gluconeogenesis	ACADM,ALDOA,ALDOC,BPGM,ENO1,ENO2,ENO3,GAPDH,GOT1,GOT2,GPD2,GPI,MDH1,MDH2,NLN,PGAM1,PGAM2,PGK1,PGM1,PPP4R3A,RANBP2,SLC25A1,SLC25A11,SLC25A12,SLC25A13,TPI1
Fc-gamma receptor signaling pathway	ACTB,ACTG1,ACTR2,ACTR3,ARPC2,ARPC3,ARPC5,BAIAP2,BRK1,CDC42,CRK,CYFIP1,CYFIP2,GRB2,HSP90AA1,HSP90AB1,IGHG1,IGHG2,IGHG3,IGKV1D-33,IGKV3-20,IGLC1,MAPK1,NCKAP1,PAK1,SRC
monocarboxylic acid catabolic process	ABAT,ACAA2,ACADM,ACADVL,ACOT2,ACOT7,AGXT,AKR1A1,ALDH3A2,ALDH4A1,ALDH5A1,CRABP1,CRYL1,DCXR,DECR1,ECH1,ECHS1,ECI1,EHHADH,ETFA,ETFB,GCDH,GOT2,HADH,HADHA,HADHB,HSD17B4,PCCA,PCCB,SORD
positive regulation of cell development	ACTR3,ADNP,APBB1,APOA1,APOE,ARF1,ARHGDIA,ARHGEF7,ARPC2,BAIAP2,BAX,C1QBP,CALR,CAMK2B,CAPRIN1,CDC42,CNTN1,COL1A1,CPNE1,CTNNB1,CXCR4,DBN1,DDX39B,DNM2,DPYSL3,DYNLT1,EEF1A1,EIF4G1,EIF4G2,ELAVL4,FDPS,FGA,FGB,FGG,FLNA,FMR1,FN1,GFAP,GSK3B,HDAC2,HNRNPK,ILK,IQGAP1,KDM1A,L1CAM,MACF1,MAP1B,MAPT,MARCKS,MYADM,NEDD4L,NEFL,NEGR1,NGFR,NME1,NOTCH1,NRCAM,NRG1,OPA1,PAFAH1B1,PALM,PAX6,PCP4,PIN1,PLXNB2,PPP2R5B,PPP2R5D,PREX1,PRMT5,PRPF19,PTBP1,PTPRZ1,RAB21,RANBP1,RELA,RHOA,RIMS1,RPL4,RTN4,RUFY3,SDCBP,SLC25A4,SMAD4,SNW1,SNX3,SRRT,SYT1,TSPO,TWF2,UBE2V2,VIM,XRCC5,XRCC6
response to insulin	AHSG,APRT,ATP6V0A1,ATP6V0D1,ATP6V1A,ATP6V1B2,ATP6V1D,ATP6V1E1,ATP6V1F,ATP6V1G2,ATP6V1H,BAIAP2,CAD,CAT,EIF6,EPM2AIP1,FABP3,GAB1,GGH,GOT1,GRB2,GSK3B,GSTP1,HADH,HADHA,HNRNPK,HSD11B2,MARCKS,MYO5A,NAMPT,NGFR,OSBPL8,PAK1,PARP1,PKM,PPAT,PRKDC,PTPN11,RAB10,RBM4,RELA,RPS6KB1,SORBS1,SORT1,SRC,SRSF3,SRSF5,STAT1,UCHL3,VAMP2,YBX1,YWHAG
vacuolar transport	ANKFY1,AP1G1,AP2A1,ARF1,CDC42,CLTC,CORO1A,DCLK1,DCTN1,DPY30,EHD1,EZR,FLNA,HSPA8,LRBA,MAPK1,MSN,PICALM,RAB10,RAB11B,RAB14,RAB21,RAB35,RAB5A,RAB5B,RAB5C,RAB6A,RAB7A,RDX,RHOB,RPS27A,SCARB2,SNAP25,SNX12,SNX2,SNX3,SORT1,SRC,SURF4,TBC1D10B,TMED9,TOM1,TSG101,VPS25,VPS26B,VPS28,VPS29,VPS33A,VPS35,VPS37B,VPS4A,VPS4B,VPS51,VTA1,WASH6P
positive regulation of cysteine-type endopeptidase activity involved in apoptotic process	AIFM1,ARL6IP5,BAX,BCL2L13,BID,CYCS,DDX3X,DIABLO,FAM162A,FIS1,GSN,HMGB1,HSPD1,HSPE1,HTRA2,MEN1,NDUFA

	13,NGFR,PDCD5,PDCD6,PPM1F,PPP2CA,RACK1,RHOA,RPS27L,RPS3,S100A8,S100A9,SNCA,STAT1,VCP
fibril organization	APP,COL3A1,FKBP1A,GPX1,GSN,HSP90AB1,HSPA8,ILK,MFAP4,PARK7,SNCA
negative regulation of neuron apoptotic process	AARS,ADNP,APOE,BAX,CACNA1A,CNTFR,CORO1A,GPI,HSP90AB1,HSPD1,HSPH1,HYOU1,ILK,KRAS,LRP1,MECP2,MSH2,NEFL,NES,NGFR,NONO,PARK7,PCP4,PIN1,PPT1,PRDX2,PRDX3,RHOA,SET,SNCA,SNCB,SOD1,SOD2,STXBP1,UBE2V2,ZPR1
cellular amino acid catabolic process	ABAT,ACAT1,AGXT,AHCY,ALDH4A1,ALDH5A1,ALDH6A1,ALDH7A1,ASRGL1,ATP2B4,AUH,DDAH1,DDAH2,DLD,DLST,DTD1,GCDH,GLS,GLUD1,GLUL,GOT1,GOT2,HIBADH,HIBCH,HSD17B10,OGDH,PCBD1,PPAT,QDPR
dendritic spine development	APOE,ARF1,ARF4,ARF6,BAIAP2,CAMK2B,CAPRIN1,CFL1,CTNND2,DBN1,EIF4G2,FMR1,GIT1,HDAC2,HDAC6,HNRNPK,MARCKS,NGFR,NRG1,PAFAH1B1,PAK1,PAK2,PALM,UBA6
tissue morphogenesis	ACTA2,ACTC1,ALDH1A1,ALDH1A3,AP2A1,AP2A2,AP2B1,AP2M1,AP2S1,BAX,CA2,CD44,CDC42,CFL1,CHD7,CLASP1,CLIC4,CLTC,COL3A1,COL4A1,CSNK2B,CTNNB1,CTNND1,CTSD,CXCR4,ENAH,ENG,EZR,FAT3,FKBP1A,FLNA,GPI,GRB2,GSN,HMGA2,ILK,KRAS,LAMA1,LAMA5,LCP1,MACF1,MSN,MTHFD1,MYLK,NCKAP1,NECTIN3,NGFR,NOTCH1,NRG1,OPA1,PAFAH1B1,PAK1,PFN1,PHB2,PLXNB2,PPP3R1,PRKACB,PRKAR1A,PSMA1,PSMA2,PSMA3,PSMA4,PSMA5,PSMA6,PSMA7,PSMB1,PSMB2,PSMB3,PSMB4,PSMB5,PSMB6,PSMB7,PSMB9,PSMC1,PSMC2,PSMC3,PSMC4,PSMC5,PSMC6,PSMD1,PSMD11,PSMD12,PSMD13,PSMD14,PSMD2,PSMD3,PSMD4,PSMD5,PSMD6,PSMD7,PSME1,PSME2,PSME3,PSMF1,PXN,RAB10,RALA,RBM15,RHOA,RHOB,RPS27A,RPS7,SCRIB,SFRP1,SLC9A3R1,SMAD4,SMARCA4,SRC,STAT1,TGM2,TMED2,TNC,TPM1,TRIM28,VCL,ZIC5
lamellipodium organization	ABLIM3,ACTR3,ARHGEF7,ARPC2,ARPC5,BRK1,CAPZB,CORO1C,CTTN,CYFIP1,DNM2,FSCN1,HSP90AA1,NCKAP1,NUP85,PXN,SNX2,SRC,TWF2,VCL,WASF1,WASF3
microtubule cytoskeleton organization	AGRN,AP1G1,ARHGEF2,ARPC5,ATAT1,BCAS3,CAPZB,CDC42,CHD4,CKAP5,CLASP1,CLTC,CNTN2,CRMP1,CRYAB,CTNNB1,CUL9,DCTN2,DYNC1H1,DYNC1LI1,DYNC1LI2,DYNLT1,EZR,FKBP4,FLNA,GAPDH,HDAC6,HDGFRP3,HSPH1,HYDIN,KATNAL2,KIF2A,KPNB1,LMNA,MAP1A,MAP1B,MAP1S,MAP2,MAP4,MAP6,MAP7D1,MAPRE1,MAPT,MYH9,NEFL,NEFM,NPM1,NTMT1,NUMA1,PAFAH1B1,PAX6,PCNT,PDCD6IP,PPP2R1A,RAN,RANBP1,RBM14,RCC1,RCC2,RHOA,RPS3,SMC1A,SMC3,SNCA,STMN1,SUN2,TBCD,TBCE,TPPP,TPPP3,TPR,TUBA1B,TUBGCP2,VPS4A,VPS4B,XPO1,ZPR1,ZW10
multi-organism transport	ALYREF,DDX39B,DERL1,DYNLT1,FMR1,KPNA4,KPNB1,NUP133,NUP160,NUP205,NUP85,NUP93,RAN,RANBP2,RPS27A,TCP1,TPR,TSG101,VPS28,VPS37B,XPO1
multi-organism localization	ALYREF,DDX39B,DERL1,DYNLT1,FMR1,KPNA4,KPNB1,NUP133,NUP160,NUP205,NUP85,NUP93,RAN,RANBP2,RPS27A,TCP1,TPR,TSG101,VPS28,VPS37B,XPO1
ephrin receptor signaling pathway	ACTB,ACTG1,ACTR2,ACTR3,AP2A1,AP2A2,AP2B1,AP2M1,AP2S1,ARHGEF7,ARPC2,ARPC3,ARPC5,CDC42,CRK,DNM1,GIT1,MYL12A,NOTCH1,PAK1,PTPN11,RHOA,SDCBP,SRC
RNA secondary structure unwinding	AGO1,DDX1,DDX17,DDX18,DDX21,DDX39A,DDX39B,DDX3X,DDX42,DDX46,DDX5,DDX50,DDX6,EIF4A1,EIF4A2,EIF4A3
positive regulation of axon extension	ADNP,APOE,DBN1,EIF4G2,FN1,GSK3B,ILK,L1CAM,MACF1,MAP1B,MAPT,NRG1,PAFAH1B1,RPL4,RUFY3,TWF2
nucleotide-excision repair, DNA damage recognition	COPS2,COPS3,COPS4,COPS7A,COPS7B,COPS8,CUL4B,DDB1,PARP1,RAD23B,RPS27A

transferrin transport	ATP6V0A1,ATP6V0D1,ATP6V1A,ATP6V1B2,ATP6V1D,ATP6V1E1,ATP6V1F,ATP6V1G2,ATP6V1H,CLTC,DNM2,RAB11B,SNX3,TFRC
positive regulation of cysteine-type endopeptidase activity	AIFM1,ARL6IP5,BAX,BCL2L13,BID,CYCS,CYFIP2,DDX3X,DIABLO,FAM162A,FIS1,GSN,HMGB1,HSPD1,HSPE1,HTRA2,MEN1,NDUFA13,NGFR,PDCD5,PDCD6,PPM1F,PPP2CA,RACK1,RHOA,RPS27L,RPS3,S100A8,S100A9,SNCA,STAT1,VCP
axon extension	ADNP,APOE,CTTN,CYFIP1,DBN1,DCLK1,DCX,DNM2,DPYSL2,EIF4G2,FN1,GSK3B,ILK,L1CAM,LAMB2,MACF1,MAP1B,MAPT,NRCAM,NRG1,OGN,PAFAH1B1,RAB21,RPL4,RTN4,RUFY3,TNR,TPBGL,TWF2,USP9X,VCL
NADH dehydrogenase complex assembly	AIFM1,BCS1L,NDUFA10,NDUFA13,NDUFA5,NDUFA6,NDUFA8,NDUFA9,NDUFB4,NDUFB9,NDUFS1,NDUFS2,NDUFS3,NDUFS4,NDUFS6,NDUFS8,NDUFV1,NDUFV2
mitochondrial respiratory chain complex I biogenesis	AIFM1,BCS1L,NDUFA10,NDUFA13,NDUFA5,NDUFA6,NDUFA8,NDUFA9,NDUFB4,NDUFB9,NDUFS1,NDUFS2,NDUFS3,NDUFS4,NDUFS6,NDUFS8,NDUFV1,NDUFV2
mitochondrial respiratory chain complex I assembly	AIFM1,BCS1L,NDUFA10,NDUFA13,NDUFA5,NDUFA6,NDUFA8,NDUFA9,NDUFB4,NDUFB9,NDUFS1,NDUFS2,NDUFS3,NDUFS4,NDUFS6,NDUFS8,NDUFV1,NDUFV2
regulation of gene expression, epigenetic	ACTB,ADAR,AGO1,ARID4A,CELF1,CNOT1,CTNNB1,DDX21,DEK,DNMT1,DPY30,EIF1,EIF6,EXOSC10,FMR1,FXR1,GPX1,GSK3B,H2AFV,H2AFY,H2AFY2,H3F3A,HAT1,HDAC2,HDAC6,HIST1H2AJ,HIST1H3A,HIST1H4D,HIST2H2AC,HIST2H3C,HMGA1,HNRNPA2B1,MBD3,MECP2,MTA1,MYBBP1A,POLR2H,POLR2L,PRKRA,RAN,RBBP4,RBM3,RBM4,SMARCA4,SMARCA5,SMARCD1,SRRT,TRIM28,UBTF,UPF1,XPO5
negative regulation of hemostasis	ABAT,ANXA2,ANXA5,APOE,APOH,F2,FGA,FGB,FGG,KNG1,KRT1,PLG,SERPINF2,SERPING1,THBS1,UBASH3B,VTN
negative regulation of blood coagulation	ABAT,ANXA2,ANXA5,APOE,APOH,F2,FGA,FGB,FGG,KNG1,KRT1,PLG,SERPINF2,SERPING1,THBS1,UBASH3B,VTN
multi-organism intracellular transport	ALYREF,DDX39B,DERL1,DYNLT1,FMR1,KPNA4,KPNB1,NUP133,NUP160,NUP205,NUP85,NUP93,RAN,RANBP2,RPS27A,TPR,TSG101,VPS28,VPS37B,XPO1
intracellular transport of virus	ALYREF,DDX39B,DERL1,DYNLT1,FMR1,KPNA4,KPNB1,NUP133,NUP160,NUP205,NUP85,NUP93,RAN,RANBP2,RPS27A,TPR,TSG101,VPS28,VPS37B,XPO1
organelle assembly	ABLIM3,ACTC1,ACTG1,ACTR2,ATP6V0D1,ATP6V1D,ATXN10,ATXN2L,C1QBP,CHD4,CIRBP,CLASP1,CLTC,CNOT1,CORO1A,CTSD,DBNL,DDX3X,DDX6,DHX30,DYNC1H1,EHD1,EIF6,EZR,FLNA,FSCN1,GABARAPL2,GSN,HDAC2,HYDIN,KIF2A,KPNB1,LAMA5,LCP1,LSM3,LSM4,MAP1LC3A,MAP1LC3B,MAP4,MRPS7,MSN,MVB12A,MYH10,NPM1,PAFAH1B1,PCNT,PDCD6IP,PDGFRB,PIP4K2A,PRKAR1A,RAB14,RAB1B,RAB5A,RAB7A,RBM14,RCC1,RDX,RHOA,RPL11,RPL12,RPL23A,RPL24,RPL3,RPL38,RPL5,RPL6,RPS10,RPS14,RPS15,RPS17,RPS19,RPS2,RPS25,RPS27,RPS27L,RPS3,RPS5,RPSA,SDC1,SDCBP,SEPT9,SH3GLB1,SRC,STX12,STX7,TBC1D10B,TBC1D9B,TPM1,TPR,TSG101,TUBGCP2,UBQLN1,UBQLN2,VDAC3,VPS25,VPS28,VPS37B,VPS4A,VPS4B,VTA1,WDR1

Title (or Source)	Grp 3_GeneSet
purine-containing compound biosynthetic process	ACACA,ADSL,AK1,AK2,AK4,AKAP12,ALDOA,AMPD2,APOE,APRT,AQP1,ATIC,ATP5A1,ATP5B,ATP5C1,ATP5D,ATP5EP2,ATP5F1,ATP5H,ATP5I,ATP5J,ATP5J2,ATP5L,ATP5O,CALM2,COASY,DCAKD,GART,GBAS,GMPS,GNAI2,GNAS,GUK1,HPRT1,IMPDH1,IMPDH2,MAT2A,MTAP,MTHFD1,NME1,NME3,NPR3,PA

	ICS,PALM,PAPSS1,PFAS,PKM,PNP,PPAT,PRPS1,RCVRN,SHMT1,SLC25A13,STAT3,STOML2,VCP
protein heterotrimerization	COL1A1,COL1A2,COL6A1,COL6A2,GNA11,GNAQ,GNB1,NUP54,NUP62,PPP2CA,WIZ
ERAD pathway	BAG6,BCAP31,CCDC47,FAF2,FBXO2,GET4,HSP90B1,HSPA5,NFE2L2,NPLOC4,PSMC1,PSMC2,PSMC3,PSMC4,PSMC5,PSMC6,SEC61B,SGTA,TRIM25,UBQLN1,UBQLN2,UBXN1,UFD1L,USP14,VCP
nucleotide-excision repair	CETN2,COPS3,COPS6,COPS7B,COPS8,DDB1,GPS1,HMGB1,LIG3,MMS19,PARP1,PCNA,POLR2A,POLR2C,POLR2E,POLR2H,PRPF19,RAD23A,RAD23B,RFC3,RPA1,RPA2,RPA3,RPS27A,SUMO2,TCEA1,UBE2I,UBE2N,UBE2V2,USP7
gene silencing	ADAR,AGO1,ARID1A,CBX8,CNOT1,DPY30,EIF6,FXR1,H2AFV,H2AFY,H2AFY2,H3F3A,HDAC2,HIST1H2AJ,HIST1H3A,HIST1H4D,HIST2H2AB,HIST2H2AC,HIST2H3C,HMGA1,HNRNPA2B1,MECP2,NCBP1,NUP155,NUP210,NUP35,NUP54,NUP62,NUP93,PABPC1,POLR2A,POLR2C,POLR2E,POLR2H,PRKRA,RAE1,RAN,RANBP2,RBM3,RBM4,SMARCA4,SMARCA5,SND1,SRRT,STAT3,TPR,TRIM28,TSN,TSNAX,UBTF,XPO5
acute-phase response	AHSG,APCS,ASS1,F2,FGA,FN1,HNRNPK,HP,ITIH4,MBL2,ORM1,ORM2,SAA1,SAA2-SAA4,SERPINA1,SERPINA3,SERPINF2,STAT3,TFRC
DNA repair	ACTL6A,APEX1,C9orf142,CBX8,CDC5L,CETN2,COPS3,COPS6,COPS7B,COPS8,DDB1,DDX1,DEK,EEF1E1,FEN1,FOXM1,GPS1,HIST1H4D,HMGA1,HMGA2,HMGB1,HMGB2,HSPA1B,HUWE1,KDM1A,LIG3,MDC1,MEN1,MMS19,MRE11A,MSH2,MTA1,NONO,NPLOC4,NPM1,OTUB1,PARP1,PCNA,PNP,POLR2A,POLR2C,POLR2E,POLR2H,PPP5C,PRKDC,PRPF19,PSMD14,RAD21,RAD23A,RAD23B,RBM14,RFC3,RMI2,RPA1,RPA2,RPA3,RPS27A,RPS27L,RPS3,RUVBL1,RUVBL2,SFPQ,SMARCA5,SMC1A,SMC3,SSRP1,SUMO2,SUPT16H,TCEA1,TERF2IP,TIGAR,TP53BP1,TRIM25,TRIM28,UBE2I,UBE2N,UBE2V2,UFD1L,USP7,VCP,WDR33,XRCC5,XRCC6,YY1
ribose phosphate biosynthetic process	ACACA,ADSL,AK1,AK2,AK4,AKAP12,ALDOA,AMPD2,APOE,APRT,AQP1,ATIC,ATP5A1,ATP5B,ATP5C1,ATP5D,ATP5EP2,ATP5F1,ATP5H,ATP5I,ATP5J,ATP5J2,ATP5L,ATP5O,CAD,CALM2,CMPK1,COASY,DCAKD,GART,GBAS,GMPS,GNAI2,GNAS,GUK1,HPRT1,IMPDH1,IMPDH2,NME1,NME3,NPR3,PAICS,PALM,PAPSS1,PFAS,PKM,PNP,PPAT,PRPS1,RCVRN,SLC25A13,STAT3,STOML2,VCP
protein sumoylation	CBX8,CETN2,CTNNB1,HNRNPC,HNRNPK,MDC1,MTA1,NOP58,NUP155,NUP210,NUP35,NUP54,NUP62,NUP93,PARK7,PARP1,PCNA,PHC2,RAD21,RAE1,RANBP2,RING1,RPA1,SAE1,SMC1A,SMC3,STAG2,SUMO2,TOLLIP,TOP1,TOP2B,TP53BP1,TPR,TRIM28,UBA2,UBE2I
maturation of LSU-rRNA	BOP1,EIF6,GTPBP4,MAK16,NHP2,PES1,RPL10A,RPL35,RPL7,RPL7A,RSL1D1,SNU13
acute inflammatory response	A2M,AHSG,APCS,APOA2,ASS1,C1QBP,C3,C4B,C4BPA,C8G,CFB,CFH,F2,F3,FGA,FN1,GSTP1,HNRNPK,HP,ITIH4,MBL2,ORM1,ORM2,PHB,PHB2,S100A8,SAA1,SAA2-SAA4,SERPINA1,SERPINA3,SERPINF2,SERPING1,STAT3,TAC1,TFRC,VTN
purine nucleotide biosynthetic process	ACACA,ADSL,AK1,AK2,AK4,AKAP12,ALDOA,AMPD2,APOE,APRT,AQP1,ATIC,ATP5A1,ATP5B,ATP5C1,ATP5D,ATP5EP2,ATP5F1,ATP5H,ATP5I,ATP5J,ATP5J2,ATP5L,ATP5O,CALM2,COASY,DCAKD,GART,GBAS,GMPS,GNAI2,GNAS,GUK1,HPRT1,IMPDH1,IMPDH2,MTHFD1,NME1,NME3,NPR3,PAICS,PALM,PAPSS1,PFAS,PKM,PNP,PPAT,PRPS1,RCVRN,SLC25A13,STAT3,STOML2,VCP

2-oxoglutarate metabolic process	DLD,DLST,GOT1,GOT2,IDH1,IDH2,IDH3A,IDH3B,KYAT3,MRPS36,OGDH
purine ribonucleotide biosynthetic process	ACACA,ADSL,AK1,AK2,AK4,AKAP12,ALDOA,AMPD2,APOE,APRT,AQP1,ATIC,ATP5A1,ATP5B,ATP5C1,ATP5D,ATP5EP2,ATP5F1,ATP5H,ATP5I,ATP5J,ATP5J2,ATP5L,ATP5O,CALM2,COASY,DCAKD,GART,GBAS,GMPS,GNAI2,GNAS,GUK1,HPRT1,IMPDH1,IMPDH2,NME1,NME3,NPR3,PAICS,PALM,PAPSS1,PFAS,PKM,PNP,PPAT,PRPS1,RCVRN,SLC25A13,STAT3,STOML2,VCP
ER-associated ubiquitin-dependent protein catabolic process	BCAP31,CCDC47,FAF2,FBXO2,HSP90B1,HSPA5,NFE2L2,NPLOC4,PSMC1,PSMC2,PSMC3,PSMC4,PSMC5,PSMC6,SEC61B,SGTA,UBQLN1,UBQLN2,UFD1L,USP14,VCP
cellular response to DNA damage stimulus	ACTL6A,ALYREF,APEX1,BAG6,BAX,BCLAF1,BID,C9orf142,CBX8,CCAR2,CD44,CDC5L,CDKN2AIP,CETN2,CLU,CNOT1,COPS3,COPS6,COPS7B,COPS8,DDB1,DDX1,DDX39B,DDX5,DEK,DNAJA1,E2F1,EEF1E1,EPHA2,FEN1,FOXM1,GNL1,GPS1,GRB2,HIST1H4D,HMGA1,HMGA2,HMGB1,HMGB2,HNRNPK,HSPA1B,HUWE1,KDM1A,LIG3,MACROD1,MAPK1,MCM7,MDC1,MEN1,MMS19,MRE11A,MRPS26,MSH2,MTA1,NDRG1,NONO,NPLOC4,NPM1,OTUB1,PARP1,PCBP4,PCNA,PEA15,PHF1,PNP,POLR2A,POLR2C,POLR2E,POLR2H,PPP5C,PRKDC,PRMT1,PRPF19,PSMD14,PTPN11,RAD21,RAD23A,RAD23B,RBM14,RFC3,RMI2,RPA1,RPA2,RPA3,RPS27A,RPS27L,RPS3,RUVBL1,RUVBL2,SETD7,SFPQ,SMARCA5,SMC1A,SMC3,SNW1,SSRP1,SUMO2,SUPT16H,TCEA1,TERF2IP,TIGAR,TIPRL,TP53BP1,TPT1,TRIM25,TRIM28,UBA1,UBE2I,UBE2N,UBE2V2,UFD1L,USP7,VCP,WDR33,XRCC5,XRCC6,YY1
chaperone-mediated protein complex assembly	APCS,CCT2,CCT6B,CLU,HSP90AA1,HSPA4,HSPD1,LONP1,PFDN6
regulation of DNA replication	CALR,CCT2,CCT3,CCT4,CCT5,CCT6A,CCT7,CCT8,CDC42,CHTF8,CTNNB1,DKC1,EHMT2,GTPBP4,HNRNPA1,HNRNPC,HNRNPU,INSR,LIG3,LONP1,MAPK1,MEN1,MRE11A,NAT10,NPM1,PCNA,PDS5A,PPP2CA,PPP2R1A,RFC3,SMC1A,SMC3,SRC,STAG2,STOML2,TCP1,WIZ
gene silencing by RNA	ADAR,AGO1,CNOT1,EIF6,FXR1,H3F3A,HIST1H3A,HIST1H4D,HIST2H3C,HNRNPA2B1,NCBP1,NUP155,NUP210,NUP35,NUP54,NUP62,NUP93,PABPC1,POLR2A,POLR2C,POLR2E,POLR2H,PRKRA,RAE1,RAN,RANBP2,RBM3,RBM4,SND1,SRRT,STAT3,TPR,TSN,TSNAX,XPO5
rRNA-containing ribonucleoprotein complex export from nucleus	EIF6,NPM1,RAN,RPS15,RPS28,RPSA,RRS1,XPO1
glyoxylate metabolic process	AGXT,DLD,DLST,GCSH,GRHPR,IDH1,IDH2,NDUFAB1,OGDH,PDHA1,PDHB,PDHX
protein localization to cytoplasmic stress granule	DDX1,DDX3X,DHX9,SSB,TIA1,YBX1
negative regulation of hydrolase activity	A2M,AGRN,AHSG,AMBP,ANXA1,APCS,APOA1,APOA2,APOC3,AQP1,C3,C4B,CD44,CNN3,COL6A3,CRYAB,CSNK2A1,CSTB,DBN1,DDX3X,DLG3,DNAJA3,DNAJB6,FKBP1A,GNAT1,GPI,GPS1,GPX1,IPO5,IQGAP1,ITIH1,ITIH2,ITIH4,KNG1,LAMTOR5,LTF,NOL3,PARK7,PCSK1N,PDE6D,PEBP1,PICALM,POR,PPP1R11,PRDX3,PRDX5,PSMF1,PTPA,RBM26,RCC2,RDX,RGN,SERPINA1,SERPINA3,SERPINC1,SERPIND1,SERPINF2,SERPING1,SERPINH1,SNCA,SRC,TFPI2,THBS1,TIPRL,TMED2,UBXN1,USP14,VTN,YWHAE
oxaloacetate metabolic process	ACLY,CS,GOT1,GOT2,MDH1,MDH2,NIT2,PCK2
tRNA metabolic process	AARS,AIMP1,AIMP2,C14orf166,C2orf49,CPSF1,CSTF2,DARS,DDX1,EEF1E1,EPRS,EXOSC2,EXOSC3,FAM98B,FARSA,FARSB,FBL,HSD17B10,IARS,KARS,LAGE3,LARS,LRRC47,LSM6,MARS,NARS,NAT10,PPA1,QTRT1,RARS,RTCB,SARS,SSB,TARS,TRMT

	1,TRMT112,VARS
Title (or Source)	Grp 4_GeneSet
modulation of synaptic transmission	ABAT,APOE,ARF1,ATP1A2,ATP2A2,ATP2B2,BAIAP2,BCAN,CA2,CLSTN1,CREB1,CRTC1,CTNND2,DBN1,DNM1,EIF4A3,EPHB2,FLOT1,FMR1,GFAP,GLUL,GNAI1,GNAI2,HNRNPK,KIF5B,LAMA2,MAPK1,MAPT,MECP2,NAPA,NCAM1,NCDN,NPTN,PCDH17,PEBP1,PFN2,PLCL2,PPP3CA,PPP3CB,RAB3A,RAB5A,RAP1B,RELN,S100B,SLC18A1,SLC1A3,SLC8A2,SNAP25,SNCA,STX1B,STXBP1,SYN1,SYNJ1,VAMP2,YWHAG,YWHAH
regulation of dendrite development	ACTR3,APOE,ARF1,BAIAP2,CAPRIN1,CFL1,CRTC1,DBN1,DCC,EIF4G2,ELAVL4,FAT3,FMR1,GSK3A,HDAC2,HNRNPK,IQGAP1,MARCKS,NRG1,PAFAH1B1,PAK3,PALM,PPP3CA,PQBP1,PTPRZ1,RELN,RHOA,SARM1,SEZ6,TNIK,YWHAH
positive regulation of ATPase activity	AHSA1,ATP1B1,ATP1B2,CHTOP,DNAJB1,DNAJB6,HNRNPU,PFN1,PFN2,RAB3A,RAB4A,RAB6A,RGN,TOR1AIP1,TPM1
regulation of ATPase activity	AGRN,AHSA1,ATP1B1,ATP1B2,CHTOP,CNN3,DBN1,DNAJB1,DNAJB6,HNRNPU,PFN1,PFN2,RAB3A,RAB4A,RAB6A,RGN,SNRNP70,TOR1AIP1,TPM1
extracellular matrix disassembly	A2M,BCAN,BSG,CAPG,CAPN1,CAPN2,CAPNS1,CD44,CLASP2,CTSG,DCN,DDR2,ELANE,FBN1,FLOT1,FN1,FSCN1,GSN,HSPG2,LAMC1,NID1,PLG
regulation of synaptic vesicle transport	ATP2A2,DNM1,FMR1,NAPA,PFN2,RAB3A,RAB5A,RAP1B,SNCA,STX1B,STXBP1,SYN1,SYNJ1
ATP hydrolysis coupled transmembrane transport	ATP1A2,ATP1A3,ATP1A4,ATP1B1,ATP1B2,ATP5A1,ATP5B,ATP6V0D1,ATP6V1A,ATP6V1B2,ATP6V1E1,ATP6V1F,ATP6V1H
positive regulation of intrinsic apoptotic signaling pathway	BAX,BCL2L1,BCLAF1,BID,CLU,DFNA5,DNM1L,FIS1,PARK7,PRKRA,RACK1,RPS3,S100A8,S100A9,SFPQ,SLC9A3R1,SOD1
regulation of neurogenesis	ACTR3,AGRN,APOE,ARF1,ARHGDIA,ARHGEF2,BAG5,BAIAP2,CALR,CAPRIN1,CFL1,CLASP2,CNTN1,COL3A1,CPNE1,CPNE6,CREB1,CRMP1,CRTC1,CTNNB1,CTTN,CXCR4,DBN1,DCC,DDX6,DOCK7,DPYSL2,DPYSL3,EEF1A1,EIF4G1,EIF4G2,ELAVL4,EPHB2,F2,FAT3,FKBP4,FMR1,FN1,GDI1,GFAP,GSK3A,HDAC2,HMG20A,HMGB2,HNRNPK,IQGAP1,ITM2C,KDM1A,L1CAM,LGALS1,LRP1,MACF1,MAP1B,MAP2,MAPT,MARCKS,MECP2,NEFL,NME1,NOTCH1,NPTN,NRG1,OGN,PAFAH1B1,PAK3,PALM,PLXNA2,PPP3CA,PQBP1,PRKCSH,PRMT5,PRPF19,PTBP1,PTPRO,PTPRZ1,RANBP1,RELN,RHOA,RPL4,RTN4,RUFY3,SARM1,SEZ6,SNAP25,SNX3,SRRT,SYNJ1,SYT4,TNIK,TSPO,UBE2V2,VIM,WDR1,XRCC5,XRCC6,YWHAG,YWHAH
cellular response to oxygen radical	ADPRHL2,APOA4,FBLN5,MPO,PARK7,PARP1,PRDX1,PRDX2,RGN,SOD1,SOD2
cellular response to superoxide	ADPRHL2,APOA4,FBLN5,MPO,PARK7,PARP1,PRDX1,PRDX2,RGN,SOD1,SOD2
positive regulation of dendritic spine development	APOE,ARF1,BAIAP2,CAPRIN1,DBN1,EIF4G2,FMR1,HNRNPK,MARCKS,NRG1,PAFAH1B1,PAK3,PALM,RELN
nucleus organization	AGAP3,BANF1,CHMP6,EMD,GOLM1,H3F3A,HMGB2,LEMD2,LMNA,NOLC1,NSFL1C,NUMA1,NUP205,NUP35,NUP93,PAFAH1B1,PPP2CA,PPP2R1A,RANBP2,RPS19,RTN4,SUN2,SYNE2,TARDBP,TBPL1,TMEM43,TOR1AIP1,TPR,VPS4A
positive regulation of dendrite development	ACTR3,APOE,ARF1,BAIAP2,CAPRIN1,CRTC1,DBN1,EIF4G2,ELAVL4,FMR1,HNRNPK,IQGAP1,MARCKS,NRG1,PAFAH1B1,PAK3,PALM,PTPRZ1,RELN,SEZ6
cellular chemical homeostasis	ACO1,ANXA6,ANXA7,AP3D1,APOC3,APOE,AQP1,AQP4,ARF1,ATP13A1,ATP1A2,ATP1A3,ATP1A4,ATP1B1,ATP1B2,ATP2A2,ATP2B1,ATP2B2,ATP2B4,ATP5B,ATP6V0D1,ATP6V1A,ATP6V1B2,ATP6V1E1,ATP6V1F,ATP6V1G2,ATP6V1H,BAX,CA2,CACNA2D1,CALM2,CALR,CAMK2D,CKB,CLN5,CLSTN1,CP,CXCR4

	,EIF5A,ELANE,F2,FIS1,FKBP1A,FN1,FTH1,FTL,GNA13,GNB1,GSTM2,GSTO1,GTF2I,HK1,HMGB1,HNRNPK,HPX,HSP90B1,IMMT,KIF5B,KNG1,LGALS1,MYO5A,NME1,NOL3,NPTN,OXCT1,PHPT1,PPP2CA,PPP3CA,PPP3CB,PPT1,PRNP,PYGM,RAB11B,RAB7A,RACK1,RANBP2,RAP1GDS1,RBM4,RGN,RMDN3,S100A8,S100A9,S100B,SLC4A1,SLC4A4,SLC8A2,SLC9A3R1,SMARCA4,SNCA,SOD1,SRI,TGM2,TPT1,VSNL1
glyceraldehyde-3-phosphate metabolic process	ALDH1A1,BPGM,PGAM1,PGD,PGLS,PGM2,TALDO1,TIGAR,TKFC,TPI1
regulation of synaptic plasticity	APOE,ARF1,ATP2B2,BAIAP2,BCAN,CREB1,CRTC1,CTNND2,DBN1,EPHB2,FMR1,GFAP,HNRNPK,MAPK1,MAPT,MECP2,NCAM1,NCDN,NPTN,PPP3CB,RAB3A,RAB5A,RELN,S100B,SLC8A2,SNAP25,SNCA,STXBP1,VAMP2,YWHAG,YWHAH

JPA associations

	Biomolecular association	NCJPA_GeneSet	JPA_GeneSet
Gene Family	Coronins	x	CORO1A,CORO1B,CORO1C,CORO2B
	CD molecules	x	ADAM10,ATP1B3,BSG,CD44,CD47,CD59,CD74,CD81,CD99,CDH2,IGLL1,IGSF8,ITGAM,ITGAV,JAM2,L1CAM,LRP1,PTGFRN,SLC4A1,THY1
Pathway	Spinal Cord Injury	x	ACAN,ANXA1,APEX1,AQP1,AQP4,BCAN,C1QB,CD47,CDC42,CSPG4,FKBP1A,GAP43,GFAP,GJA1,LGALS3,MAPK1,MAPK3,MBP,MIF,NCAN,OMG,PPP3CA,PRKCA,PTPRZ1,RHOA,RHOB,RHOC,RTN4,VCAN,VIM
	Leigh Syndrome	x	ACAT1,AKR1B1,ALDH2,DLD,GLO1,MDH1,ME2,PC,PDHA1,PDHB,PKLR
	Pyruvate Metabolism	x	ACAT1,AKR1B1,ALDH2,DLD,GLO1,MDH1,ME2,PC,PDHA1,PDHB,PKLR
	Gap junction degradation	x	AP2M1,CLTA,CLTB,CLTC,DNM1,DNM2,GJA1,MYO6
	Membrane Trafficking	x	AP1B1,AP1M1,AP2M1,ARCN1,CHMP4B,CHMP6,CLTA,CLTB,CLTC,COPA,COPB1,COPB2,COPE,COPG1,CTSZ,DNASE2,DNM1,DNM2,FTH1,FTL,GJA1,HIP1R,HSPA8,MYO6,NAPA,PICALM,RAB10,RAB5C,RALA,SEC13,SEC23A,SEC24C,SEC31A,SH3GL2,SNAP23,SNAPIN,SNX5,SRC,TJP1,TXNDC5,VAMP2,VTA1,YWHAB,YWHAE,YWHAG,YWHAH,YWHAQ,YWH

			AZ
	Complement cascade	x	C1QA,C1QB,C3,C4A,C4BPA,C6,C7,C8B,C9,CD59,CFB,CFH,CFI,IGHG1,IGHG2,IGHG3,IGHG4,IGKC,IGKV1D-33,IGKV3-20,IGKV4-1,VTN
	Regulation of Complement cascade	x	C3,C4A,C4BPA,C6,C7,C8B,C9,CD59,CFB,CFH,CFI,VTN
	Bacterial invasion of epithelial cells	x	ACTG1,ARPC1A,ARPC2,ARPC5L,CDC42,CLTA,CLTB,CLTC,CRK,CRKL,CTNNA1,CTNNA2,CTNNB1,CTTN,DNM1,DNM2,DNM3,FN1,RHOA,RHOG,SRC,VCL,WASF2,WASL
	Cytosolic tRNA aminoacylation	x	AARS,DARS,FARSA,FARSB,KARS,LARS,NARS,PPA1,QARS,RARS,SARS,TARS,VARS,WARS
	Prion diseases	x	BAX,C1QA,C1QB,C6,C7,C8B,C9,HSPA5,LAMC1,MAPK1,MAPK3,NCAM1,NCAM2,SOD1,STIP1
	Opioid proopiomelanocortin pathway	x	GNAI2,GNAI3,GNAO1,GNB1,GNB2,GNG10,GNG12,GNG2,GNG4,GNG7,SNAP23,SNAP25,VAMP2,VAMP3
	Opioid prodynorphin pathway	x	GNAI2,GNAI3,GNAO1,GNB1,GNB2,GNG10,GNG12,GNG2,GNG4,GNG7,SNAP23,SNAP25,VAMP2,VAMP3
	S1P4 pathway	x	CDC42,GNA13,GNAI2,GNAI3,GNAO1,GNAZ,MAPK1,MAPK3,RHOA
	Complement and Coagulation Cascades	x	A2M,APOA2,C1QA,C1QB,C3,C6,C7,C9,F12,F2,FGB,KNG1,PLG,SERPINA1,SERPINC1,SERPIND1,SERPINF2,SERPING1
	Citric Acid Cycle	x	ACO2,CS,DLST,FH,IDH3A,MDH2,OGDH,PC,PDHA1,PDHB
	Thrombin signalling through proteinase	x	F2,GNA11,GNA13,GNAQ,GNB1,GNB2,GNG10,

	activated receptors (PARs)		GNG12,GNG2,GNG4,GNG7,MAPK1,MAPK3,SRC
	Clathrin derived vesicle budding	x	AP1B1,AP1M1,CLTA,CLTC,CTSZ,DNASE2,DNM2,FTH1,FTL,HIP1R,HSPA8,NAPA,PICALM,RAB5C,SH3GL2,SNAP23,SNAPIN,SNX5,TXNDC5,VAMP2
	trans-Golgi Network Vesicle Budding	x	AP1B1,AP1M1,CLTA,CLTC,CTSZ,DNASE2,DNM2,FTH1,FTL,HIP1R,HSPA8,NAPA,PICALM,RAB5C,SH3GL2,SNAP23,SNAPIN,SNX5,TXNDC5,VAMP2
	Cortocotropin releasing factor receptor signaling pathway	x	GNA11,GNAQ,GNB1,GNB2,GNG10,GNG12,GNG2,GNG4,GNG7,SNAP23,SNAP25,VAMP2,VAMP3
	Formation of annular gap junctions	x	AP2M1,CLTA,CLTB,CLTC,DNM1,DNM2,GJA1
	p130Cas linkage to MAPK signaling for integrins	x	CRK,FGA,FGB,FGG,FN1,RAP1A,RAP1B,SRC,TLN1
	GRB2:SOS provides linkage to MAPK signaling for Intergrins	x	FGA,FGB,FGG,FN1,GRB2,RAP1A,RAP1B,SRC,TLN1
	2-Hydroxyglutric Aciduria (D And L Form)	x	ABAT,ACAT1,ACSM1,ALDH2,ALDH5A1,ILVBL,OXCT1,PDHA1,PDHB
	M Phase	x	BANF1,CKAP5,CLASP2,KIF2A,LMNA,LMNB1,MAPK1,MAPK3,MAPRE1,NEK9,NUP93,PAFAH1B1,PPP1CC,PPP2R1A,PPP2R2A,PSMA2,PSMA3,PSMA5,PSMA6,PSMB1,PSMB2,PSMB3,PSMB4,PSMB5,PSMB6,PSMB9,PSMC1,PSMC2,PSMC3,PSMC4,PSMC5,PSMD1,PSMD11,PSMD2,PSMD3,PSMD5,PSMD6,PSME1,PSME2,PSMF1,RAB1B,RAB2A,SEC13,TMPO,

			TPR,USO1,XPO1
	Mitotic Anaphase	x	BANF1,CKAP5,CLASP2,KIF2A,LMNA,LMNB1,MAPRE1,PAFAH1B1,PPP1CC,PPP2R1A,PPP2R2A,PSMA2,PSMA3,PSMA5,PSMA6,PSMB1,PSMB2,PSMB3,PSMB4,PSMB5,PSMB6,PSMB9,PSMC1,PSMC2,PSMC3,PSMC4,PSMC5,PSMD1,PSMD11,PSMD2,PSMD3,PSMD5,PSMD6,PSME1,PSME2,PSMF1,SEC13,TMPO,XPO1
	Mitotic Metaphase and Anaphase	x	BANF1,CKAP5,CLASP2,KIF2A,LMNA,LMNB1,MAPRE1,PAFAH1B1,PPP1CC,PPP2R1A,PPP2R2A,PSMA2,PSMA3,PSMA5,PSMA6,PSMB1,PSMB2,PSMB3,PSMB4,PSMB5,PSMB6,PSMB9,PSMC1,PSMC2,PSMC3,PSMC4,PSMC5,PSMD1,PSMD11,PSMD2,PSMD3,PSMD5,PSMD6,PSME1,PSME2,PSMF1,SEC13,TMPO,XPO1
	Neurofascin interactions	x	ANK1,CNTN1,CNTNAP1,DCX,NFASC,NRCAM
	Nef Mediated CD8 Down-regulation	x	AP2A1,AP2A2,AP2B1,AP2M1,AP2S1,ATP6V1H
	TCA cycle	x	ACO2,CS,DLD,DLST,FH,IDH3A,MDH2,OGDH,SUCLG2
	Shigellosis	x	ACTG1,ARPC1A,ARPC2,ARPC5L,CD44,CDC42,CRK,CRKL,CTTN,MAPK1,MAPK3,PFN1,PFN2,RELA,RHOG,SRC,VCL,WASF2,WASL
	Opioid proenkephalin pathway	x	GNAI2,GNAI3,GNB1,GNB2,GNG10,GNG12,GNG2,GNG4,GNG7,SNAP23,SNAP25,VAMP2,VAMP3
	S1P3 pathway	x	GNA11,GNA13,GNAI2,

			GNAI3,GNAO1,GNAQ,GNAZ,ITGAV,MAPK1,MAPK3,RHOA,SRC
	Uptake of Oxygen and Release of Carbon Dioxide by Erythrocytes	x	AQP1,CA1,CA2,HBA1,HBB,HBD,SLC4A1
	Uptake of Carbon Dioxide and Release of Oxygen by Erythrocytes	x	AQP1,CA1,CA2,HBA1,HBB,HBD,SLC4A1
	O2/CO2 exchange in erythrocytes	x	AQP1,CA1,CA2,HBA1,HBB,HBD,SLC4A1
	Adaptive Immune System	x	ACTR1A,ACTR1B,AP1B1,AP1M1,AP2A1,AP2A2,AP2B1,AP2M1,AP2S1,C3,CALR,CANX,CD74,CD81,CDC42,CLTA,CLTC,CTSB,CTSC,CTSD,DCTN2,DCTN5,DNM1,DNM2,DNM3,DYNC1H1,DYNC1LI2,DYNLL2,ENAH,FBXO2,FGF1,GRB2,HLA-A,HLA-B,HLA-DQB1,HLA-DRA,HLA-DRB1,HSPA5,HUWE1,IGHD,IGHM,IGKC,IGKV1D-33,IGKV3-20,IGKV4-1,ITGAV,ITPR1,ITPR3,KIF2A,KIF5B,NPEPPS,NRAS,PDIA3,PPP2R1A,PSMA2,PSMA3,PSMA5,PSMA6,PSMB1,PSMB2,PSMB3,PSMB4,PSMB5,PSMB6,PSMB9,PSMC1,PSMC2,PSMC3,PSMC4,PSMC5,PSMD1,PSMD11,PSMD2,PSMD3,PSMD5,PSMD6,PSME1,PSME2,PSMF1,PTPN11,RAB7A,RAP1A,RAP1B,RAP1GAP,RBCK1,RELA,SEC13,SEC23A,SEC24C,SEC31A,SH3GL2,SKP1,SPTBN2,SRC,TAPBP,TCEB2,UBA1,UBE2L6,UBE2N,UBE2V2,YWHAB,YWHAZ
	Synthesis of DNA	x	PSMA2,PSMA3,PSMA5,

			PSMA6,PSMB1,PSMB2, PSMB3,PSMB4,PSMB5, PSMB6,PSMB9,PSMC1, PSMC2,PSMC3,PSMC4, PSMC5,PSMD1,PSMD1 1,PSMD2,PSMD3,PSM D5,PSMD6,PSME1,PSM E2,PSMF1
	Chylomicron-mediated lipid transport	x	APOA1,APOA2,APOA4, APOA5,APOB,APOC3,A POE,HSPG2,P4HB
	Complement Activation, Classical Pathway	x	C1QA,C1QB,C3,C4A,C4 B,C6,C7,C8B,C9
	Dopamine Neurotransmitter Release Cycle	RAB3A,SNAP25,STX1A, STXBP1,SYN1,SYN2,SYT 1,VAMP2	x
	Serotonin Neurotransmitter Release Cycle	RAB3A,SNAP25,STX1A, STXBP1,SYN1,SYN2,SYT 1,VAMP2	x
	Ensemble of genes encoding core extracellular matrix including ECM glycoproteins, collagens and proteoglycans	ACAN,AGRN,BCAN,BG N,COL14A1,COL18A1,C OL1A1,COL1A2,COL3A 1,COL4A2,COL5A2,COL 6A1,COL6A2,COL6A3,D CN,DPT,EFEMP1,EMILI N1,FBLN5,FBN1,FGA,F GB,FGG,FN1,HAPLN1,H APLN2,HSPG2,IGFBP3,L AMA2,LAMA4,LAMB1, LAMB2,LAMC1,LRG1,L UM,MFAP2,NCAN,NID 1,NID2,OGN,POSTN,PR ELP,SPARC,TGFBI,THBS 1,TNC,TNR,VCAN,VTN, VWA1	x
	Formation of ATP by chemiosmotic coupling	ATP5A1,ATP5B,ATP5C1 ,ATP5D,ATP5F1,ATP5H, ATP5I,ATP5J,ATP5O	x
	Selenium Pathway	ALB,APOA1,CAT,F2,GP X1,HBA1,HBB,ICAM1, MPO,PLG,PNPO,PRDX1 ,PRDX2,PRDX3,PRDX4, PRDX5,SERPINA3,SOD1 ,SOD2,SOD3,TXN	x
	Mitochondrial Electron Transport Chain	ATP5A1,ATP5B,ATP5C1 ,ATP5D,ATP5F1,GAPDH ,GPD1,GPD2,UQCRC1	x

	GABA synthesis, release, reuptake and degradation	ABAT,ALDH5A1,HSPA8, RAB3A,SNAP25,STX1A, STXBP1,SYT1,VAMP2	x
	Post-chaperonin tubulin folding pathway	TBCA,TBCB,TUBA1B,TU BA4A,TUBB2B,TUBB3,T UBB4A,TUBB4B,TUBB6	x
	oxidative phosphorylation	ATP5A1,ATP5C1,ATP5F 1,ATP5J,ATP6V0D1,AT P6V1B2,COX4I1,CYC1, NDUFA6,NDUFAB1,ND UFB10,NDUFB8,NDUFS 3,NDUFV2,UQCRH	x
	Citrate cycle, first carbon oxidation, oxaloacetate => 2-oxoglutarate	ACO1,ACO2,CS,IDH1,ID H2,IDH3A	x
	Genes encoding proteoglycans	ACAN,BCAN,BGN,DCN, HAPLN1,HAPLN2,HSPG 2,LUM,NCAN,OGN,PRE LP,VCAN	x
	Transmission across Chemical Synapses	ABAT,ACHE,ALDH2,ALD H5A1,AP2A1,AP2A2,AP 2B1,AP2S1,CACNA2D1, CAMK2A,CAMK2B,CA MK2D,COMT,EPB41L1, GLUL,GNAI2,GNB1,GN B2,GNG2,GNG4,HSPA8 ,MAPK1,NSF,PRKCA,RA B3A,SLC1A2,SLC1A3,SN AP25,STX1A,STXBP1,SY N1,SYN2,SYT1,VAMP2	x
	Caspase-mediated cleavage of cytoskeletal proteins	ADD1,DBNL,GSN,MAPT ,PLEC,SPTAN1,VIM	x
	Focal Adhesion	ACTG1,ACTN1,CAPN1, CDC42,COL1A1,COL1A 2,COL3A1,COL4A2,COL 5A2,COL6A2,CRK,FLNA, FN1,GRB2,ITGAV,ITGB8 ,LAMA2,LAMA4,LAMB 1,LAMB2,LAMC1,MAP K1,MYL6,RAP1B,RHOA, THBS1,TLN1,TNC,TNR, VCL,VTN,ZYX	x
	Cytoskeletal regulation by Rho GTPase	ACTG1,ARHGAP1,ARPC 2,ARPC5,CDC42,CFL1, MYH10,MYH9,PFN1,PF N2,STMN1,TUBB2B,TU	x

		BB3,TUBB4A,TUBB4B,TUBB6,TUBB8	
	NCAM signaling for neurite out-growth	AGRN,COL4A2,COL6A1,COL6A2,COL6A3,GRB2,MAPK1,NCAM1,NCAN,NRAS,SPTA1,SPTAN1,SPTB,SPTBN1,SPTBN2,YWHAB	x
	Rho cell motility signaling pathway	ACTR2,ACTR3,ARHGAP1,ARPC2,ARPC5,CFL1,GSN,PFN1,RHOA,TLN1,VCL	x
	2-Oxocarboxylic acid metabolism	ACO1,ACO2,CS,GOT1,GOT2,IDH1,IDH2,IDH3A	x
	Gluconeogenesis, oxaloacetate => fructose-6P	ALDOA,ALDOC,ENO1,ENO2,GAPDH,PGAM1,PGK1,TPI1	x
	Vasopressin-regulated water reabsorption	AQP4,ARHGDIA,DCTN2,DYNC1H1,DYNC1I1,DYNC1LI2,GNAS,NSF,RAB11B,RAB5A,RAB5B,RAB5C,VAMP2	x
	Respiratory electron transport	COX4I1,COX5A,COX6B1,CYC1,ETFA,ETFB,MT-CO2,NDUFA13,NDUFA6,NDUFAB1,NDUFB10,NDUFB8,NDUFS1,NDUFS3,NDUFV2,UQCRC1,UQCRC2,UQCRH	x

Table s1: Validated peptide markers in JPA cases by targeted MS

Protein	Peptide transition	JPA poor outcome	JPA favourable outcome
FBN1	TCVDINECLLEPR - 809.8818++	341972	5923980
INA	HSAEVAGYQDSIGQLENDLR - 1101.5247++	75887	66058
IGALS3BP	ELSEALGQIFDSQR - 796.8994++	4665810	23402382
	ASHEEVEGLVEK - 442.8894+++	507009	3702404

DPSYL5	IPHGVSGVQDR - 388.8755+++	35732700	3127707
	TISASTQVQGGDFNLYENMR - 744.3514+++	74190	57355
CELF2	ELFEPYGAVYQINVLR - 637.6719+++	54092	2905688
	VMFSPFGQIEECR - 533.9147+++	10850	1068330
GAB1	IFYLVADSEEEMNK - 844.3978++	280583	4133221
	APSASVDSSLYNLPR - 526.2704+++	46223800	541610240
HSD11B2	LAMSDLTPVVDAITDALLAARPR - 803.7772+++	2524755	547753
ARAP1	AFVPPLAEDLLAR - 471.2696+++	21773538	59958
	LGSVSLIPLR - 352.2255+++	2261316	1551352
GTPBP1	LNDTLLLGPDPLGNFLSIAVK - 737.4192+++	77778	358953
DDA1	EYPSEQIIVTEK - 479.2487+++	352350	1249111
	DQEQVELEGESSAPPR - 590.9429+++	933212	8015377
TPD52L2	MDSAGQDINLNSPNK - 535.2509+++	32086692	0
	TPAVEGLTEAEEEELR - 591.6231+++	400394	18064
LUC7L2	LAETQEEISAEVAAK - 530.2737+++	38215	414494
	VEQLGAEGNVEESQK - 539.5969+++	213491	950906
LUC7L3	MISAAQLLDELMGR - 516.6022+++	259302	3621508
	LALSQNQQSSGAAGPTGK - 572.2955+++	110442	3501737
PLLP	TSSPAQGAEASVSALRPDLGFVR - 772.7363+++	512380	665204
	GVGSNAATSQMAGGYA - 481.2174+++	30832	31861
DTNA	LAAESSSSQPPQQR - 495.9146+++	1713247	11368666
	NDLLVAADSITNTMSSLVK - 664.6821+++	1491045	2514029
EPN2	NIVNNYSEAEIK - 465.2368+++	4516	1740660
	TGAPLGQSEELQPLSQR - 604.3146+++	10154688	58257556
*XRCC5	IQPGSQQADFLDALIVSMDVIQHETIGK - 1018.5253+++	50460	66992

	TEQGGAHFSVSSLAEGSVTSVGSVNPAENFR - 1041.1656+++	285516	611788
ILF3	HSSVYPTQEELEAVQNMVSHTER - 891.0854+++	0	1459681
	AVSDWIDEQEK - 440.5420+++	1977417	2184919
*XRCC6	DIISIAEDEDLR - 463.5683+++	2627387	6023524
ANXA2	RAEDGSVIDYELIDQDAR - 688.9993+++	257419	1115858
ITIH2	IYGNQDTSSQLK - 451.8930+++	518450	2711510
	LDQIESVITATSANTQLVLETLAQMDDLQDFLSK - 1250.9713+++	47314	51746

* Referenced in main text